IN VITRO CHARACTERISATION OF THE NEUTROPHIL IN RESPIRATORY SYNCYTIAL VIRUS BRONCHIOLITIS

Gemma Louise Saint

A thesis submitted in accordance with the requirements of the University of Liverpool for the Degree of Doctor of Philosophy

June 2015

Department of Women's and Children's Health
Institute of Translational Medicine
University of Liverpool

Abstract

Background: Respiratory Syncytial Virus (RSV) is a common cause of bronchiolitis during infancy; virtually all children are infected with this virus by the age of 2 years. Although the majority have a self-limiting, mild infection, 1-3% have disease severe enough to warrant hospital admission. These children have an abundance of neutrophils (>80% of bronchoalveolar lavage cells) within their airways. There is however, a lack of detailed investigation into their role in viral infection. Our group has previously shown RSV associated with *ex vivo* neutrophils from infected infants. To explore this observation further, I have modelled and visualised the RSV-neutrophil interaction, hypothesising that neutrophils play a role in the innate viral response in the airway.

Aims: The aims of this thesis were to (i) establish an *in vitro* model of RSV-neutrophil interaction, (ii) determine whether RSV is taken up into the neutrophil, (iii) determine if RSV productively replicates inside the neutrophil, (iv) compare neutrophil-RSV interaction in adult and infant neutrophils and (v) investigate the response of the neutrophil to RSV.

Methods: An *in vitro* model of RSV-neutrophil interaction was established using highly purified adult and cord blood neutrophils. Neutrophils were analysed by quantitative RT-PCR, western blot, and by confocal microscopy using indirect immunocytochemistry. In addition, *ex vivo* BAL neutrophils from RSV infected infants were examined by confocal microscopy. Following validation of this model, confirming the presence of virus within the neutrophil, a human gene microarray was performed.

Results: Interaction of neutrophils with RSV was modelled *in vitro* and demonstrated by PCR analysis and western blot. RSV N gene expression revealed maximal neutrophil uptake at 4 hours. A time course over 20 hours showed no increase in RSV expression, implying that active RSV replication was not occurring. Confocal microscopy revealed internalisation of RSV, with virus distributed throughout the cytoplasm. Imaging of *ex vivo* neutrophils extracted from bronchoalveolar lavage of RSV-infected infants showed a similar distribution. RSV induced significant change in neutrophil gene expression with over 1000 differentially expressed genes being identified. Pathway analysis revealed an RNA virus specific transcriptional response. Results for key molecules were subsequently validated by RT-PCR.

Conclusions: Neutrophils do not allow RSV to replicate within them. In contrast, following interaction with RSV, they alter their gene expression profiles through the modulation of interferon responses and other pathways, thereby inhibiting viral replication. Evidence presented in this thesis supports a novel role for neutrophils as innate cells at the frontline of antiviral immunity in RSV disease.

Table of contents

Table of figures

Table of tables

Acknowledgments

I have enjoyed the past 3 years immensely and feel incredibly privileged to have been able to undertake this PhD. I cannot possibly thank everybody fully here, but would like to record those who have been of particular importance. Firstly, thanks to my supervisors who have allowed me three different perspectives, to have their direction and encouragement has been instrumental to this work. Dr Brian Flanagan has always been on hand for impromptu meetings and has coped admirably well with my bad science day grumps! I am very grateful to Dr Paul McNamara for his support, guidance and most excellent tutoring in the art of removing extraneous words! I am most appreciative of Prof Rosalind Smyth who always bought thoughtful critique to the project and pushed me to work to the highest standard.

A number of people from research groups at the University of Liverpool and around the country have given generously of their time, and offered invaluable advice and tutoring. My particular thanks to Ian Sabroe, Lynne Prince, Claire Smith, Rob Hirst, Marco Marcello, Lucille Rainbow, Mark Turner, David Mason and Jonathon David. I thank the research nurses who have supported the studies, both at Alder Hey and Liverpool Women's Hospital. The kind participation of the children and families involved in this study is so appreciated and I thank them for their contribution. The support of the Alder Hey PICU physiotherapy team and the Liverpool Women's midwifery team is also appreciated. I give heartfelt thanks to the ICH team, with particular recognition to members of the ABLE group, including Rachel Corkhill, Angela Hackett, Kate Phillips and Katie Rose. Thank you also to Moira Saphier, the true boss! I would like to thank my charitable funder, the Wellcome Trust: their generous Fellowship award has allowed me to carry out this research which has fostered a desire to continue in paediatric medical research.

I am so very thankful to my ever supportive friends who have listened to me (a lot!), laughed with me, run with me, made me countless cups of tea and who are always there for me. Thank you to God, I have completed this PhD through Him who gives me strength, and thank you for providing me with my church family at ACC. To my brother Richard, the first 'real' doctor of the family, thank you so much for your patience and invaluable thesis formatting support! Finally, to my family, I dedicate this thesis to you all. You have provided the support required for me to do all that I have done so far, and your love and encouragement carries me through.

Author's declaration

I declare that, except where explicit reference is made to the contribution of others, this thesis is the result of my own work. The material contained in this thesis has not been presented, nor is currently being presented, either wholly or in part for any other degree of qualification.

This research was carried out at Alder Hey Children's Hospital, the Institute of Child Health and the Institute of Integrative Biology, University of Liverpool.

Signature…….

Printed name……

Abbreviations

ADE	antibody dependant enhancement
ALRI	acute lower respiratory infection
APC	antigen presenting cell
AU	airy unit
BAL	bronchoalveolar lavage
CCA	chimpanzee coryzal agent
CGR	Centre for Genomic Research
CMV	cytomegalovirus
DC	dendritic cell
DDX58	DEAD(Asp-Glu-Ala-Asp) box polypeptide 58
DHX58	DEXH (Asp-Glu-X-His) box polypeptide 58
DICER1	double stranded RNA-specific endoribonuclease
DMEM	Dulbecco's modified eagle medium
DNA	deoxyribonucleic acid
DTT	dichlorodiphenyltrichloroethane
EBV	Epstein-Barr virus
ERS	European Respiratory Society
FCS	foetal calf serum
FDR	false discovery rate
FI-RSV	formalin inactivated RSV
FSC	forward scatter
GA	gestational age
GFP	green fluorescent protein
GM-CSF	granulocyte macrophage-colony stimulating factor
HMPV	human metapneumovirus
IFN	interferon
Ig	immunoglobulins
IL-1RA	IL-1 receptor antagonist
IPA	Ingenuity Pathway Analysis
IPS-1	interferon promoter-stimulating factor 1
IRF	interferon regulatory factor
ISG	interferon stimulated gene

LRTI	lower respiratory tract infection
LXA4	lipoxin A4
MAVS	mitochondrial antiviral signalling protein
MDA-5	melanoma differentiation associated gene 5
MDC	monodansylcadaverine
MHC	major histocompatability complex
MOI	multiplicity of infection
MPO	myeloperoxidase
MX1	myxovirus resistance 1
NETs	neutrophil extracellular traps
NFKB	nuclear factor-KB
NK cells	natural killer cells
NO	nitric oxide
NPA	nasophayngeal aspirate
P value	probability value
PAMPs	pathogen-associated molecular patterns
PBS	phosphate buffered saline
PCA	principal component analysis
pDC	plasmacytoid dentritic cell
PEV	primary endocytic vesicle
PFA	paraformaldehyde
PFU	plaque forming units
PI	propidium iodide
PICU	paediatric intensive care unit
PMNL	polymorphonuclear neutrophil leucocytes
PRR	pattern recognition receptor
PVDF	polyvinylidene difluoride
qPCR	quantitive polymerase chain reaction
REC	research ethics committee
RIG-I	retinoic acid-inducible gene I-like receptor
RIN	RNA integrity number
RNA	ribonucleic acid
ROS	reactive oxygen species

RSV	Respiratory Syncytial Virus
RT	real time
SDS	sodium dodecyl sulfate
SEM	standard of error
SSC	side scatter
ssRNA	single stranded RNA
STAT	signal transducer and activator of transcription
TBST	Tris-buffered saline and Tween 20
TGF	transforming growth factor
Th	T helper
TLR	toll like receptor
TNF	tumour necrosis factor
TRAIL	TNF-related apoptosis-inducing ligand
TRIM	tripartite motif-containing proteins
URTI	upper respiratory tract infection
USP18	ubiquitin specific peptidase 18
WHO	World Health Organisation
WNV	Western Nile virus

Chapter 1 General Introduction

1.1 Respiratory Syncytial Virus

Since its discovery in 1956, respiratory syncytial virus (RSV) has been recognised as a pathogen causing a significant burden of disease to the paediatric population. It is an important cause of severe respiratory illness in infants and young children and the leading cause of bronchiolitis. Despite increasing understanding of the immunology and pathology of the virus, the number of admissions to hospital continues to rise. In the UK, admissions coded as acute bronchiolitis increased from 21 330 in 2004/5 to 34 668 in 2012/13 (1).

RSV was first identified in chimpanzees with symptoms of an upper respiratory tract infection (2). It was initially named Chimpanzee Coryzal Agent (CCA). In 1957, a virus which was indistinguishable from CCA, was isolated from throat swabs from two separate infants by Chanock and Finberg (3). These three isolates were grouped and named respiratory syncytial virus because of the ability they showed in culture to cause epithelial cells to fuse forming syncytia.

1.1.1 Classification

RSV is an RNA virus of the *Paramyxoviridae* family. The *Paramyxoviridae* family is subdivided into *Paramyxovirinae* and *Pneumovirinae. The Pneumovirinae* family is split into the *Pneumovirus* and *Metapneumovirus* genus, with RSV belonging to the *Pneumovirus* genus. Avian pneumovirus and human metapneumovirus belong to the *Metapneumovirus* genus. RSV contains more genes/proteins than any other member of the *Paramyxoviridae* family.

1.1.2 Structure

RSV is a negative-sense, single-stranded RNA virus consisting of 15,191 base pairs. The genome is found encapsidated by the nucleocapsid N protein and has 10 genes encoding 11 proteins. The virus, which is 150-300nm in diameter, is enveloped in a lipid bilayer, and has 3 surface glycoproteins: the

large glycoprotein G, fusion protein F and small hydrophobic protein SH. These viral glycoproteins form separate homo-oligomers that appear as short surface spikes **(Figure 1-1).** RSV lacks neuraminidase or haemagglutinin activity.

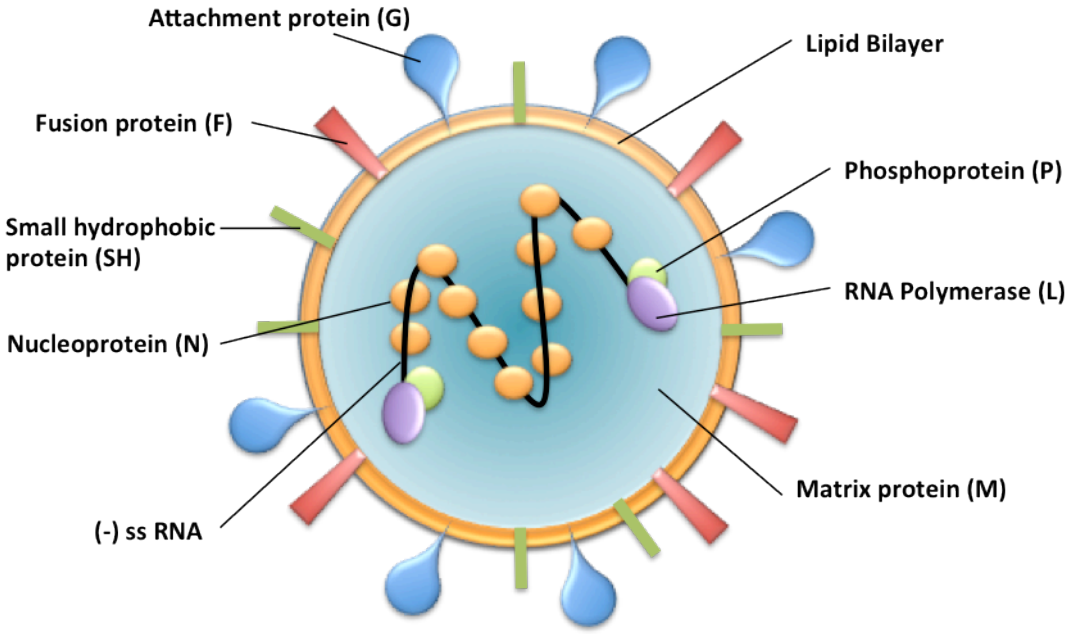

Figure 1-1 Schematic representation of an RSV virion identifying key proteins

The RSV virion is composed of a lipid bilayer which encapsulates the negative sense single stranded RNA. There are 3 surface glycoproteins, G, F, and SH. Inside the lipid bilayer is the matrix protein (M). The nucleocapsid is made up of 4 proteins, L, M, N and P.

Lipid envelope

The F protein, typical of a paramxyoviridae F protein, directs the fusion between the virus and the host plasma membrane. In addition, it is capable of attaching to neighbouring cells and promoting syncytia formation. The G protein is the major attachment protein, containing a single hydrophobic region. It is a type II transmembrane glycoprotein. The SH protein is a transmembrane protein which appears to be a viroporin, a small viral protein which can modify membrane permeability and affect budding (4). The non-glycosylated matrix protein M has a role in virus particle formation.

Ribonucleocapsid

The nucleocapsid, contained inside the lipid bilayer, is 12-15nm in diameter and made of 4 nucleocapsid proteins which replicate and transcribe the RSV genome, these are the nucleocapsid protein N, the phosphoprotein P, the anti-termination factor M2-1 and the large polymerase subunit L. M2 is the second matrix protein encoding both M2-1 (elongation factor) and M2-2 (transcription regulation)

Non-structural proteins

NS1 and NS2 are non-structural proteins that are unique to the *Pneumovirus* genus. These proteins act cooperatively to interfere with innate immune responses including interferon induction and signalling. They suppress the activation and nuclear translocation of the IFN-regulatory factor IRF-3 (5). NS1 and NS2 have also been shown to activate antiapoptotic genes of the host cell, thereby prolonging the life of the cell and increasing viral yield (6).

1.1.3 Viral replicative cycle

Attachment and viral entry are mediated by the G and F glycoproteins. Much of our understanding of RSV cell entry is inferred from our knowledge of other enveloped viruses. These can be grouped into two broad categories; those that require acidic pH for fusion and entry and those that fuse at neutral pH. The latter group include the paramyxovirus family, including RSV, which enter irrespective of drugs that inhibit acidification (7, 8). Entry to host cells therefore is presumed to be by plasma membrane fusion of the viral envelope and the cell plasma membrane (9). There is some evidence, discussed in detail in **Chapter 4**, that entry can occur by endocytosis, both clathrin-mediated and macropinocytosis (10, 11). Transcription and replication of the genome occurs in the cytoplasm. RSV mRNAs and proteins can be detected at 4–6 hours post infection of epithelial cells, reaching a peak by 15–20 hours (12). Progeny virus begins by 10–12 hours post infection, and continues until the cells die by 30–48 hours (13).

1.2 Respiratory Syncytial Virus bronchiolitis

Viral bronchiolitis occurs predominantly in infants under the age of one year and is the commonest reason for hospitalisation in this age group. Approximately 1 in 5 infants will develop bronchiolitis in their first year of life. RSV is the leading cause of bronchiolitis, resulting in up to 80% of cases.

1.2.1 Epidemiology

RSV is a common infection during infancy; virtually all children will be infected by the age of 2 years (14). Although the majority have a self-limiting, mild infection, 1-3% of all infants have disease severe enough to warrant admission to hospital (15-18). Most of these hospitalised children are previously healthy, although several groups of infants are predisposed to severe RSV infection; premature or extremely low birth weight infants, and those with chronic lung disease, congenital heart disease or immunodeficiency (19-21). Incomplete development of the airway and airway hyperreactivity may contribute to the increased risk of disease seen in preterm infants. Pulmonary hypertension and cyanosis are associated with worse outcome in those infants with pre-existent heart disease (22). RSV epidemics occur annually. In temperate climes this occurs during the winter season. In Liverpool, at Alder Hey Children's Hospital, peak RSV bronchiolitis is seen between November and January **(Figure 1-2)**.

1.2.2 Incidence

RSV is believed to be the most important acute lower respiratory infection (ALRI) causing viral pathogen worldwide. In 2010, a systematic review was carried out, funded by the World Health Organisation (WHO) and Bill and Melinda Gates Foundation, which included unpublished data and produced a global estimate of RSV burden of disease (23). They estimated the incidence of RSV-associated ALRI in under 5 year olds to be 33.8 (95% CI 19.3-46.2) million new episodes in 2005. Severe RSV requiring a hospital admission accounted for 3.4 (2.8-4.3) million of these episodes. It was estimated that 66 000 – 199 000 under 5 year olds died from RSV associated ALRI in 2005, 99% of these deaths occurring in developing countries. RSV has been a

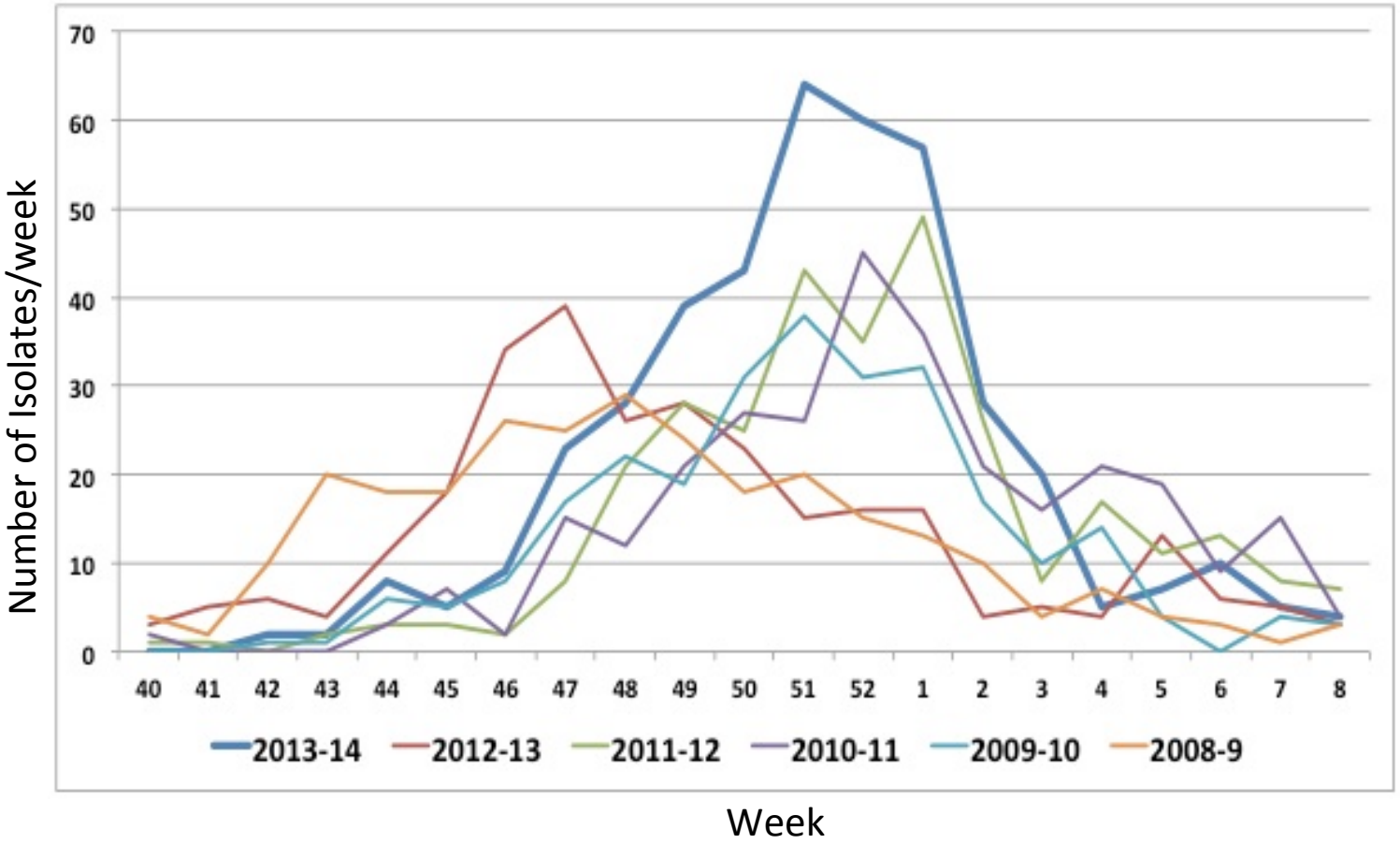

Figure 1-2 Number of RSV/week at Alder Hey Hospital

Line graph showing number of RSV isolates/week from 1st week of October to end of February during 2008-2014 at Alder Hey Children's Hospital, Liverpool

Image generated from data collated by the Microbiology department at Alder Hey Children's Hospital, Liverpool

priority for many national health organisations for over 20 years, with renewed attention in 2000 following the establishment of the Millennium Development Goals, which included reduction in child mortality (23). The WHO have also recognised the importance of vaccine development for RSV and their 'Product Development for Vaccines Advisory Committee' (PDVAC) have identified it as a priority area (24).

1.2.3 Spread of RSV

RSV is one of the most contagious human pathogens (25). It is spread by droplet and secretion transmission between individuals in close contact. The incubation period is between two to eight days. By two years of age, almost all children will have had an RSV infection at least once (26).

1.2.4 Clinical presentation

Initial symptoms are generally those of an upper respiratory tract infection with coryza, rhinitis and cough (27). A third of children develop otitis media (28). Symptoms can progress over 3-4 days to involvement of the bronchioles leading to dyspnoea, subcostal recession and poor feeding. When examined, chest auscultation may reveal wheeze and/or crackles. Infants younger than 6 weeks of age may present with apnoea and no other clinical signs. Bronchiolitis can lead to acute respiratory failure, characterised by hypoxia and carbon dioxide retention. The acute illness improves over 5-7 days but a persistent cough lasting for more than two weeks occurs in 50% of children (29).

1.2.5 Delayed respiratory sequelae of RSV bronchiolitis

In some children, a 'post bronchiolitis syndrome' occurs characterised by months of episodic wheeze, typically with other viral infections. Stein *et al* showed that RSV bronchiolitis carried the highest independent risk ratio for asthma (30). The Tucson study, a longitudinal study investigating development of asthma, revealed that RSV significantly increased the risk for wheezing in the first 10 years of life but that was no longer significant at 13 years of age (30). However, in 2007 Simoes *et al* offered the first evidence that RSV causes recurrent wheezing. A prospective, multicentre, double-

cohort, follow-up study in 27 centres recruited 421 pre-term infants, who either did or did not received prophylactic palivizumab. The recruits were followed up for two years, and an association between palivizumab prophylaxis and improved respiratory outcomes was statistically significant even after adjustment for confounding factors. The authors concluded that preventing RSV LRTI using palivizumab may reduce subsequent recurrent wheezing in pre-term infants (31). In 2013 Blanken et al showed that palivizumab treatment resulted in a significant reduction in wheezing during the first year of life, even after the end of treatment, thus implicating RSV as an important cause of recurrent wheeze during the first year of life in such infants.

1.2.6 Management

Supportive care is the mainstay of treatment. Children are admitted to hospital if they have apnoea, take less than 75% of usual feed volume, and/or have severe respiratory distress and/or hypoxia. Care is given in the form of hydration (nasogastric feeds or intravenous fluid), and/or supplemental oxygen for hypoxaemia. To date, no treatments for bronchiolitis have been shown to be efficacious, despite many being trialled, including antibiotics, hypertonic saline, adrenaline, salbutamol, montelukast, ipratropium bromide or systemic inhaled corticosteroids for bronchiolitis (32). However, there are a number of new promising anti-virals coming through (33). In particular, oral GS-5806, an oral RSV-entry inhibitor, has shown promising results in an RSV challenge model using healthy adults; reducing viral load and severity of clinical disease (34).

1.2.7 Prophylaxis

Palivizumab is a humanised monoclonal antibody ($IgG1_{1K}$) that is used to prevent RSV infection in high-risk infants. It is directed towards an epitope in the ‘A’ antigenic site on the F protein, the protein responsible for fusing the virus with the host cell (35, 36). The half-life of palivizumab is 18 – 21 days and therefore it must be given monthly to maintain protection over the winter months/RSV season (35). It is licensed in the UK only for certain high-risk

infants for whom RSV infection is likely to cause significant illness or death (37). These are:

- Preterm infants who have chronic lung disease (defined as oxygen dependency for at least 28 days from birth). Eligibility however, depends on their gestational age at birth and their corrected age at the start of the RSV season.
- Pre-term infants who have haemodynamically significant, acyanotic congenital heart disease.
- Infants < 24 months with severe combined immunodeficiency disorder.
- Infants on long term ventilation under certain conditions (38).

1.3 Innate immune response in RSV bronchiolitis

Inoculation of RSV into the nose or eyes results in virus entering the nasopharynx. Once within the respiratory tract, it can be trapped by mucus lining the airways. Over several days the virus can spread to the lower airways. The mechanism by which this occurs is not known but may be due to spread along the epithelium or through aspiration of the nasopharyngeal secretions. It is the ciliated cells of the small bronchioles and type 1 pneumocytes in the alveoli that are infected, with the basal cells being spared (39).

1.3.1 Viral recognition

Viral infection of epithelial cells leads to recognition of viral components within these cells by pattern recognition receptors (PRRs). RNA viruses are detected by two kinds of PRR; cytoplasmic recognition receptors such as retinoic acid-inducible gene I-like receptor (RIG-1), and Toll-like receptors (TLRs). RIG-1 is a highly inducible cytoplasmic RNA helicase that signals antiviral responses after binding dsRNA (40, 41). In contrast to TLRs, these receptors are cytoplasmic and can therefore recognise intracellular virus (42). TLRs are membrane bound receptors. In RSV infection, TLR 3 and TLR 4 are thought to mediate RSV signalling (43-45). This signalling takes the form of nuclear factor $_K$B (NF_KB) activation and cytokine secretion. TLR2 and TLR6 have also been implicated in the control of RSV replication, as well as in the production of inflammatory cytokines by leucocytes, and neutrophil

migration into the lungs (46). RSV can modulate changes in the expression of these TLRs, enhancing inflammatory responses, for example in epithelial cells an upregulation of TLR4 has been described (47). In addition, neutrophils from BAL of RSV infected pre-term infants express higher levels of TLR4 than healthy infants (48).

1.3.2 Inflammatory response

NF_KB is translocated to the nucleus upon activation of PRRs, leading to the production and secretion of cytokines and chemokines (illustrated below in **Figure 1-3** by airway epithelium infected with RSV). Of particular significance to viral infection are type I interferons (IFNs). Not only produced by epithelial cells, they are also produced by plasmacytoid dendritic cells (pDCs) and macrophages in response to TLR and RIG-1 activation by virus. Type I IFNs bind to cell surface receptors activating signalling pathways, promoting an anti-viral response. Downstream signalling molecules vary depending on the cell type but transcription of over 100 IFN stimulating genes (ISGs) lead to an anti-viral state. STAT1/STAT2 signalling is the best described of these pathways. As well as the production of these specific antiviral factors there is also expression of CXC and CC chemokines that stimulate the recruitment of a number of cells including neutrophils, natural killer (NK) cells, and dendritic cells (49). One of the first cells, alongside epithelial cells, to encounter RSV in the airways, is the macrophage.

1.3.3 Macrophages

Macrophages help to control viral infection through direct interaction with helper and cytotoxic T cells and also through the production of cytokines, in particular type I IFN (50). In response to RSV they secrete a host of cytokines, which in turn activate and recruit neutrophils, lymphocytes and NK cells to the site of infection. They destroy invading pathogens by phagocytosis and subsequently function as antigen presenting cells (APCs) by presenting protein on their cell membrane (51, 52).

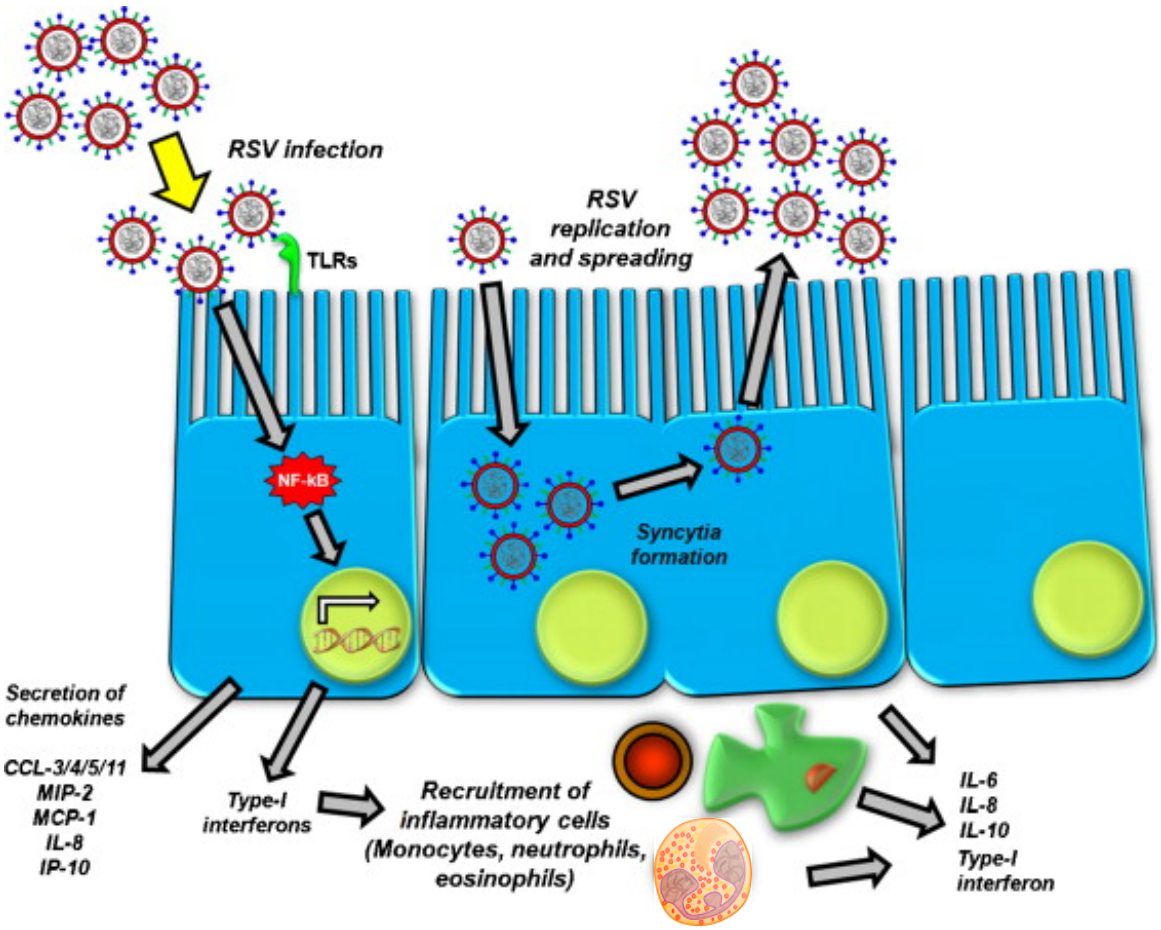

Figure 1-3 RSV infection modifies the inflammatory environment in the airways.

This image illustrates how RSV infection of the epithelium modifies the inflammatory environment of the airways. RSV infects the ciliated airway epithelial cells, and as a result the infected cells mount a defence mechanism. Activation of NFkB by RSV-derived molecular patterns precedes secretion of type I IFNs. Engagement of surface PRRs, such as TLR4, by RSV induces production of several chemokines and cytokines. These messengers trigger an influx of inflammatory cells, including neutrophils. In the meantime viral replication is ongoing inside the cells, spreading from cell to cell.

Adapted from Bueno *et al*. (2011) (54)

1.3.4 Neutrophils

Neutrophils intensify the cellular response through the production of further chemokines (53). Although these cells are numerically the major inflammatory cell within the airway in infants with RSV bronchiolitis, their specific role is largely undetermined (55). The function of these important cells is discussed in more detail in **Section 1.6**.

1.3.5 Natural Killer Cells

Work in mice has revealed that natural killer cells are present in the lung in the initial stages of infection and produce abundant quantities of IFN-γ, which appears to shape the subsequent T cell response (56). Virus infected cells are recognised by decreased MHC class 1 molecule expression.

1.3.6 Dendritic cells

Dendritic cells (DCs) link the innate to the adaptive immune response. From murine studies it has been shown that plasmacytoid DCs, thought to limit viral replication, are recruited early on in infection (57). In contrast myeloid DCs increase in number later in the infection and are matured by RSV, and subsequently activate naïve T cells (58).

1.4 Adaptive Response in RSV bronchiolitis

1.4.1 Humoral response

Only the two major RSV surface viral glycoproteins (F and G) induce antibodies that confer protection (59). Secretory IgA in the mucosa is important for local protection in the upper airway but its effect is short-lived. Serum-derived RSV antibody (mainly IgG) accesses the lower but not the upper airways relatively effectively; in the nasal mucosa access occurs via passive transudation (25, 60). During acute infection, IgM is present within a few days and lasts up to 1-2 weeks. IgG appears after a week, peaks after a month and declines thereafter. The protection resulting from serum antibody production following RSV infection is therefore short-lived (61).

Most term newborn babies have RSV neutralising antibodies due to placental transfer of maternal immunoglobulin. These antibodies appear to confer a degree of protection; correlation has been noted between low cord blood RSV antibody titres and severe RSV disease (27) and early RSV disease (62). In addition, prophylactic administration of RSV-neutralising antibody provides protection to high-risk infants (63, 64).

1.4.2 Cell-mediated immune response

Both $CD4^+$ T helper and CD8 cytotoxic T^+ cells are recruited to the lung in response to RSV infection and are believed to play a critical role in terminating acute RSV infection (65, 66). Humans with compromised T cell immunity shed virus for months, and in mice depletion of $CD4^+$ and CD8 T^+ cells also cause prolonged shedding (20). In mice, this T cell depletion despite causing prolonged viral replication, reduces pulmonary disease (65).

1.5 RSV pathogenesis

RSV infection is usually completely resolved by the innate and adaptive immune responses described above (67, 68). However, infection does result in widespread alteration in cellular gene expression, and upregulation of cytokines and chemokines as the body mounts its immune response. The combination of host immune response and viral factors are thought to be responsible for RSV induced pathology although their relative contributions are debated.

1.5.1 Infant and viral factors contributing to pathogenesis

RSV occurs more frequently and severely in younger children, with the peak for hospitalisation being 2 months of age. Rhinovirus, influenza, and human metapneumovirus commonly infect children less than 6 months of age (69). Rhinovirus in particular is associated with wheezing but in infants less than 6 months old, its incidence is much less than that of RSV (70). It is perhaps the unusual ability of RSV to evade maternal antibodies, which allows infection of very young infants. Due to the narrow diameter of these infants' bronchiolar airway lumens it has been suggested that they are more susceptible to mechanical obstruction and severe disease. In addition, these

infants are vulnerable due to the absence of previous exposure and consequent lack of immune memory. Reinfection is common, even within the same season (26). This is not unique to infants; the same is true for healthy adults and even more commonly in exposed adults such as health-care workers (68, 71). Reinfection of healthy individuals usually results in disease of reduced severity but this ability to re-infect ensures that RSV remains present within the population, at all ages.

Individual proteins within the RSV virion contribute to its pathogenicity. RSV subverts the antiviral IFN response through two IFN antagonists, NS1 and NS2 (72). They inhibit the induction of IFN-alpha/beta by blocking the activation of IFN regulatory factor 3 and by inhibiting type I IFN signalling through the JAK/STAT pathway (5). The JAK/STAT pathway would otherwise amplify the IFN response and upregulate IFN stimulated genes, resulting in the antiviral state described in **Section 1.3**.

RSV F and G surface proteins induce neutralising antibody production and are the major antigenic determinants of protection. The G protein differs from most other receptor binding proteins of the *Paramyxoviridae* family with respect to its structure and antigenic properties. For not fully elucidated reasons, the G protein requires multiple antibodies in order to be efficiently neutralised (73). It also influences epithelial and antigen presenting cell responses by down-regulating expression of inflammatory mediators through the inhibition of the NF-kB-pathway (74) (75).

There is increasing recognition that the magnitude of the viral load correlates with disease severity. Nasal viral loads are used in a number of studies as a surrogate for lower airway measurement, as the agreement of viral load between the two has been shown to be good (76). Higher viral load correlates with longer hospital stay, increased risk of intensive care and of mechanical ventilation (77, 78). In an adult RSV model, viral load, measured by RT-PCR has been shown to correlate with disease severity (79). The degree to which this is due to viral damage or an increased immune response is not elucidated.

1.5.2 Immune pathogenesis

Disease manifestation of RSV infection varies widely from upper respiratory tract infection (URTI), through to lower respiratory tract infection (LRTI), which can be mild or life threatening. Although the direct cytopathic effect of the virus and viral load likely contribute to these different manifestations, several observations lead us to believe that the host's own immunity plays a role in disease severity.

Histopathology of the lung from an infant with RSV who died in a car accident rather than as a result of infection, revealed significant numbers of immune cells, specifically T lymphocytes, monocytes and neutrophils (39). Inflammatory cells were noted in the submuscularis between the arterioles and bronchioles, but also identified moving through gaps in smooth muscle. This, the author's conjecture, could impact smooth muscle tone and affect airway hyperreactivity. The small airways were noted to contain inflammatory cells, fibrin and mucus, suggesting that mechanical obstruction of these airways plays a role in disease (39).

Murine studies have suggested that, in addition to clearing infection, T cells contribute to disease severity (66). A further mouse study suggested that the presence of alveolar lymphocytes correlated with disease severity, with a reduction in illness observed after ablation of $CD4^+$ or $CD8^+$ T cells despite ongoing RSV replication (65). There are opposing views in the literature regarding T cells in human infant disease. *Sanchez et al* report that T cells are not frequently observed in the airway or lung tissue of RSV infected infants (80). *Lukens et al* however report that there is a robust T cell activation and response in RSV (81). It is worth noting however that *Sanchez et al* used a group of infants with fatal bronchiolitis, a number of who had pre-existing medical conditions including Down's syndrome. Juxtaposed to host immunity causing the burden of pathogenesis is that RSV disease is more severe and occurs more frequently in immunocompromised individuals for example children with low T cell numbers have an increased risk of severe disease (82).

The failure of the formalin inactivated RSV (FI-RSV) vaccination in the 1960s provides further evidence of the potential for immune mediated pathogenesis. This vaccine, given to RSV naive infants, was not protective and primed for severe disease on infection with naturally occurring RSV infection. When this occurred, 80% required hospitalisation and two infants died. Histopathological analysis, supported by subsequent animal data, revealed that an atypical antibody response resulted in antigen-antibody complexes and complement activation in the lungs (83, 84). In addition, a Th2 biased response contributed to immunopathology with an overly robust response of virus-specific $CD4^+$ T lymphocytes (85). It is not clear however what relevance the pathogenesis of FI-RSV disease has to naturally occurring human disease as similar heightened responses do not occur.

There are an abundance of inflammatory cytokines and granulocytes in the airways of infants with severe RSV, with the neutrophil being the most abundant inflammatory cell, accounting for up to 84% of airway leucocytes (55, 86). This is much greater than that seen in influenza virus infection (87). There is a high airway concentration of predominantly epithelial derived CXCL8, a major neutrophil chemoattractant (49). In a study of the dynamics of neutrophil responses in infants admitted to the intensive care unit, the appearance of neutrophil precursors in the blood, preceding their influx into the lungs, closely followed the peak of virus shedding and was concurrent with clinical symptoms. Whether this represented a protective response or a contributor to the disease severity cannot be determined (81).

The magnitude of the neutrophil response to RSV infection, which appears greater than that for other viral infections, does lead one to deliberate what the role of the neutrophil is in RSV disease. Beyond the appreciation that they may contribute indirectly to viral clearance through their ability to phagocytose RSV infected and apoptotic cells, their contribution to the antiviral response within the airways has not been investigated. The extent to which RSV neutrophilia is protective versus pathogenic is unclear.

1.6 The Neutrophil

Paul Ehrlich in 1886 first described as ‘polynuclear cells’, the cells we now know as polymorphonuclear neutrophil leucocytes, PMNL, PMN or just neutrophils (88). When it was recognised that the neutrophil had in fact a single multi-lobed nucleus rather than a number of nuclei they were re-named to the present terminology (89). Initially there was misunderstanding as to the role of the neutrophil in inflammation, with the belief that the neutrophil spontaneously generated until Waller demonstrated that they originated from blood (90). Secondly it was thought that the presence of neutrophils, which were now known to produce pus, assisted the growth of microorganisms. However, Metchnikoff showed that neutrophils were capable of chemotaxis and could phagocytose. He argued that the presence of phagocytic cells were beneficial to mammals as a natural immunity against infection by microorganism (91). Other scientists in the field initially refuted Metchnikoff’s theory on the killing ability of neutrophils but in 1905 he was awarded a Nobel Prize for his findings. Previously considered to be short-lived, phagocytic cells, they are increasingly being found to have more complex and far-reaching functions. Their role as the first immune cell to respond to invasion by bacteria and fungi has been extensively demonstrated and, neutrophil depletion generally results in catastrophic consequences to whichever species is being studied. Neutrophils are recruited in large numbers to the site of many viral infections and although there is evidence that they play a role in anti-viral innate immunity, the evidence is limited and more investigation is warranted.

1.6.1 Structure

Neutrophils, 10-15μm in diameter (92), consist of 63% cytoplasm, 21% nucleus, 15.4% granules and 0.6% mitochondria (93) **(Figure 1-4)**. The cytoplasm contains primary (azurophilic) granules, secondary (specific) granules and tertiary granules, which contain enzymes and proteins **(Table 1-1).** Ingested pathogens are contained within phagosomes that then fuse with primary granules, termed lysosomes. The granules can also be released

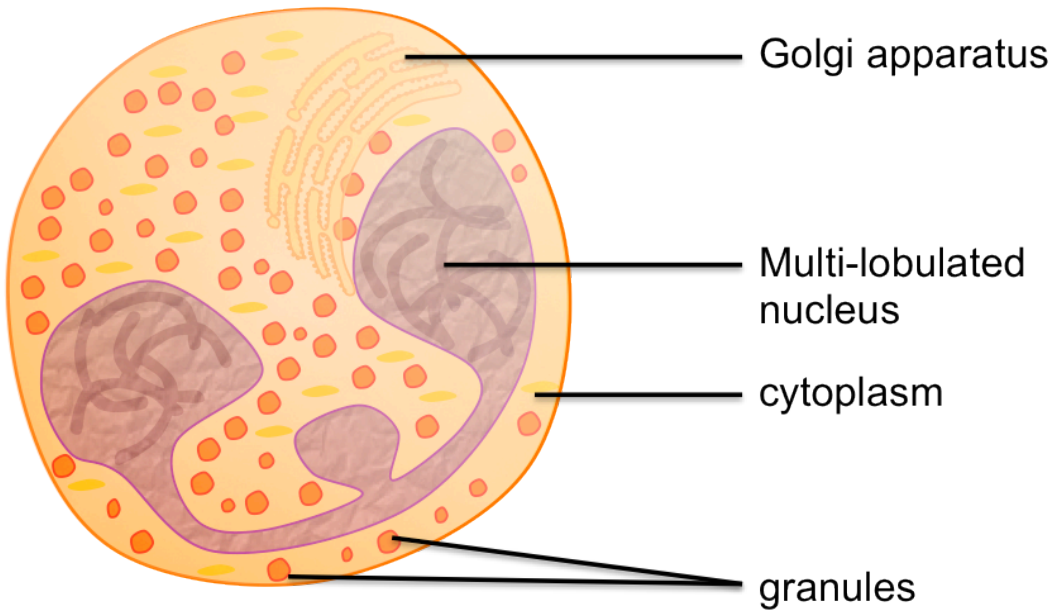

Figure 1-4 Neutrophil granulocyte

This is a schematic diagram of a neutrophil showing the component parts. The nucleus has a characteristic multi-lobed shaped. Within the cytoplasm is the small golgi apparatus, and multiple granules.

Granule type	**Content**
Azurophilic (primary)	myeloperoxidase, permeability-increasing protein, defensins, neutrophil elastase and cathepsin G
Specific (secondary)	alkaline phosphatase, lysozyme, NADPH oxidase, collagenase, lactoferrin, cathelicidin
Tertiary	cathepsin, gelatinase

Table 1-1 Neutrophil granule types and contents

The neutrophil contains about 200 granules of 3 different types; azurophilic, specific and tertiary.

extracellularly along with cytotoxic substances when activated through Fcγ receptors.

During the inflammatory response, the neutrophil functions in a variety of ways, with regulatory factors at every step. Their killing capability is three pronged, and comprises engulfment of the organism (phagocytosis), release of secretory granules containing reactive oxygen species (degranulation) and release of neutrophil extracellular traps (NETs) capable of trapping microorganisms and potentially killing them with the aid of attached antimicrobial peptides.

1.6.2 Pathogen destruction

That neutrophils are essential for an effective innate immune response, is evidenced by the life-threatening conditions associated with congenital abnormalities of neutrophil function (94). Their primary role is in their ability to act as phagocytic cells. The neutrophil senses chemotactic factors that are generated at the site of an infection via plasma membrane receptors on their surface. The neutrophil attaches to endothelium by means of binding to P-selectin and E-selectin via glycosylated ligands. These tethered neutrophils roll along the endothelium in the direction of blood flow (95). They squeeze through gaps between endothelial cells, a process called transmigration. This involves rearrangement of the neutrophil cytoskeleton. They then migrate up a chemoattractant gradient by chemotaxis towards the site of infection (96). The microorganisms by this stage may have been opsonised by serum proteins such as complement or immunoglobulin. The neutrophil will have upregulated surface expression of receptors required for phagocytosis. Thus primed, they will carry out phagocytosis, degranulation and activation of respiratory burst in order to kill the microorganism. Since 2004, the role of neutrophil extra-cellular traps (NETs) was recognised as part of the cells armoury against invading pathogens. A web of chromatin fibres and serine proteases are released, as the neutrophil's final act, to trap and kill microbes extracellularly (97). The neutrophil may augment the inflammatory response by production of neutrophil chemoattractants, drawing in additional neutrophils, and cytokines activating and recruiting other immune cells. The

principle role of the neutrophil is to destroy invading microorganisms and this it does most effectively as described above. The paradox however is that in order to do so it generates chemicals such as ROS and defensins, which not only destroy the invading organism but potentially also damage host tissue (98, 99). Thus to limit this damage, controlled cell death or apoptosis, is required (100).

1.6.3 Resolution of inflammation

Apoptosis is not the only way that the neutrophil contributes to the resolution of inflammation. Neutrophils also have anti-inflammatory capabilities through their ability to block and scavenge chemokines such as CCL3 and CCL5 (101), and produce anti-inflammatory cytokines such as IL-1 receptor antagonist (IL-1RA) and TGF-β1&2 (102). They can also produce pro-resolving lipid mediators such as lipoxin A4 (LXA4) that inhibit further neutrophil recruitment (103). Furthermore, they contribute to the biosynthesis of resolvins, which contribute to inhibit neutrophil transendothelial migration (103).

1.6.4 Neutrophil-derived cytokines

Chemokines, pro-inflammatory, anti-inflammatory, immunoregulatory, angiogenic and fibrogenic cytokines as well as ligands to the TNF superfamily are all expressed and produced by the neutrophil **(Figure 1-5)** (102). Neutrophils produce cytokines either constitutively or upon activation. There are a variety of neutrophil receptors, including colony-stimulating factor and cytokine receptors, G protein coupled-, FCy and complement receptors, and PRRs that trigger this activation. They express all TLRs except TLR-3 (104). Neutrophils control the expression and production of cytokines through regulation at different levels, including mRNA transcription, translation and protein secretion. For example, TNF-related apoptosis-inducing ligand (TRAIL), CXCL8, CCL20 and IL1- RA are synthesised but then stored in intracellular pools, requiring further stimulation by secretagogue-like molecules for rapid secretion (105).

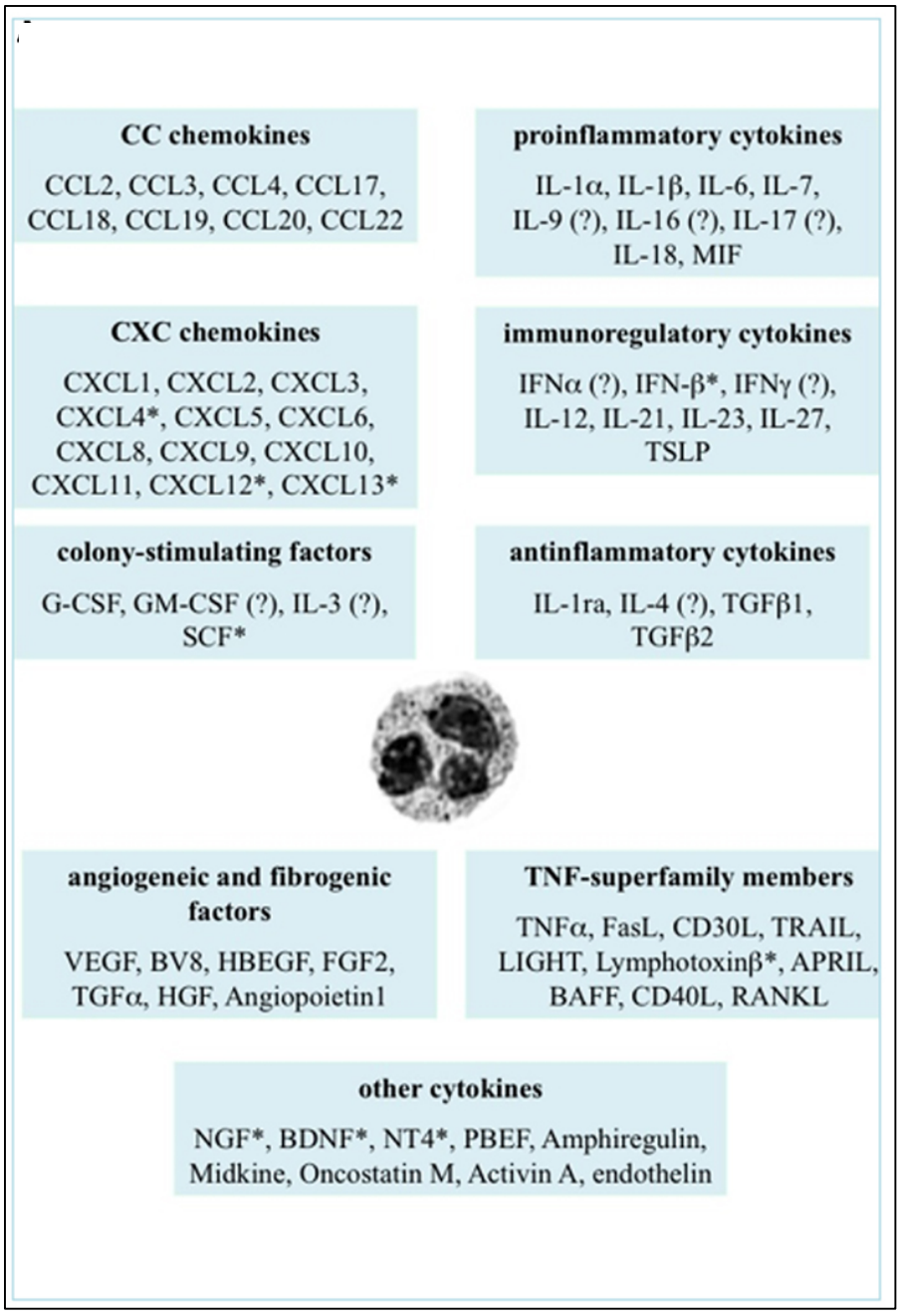

Figure 1-5 Cytokines expressed and/or produced by human neutrophils

This figure lists the cytokines that have been validated in human neutrophils through gene expression techniques, immunohistochemistry, enzyme-linked immune-adsorbent assays or biological assays. * refers to studies only performed at the mRNA level. ? refers to controversial data.

(Taken from Cassatella *et al,* 2014 (105))

1.6.5 Crosstalk with other immune cells

Through its ability to produce cytokines and chemokines, the neutrophil can recruit discrete cell populations as and when needed. Neutrophils produce chemotactic signals that recruit monocytes, dendritic cells, NK cells, and T-helper type 1 and type 17 cells (106). TNF-alpha is produced by neutrophils, which can drive DC and macrophage differentiation. This crosstalk is bi-directional with products from macrophages and DCs activating neutrophils as well. Cell to cell contact between CD11b on neutrophils and DC-SIGN (DC-specific ICAM3 grabbing non-integrin) on monocyte derived DCs induces maturation (107). Neutrophils are also a source of BAFF, a member of the TNF superfamily, which is needed for B cell function, maturation and survival (108). Neutrophils can also modulate NK cell survival, proliferation and IFNy production through the release of ROI and granule components (109). There is complex interplay between T cells and neutrophils, with effects on recruitment to inflamed sites and cell survival (102).

1.6.6 Neutrophils in viral infection

A number of factors support a role for phagocytes such as neutrophils in the early defence against viruses. It has long been known that viral infections can lead to a transient neutropenia (110) and this has been postulated to be due to cells being recruited *en masse* to the site of infection (55, 111). Through phagocytosis, virally infected cells and potentially individual virions, can be cleared (112). Neutrophils also produce a variety of mediators, including some that have anti-viral activities such as TNFα and TRAIL (105). More recent data reveals that the neutrophil can respond specifically to viral invasion and recognise potentially dangerous 'non-self' RNA and DNA, via intracellular sensor systems, such as RIG-1 (113). Cassetella *et al* have shown that RIG-1 and melanoma differentiation associated gene 5 (MDA-5) - mediated signal cascades occur in human neutrophils as evidenced by the expression of antiviral and immunomodulatory molecules in response to poly(I:C) transfection (114). That neutrophils possess RNA recognition receptors, such as RIG-1, MDA-5 and TLR-8, that are non-canonically expressed at the mRNA and protein level has since been shown (115).

1.7 Neutrophils and RSV

On the basis of the studies presented above, it would appear that neutrophils have a role at the frontline of antiviral immunity. What is known about their contribution in RSV infection? As referenced previously neutrophils are the predominant cell in the airways of infants with RSV bronchiolitis. Epithelial cells drive this migration through the production of neutrophil chemoattractants in response to RSV, particularly CXCL8 (53, 116-119). CXCL8 concentration is elevated in the bronchoalveolar lavage (BAL) fluid of severely infected infants and at levels higher than in other viral pulmonary infections such as adenovirus and rhinovirus (118, 120, 121). *In vitro* studies show that there is an initial CXCL8 peak two hours after RSV infection suggesting establishment of viral infection is not required for this early inflammatory response. A further peak is seen at 24 hours with a requirement for active viral replication at this later stage (122). There is evidence to suggest that CXCL8 correlates with disease severity, the NPA CXCL8 mRNA showing a strong dose response correlation (123). Neutrophils have been found to represent a median of 93% of cells in the upper airway, collected by nasopharyngeal aspiration, and between 76% and 84% in the lower airway, counted from BAL fluid (55, 86). There is some evidence, from *in vitro* studies, that RSV infection increases neutrophil adherence to epithelial cells, which is hypothesised to contribute to epithelial damage and detachment (124, 125). Most studies on the role of neutrophils in RSV disease have concentrated on the damage inflicted by the neutrophil (119, 126). There is one report, albeit published 30 years ago, which describes neutrophil mediated cytotoxicity against RSV. Human neutrophils were shown to mediate cytotoxicity, in the form of cell lysis, of RSV infected epithelial cells (HEP-2) measured by a chromium-51 release assay, in the presence of complement. Activation of complement by RSV-infected epithelial cells was observed only in the presence of neutrophils, not lymphocytes or monocytes (127).

One would expect, given their ability to cause damage, that depleting neutrophil numbers would reduce the pathogenesis of RSV disease. In a

murine model of RSV, a monoclonal antibody Ly6G was used effectively to deplete neutrophils in blood and lungs. Neutrophil depleted mice lost more weight and had increased lung damage evidenced by greater bronchiolar and alveolar oedema, alveolar haemorrhage, and vasculitis. There was no significant change in viral load but there was a reduction in mucin production and a change in cytokine expression, with a reduction in Th2 cytokines (128). This study, albeit in mice, would suggest that the neutrophil protects against lung damage and disease severity rather than causing it.

One further important study, discussed in more detail in **Chapter 3**, explored the *in vivo* interaction between RSV and neutrophils, and showed that RSV proteins and mRNA transcripts are present within blood and bronchoalveolar lavage neutrophils from infants with RSV disease (129). Although the majority of RSV replication occurs within the respiratory epithelium, these findings suggest that RSV replication may also occur within the neutrophil. Given that neutrophils are one of the first immune cells to encounter and interact with RSV in the lung, are numerously present, and have recently been demonstrated to contain viral sensors specific to RNA, this piece of work aiming to explore this interaction and characterise any antiviral mechanisms is warranted.

1.8 Aims of the study

The overall aim of this study is to explore the interaction between neutrophils and RSV. Specifically I aim to:

1. Establish an *in vitro* model of neutrophil-RSV interaction
2. Determine whether RSV is taken up into the neutrophil
3. Determine if RSV productively replicates inside the neutrophil
4. Compare neutrophil-RSV interaction in adult and infant neutrophils
5. Investigate the response of the neutrophil to RSV

Hypotheses relating to these specific aims are stated in the relevant chapters.

Chapter 2 Methods and optimisation of an *in vitro* model of neutrophil-RSV interaction

In order to realise the aims outlined in Chapter One, an *in vitro* model of RSV - neutrophil interaction needed to be established. **Sections 2.1 – 2.12** describe the materials, method and experiments undertaken to optimise this *in vitro* model. **Sections 2.13 – 2.17** describe the standard methods and materials used for subsequent chapters.

2.1 Participant recruitment

Three groups of participants were recruited; healthy adult controls for peripheral blood, ventilated RSV infected infants for BAL samples, and term infants delivered by caesarean section for cord blood. Ethical approval to obtain samples from these participants came from one pre-existing study and one new study as described below.

2.1.1 Mucin study

This on-going study was originally conceived to investigate inflammation and mucus production in the airways of children with a variety of respiratory conditions (REC reference mucin study 06/Q1502/142). For my experiments, I recruited infants who were ventilated for RSV bronchiolitis at Alder Hey Children's Hospital, Liverpool, UK during 2012/13, 2013/14, and 2014/15 seasons. Term and pre-term infants ventilated for RSV-positive bronchiolitis and less than one-year of age were eligible for enrolment. Infants who had congenital heart disease, genetic syndromes or immune dysfunction were not eligible. Demographic details including gestational age at birth, time since intubation, and weight were recorded. All parents received written information about the study **(Appendix 1)** and gave written informed consent prior to collection of data or clinical samples **(Appendix 2)**.

2.1.2 Cord blood study

This new study was set up to investigate the immune system in newborn babies, in particular the functional capacity of the neutrophil to RSV (REC

reference cord blood study 08/H1017/147). Research nurses gave written information about the study to pregnant women at elective caesarean section pre-assessment clinics at Liverpool Women's Hospital **(Appendix 3)**. Consent was taken to collect up to 60mls of cord blood from the placenta after delivery by elective caesarean section. Women were eligible if they were having a planned section for maternal reasons from 37/40 gestational age (GA). They were not eligible if there were any concerns regarding the baby's health. The control group consisted of healthy adult volunteers who gave informed consent for up to 40mls of peripheral blood to be collected. Adults were not eligible for inclusion if they had a chronic illness or were taking regular medication.

2.2 Blood neutrophil collection and processing

Neutrophils were initially isolated from whole blood using polymorphprep™ (Axis-Shield). Whole blood, taken directly into tubes containing 3.8% sodium citrate, an anti-coagulant, at a ratio of 1:9, was layered at 1:1 ratio over polymorphprep™. This was centrifuged at 1800rpm for 40 minutes, with the brake set to zero. Neutrophils were analysed by flow cytometry to establish the percentage of CD66c positive cells. CD66c is a granulocyte marker, which is highly expressed by neutrophils (130). Purity of the enriched neutrophil population was 61.3% **(Figure 2-1)**. The majority of the contaminating cells were red blood cells but of more concern was the potential for monocyte contamination. It has been shown that the presence of monocytes, even in small numbers, can alter the behaviour of neutrophils (131). To ensure that all responses observed were neutrophil specific, magnetic immunoselection was adopted as the neutrophil purification technique **(Figure 2-2)**. This method is described below and yielded 99.8% CD66c positive cells.

Antibody	Concentration	Host	Supplier
Anti- human CD66c PE (monoclonal)	0.125µg per sample	Mouse	ebioscience
IgG1 isotype PE (monoclonal)	0.125µg per sample	Mouse	Beckman Coulter

Table 2-1 Antibodies used for neutrophil identification

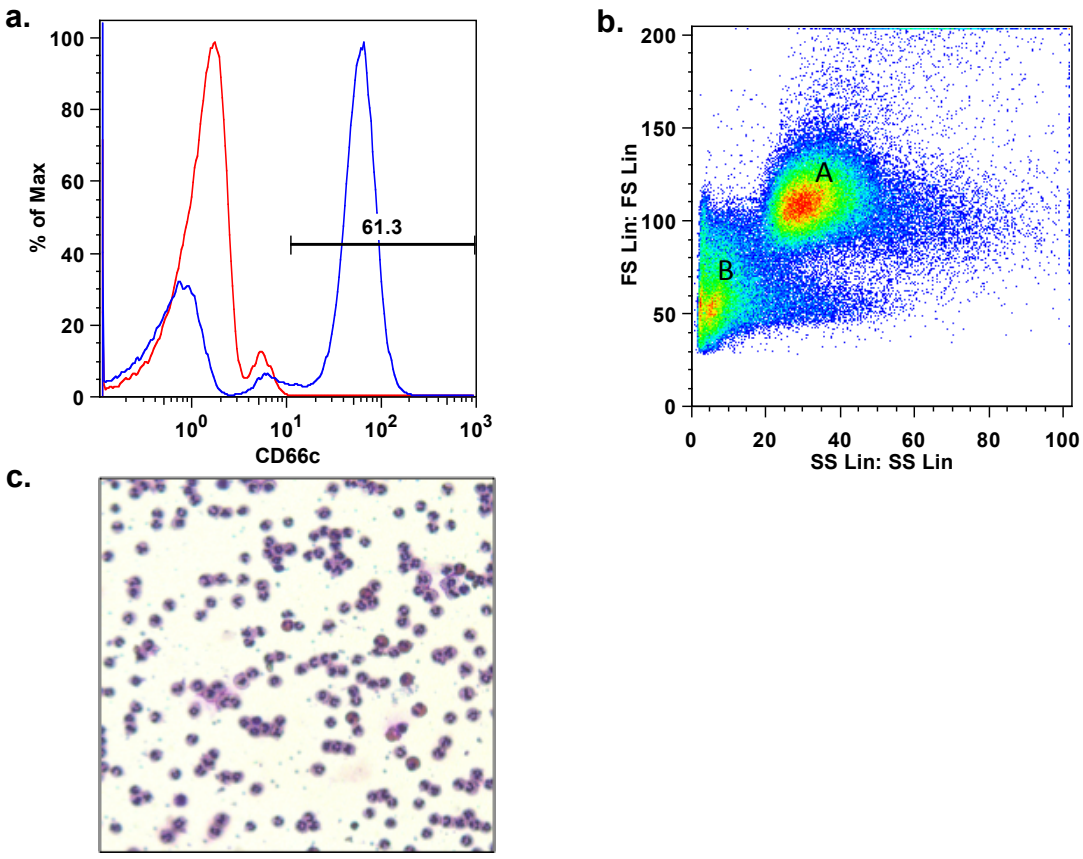

Figure 2-1 Neutrophil purity using polymorph preparation method

a) Histogram showing percentage of cells that are CD66c positive measured by flow cytometry. Neutrophils were isolated using the polymorph preparation method. Blue line = neutrophils labelled with a monoclonal antibody to CD66c conjugated to PE. Red line = matched isotype control. In this sample 61.3% of neutrophils expressed CD66c. b) Flow cytometry scatter plot demonstrating the neutrophil population (A) and contaminating cell population (B) on the basis of forward and sidelight scatter properties. c) Neutrophils were spun onto a slide, then stained using a Romanowsky staining protocol, before being imaged using a Leiss microscope. Cells were histologically identified as neutrophils by their multi-lobed nucleus and stain uptake pattern.

2.2.1 Negative immunoselection methodology

Antibody complexes and dextran-coated magnetic particles were used to isolate the neutrophils by removing unwanted cells from the cell suspension. The antibody complexes link targeted cell populations to the magnetic particles. Labelled cells are pulled to the sides of the tube when the sample is placed in the EasySep™ magnet. Magnetically labelled cells (the positive fraction) remain in the tube while untouched cells (the negative fraction) can be poured into a new tube. For neutrophil isolation, the tetrameric antibody complexes recognize CD2, CD3, CD9, CD19, CD36, CD56, glycophorin A and dextran coated magnetic particles.

2.2.2 Neutrophil ultra-purification by magnetic immunoselection

Neutrophils were isolated from the venous blood of healthy adult volunteers. Blood was taken directly into tubes containing 3.8% sodium citrate. Blood was centrifuged at 270g for 20 minutes at 18°c before plasma was aspirated from the top. Plasma was further centrifuged at 1155g for 10 minutes at 18°C to make platelet poor plasma (PPP). To the cell pellet, 6 ml of 6% dextran was added and total volume made up to 50ml with warmed 0.9% sodium chloride. After 25 minutes, the upper layer, which is red cell depleted following dextran sedimentation, was removed and cells pelleted by centrifugation at 185g for 6 minutes. Neutrophils were separated by discontinuous plasma:Percoll gradient centrifugation, pelleted at 420g for 6 minutes and resuspended in RoboSep™ buffer (Stemcell™ Technologies).

Ultra-purification of neutrophils was performed using negative immunoselection. Resuspended neutrophils were mixed with EasySep™ Human Neutrophil Enrichment Cocktail (Stemcell™ Technologies) at 50ul/ml cells, mixed well and incubated at room temperature for 10 minutes. EasySep™ Nanoparticles (Stemcell™ Technologies) were then vigorously pipetted before addition of 100ul/ml cells. After mixing well they were incubated at room temperature for 10 minutes. The whole suspension was then made up to a total volume of 2.5ml by the addition of RoboSep™ buffer before being thoroughly mixed and placed into the EasySep™ magnet for 5 minutes. The desired fraction was poured off by inverting the magnet and

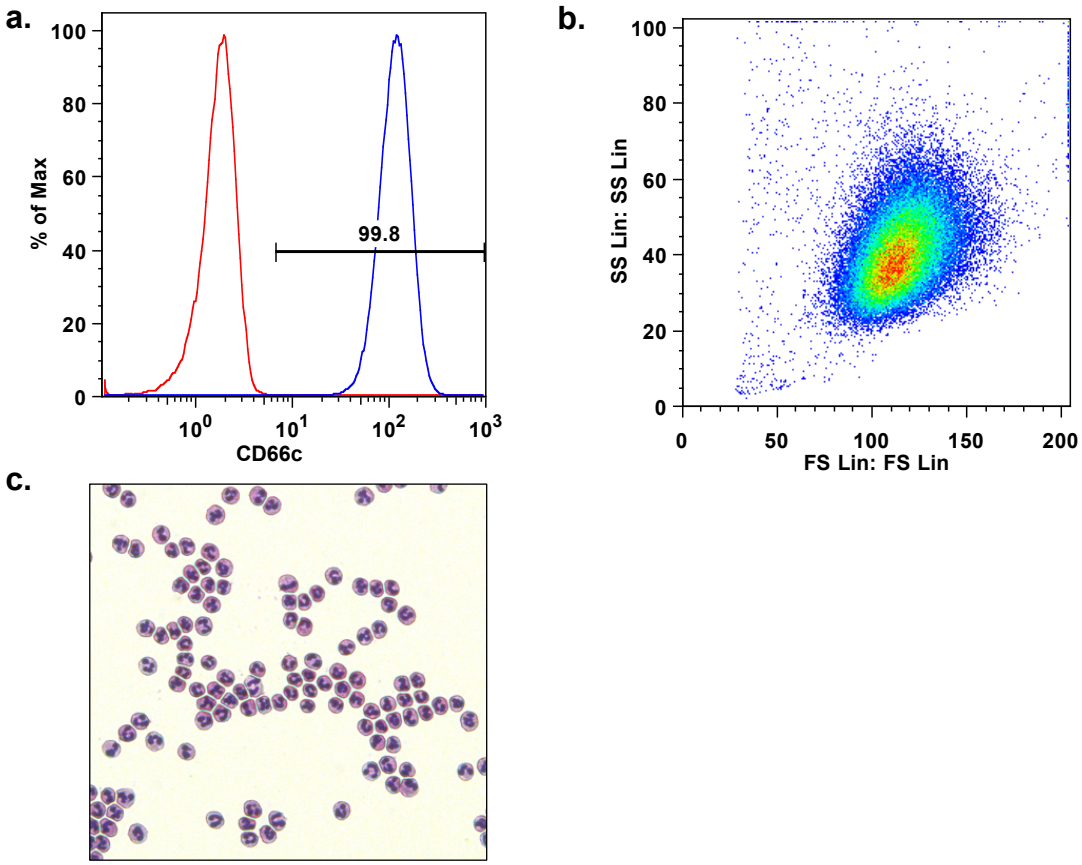

Figure 2-2 Neutrophil purity using negative immunoselection method

a) Histogram showing percentage of cells that are CD66c positive measured by flow cytometry. Blue line = neutrophils labelled with a monoclonal antibody to CD66c conjugated to PE. Red line = matched isotype control. Following negative immunoselection where antibody complexes link to CD2, CD3, CD9, CD19, CD36, CD56 and glycophorin A and bind to magnetic particles leaving a pure preparation of neutrophils, 99.8% of neutrophils expressed CD66c. b) Flow cytometry scatter plot demonstrating the one cell population on the basis of forward and sidelight scatter properties. c) Neutrophils were spun onto a slide then stained using a Romanowsky staining protocol, before being imaged using a Leiss microscope. Cells were histologically identified as neutrophils by their multi-lobed nucleus and stain uptake pattern.

tube into a new tube, which was then placed into the magnet for a further 5 minutes. This was repeated once, leaving the negatively selected enriched cells in the new tube ready for use.

2.3 Romanowsky staining technique

Cells were spun onto slides using a cytospin and air-dried. Rapid Romanowsky Stain (HD Supplies) was used. 25 mls of each solution (A - fixative solution containing thiazine dye in methanol, B - Eosin Y in phosphate buffer, and C - Methylene blue in phosphate buffer) were placed in sequentially positioned Coplin jars. Slides were placed in solution A for 30 seconds, then solution B for 30 seconds and finally solution C for 30 seconds, with no rinsing between each immersion. Slides were washed gently in running water before being allowed to air dry for 5 minutes. Slides were then examined by Leica microscope (40x/0.5 objective) and images recorded using Leica IM50 Image Manager. Leukocytes show excellent nuclear and cytoplasmic staining. Immature granulocytes show bright azurophilic granules. Erythrocytes are orange-red.

2.4 Neutrophil culture

Neutrophils were counted using a manual haemocytometer and suspended at 5 million/ml in Dulbecco's Modified Eagle Medium (DMEM) in 10ml falcons for experiments. If serum was required this was either 5% autologous serum, or 5% AB serum. Neutrophils were incubated at 37^{o}C/5% CO_2.

2.5 RSV preparation

30 000 Hep2 Cells/cm^2 in a volume of 30ml were seeded into a T175 cm^2 flask and left to grow to approximately 50% confluence overnight at 37^{o}C/5% CO_2 in DMEM and 10% foetal calf serum (FCS). Medium was removed from the flask and cells washed twice with PBS. 1 vial of RSV (MOI 1) and 8mL of serum free medium were added to the flask which was left to rock gently at 37°C for 2hrs. After 2hrs, 22mL of DMEM containing 2% FCS was added and cells incubated for 24 hours at 37^{o}C/5% CO_2. Media was replaced after 24 hours with DMEM with 10% FCS. Cells were harvested at the first sign of cytopathic effects such as dead cells floating; this usually occurred 48 hours

following infection. At this time, all but 4mls of media was removed. The cells were scraped from the bottom of the flask using a cell scraper and placed in a universal container on ice before being passed through a 25 gauge needle 10 times. Cells were then spun down at 4^{o}C at 1500rpm for 5 minutes. The supernatant was quickly transferred in 500ul aliquots into pre-labelled cyrovials before being snap frozen in liquid nitrogen and placed in the -80 ^{o}C freezer for storage. As RSV is most stable when within cells and unbound virus degrades rapidly, work was carried out quickly when thawing and freezing down virus containing cryovials. For thawing, the cryovial was agitated in a water bath set to 37°C. When the pellet was almost completely thawed it was opened in a tissue culture or lamina flow hood and gently pipetted up and down to thaw remaining virus and used as quickly as possible. The RSV preparation used in the majority of the experiments was a gift from Dr. Paul Fitch (University of Edinburgh). This was 50 vials from 1 batch of propagated RSV A2 strain (PFU 1.79x10^{6}).

2.6 Plaque assay

A plaque assay was used to quantify the amount of virus propagated. Hep2 cells were seeded into a 96 well plate in DMEM containing 10% FCS for 24 hours. A doubling dilution was made of virus stock staring at 1/100 and producing 8 dilutions in serum free DMEM. The Hep2 cells were washed with PBS and 50ul of virus was added to each well, with each dilution plated in triplicate and a virus free control included. After 2 hours at 37^{o}C/5% $CO_{2,}$ 150ul of DMEM with 10% FCS was added and the cells cultured overnight. After this time the cell were washed with PBS (100ul/well) and fixed for 20 minutes at room temperature with 100% methanol containing 2% hydrogen peroxide. The cells were washed with PBS before 100ul of biotinylated anti-RSV antibody (1/200 dilution with PBS/1%BSA) per well was added for 1 hour at room temperature. The wells were then washed twice with PBS/1% BSA and 100ul of extravidin peroxidase (1/500 dilution in PBS) was added for 30 minutes at room temperature. After 2 washes, with PBS/1%BSA, 50ul of 3 amino-ethylcarbazole substrate was added per well, for up to 40 minutes. When plaques appeared the reaction was stopped using a PBS wash. The plaques in wells that appeared to have around 100 were counted,

as were all replicates of that dilution. The numbers of plaques in the wells in the 2 dilutions below were also counted. Plaque forming units (PFU) for each virus batch were then calculated using the formula:

Number of plaques x dilution x 20 = PFU/ml

2.7 Phagocytosis assay

For this assay pHrodo™ E. coli BioParticles® Phagocytosis Kit for Flow Cytometry (Invitrogen) was used. Assays were carried out according to the manufacturer's protocol except that 100ul of neutrophil preparation was used rather than whole blood. Lyophilized pHrodo E. coli BioParticles® Conjugate was stored in the freezer. When required, 2ml uptake buffer (HBSS + 20mM HEPES, pH 7.4 (NaOH added if necessary)) was placed into the vial containing the 2mg lyophilized product and vortexed to resuspend. Neutrophils were suspended at 5 million/ml in DMEM. 50ul of pHrodo was added to each tube, except the control. When required, 10-20% autologous serum was added. Cells were left to incubate at 37^{o}C/5% $CO_{2,}$ except for the ice control sample. At 15, 30, 60, 90, 120, 150 and 180 minutes, samples from each tube were collected, washed twice and then analysed by flow cytometry. Neutrophils that have phagocytosed bacteria emit fluorescence in the FL3 channel **(Figure 2-3a)**. Neutrophils that have been incubated with pHrodo E. coli on ice were used as a negative control.

This technique was used to quantitatively assess the phagocytic activity of the isolated neutrophils and to ascertain the percentage of autologous serum needed to enhance phagocytosis.

2.7.1 Isolated neutrophils are capable of phagocytosis

The number of neutrophils that had phagocytosed bacteria increased with time up to 120 minutes and then plateaued **(Figure 2-3c)**. Neutrophils are thought to be able to recognise and internalise targets within minutes of exposure. However, the conditions within the phagosome which trigger the fluorescence of the E. coli pH sensitive label, takes one to several hours

(132). Phagocytosis plateaus at 2 hours as the maximal capacity of the neutrophil is reached.

2.7.2 Autologous serum enhances neutrophil phagocytosis

Neutrophils incubated with pHrodo E. coli for 2 hours were analysed by flow cytometry and percentage phagocytosis measured by percentage of neutrophils that were FL3 +ve. Comparison was made between incubations carried out with no serum, and in the presence of 10 and 20% autologous serum **(Figure 2-4).** Phagocytosis increased significantly in the presence of both 10% serum, from 62.72% (+/- 0.88) to 85.60% (+/- 3.06) $p<0.0001$ and 20% serum, to 86.85% (+/- 3.10) $p = 0.0001$. One-way ANOVA was performed with Bonferroni's post hoc test to allow for multiple testing.

That serum enhances phagocytosis is an anticipated result, as serum contains complement and immunoglobulin, capable of opsonising the target microorganism and amplifying phagocytosis. Increasing the quantity of serum beyond 10% did not further improve uptake, most likely due to all E. coli targets being quenched by immunoglobulin and complement with this quantity of serum.

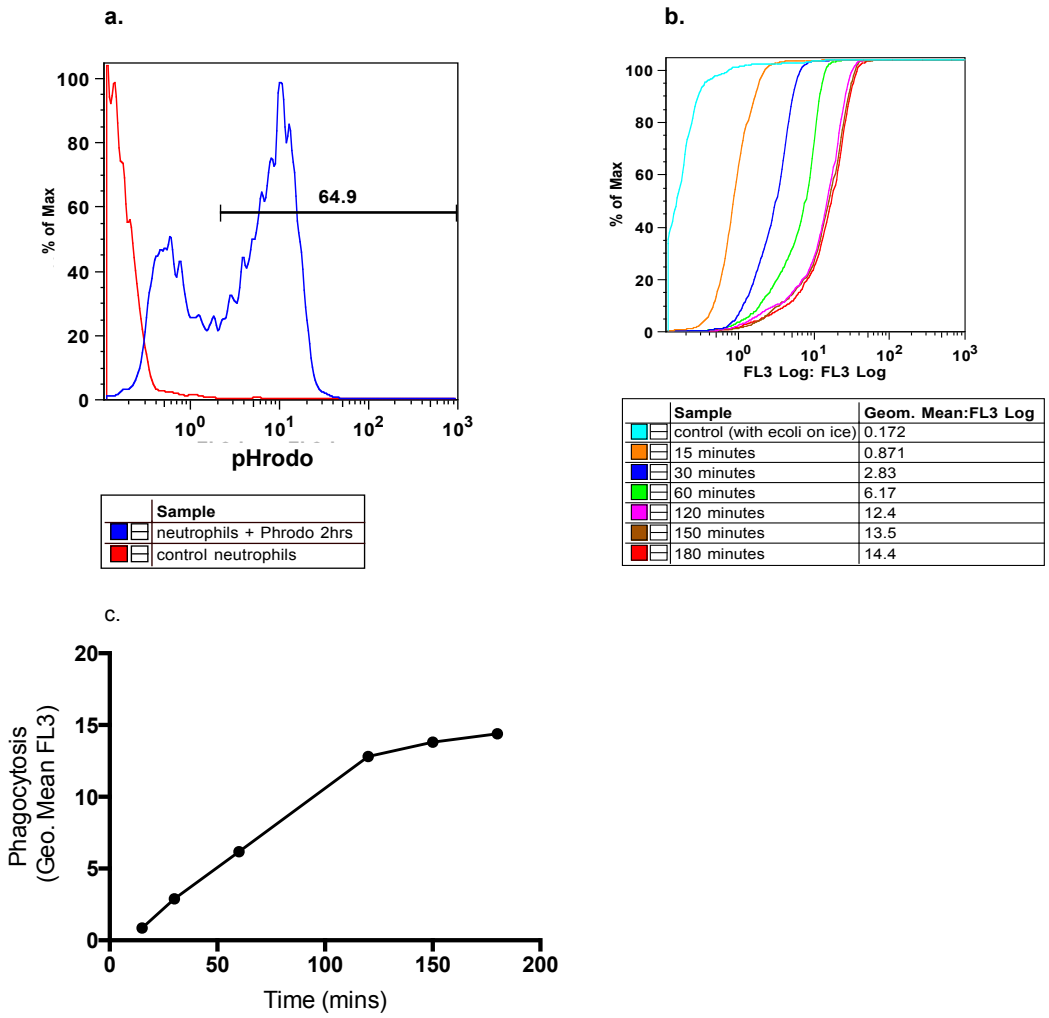

Figure 2-3 Neutrophil phagocytosis using pHrodo E. coli

Neutrophils were incubated with pHrodo labelled E. coli particles. Samples were taken at a range of time points and analysed by flow cytometry. Using mean fluorescent index FL3 for the neutrophil population, a time course was constructed. a) Representative flow cytometry histogram plot showing the fluorescence in FL3 channel of neutrophils and E. coli on ice (as a control) and neutrophil + E. coli at 37°C. 1. b) Time course of pHrodo E. coli phagocytosis, the geometric mean of FL3 is plotted for each time. c) Time course of pHrodo E. coli showing increasing phagocytosis until 2 hours when the increase plateaus.

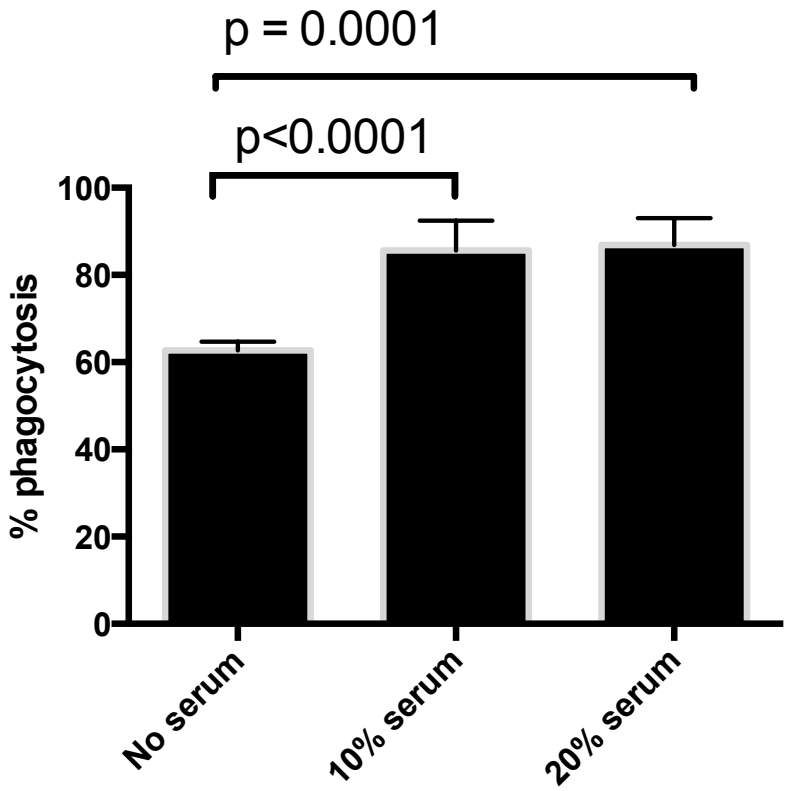

Figure 2-4 Autologous serum enhances neutrophil phagocytosis of pHrodo

Neutrophils incubated with pHrodo E. coli for 2 hours were analysed by flow cytometry. The percentage of FL3 +ve neutrophils was used as a surrogate measure for the percentage of neutrophils exhibiting phagocytosis. Neutrophil incubation was carried out in the presence of no serum, 10% or 20% autologous serum. A statistically significant increase in phagocytosis was observed in the presence of 10 and 20% serum. (4 independent experiments/ n=4)

2.8 Flow cytometer analysis and set-up

All flow cytometer analysis was performed using a Beckman Coulter Cytomis FC 500MPL flow cytometer equipped with a 488 nm argon-ion laser. To analyse samples, two dot plots were set up, one showing forward scatter (FSC) vs. side scatter (SSC), and another showing a histogram of cell count against fluorescence. A negative control was always applied first. In the pHrodo phagocytosis experiment, this consisted of neutrophils with no pHrodo™ BioParticles® conjugate that have been through the whole methodological procedure. Linear FSC and SSC voltages were set to locate the neutrophil scatter pattern. All flow data was analysed using FlowJo 9.4.11.

2.9 Annexin V/PI apoptosis assay

Annexin V FITC apoptosis detection kit (Sigma) was used to carry out this assay. Cells were suspended in 300ul Annexin binding buffer with 3ul of Annexin V for 15 minutes in the dark at room temperature. They were then flash stained with propidium iodide (PI), 10ul in 900ul of Annexin binding buffer and analysed on the flow cytometer. 10,000 events were collected. Early apoptosis is identified by Annexin V positivity and cell death by PI staining **(Figure 2-5)**.

2.10 Neutrophil survival

2.10.1 Neutrophil survival can be extended *in vitro* by GM-CSF

Flow cytometry Annexin V/PI analysis was used to assess the percentage of viable neutrophils at time points up to 20 hours in the presence or absence of 5ng/ml human recombinant GM-CSF (Peprotech). In the absence of GM-CSF, mean (SEM) neutrophil survival was 98.87% (+/- 0.296), 88.97% (+/- 6.470), 76.27% (+/- 8.03), 42.83% (+/- 15.04) at 0, 2, 4 and 20 hours respectively **(Figure 2-6)**. There was a significant decrease in cell viability at 4 hours ($p=0.0216$) and 20 hours (<0.0001) when compared to 0 hours.

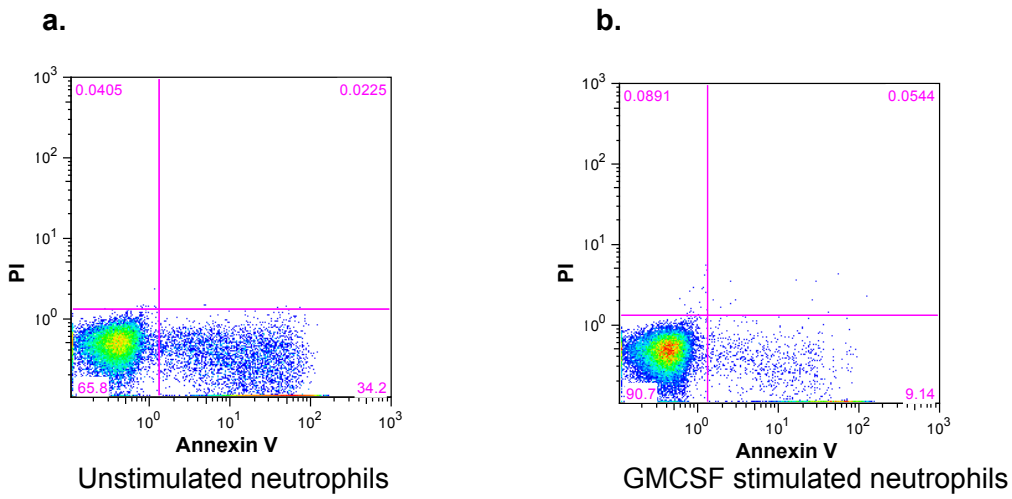

Figure 2-5 Illustration of flow cytometric analysis of Annexin V/PI apoptosis assay

At appropriate time points, samples were stained with Annexin V (marker of apoptosis (FL1)) and propidium iodide (PI - marker of necrosis (FL3)), and analysed by flow cytometry. a) Scatter plot shows neutrophils stained for Annexin V/PI. 85.8% of cells are viable (Annexin V -ve/PI -ve, *Q1*), 34.2% are apoptotic (Annexin V +ve/PI -ve *Q2*), and 0% are apoptotic and necrotic (Annexin V +ve/PI +ve, *Q3*). b) Scatter plot shows neutrophils stained for Annexin V and PI, and exposed to GM-CSF. 90.7% cells are viable (*Q1*), 9.14% cells are apoptotic (*Q2*) and 0% cells are apoptotic and necrotic (*Q3*).

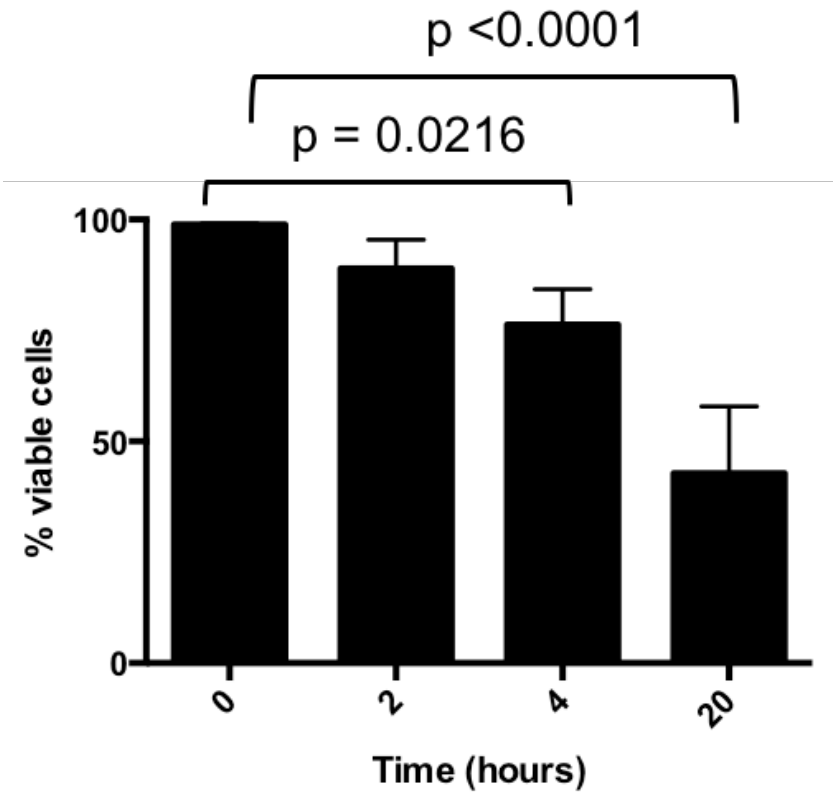

Figure 2-6 Neutrophil survival time course

Bar chart showing percentage of viable neutrophils at 0, 2, 4 and 20 hours. There was a significant decrease in cell viability at 4 hours (p=0.0216) and 20 hours (<0.0001) when compared to 0 hours. (3 independent experiments/ n=3)

With the addition of GM-CSF cell viability increased to 97.20% (+/- 0.635), 93.47% (+/- 3.45), 95.00% (+/- 1.44) and 75.47% (+/- 5.28) at 0, 2, 4 and 20 hours. Cell viability was still significantly decreased at 20 hours (p=0.0059) but there was significantly improved cell survival when compared to untreated neutrophils (p=0.0458) **(Figure 2-7)**. A two-way ANOVA with Bonferroni's post hoc test was used to allow for multiple testing.

2.10.2 The effect of RSV on neutrophil survival

Highly purified neutrophils were incubated with RSV (MOI 0.1) preparation for 0, 2, 4 and 20 hours without GM-CSF. At these time points neutrophil viability, with and without RSV exposure was measured by flow cytometry. Mean (SEM) survival of neutrophils exposed to RSV was 97.10% (+/-2.201), 96.23% (+/-1.619), 94.67% (+/-1.656) and 78.07% (+/-3.896) at 0, 2, 4 and 20 hours respectively. The percentage of viable neutrophils was significantly higher at 20 hours when compared to RSV unexposed cells (p value =0.007) **(Figure 2-8)**.

2.11 *In vitro* neutrophil-RSV culture system

An *in vitro* Neutrophil-RSV culture system was established by combining the various optimised methods and techniques described above in **Sections 2.2 - Section 2.11**. This system is illustrated schematically **(Figure 2-9)**.

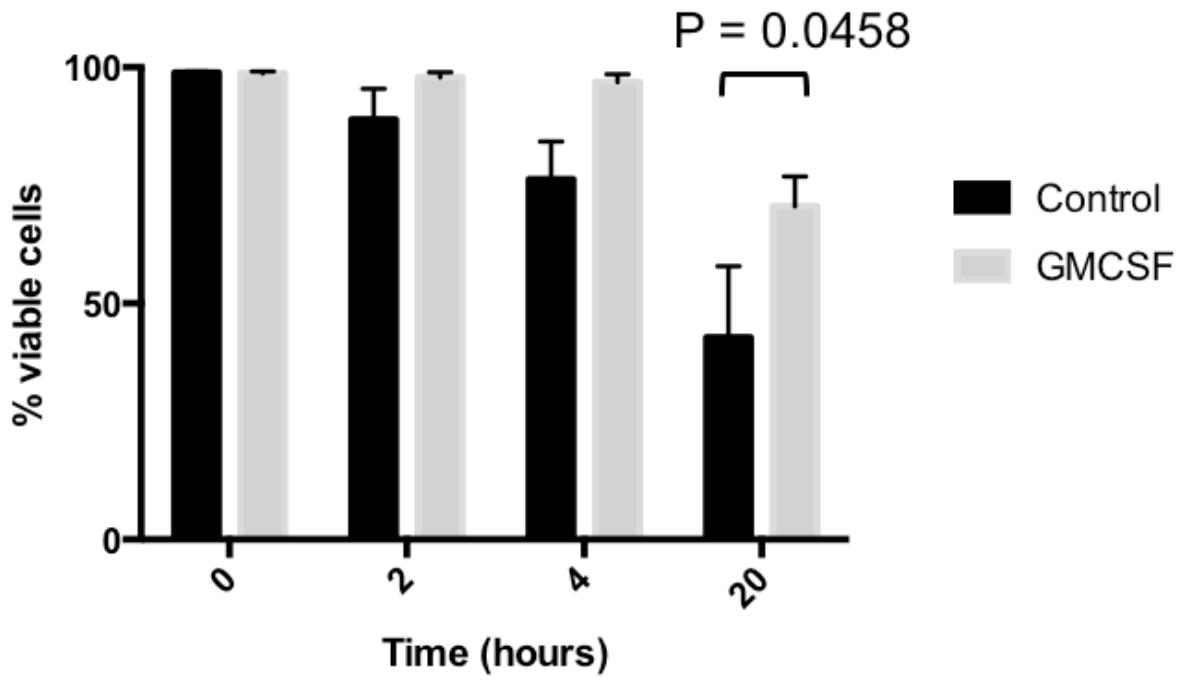

Figure 2-7 Neutrophil survival can be extended *in vitro* by GM-CSF

Grouped bar chart showing survival of GM-CSF treated and untreated cells at 0, 2, 4 and 20 hours. With GM-CSF no significant apoptosis was observed until the neutrophils were 20 hours old, at which point, survival was significantly better than for untreated cells ($p = 0.0458$) (3 independent experiments/ n=3)

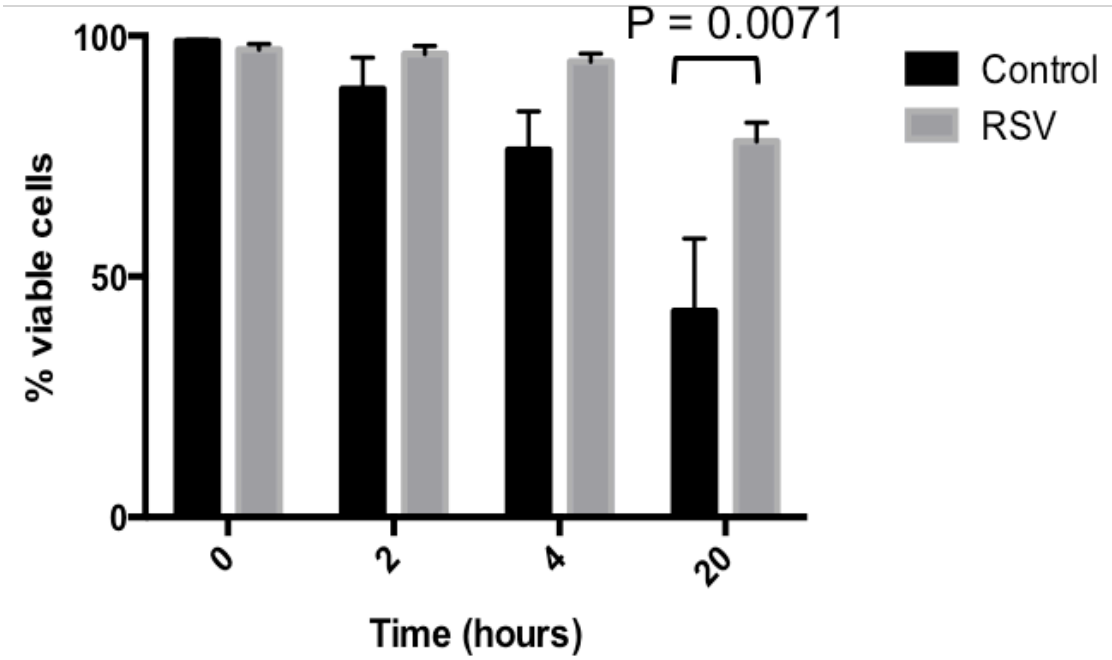

Figure 2-8 Neutrophil survival is affected *in vitro* by RSV

Grouped bar chart showing neutrophil survival +/- RSV at 0, 2, 4, and 20 hours. Neutrophil survival was extended *in vitro* by RSV. There was no significant apoptosis measured until 20 hours, and survival was statistically better at 20 hours than untreated cells (p value =0.007). (3 independent experiments/ n=3)

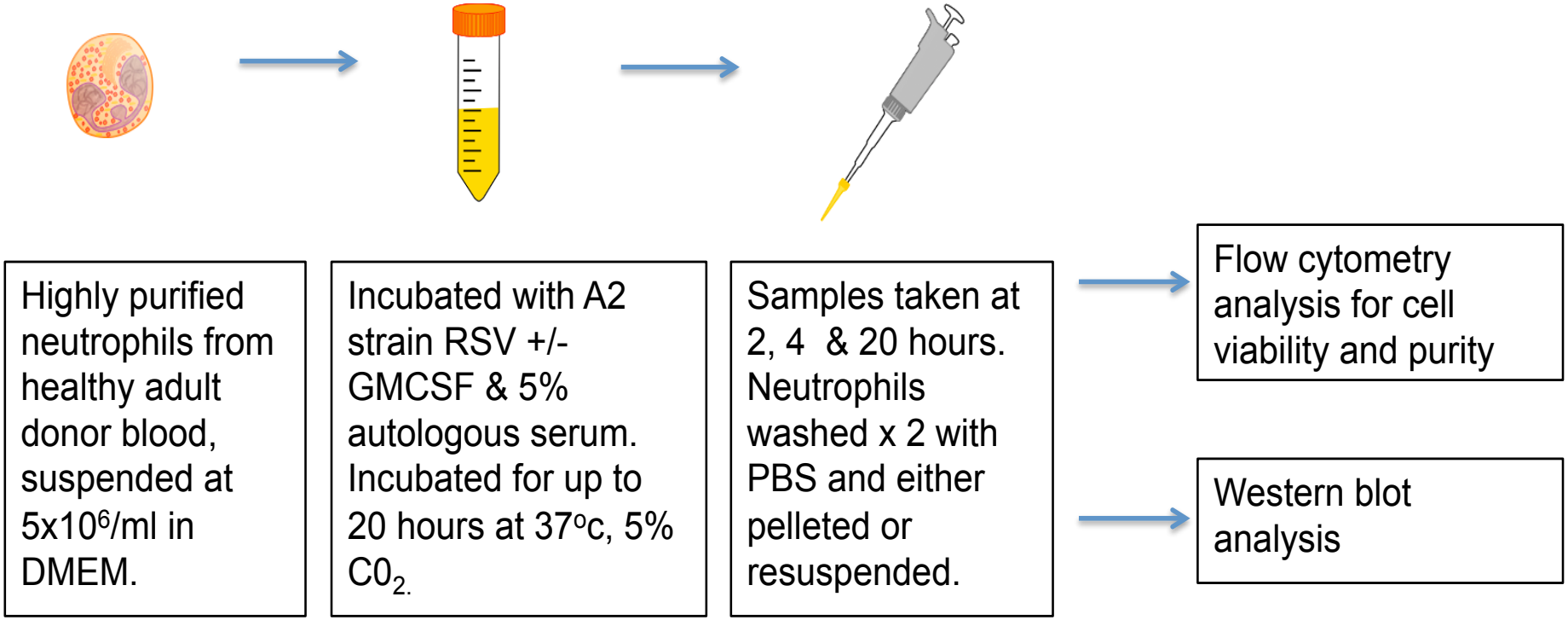

Figure 2-9 *In vitro* culture system for neutrophil-RSV infection

Highly purified neutrophils were isolated by negative immunoselection from healthy adult donor blood. Cells were suspended in DMEM at $5x10^6$/ml with the addition of 5% autologous serum. If GM-CSF was used this was added at a concentration of 5ng/ml. A2 strain RSV (MOI 0.1) was rapidly thawed and added to the neutrophils. If no RSV was added the equivalent volume of DMEM was added to the control tubes. Neutrophils were incubated at 37°C, 5% $C0_2$ for up to 20 hours. At each time point the neutrophils were washed in PBS twice before either being resuspended for flow cytometric analysis or pelleted for Western blot analysis.

2.12 Western blotting

Western blotting was used to identify RSV proteins, firstly from infected epithelial cells and then from RSV exposed neutrophils. The primary and secondary antibodies used in western blotting analysis are listed in **Table 2-2** and **Table 2-3**.

2.12.1 Principle of western blotting

Western blotting is a widely used analytical technique for the study of proteins. It allows the detection of a single protein within a mixture of proteins derived from a biological sample. The sample is broken down by homogenisation and then cell lysis, using detergents and buffers in the presence of protease inhibitors, to prevent digestion of the sample by its own enzyme. The sample is then loaded onto a gel where the proteins are separated, by gel electrophoresis, dependant on their molecular weight. A ladder containing a mixture of proteins with defined molecular weights is also loaded to aid identification of proteins. The proteins migrate along the gel at different speeds dependant on their molecular weight, and separate into bands. These protein bands are then transferred from the gel onto a membrane using electroblotting in order that the protein of interest can be detected using an antibody. Following incubation of the blot with the chosen primary antibody, a secondary antibody is used. This is linked to a reporter enzyme, which by cleaving a chemiluminescent agent produces luminescence signal in proportion to the amount of protein. This light output can then be detected and imaged using a scanner. Any visible protein bands can be identified based on the antibody used and expected size confirmed by position in relation to the molecular weight ladder.

2.12.2 Tissue preparation

The extracted samples were prepared in 100ul of 89% lysis buffer (10% glycerol (Fisher Scientific), 125nM Tris (Fisher Scientific), 3% Sodium dodecyl sulfate (SDS) (Bio-Rad), 0.2% bromophenol blue (Sigma), 1% protease inhibitor (Thermo Scientific) and 10% dichlorodiphenyltrichloroethane (DTT) (Sigma) at pH6.8). Samples were

denatured for 3 minutes using a heating block set at 100°C, vortexing every 60 seconds, before being loaded on to a gel or stored at -20°C for later use.

2.12.3 Running gel and blotting

12% Mini-PROTEAN® TGX™ pre-cast gels (Bio-Rad) were used. Precision protein plus standard (Bio-Rad) was loaded into the first well followed by the samples, 20ul of neutrophil samples, 10ul of epithelial samples, and allowed to settle evenly on the bottom of the wells. Following sample loading with 1x electrophoresis running buffer (3.03g Tris Base, 14.4g Glycine, 1g SDS made up to 1 litre in H_20), the gel was run at 140V for 45 minutes before the gel was removed for blotting. The Trans-blot ® Turbo™ Mini Polyvinylidene Difluoride (PVDF) transfer packs (Bio-Rad) were used with Trans-Blot ® Turbo™ rapid western blotting system for protein transfer.

2.12.4 Antibody staining

The PVDF membrane was placed into a small tissue culture flask containing blocking buffer for 1 hour. The blocking buffer used was 5% (w/v) non-fat dry milk/TBST (100ml 10xTBS, 900ml dH_20, 1ml TWEEN 20 (Fisher)). The membrane was then incubated overnight at 4°C on an orbital shaker with the primary antibody. The primary antibody solution was then removed and the blot washed three times for five minutes before addition of the secondary antibody. The blot was incubated with the secondary antibody for 1 hour at room temperature on a shaker before being washed three times and read.
Chemiluminescence substrate (Li-Cor) was prepared by adding equal volume of the Solution A to an equal volume of the Solution B; approximately 800µl was needed in total per blot. This was then pipetted on to the protein side of the membrane ensuring the mixture covered the membrane evenly and incubated for 5 minutes before reading on the C-Digit scanner (Li-Cor). Data was analysed using ImageStudioLite (Li-Cor).

Antibody	Dilution	Host	Supplier
Anti-F RSV (monoclonal)	1:500	Mouse	Abcam
Anti-RSV biotin conjugated (polyclonal)	1:2000	Goat	Biorad
Anti-histone H3	1:30 000	Rabbit	Sigma

Table 2-2 Primary antibodies used for western blot analysis

Antibody	Dilution	Host	Species Against	Supplier
IgG Streptavidin HRP	1:200	Mouse	Goat	R&D
Anti-Mouse	1:1000	Goat	Mouse	R&D
Anti-Rabbit	1:1000	Goat	Rabbit	R&D

Table 2-3 Secondary antibodies used for western blotting

2.12.5 RSV proteins measured by Western Blot from infected epithelial cells

Western blot was carried out on pellets harvested at 24 hours from epithelial cells infected with RSV (MOI 1). A polyclonal RSV antibody (1/100) was used with streptavidin secondary (1/1000). Five bands were clearly seen and identified based on their predicted molecular weights as F, G, M, N and P proteins. Bands were not detected in non-infected control cells **(Figure 2-10).**

2.12.6 RSV proteins measured by Western blot from neutrophils incubated with RSV

A Western blot was carried out on pellets harvested at 2 hours from neutrophils incubated with RSV (MOI 0.1). A polyclonal RSV antibody (1/100) was used with streptavidin secondary (1/1000). Four bands were clearly seen and identified based on their predicted molecular weights as F, G, M, and N proteins. Bands were not detected in neutrophils not incubated with RSV **(Figure 2-11)**. A P protein band was not identified, unlike the epithelial cell experiment. This may be due to degradation of the RSV proteins within the neutrophil, which does not occur in the epithelial cell.

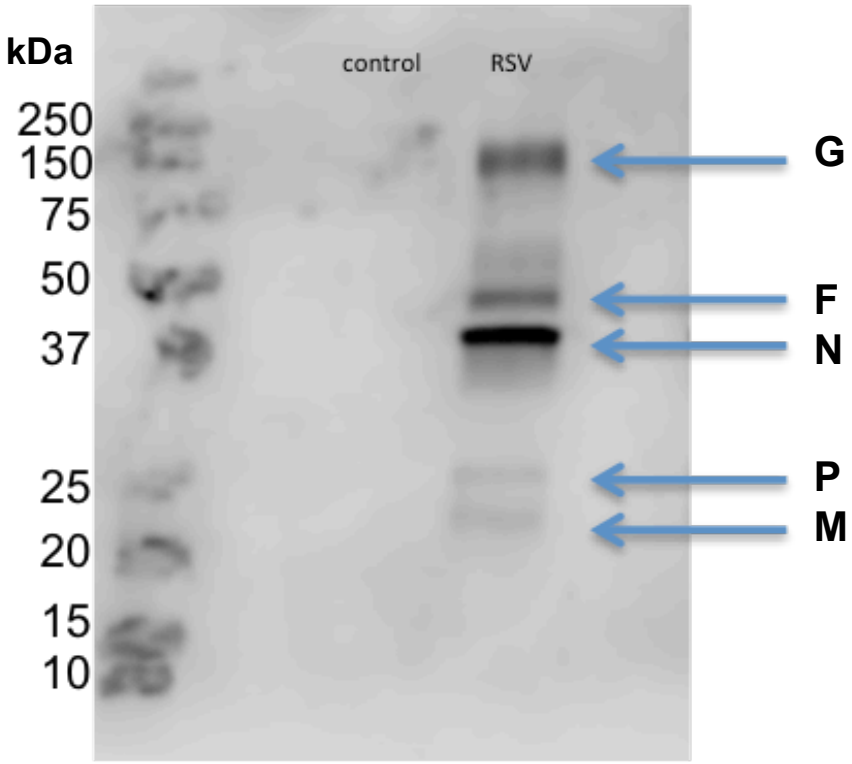

Figure 2-10 RSV proteins identified from infected epithelial cells

Western blot was carried out on pellets harvested at 24 hours from epithelial cells infected with RSV (MOI 1). Control pellets consisted of epithelial cells that had not been infected. RSV polyclonal antibody with anti-mouse secondary was used. RSV F, G, M, N and P proteins were identified from infected cells. Molecular weight of protein ladder is shown in kDa.

a.

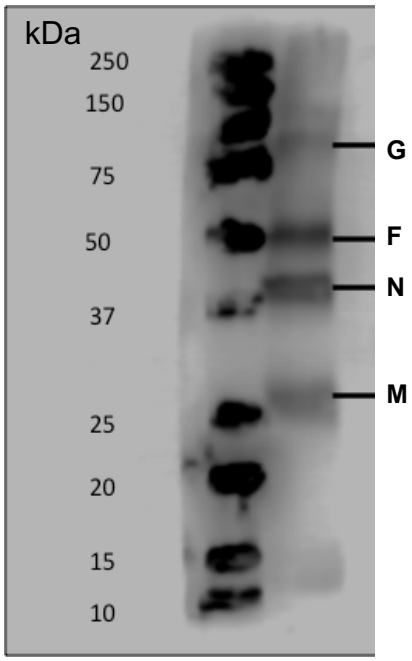

b.

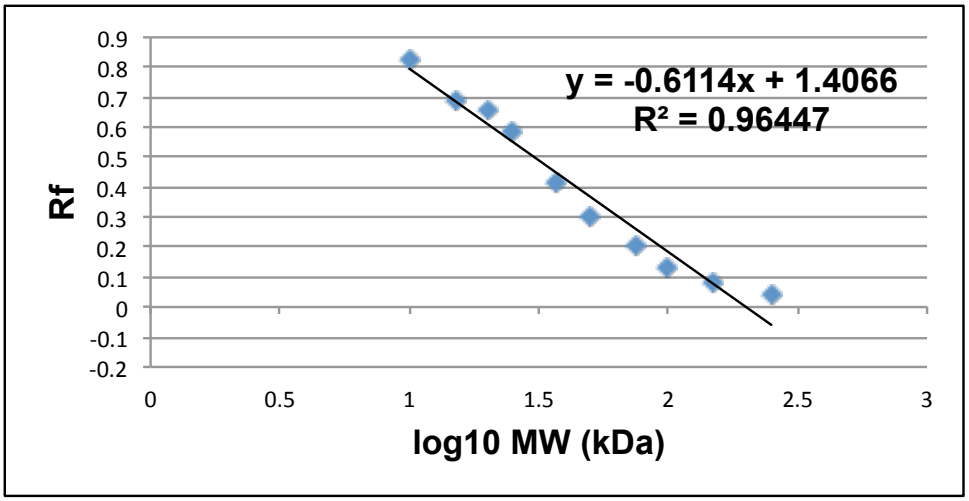

Protein of Interest	Calculated MW (Kda)	Expected MW (Kda)
G	120	90
F	57	58
N	44	43
M	24	22

Figure 2-11 RSV proteins identified from neutrophils incubated with RSV

a) Western blot image of neutrophils incubated for 2 hours with RSV. RSV polyclonal antibody with anti-mouse secondary was used. 4 bands are seen at 24, 44, 57 and 120 kDa, which correlate with RSV G, F, N and M proteins respectively. Reference protein markers are also visualised, which indicate the position of proteins of known molecular weights. b) Correlating scatter plot of the protein migration distance (R_f) of the reference protein markers against the log of their molecular weight. The calculated equation of the line is shown which has then been used to calculate the molecular weight of the RSV proteins. Individual RSV proteins were then identified using their expected molecular weights.

Quantitative Polymerase Chain Reaction (qPCR) was used in the work described in **Chapter 3** to establish a time course of RSV N gene expression using infected epithelial cells and RSV exposed neutrophils. qPCR was also used in the work described in **Chapter 6** to validate the findings of a microarray analysis.

2.12.7 Principle of Reverse Transcription qPCR

qPCR allows exponential amplification of short deoxyribonucleic acid (DNA) sequences (usually 100 to 600 bases) within a longer double stranded DNA molecule in order to detect and quantify gene expression. It involves reverse transcription of RNA into cDNA followed by PCR to amplify a specific cDNA molecule. This can be quantified in real time by the accumulation of fluorescence after each amplification cycle (133).

There are two established methods of PCR quantification, relative and absolute. Relative quantification determines the mRNA quantity relative to the quantity of an internal reference gene. Mathematical algorithms have been developed to calculate the corrected relative expression ratio; these include the Pfaffl method and the **ΔΔ**CT method (134, 135). Absolute quantification can also be used which relies on a standard curve of Ct values, generated from a dilution series of a standard with known initial target copy number. The reliability of the standard used is paramount for accuracy (136, 137). Relative quantification has been used for all qPCR analysis in this thesis.

The efficiency of each target assay was calculated by performing a serial dilution experiment. The slope of the standard curve was used to measure an efficiency value as described in **Figure 2-12**.

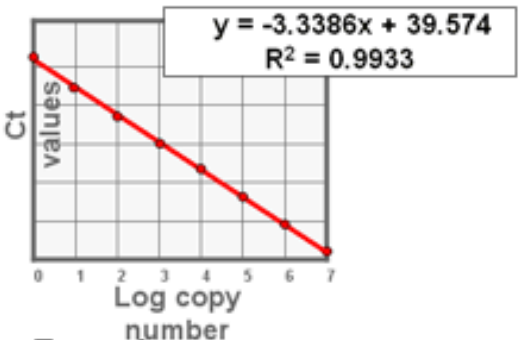

Slope = -3.3386

Efficiency = $10^{(-1/slope)} - 1$

= $10^{(0.30)}$ -1

= 0.995 = 99.5%

Figure 2-12 Calculation of PCR efficiency

PCR efficiency was assessed by plotting the results of serial dilution experiments, and then calculating the equation for the slope of the line of best fit. Dilution Log10 was plotted against the Ct values. The slope of the standard curve can be translated into an efficiency value. The efficiency of the PCR should be between 90–100% (−3.6 ≥ slope ≥ −3.3). If efficiency is 100%, the Ct values of the dilution experiment will be 3.3 cycles apart i.e. 2 fold change for each change in Ct.

(Image adapted from applied biosystem PCR manual)

The amplification curve for each experiment was inspected to ensure i) that the fluorescent threshold was set within the exponential phase of the PCR reaction, ii) that the curve continued to rise and was not limited by reagent availability, and iii) that the non-template control did not show fluorescence. The **ΔΔ**CT method used for quantification relies on absolute PCR efficiency, which must be between 90 - 100%. The slope of the curve is directly related to the amplification efficiency, so amplification curves were reviewed to ensure that R^2, the indicator of quality of fit of the curve, was ≥ 0.95. This was the case for all but two of target genes analysed **(Table 2-4)**.

Gene	R^2	Slope	Efficiency (%)	Threshold
DICER 1	0.94	-3.59	90	0.2
DDX58	0.96	-3.49	93	0.2
DHX58	0.95	-3.30	100	0.2
IRF7	0.90	-3.30	100	0.1
MX1	0.98	-3.48	94	0.2
STAT1	0.98	-3.50	93	0.2
USP18	0.95	-3.28	95	0.2
RSV	0.97	-3.61	89	0.2
GAPDH	0.97	-3.49	93	0.015
B2M	0.97	-3.50	93	0.15

Table 2-4 Standard curve characteristics of qRT-PCR experiments

2.12.8 RNA Extraction

Samples for PCR analysis were stored in TRIzol (life technologies) at -30°C for short-term storage and -80°C for long-term storage. Samples were thawed on ice when required. 100ul chloroform (Sigma) was added to each 500ul sample, and the sample vortexed prior to centrifugation at 1300g/10 minutes. The top aqueous layer was pipetted off into a new Eppendorf to which 400ul isopropanol (Sigma) was added and the sample vortexed and then cooled at -20°C for 30 minutes. The sample was centrifuged at 1300g/15 minutes after which the supernatant was removed and 500ul RNAse free 70% ethanol (Sigma) added before centrifugation at 1300g for 5

minutes. All ethanol was removed and the sample left to dry for 10 minutes prior to the addition of 10ul RNAse free water.

2.12.9 cDNA synthesis

RNA samples were converted to cDNA using High Capacity cDNA Reverse Transcription Kit (applied biosystems). To each tube, 2ul RT buffer, 2ul random primers, 1ul dNTP mix, 4ul RNAse free water and 1ul Multiscribe Reverse Transcriptase enzyme were added. Samples were then placed at 37°C in a heating rack for 1 hour. The cDNA was then diluted 1:4 (final volume 100ul) with RNAse free H_20 and stored at -80°C until use.

2.12.10 Quantitative Polymerase Chain Reaction

Probe based Taqman® qPCR detection was used for all qPCR experiments. All assays used are detailed in **Table 2-5**. All target gene expression was normalised to an internal standard. The internal reference gene L32 was selected for use in all experiments. An RSV Taqman probe (Applied biosystems) was used. Primer and probe sequences are described in **Table 2-6**, and the methods described in Pachet *et al* paper on the development of quantitative TaqMan RT-PCR for RSV (138). For all reactions 1.25ul of a specific gene expression assay probe (Taqman®), 12.5ul Taqman Master Mix and 11.25ul cDNA were used and reactions were run in a 96 well PCR plate. Plates were sealed with adhesive film and run on Applied Biosystems 7500 fast Real-Time PCR System. Cycling conditions were – 2 minutes at 50°C, hold at 95° for 10 minutes, followed by 40-60 cycles of 95°C for 15 seconds and 60°C for 60 seconds.

2.12.11 Analysis of qPCR data

Quantification of gene expression was by comparative quantification method (**ΔΔ**CT method). Analysis was performed by: calculation of the mean Ct values of target gene and internal reference gene, and calculation of the arithmetical mean of the selected internal reference gene to generate the mean reference value for each sample.

Δ*CT = Ct (target) – Ct (mean reference)*

Target gene expression, relative to interval reference gene expression was then calculated using the following equation.

Relative gene expression = $2^{-\Delta CT}$

Gene	Assay ID	Supplier
Mitochondrial ribosomal protein L32	Hs00388301_m1	Life technologies
DICER 1	Hs00229023_m1	Life technologies
DDX58	Hs00204833_m1	Life technologies
DHX58	Hs01597843_m1	Life technologies
IRF7	Hs00185375_m1	Life technologies
MX1	Hs00895608_m1	Life technologies
STAT1	Hs01013996_m1	Life technologies
USP18	Hs00276441_m1	Life technologies

Table 2-5 Pre-designed gene expression assays used for qPCR analysis

Gene	Forward Primer	Reverse Primer	Probe
RSV N gene	CTCAATTTCCTCACT CTCCAGTGT	CTTGATTCCTCGGTGT ACCTCTGT	TCCCATTATGCCTAGGC CAGCAGCA

Table 2-6 RSV Primer and probe for qPCR

2.13 Imaging

Confocal microscopy was used in **Chapters 3, 4 and 5** to identify RSV from neutrophils, both from the *in vitro* system and also from *ex vivo* neutrophils collected from RSV infected infants' BAL. All antibodies, both primary and secondary, used for immunocytochemistry are listed **in Table 2-7** and **Table 2-8** respectively.

2.13.1 Sample preparation for imaging

Cytospin slides of purified neutrophils (approximately 50,000 cells) were prepared from both BAL and blood. Samples were diluted in PBS if required. The samples were pipetted on to cyto-chambers secured in slide carries containing superfrost® plus slides (Thermo Scientific) and centrifuged at 400g for 4 minutes in a Rotofix 32A. Following air-drying slides were fixed with either ice cold 100% methanol or paraformaldehyde (PFA) (Sigma).

2.13.2 Indirect immunocytochemistry staining

Cytospin slides were stored at -30°C until required. They were then removed and left to thaw before rehydrating them in PBST (PBS plus 0.1% TWEEN) for 5 minutes. A circle was drawn around cytospun cells with a hydrophobic marker prior to 1 hour of blocking with 5% milk in PBST. Slides were then washed with PBST 3 times for 5 minutes. The primary antibody (diluted in PBST/5% milk) was added and slides left for 1 hour at room temperature in a humid chamber. They were then washed 3 times in PBST before the secondary antibody was used, at the required concentration in PBST/5% milk, for a further hour. Slides were washed 3 times in PBST before being dried and mounted using VECTASHIELD® Mounting Media (vectorlabs) and cover slips sealed with clear nail varnish. Co-stains DAPI (1:10,000) (Sigma) and Evans Blue (Sigma) were used after application of the secondary antibody and prior to mounting. Slides were stored at 4°C until needed.

Antibody	Dilution	Host	Supplier
Anti- human CD66c PE (monoclonal)	0.125µg per sample	Mouse	ebioscience
IgG1 isotype PE (monoclonal)	0.125ug per sample	Mouse	Beckman Coulter
Anti-F RSV (monoclonal)	1:100	Mouse	Abcam
Anti-N RSV (monoclonal)	1:100	Mouse	Abcam
Anti-G RSV (monoclonal)	1:100	Mouse	Abcam
IgG1 isotype (monoclonal)	1:50	Mouse	R&D

Table 2-7 Primary antibodies used for indirect immunocytochemistry staining

Antibody	Dilution	Host	Species Against	Supplier
IgG Alexa Fluor® 488	1:1000	Goat	Mouse	Life technologies
IgG Alexa Fluor® 594	1:1000	Goat	Mouse	Invitrogen

Table 2-8 Secondary antibodies used for indirect immunocytochemistry staining

2.13.3 Confocal microscopy

Immunofluorescence images were captured with Multiphoton Zeiss Observer Z.1 confocal laser microscope. Zeiss Fluor 40x oil and 63x oil immersion

objective were used. IgG Alexa Fluor 488 dye was excited at 488nm, using an Argon laser (530nm). IgG Alexa fluor 554 dye was excited at 561nm using a diode-pumped solid-state laser (575nm). The pinhole was set at 1 airy unit (AU) to provide the optimal signal to noise ratio. For Z-stack images the slice thickness was between 0.5 – 1µm.

2.13.4 Image Processing

Images were exported from Zen 2010 and edited in Fiji ('Fiji is just Image J') (139). This is an open source, multi-platform software for acquisition, visualisation and analysis of biological data. When multidimensional data was required, Imaris (Bitplane) software was used. When Z-stacks are presented these are seen as single slices, unless specified. Co-localisation analysis was carried out in Fiji. Mander's coefficient was used to measure the significance of any observed co-localisation. This significance test evaluates the probability that the measured value of fluorescent overlap from the two colours is significantly greater than the fluorescent overlap that would be expected if there were only random overlap.

2.14 Statistical Analyses

The statistical analysis software Graph pad Prism (version 6.0) was used for graphical representation of data and statistical analysis (GraphPad software, Inc). All data were assessed to ascertain whether they were normally distributed using the Shapiro-Wilk test. Normally distributed data were compared using a student t-test when there 2 experimental groups. When there were more than 2 groups, one-way ANOVA was performed with Bonferroni's post hoc test, to identify for significant differences and to allow for correction for multiple testing. In one instance a two-way ANOVA was used as there were 2 experimental variables (Section 2.10.1). Non-parametric data were compared using the Mann-Whitney U test when there were 2 experimental groups. When there were more than 2 groups Kruskal-Wallis test was used for unpaired data or Friedman test when data were paired, with Conover Inman post hoc test. Throughout this thesis a statistically significant difference was taken as a probability (p) value < 0.05.

Chapter 3 Characterisation of RSV-neutrophil interactions

3.1 Introduction

In **Chapter 2**, I described an optimised method for the *in vitro* assessment of the interaction between neutrophils and RSV. I showed that RSV could be identified within human adult neutrophils, an observation previously only made *in vivo* (129). The logical question to arise from these results is 'what is the nature of this interaction'? A number of studies have explored the role of the neutrophil in the pathogenesis of viral disease. Some have shown viral components inside the neutrophil and others have purported to show viral replication in the neutrophil. Very few have considered mechanisms by which virus enters the cell. The word 'infection' is frequently used, often rather loosely. Sometimes it is used to describe just the entry of virus into the cell, whilst at other times, it is used to describe proliferation of the virus with the result of viral spread.

A number of groups have reported virus replication inside neutrophils. Some have used elegant methods, such as a study into the pathogenesis of West Nile virus, in which the authors measured both positive and negative sense viral RNA within neutrophils from mice. The presence of negative sense RNA was used to indicate active replication, as viral RNA polymerase generates negative sense RNA to serve as a template for replication. At 8 hours negative-sense RNA was detected. No later time points were used to measure production of actual whole virus however, and neutrophil depletion resulted in higher viral loads (140). Other studies, on H5N1 influenza, have simply used the localization of virus to the neutrophil nucleus as evidence of its ability to replicate within. H5N1 viral proteins were found in placental neutrophils from virus infected patients. The investigators hypothesised entry by phagocytosis and immunohistochemistry localized the virus to the cytoplasm that replication was likely to be occurring. No further evidence was sought (141, 142). EBV genome has been found *in vitro* in neutrophil nuclei, but no viral transcripts were detected. It was concluded that the cell

undergoes apoptosis too rapidly to allow for replication (143). Cytomegalovirus replication in neutrophils has been extensively studied. Replication has previously been claimed based upon detection of viral transcripts within neutrophils (144-146). However, later studies have subsequently concluded that the presence of viral proteins and transcripts do not represent replication as they lead to only small quantities of viral nucleic acids (147).

Other studies have shown virus within neutrophils but with no evidence of replication. Nakanishi *et al* demonstrated in mice that both macrophages and neutrophils recruited to the lung during H1N1 influenza infection contained influenza infected apoptotic cells (148). Garcia-Sastre *et al* used whole-organ imaging and flow cytometry to track the dynamics of a recombinant influenza virus carrying a green fluorescent protein (GFP) reporter gene in mice (149). GFP virus was present not only in epithelial but also hematopoietic cells including neutrophils. The authors concluded that intracellular detection of virus was due to direct 'infection' of the neutrophils, or secondary to phagocytosis of infected cell debris. A preceding study looking specifically at virus-infected neutrophils with influenza had shown similar uptake but had proved, by use of a plaque assay on supernatant fluid, that infectious progeny were not produced by neutrophils (150). Recent work on H3N2, a highly virulent influenza virus, revealed a small proportion of neutrophils that were positive for virus in an *in vitro* model system. The authors used fluorescently labelled influenza virus and used flow cytometry to quantify positivity. They found neutrophils did not support active replication, as virus titres remained unchanged in the supernatants of the infected neutrophils (151).

It is worth noting that the word 'infection' is often used indiscriminately in these studies. Within this thesis, the term 'replicative infection' will be used henceforth to describe such an event occurring. 'Virus positive' will be used to describe the presence of virus in the cell where no evidence of replication is presented. Overall, there certainly appears to be evidence of viruses being

found within neutrophils in many studies, but evidence that these cells actually allow viruses to replicate within them tends to be weak.

There is only one paper that presents evidence of potential RSV replication inside the neutrophil. Our group previously identified RSV F, G and N proteins within blood and BAL neutrophils taken from intubated infants with severe RSV bronchiolitis. The same neutrophils that were positive for RSV proteins, were also found to be RSV mRNA positive raising the possibility that active viral transcription was occurring (129). Potentially this could happen as part of an abortive replicative process or represent whole viral replication. Either scenario could be detrimental to the host, with a build up of RSV transcripts and proteins potentially exacerbating inflammation, and whole viral replication potentially enabling the neutrophil to contribute to viral dissemination. However, it is also possible that neutrophil take-up of virus is a mechanism for enabling viral clearance. Understanding the mode of viral entry and the kinetics of virus uptake, in particular whether the neutrophil is a site of viral replication, will contribute to our understanding of the role of the neutrophil in the airway.

3.2 Hypothesis

RSV does not infect and productively replicate within the neutrophil but is taken up actively by the neutrophil through endocytosis.

3.3 Aims

To answer the above hypothesis the work described in this chapter aimed to:

1. Establish the kinetics of RSV uptake and whether RSV replicates within purified healthy adult neutrophils in vitro.
2. Determine whether neutrophils release RSV progeny into the supernatant that are capable of epithelial cell infection
3. Determine whether autologous serum enhances uptake of RSV
4. Establish whether the mechanism of viral entry uptake is through endocytosis.

3.4 Specific methods

Adult neutrophils and RSV were cultured *in vitro* using the conditions laid out in **Chapter 2 (Section 2.12)** and illustrated in **Figure 2-9**. In brief, highly purified neutrophils from the whole blood of healthy adults were isolated and incubated with A2 strain RSV MOI 0.1 in the presence of 5ng/ml GM-CSF and 5% autologous serum for up to 20 hours. From henceforth, all experiments on neutrophils were undertaken using these conditions. Samples were examined at appropriate time points using a range of analysis methods for the presence of RSV using the methods outlined in **Chapter 2 (Sections 2.13 - 2.15)**. RSV N gene was measured using RT qPCR. Productive viral progeny was looked for using a plaque assay. RSV proteins were identified across a time course using the Western Blot technique. Lastly, indirect immunocytochemistry was used to identify RSV by confocal microscopy.

3.5 Results

3.5.1 RSV measured by qPCR using a RSV N primer

To show that RSV could be quantified by RSV N gene qPCR and demonstrated to be replicating over time, a positive model of replicative infection was used. This model used the epithelial cell line A549. A549 cells were infected with RSV (MOI 1) for up to 20 hours and cells harvested, washed and pelleted at time points 2 and 20 hours before being stored in TRIzol at -30^{o}c. Following reverse transcription, RSV was quantified using qPCR and comparative quantification. RSV N quantity significantly increased over time ($p=0.032$) indicating active replication **(Figure 3-1)**.

3.5.2 No evidence of RSV replication in neutrophils

To determine whether RSV replication occurred over time in a similar fashion to that seen in the epithelial cells RSV N gene qPCR was carried out on RSV exposed neutrophils. Highly purified neutrophils at $5x10^{6}$/ml in DMEM were incubated with RSV preparation for 2, 4 and 20 hours, in the presence of GM-CSF and with or without 5% autologous serum. At these time points neutrophils were pelleted for 5 minutes at 1800rpm. Supernatant was

removed and stored at -80^{o}C. Neutrophils were washed in 10 mls PBS twice before a dry pellet was resuspended in 500ul TRIzol and stored at -30 ^{o}C prior to RNA extraction. RNA extraction and reverse transcription was carried out as described in **Section 2.9**. RSV expression was measured at each time point and quantified relative to the internal housekeeping gene L32 **(Figure 3-2)**. RSV expression without serum was not significantly different at any time point although there was a trend towards a decrease over time. RSV expression with serum showed maximal uptake at 4 hours and a decrease by 20 hours, although this trend did not reach statistical significance. Uptake was observed to be greater in the presence of 5% autologous serum.

3.5.3 RSV uptake is optimally enhanced by 10% autologous serum

Given the results described above, I sought to determine the optimum concentration of autologous serum to maximize neutrophil uptake of RSV for my future studies. Highly purified neutrophils at 5x10^{6}/ml in DMEM were incubated with RSV preparation for 2 hours, in the presence of GM-CSF and either 0%, 0.1%, 1% or 10% serum autologous serum. At these time points neutrophils were pelleted for 5 minutes at 1800rpm. Supernatant was removed and stored at -80^{o}C. Neutrophils were washed in 10 mls PBS twice before a dry pellet was resuspended in 500ul tryzol and stored at -30 ^{o}C prior to RNA extraction. RNA extraction and reverse transcription was carried out as described in **Chapter 2**. RSV expression was measured at each time point and quantified relative to the internal housekeeping gene L32 and **ΔΔ**Ct method was used to quantify RSV expression compared to expression in neutrophils unexposed to serum. There was a significant increase in uptake with 10% serum compared to no serum (p value = 0.0231) and compared to 0.1% serum (p value = 0.0408) **(Figure 3-3)** (Friedman test with Conover Inman post hoc test was carried out following non parametric distribution confirmation by Shapiro-Wilks).

As a result of the above experiment it would have been ideal to carry out subsequent experiments using 10% autologous serum, however the usual quantity of serum yielded from the blood samples only allowed the use of

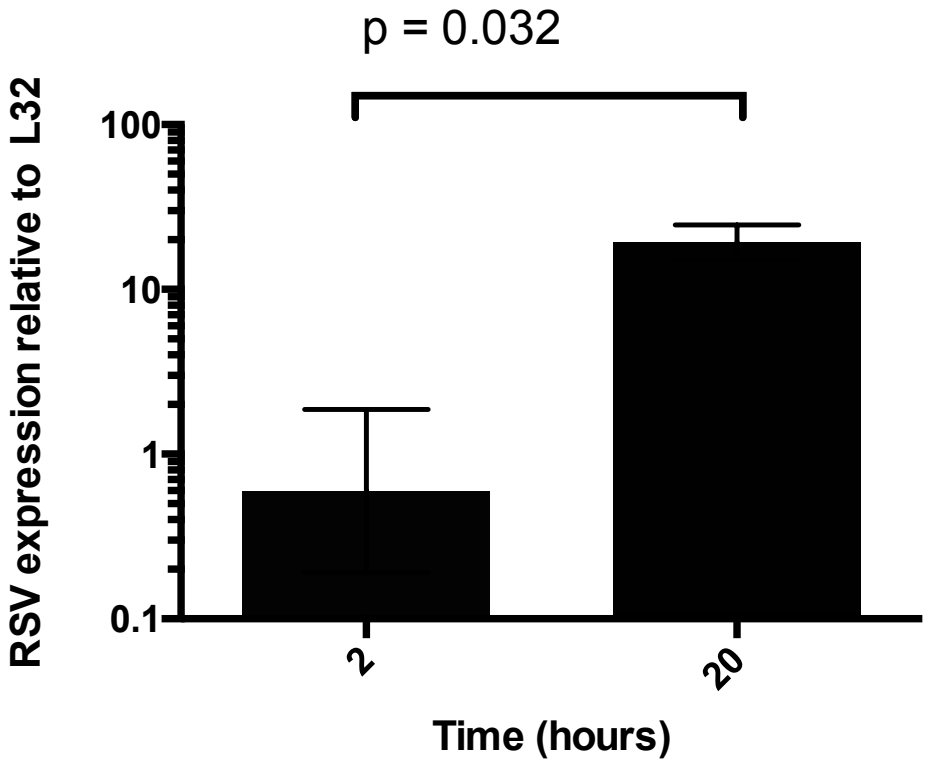

Figure 3-1 RSV N gene expression relative to L32 in the epithelial cell line A549

A549 cells were infected with RSV MOI 1. Cells were harvested at 2 and 20 hours and stored in TRIzol prior to RNA extraction and reverse transcription. RSV N gene was measured by qPCR and is expressed relative to L32 on a log axis. RSV N gene expression increases significantly from 2 to 20 hours (p value = 0.032).

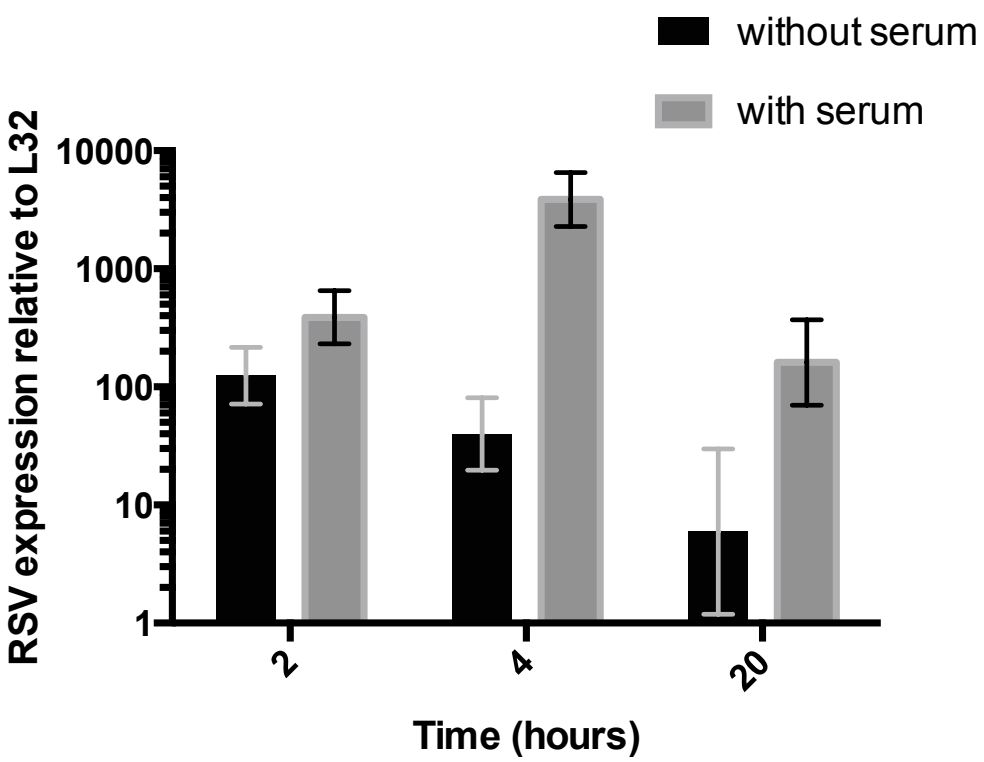

Figure 3-2 RSV N gene expression relative to L32 in neutrophils incubated with RSV.

Neutrophils were incubated with RSV in the presence of GM-CSF and in the presence or absence of 5% autologous serum. Cells were harvested at 2, 4 and 20 hours and stored in TRIzol prior to RNA extraction and reverse transcription. RSV N gene was measured by qPCR and is expressed relative to L32 on a log axis. RSV expression without serum was not significantly different at any time point although there was a trend towards a decrease over time. RSV N gene expression with serum showed maximal uptake at 4 hours and a decrease by 20 hours, although this trend did not reach statistical significance. Uptake was observed to be greater in the presence of serum.

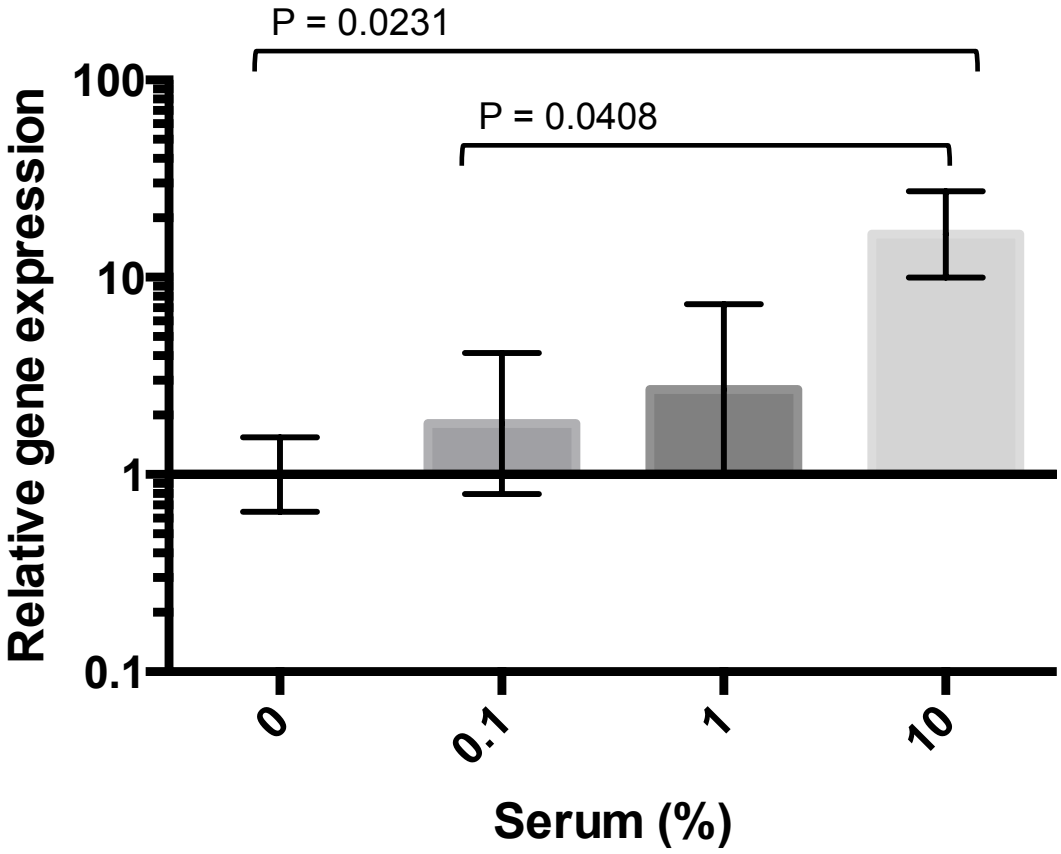

Figure 3-3 RSV uptake is enhanced by the presence of 10% autologous serum

RSV N gene expression is shown for cells incubated with RSV for 2 hours in the presence of 0, 0.1%, 1% and 10% autologous serum. There was a significant increase in uptake with 10% serum compared to no serum (p value = 0.0231) and compared to 0.1% serum (p value = 0.0408)

5%. For this reason, future experiments were carried out with 5% autologous serum.

Of note the stability of housekeeping gene L32 with and without RSV was not measured at this point. This is addressed in **Section 6.4.3**.

3.5.4 Western blot analysis confirms qPCR time course results

As RSV N gene was measured from the neutrophils but decreased over time, I sought to measure the RSV protein at the same time points. A Western blot was carried out on pellets harvested at 2, 4 and 20 hours from neutrophils incubated with RSV in DMEM, in the presence of GM-CSF and 5% autologous serum. A polyclonal RSV antibody (1/100) was used with streptavidin secondary (1/1000). 4 bands were clearly seen and identified based on their predicted molecular weights as F, G, M and N. The density of the bands reduces clearly at 20 hours suggesting degradation of internalised RSV protein **(Figure 3-4).** The figure shown is representative of 3 identical, separate experiments, which revealed the same finding.

3.5.5 Neutrophils can not disseminate virus to epithelial cells

In order to confirm the absence of productive RSV infection in the neutrophil, the neutrophil supernatant was analysed for infectious progeny. Supernatant collected from neutrophils, which had been incubated with RSV for 2 hours, using the conditions previously outlined, then washed and cultured for a further 22 hours, was added to A549 cells cultured to 80% confluence. At 48 hours, a plaque assay, measuring the infective capacity of the supernatant, was carried out. This revealed that the supernatant from the neutrophils exposed to RSV did not cause infection of the epithelial cells. A positive control, supernatant from RSV infected epithelial cells, did cause infection as evidenced by the level of plaque formation **(Figure 3-5).**

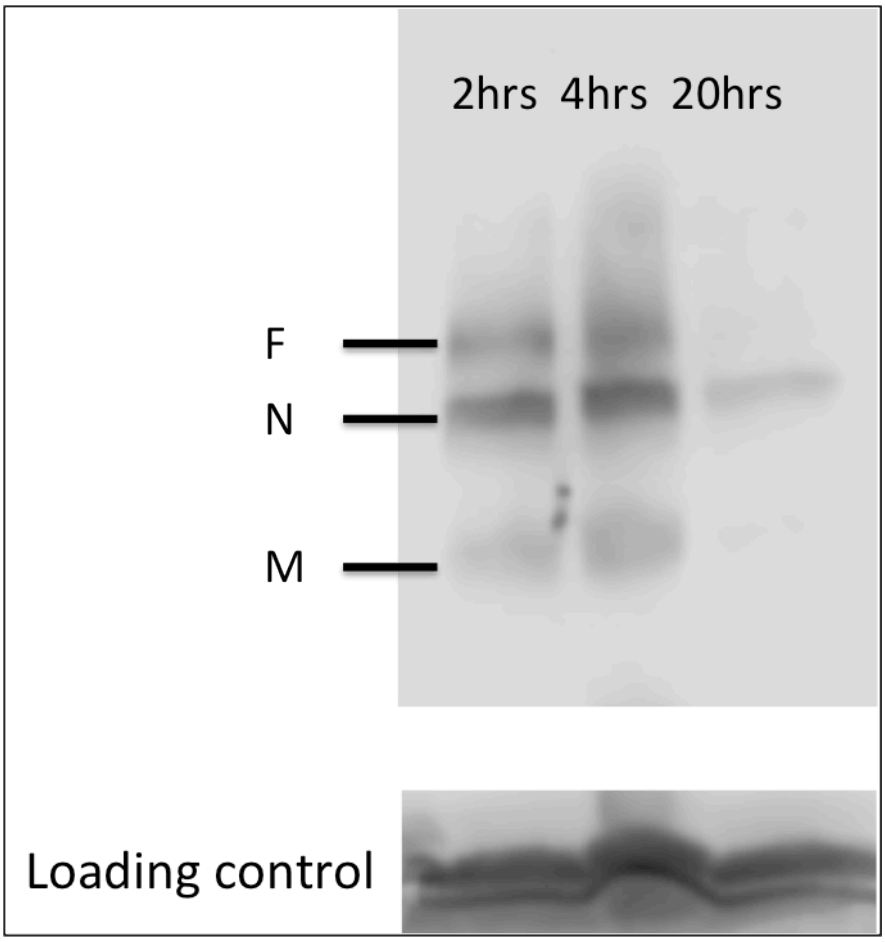

Figure 3-4 Western blot time course for RSV from neutrophils

A Western blot was carried out on pellets harvested at 2, 4 and 20 hours from neutrophils incubated with RSV and 5% autologous serum. The quantity of RSV, as shown by the density of the 3 RSV protein bands F, N and M, is markedly reduced by 20 hours.

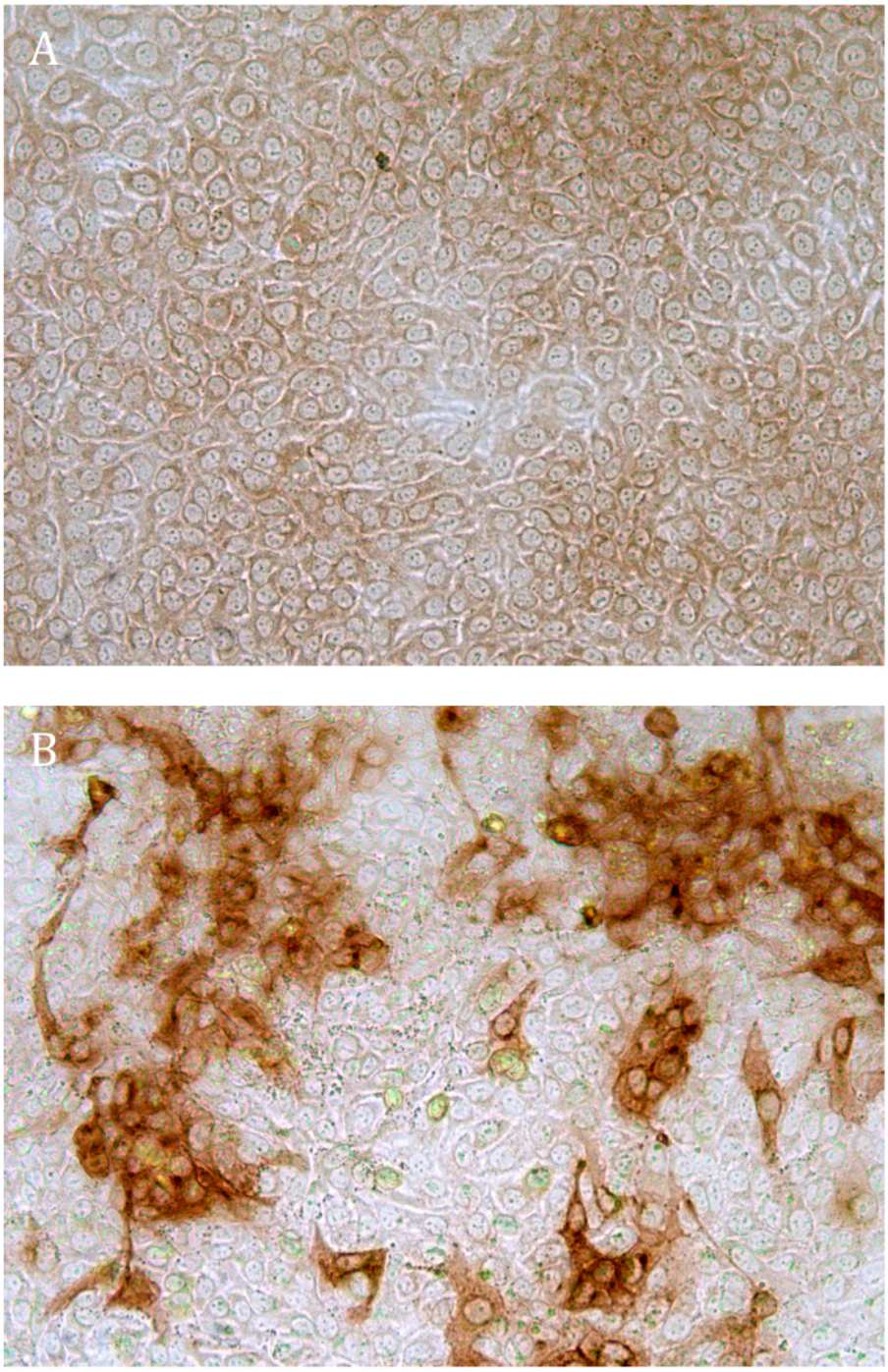

Figure 3-5 Plaque assay of A549s exposed to supernatant from RSV exposed neutrophils and A549s

Neutrophils and A549s were incubated with RSV for 2 hours, after which time they were washed and left in culture media for a further 22 hours. Supernatant was then removed and added straight to A549 cells cultured to 80% confluence. After 48 hours a plaque assay was performed revealing that those cells with neutrophil supernatant (A) had not been infected with RSV but the A549s that were cultured in media taken from RSV treated epithelial cells (B) had been infected as evidenced by the plaques.

3.5.6 Cytochalasin D is an effective phagocytosis inhibitor

The inhibition of neutrophil uptake of pHrodo E. coli by cytochalasin D, a known potent inhibitor of phagocytosis, was tested to check the efficacy and concentration of the inhibitor (152). Neutrophils were incubated with pHrodo E. coli for 2 hours, as outlined in **Chapter 2**, following 15 minute pre-treatment with or without cytochalasin D (concentration = 0.1mg/ml.) Neutrophils were analysed by flow cytometry as previously described; phagocytosis was quantified by measuring the percentage of neutrophils that were FL3 +ve. Comparison was made between those neutrophils exposed and unexposed to pHrodo E. Coli both with and without pre-treatment with cytochalasin D **(Figure 3-6)**. Cytochalasin D successfully reduced phagocytosis to 2.38% from 83.9%.

3.5.7 RSV uptake is not inhibited by the cytochalasin D

Following the above optimisation, to determine whether RSV was being taken up by the neutrophil using phagocytosis, cytochalasin D was used. RSV uptake was measured by RSV N gene qPCR. Highly purified neutrophils were incubated with RSV preparation for 2 hours, in the presence of GM-CSF and 5% autologous serum +/- 15 minute pre-exposure to 0.1mg/ml cytochalasin D. At 2 hours neutrophils were washed in 10 mls PBS twice before a dry pellet was resuspended in 500ul tryzol and stored at -30 ^{o}C prior to RNA extraction. RNA extraction and reverse transcription was carried out as described in **Chapter 2**. RSV expression was measured at each time point and quantified relative to the internal housekeeping gene L32 and ΔΔ Ct method was used to quantify RSV expression against expression in neutrophils unexposed to cytochalasin D **(Figure 3-7a)**. There was no statistically significant difference in RSV expression. Friedman test with Conover Inman post hoc test was performed.

3.5.8 RSV uptake is not enhanced by a RSV monoclonal antibody

To determine whether RSV uptake could be enhanced by an RSV monoclonal antibody, palivizumab was tested in the culture system. Highly

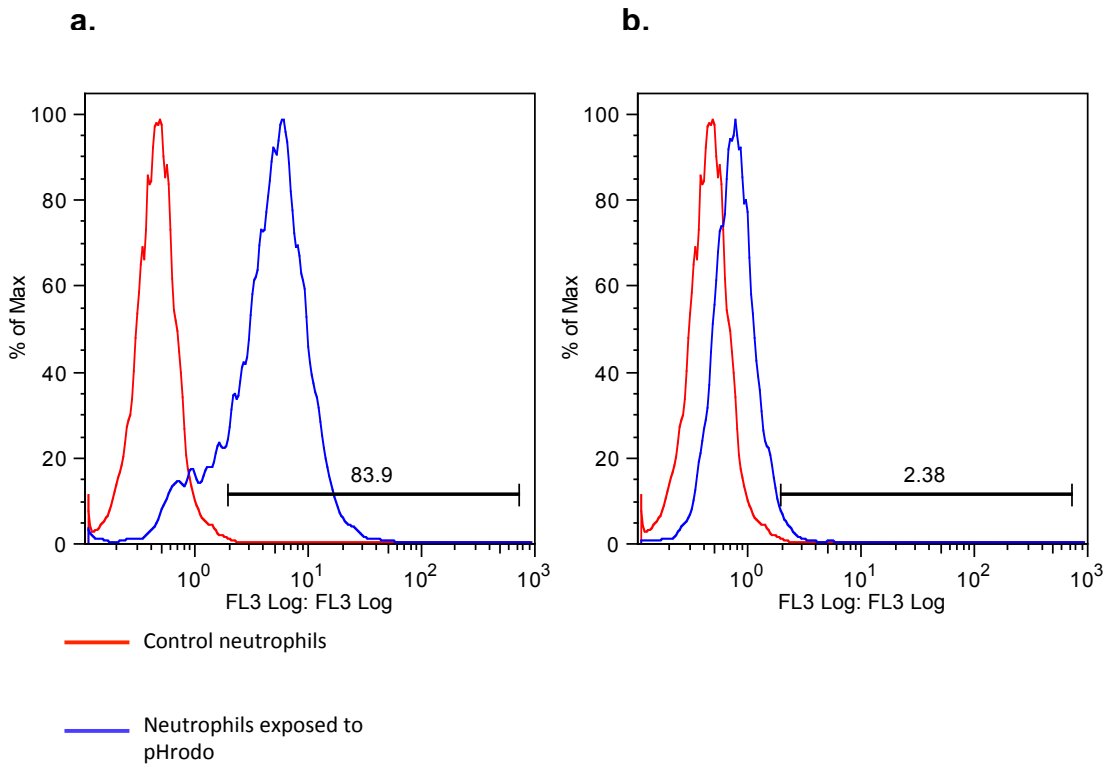

Figure 3-6 Cytochalasin D reduces phagocytosis of pHrodo E. coli

a) Histogram showing percentage of neutrophils that were FL3 positive following exposure to pHrodo E. Coli. Neutrophils were incubated with (blue line) or without pHrodo labeled E. coli particles (red line) for 2 hours. Samples were then taken and analysed by flow cytometry. b) Histogram showing percentage of neutrophils that were FL3 positive following exposure to pHrodo E. Coli following 15-minute treatment with Cytochalasin D (blue line) compared to neutrophils not exposed to E. Coli (red line). Phagocytosis was reduced from 83.9% to 2.38% by exposure to cytochalasin D.

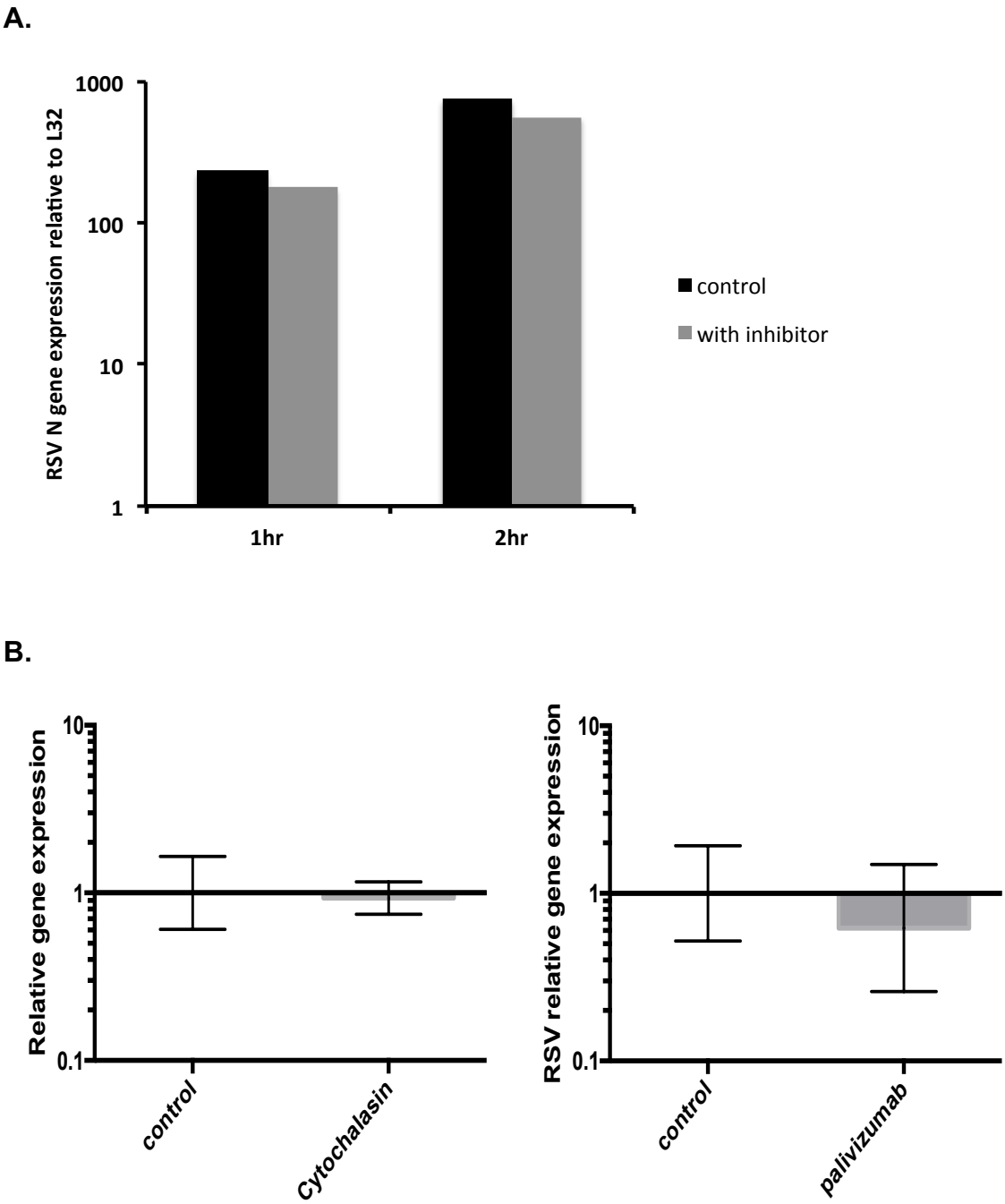

Figure 3-7 RSV uptake following pre-treatment with cytochalasin D or palivizumab.

A. Neutrophils were exposed to RSV +/- pre-treatment with the inhibitor cytochalasin D. This figure is representative of 3 independent experiments showing RSV N gene expression relative to L32, the results of which are summarised in B.
B. Neutrophils were exposed to RSV +/- pre-treatment with cytochalasin D. Neutrophils were exposed to RSV +/- pre-treatment with palivizumab. There was no statistically significant difference in RSV N gene expression in either case.

purified neutrophils at $5x10^6$/ml in DMEM were incubated with RSV preparation for 2 hours, in the presence of GM-CSF, but not the autologous serum usually used +/- the monoclonal RSV antibody palivizumab. At 2 hours, neutrophils were washed in 10 mls PBS twice. The dry pellet was then resuspended in 500ul tryzol and stored at -30 ^oC prior to RNA extraction. RNA extraction and reverse transcription was carried out as described in **Chapter 2**. RSV expression was measured at each time point and quantified relative to the internal housekeeping gene L32 and ΔΔ Ct method was used to quantify RSV expression against expression in neutrophils unexposed to palivizumab **(Figure 3-7b).** There was no statistically significant difference in RSV expression. Friedman test with Conover Inman post hoc test was performed.

3.5.9 RSV can be visualised by confocal microscopy

Using the RSV polyclonal antibody utilised in the previous Western blot, and an IgG Alexa Fluor® 594 secondary (Invitrogen), indirect immunocytochemistry was carried out on neutrophils that had been in culture with RSV preparation for 2 hours, in the presence of GM-CSF and 5% autologous serum. Immunocytochemistry was carried out as described in **Section 2.14**. The nucleus was co stained with DAPI. The image presented is an overlay of the 3 channels used for DAPI, RSV and a brightfield image **(Figure 3-8)**. Neutrophils are shown with positive staining for RSV diffusely in the cytoplasmic area, with exclusion of the DAPI stained nucleus.

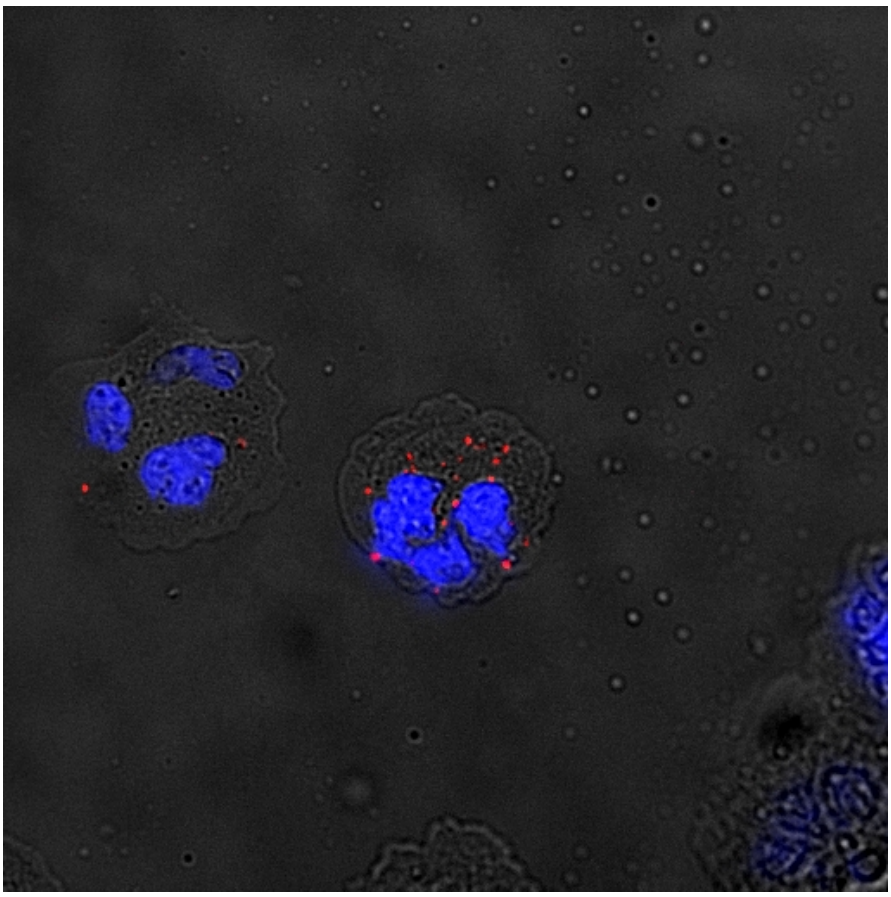

Figure 3-8 Confocal fluorescence microscopy with superimposed brightfield microscopy

Neutrophils that had been incubated for 2 hours with RSV were spun onto slides and fixed with methanol, following which they were stained for RSV and co-stained with DAPI. Images were taken using a Multiphoton Zeiss microscope. 3 channels were used for DAPI, RSV and a brightfield image. The red indicates RSV and blue the nucleus.

3.6 Discussion

Having established and optimised the *in vitro* model of RSV and neutrophil culture in **Chapter 2**, I wanted to investigate the nature of the viral-neutrophil interaction in more detail. **Chapter 2** revealed that the neutrophils had been isolated to a high degree of purity and were functionally competent with respect to phagocytosis. I also showed that the neutrophil remained viable *in vitro* in short-term culture, up to 20 hours, in the presence of RSV and by using the pro-survival factor GM-CSF. Direct interaction of RSV and healthy adult neutrophils was demonstrated *in vitro*. In this chapter, I sought to investigate what happens to the quantity of RSV once it is inside the neutrophil; does viral replication occur?

Studies referenced in this chapter's introduction used a variety of methodologies to establish whether viral replication occurred within the neutrophil. Conventionally, when assessing whether a particular target reduces or enhances viral replication of RSV in cell culture, RT-qPCR is used to measure the expression of virus either against a control value or against an internal housekeeping gene (153, 154). To this end, the approach utilised here was similar. Firstly, A549 cells exposed to RSV and then analysed for RSV N gene expression over time by qPCR, were used as a positive control. Expression at 2 hours represented RSV initially taken up by the cell, whilst increased RSV expression at 20 hours represented newly formed RSV N, indicating transcription of RSV in the cells.

The same methodology was applied to studies of neutrophils incubated with RSV. However, despite an initial robust uptake of RSV at 2 hours, RSV N gene expression did not increase over subsequent time points (4 and 20 hours). In fact there was a trend for RSV N gene expression to decrease over this time. Western blot analysis of the RSV protein content of the neutrophils over time adds weight to this finding, as there was a marked decrease at 20 hours. This suggests that RSV does not replicate inside the neutrophil, and that in fact, virus is being degraded over time within these cells.

In order to ascertain whether viable viral progeny are released from the neutrophil after exposure to RSV as occurs with infected epithelial cells, a further experiment was carried out. Supernatant, from both RSV exposed A549s and neutrophils, was used as media on sterile A549 cells with the intention of transmitting any live virus and causing subsequent infection. This procedure resulted in infection of the A549s by the supernatant of the RSV exposed A549s, but no infection was evident with the supernatant from the RSV exposed neutrophils. This supports the conclusion that viable virus is not released, and most probably not manufactured by the neutrophil.

Contrary to these results the paper by Halfhide *et al*, from our group, suggested that RSV does replicate inside neutrophils, as evidenced by the finding of mRNA in BAL neutrophils from RSV infected infants (129). Understanding the RSV replicative process helps us to understand how RSV mRNA might be manufactured without viral progeny being produced. Upon host infection, viral RNA polymerases synthesise a positive sense mRNA strand. These mRNAs then use host-cell machinery to synthesise viral proteins. Replication of the genome occurs via the production of a positive sense intermediate RNA strand, which is then used for the synthesis of further negative strand sense genome. The dynamics of RSV infection have been tracked in mice using PCR primers specifically targeting the positive sense (replicative intermediate and mRNA) or negative sense (genome) strand RSV RNA (154). Mice are not known to be particularly permissive to RSV and require high inoculation titres. Positive sense strands were found in significantly higher numbers than the negative sense strands, in the whole mouse lung, suggesting that viral replication was impaired. Similar findings were seen in experiments with cotton rats where increasing expression of viral transcripts and genome replication did not lead to the production of detectable progeny virus. This phenomenon has been termed abortive replication (155). The authors hypothesise that this inability to produce viral progeny, despite the presence of transcription, might be due to viral-host cell dynamics, with the murine cells not facilitating effective RSV RNA synthesis. Primarily, RSV infects and replicates in respiratory epithelial cells (156)

(157). However, there are reports of DCs (158), monocytes (159), and macrophages (160) being infected. Monocyte-derived DCs were considered infected on the basis of positivity for GFP expressing virus, a median of 4.9% were positive by flow cytomtery analysis. In monocytes, infection was determined on the basis of RSV gene expression in the monocytes, but not on the release of virus, suggesting that this transcription is abortive. Similarly, *in vitro* work on macrophages showed initial low-level release of infectious progeny, which quickly waned. It would appear that the neutrophil is an additional immune cell that is receptive to RSV entry but not permissive of productive infection.

Given what is known about the hostile environment inside the neutrophil, and its very purpose (i.e. to kill microbes), it is perhaps not surprising that virus, once within the cell, is not able to complete its replicative cycle. The first stage of replication, the production of the mRNA by viral RNA polymerase, could feasibly occur prior to the degradation of RSV. This could explain the measurable presence of RSV mRNA in the Halfhide *et al* study. However, when neutrophils come into contact with foreign particles, NADPH production and the resultant oxidative burst (161, 162), leads to the generation of antimicrobial molecules such as hydroxyl radicals and hydrochlorous acid (163), proteases, defensins and antimicrobial peptides (164). Mostly these processes occur in the neutrophil endosome. Thus if RSV was to be taken up into endosomes, its destruction would be likely. How does RSV gain entry, and concomitant to this, where is the internalised RSV located?

As endocytosis was considered a likely mode of viral entry, and serum contains antibodies and complement, it seemed likely that serum would enhance virus uptake by neutrophils. Phagocytes such as neutrophils express receptors that bind opsonin molecules, enhancing phagocytosis and eventual intracellular killing (165). This was indeed the case. Furthermore, a serum dose response was observed with uptake significantly enhanced with the addition of 1 or 10% autologous serum. The serum enhancement of uptake suggested that RSV was being taken up into the cell by endocytosis. If this were the case then an endocytosis inhibitor should inhibit uptake.

Cytochalasin D was chosen as said inhibitor. It disrupts the cytoskeleton by disrupting actin filaments, preventing formation of a phagosome. Optimisation work using the pHrodo E-coli as the target of phagocytosis confirmed successful inhibition and established the concentration needed for this. Cytochalasin however, did not inhibit uptake of RSV into neutrophils. There is disagreement in the literature over whether all endocytosis pathways are inhibited by cytochalasin. Conventionally it is considered to inhibit phagocytosis, an inherently actin dependant process (166). More recently the actin cytoskeleton has been implicated in clathrin-dependant mechanisms such as macropinocytosis (167), and there is less consensus over the ability of cytochalasin to inhibit these mechanisms. Macropinocytosis is exploited by many viruses as a way of gaining entry into host cells (168). The mechanism involves nonspecific binding to any cell surface component. This triggers the plasma membrane to 'ruffle', leading to the membrane forming macropinocytic protrusions. These protrusions allow uptake of fluid along with suspended particles including virus into the cell **(**Figure 3-9**)**. There is no specific test that will define whether virus gains entry by macropinocytosis, although some believe that as it is reliant on actin dynamics, it should be inhibited by cytochalasin (168). However, it has also been shown that actin filament disruption may allow greater 'ruffling' of the membrane, thus potentially allowing increased entry (169) **(Figure 3-10)**.

If pinocytosis is the mechanism of uptake, which does not rely on opsonisation by antibodies or complement, how does serum enhance uptake? A possible explanation is that of antibody dependant enhancement (ADE), a phenomenon observed in other viral infections such as Dengue Fever, Ebola and HIV (170-172). Non-neutralising antiviral proteins, such as antibodies, facilitate viral entry through interactions of the complement system and receptors. There are several postulated mechanisms. All viruses initiate infection by attaching to host cells via viral surface proteins and their corresponding receptors. Antibodies specific to the viral surface proteins can inhibit or 'neutralise' this process. However, these antibodies may also potentiate this process via crosslinking of virus-antibody complexes through

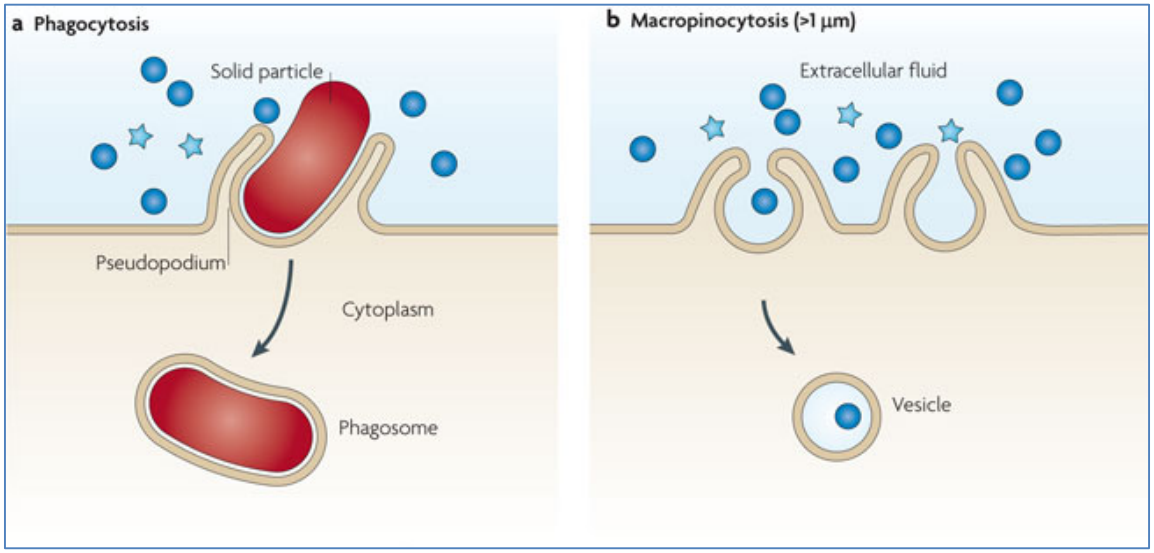

Figure 3-9 Modes of cellular internalisation by phagocytes

a) Internalisation of large particles is facilitated by phagocytosis, and enhanced by opsonisation. b) Non-specific uptake of small particles can occur through macropinocytosis. (Adapted from Petros *et al*, (2010)) (173)

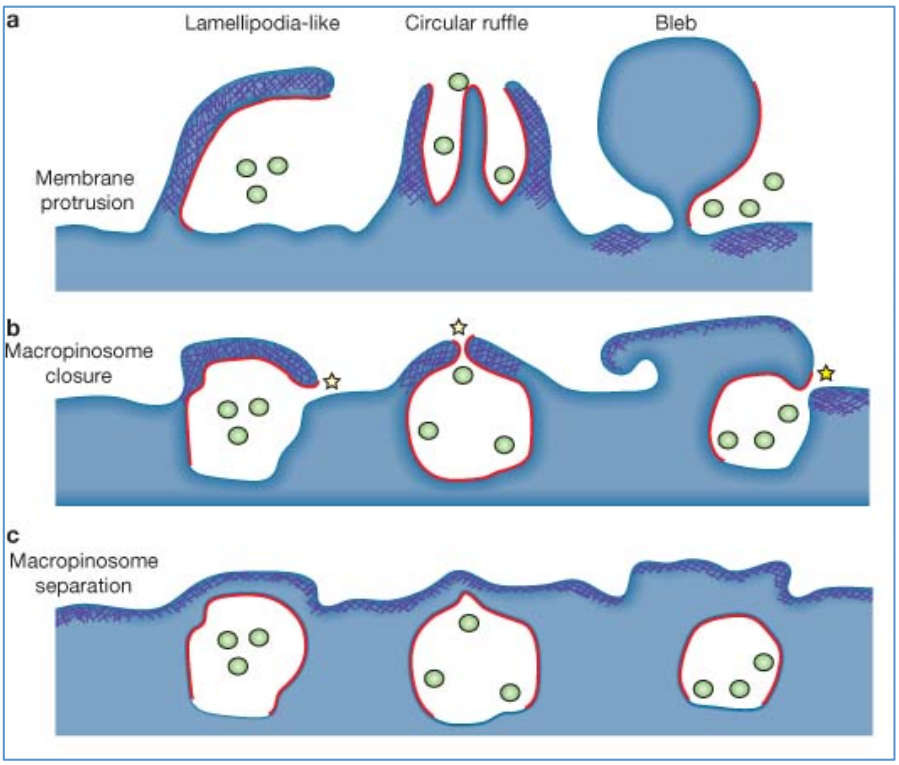

Figure 3-10 Macropinosome ruffling formation

The membrane protrusions involved in macropinocytosis can take the form of planar lamellipodia, circular ruffles or blebs, depending on the cell type. Lamellipodia and circular ruffles require polymerisation of actin. Bleb formation is probably the result of local actin cortex destabilization. The blue lines represent actin and the red lines the portion of the protrusion that will constitute the membrane of the macropinosome. The three different forms are shown going through three stages a) membrane protrusion, b) macropinosome closure, and c) separation of the macropinosome. The star shows the site of closure. (Taken from Mercer & Helenius, (2009)) (174)

interaction with cellular Fc receptors (175). *In vitro* uptake of RSV in the presence of RSV specific antibodies has previously been investigated in airway epithelial cells. Monoclonal antibodies to RSV surface F and G glycoproteins were found to have neutralizing and enhancing properties (176). Palivizumab, which is known to neutralize RSV infection of epithelial cells, was investigated in our culture system. Palivizumab did not appear to neutralise or enhance uptake of the RSV when compared with the usual culture conditions. This would suggest that the presence of antibody in the culture system might not be a contributing factor to the enhancement of uptake. It also shows that neutralisation by an IgG RSV antibody does not prevent uptake by the neutrophil.

Pharmacological inhibition of endocytosis is an inherently difficult process to investigate because of the nonspecific effects of the available inhibitors used to distinguish the major endocytic pathways (177). My lack of success elucidating a mechanism of uptake with cytochalasin and the high likelihood of similar results with other pharmacological inhibitors of endocytosis, led me to attempt using visualisation to gain more insight into the biological processes at play. Visualisation has played an important role in our understanding of biology since the 17th century when Robert Hooke, a natural philosopher, published his book *Micrographia* with hand drawn images of biological objects, termed cells (this term was first coined in this book) observed by microscope. The book was a best seller and sparked public interest in microscopy. Visualisation in biology has gone on to become more complex particularly with the advent of computer technology. Visualisation is particularly useful for conveying information, especially where data is not easily summarised by equations or algorithms. I therefore used indirect immunocytochemistry to fluorescently label RSV in situ. This serves two purposes. Firstly, to confirm true internalisation of the virus, as all previously used methodologies could have been detecting/measuring attached rather than internalised virus. Secondly, if internalised virus was confirmed then the location of it could be explored.

The confocal image shows diffuse cytoplasmic speckling of fluorescently antibody labelled RSV. The size and distribution of RSV within the cells is suggestive of an endosomal location. This result confirms that it is possible to identify virus using microscopy and further validates the association of the neutrophil and virus *in vitro*. However, this image does not prove internalisation - the virus could still be attached to the outside of the cell. This is because if the 'pinhole' within the confocal microscope is wide open, then it is possible for the whole cell to be imaged rather than a slice in the image so generated. However, several aspects of the image taken suggest that this does indeed represent internalised virus, such as the lack of virus 'in' any of the nuclei and the lack of virus seen around the edge of the neutrophil. Additional confocal work is required to verify this result and this is described in the following chapter.

The quantity of RSV used for all the neutrophil experiments in this and subsequent chapters should be discussed. RSV MOI 0.1 was used, initially because producing RSV of high enough titre to have a higher MOI was difficult. However, it became apparent that this MOI was adequate to both quantify and visualise RSV in conjunction with the neutrophil. MOI relates to the number of infective particles per cell and thus only measures the infective capability of the virus. It has long been recognised that a large number of non-infective particles are produced in the laboratory propagation process and as the RSV – neutrophil interaction is not one of replicative infection, the measurement of MOI becomes less relevant; both infective and non-infective virions may participate in the interaction (178, 179).

3.7 Summary

The data presented in this chapter do not suggest that RSV replicatively infects neutrophils. Rather, it reveals that RSV is taken up by neutrophils with maximal uptake at 4 hours and reduction by 20 hours. RSV uptake is improved by serum, which may be as a result of antibody mediated enhancement. The mechanism of uptake has not been confirmed but macropinocytosis is a possible pathway. This would lead RSV to be localised

in endosomes in the cytoplasm as suggested by the initial confocal images, whilst not necessarily being inhibited by actin disruption.

Chapter 4 Visualisation of RSV within the neutrophil by confocal microscopy

4.1 Introduction

In **Chapter 3**, I established that RSV appears to enter neutrophils, in a serum dependant manner, before being degraded. Initial confocal microscopy showed that the virus was localised to the cytoplasm, in small discrete pockets resembling endosomes. Cytochalasin D, an actin cytoskeleton disruptor, did not prevent uptake of the virus, from which it can be inferred that phagocytosis is not the mechanism of uptake, as this is an actin dependant process. In addition, phagocytosis is not a common mechanism used by a virus to enter host cells; other forms of endocytosis are more commonly exploited due to the particle size of viruses (180).

As obligate intracellular parasites viruses must enter host cells to replicate. They can do this in two ways: by a direct mechanism at the plasma membrane or by hijacking the host cell's endocytic pathways (181). Internalisation itself is generally not sufficient for productive infection. An incoming virus contained within an endosome can be construed as still being within the extracellular space. Therefore, endocytosed viruses must penetrate or fuse with the endosomal membrane to be released into the cytoplasm (182). Viruses not only depend on the machinery of the cell for internalisation but also for trafficking within the cytoplasm to the site of replication. For nuclear replicating viruses especially, the endosome can enable delivery of its viral cargo to the nuclear pore, ready for translocation into the nucleus.

Endocytosis is used by cells to internalise extracellular particles, and starts with the formation of primary endocytic vesicles (PEVs). It is the formation of these PEVs that varies between the different types of endocytosis. PEVs are then routed to endosomes, where processes such as recycling, degradation, and storage occur. There are six known endocytic pathways used by viruses to gain entry into cells. However, there is considerable overlap between

pathways and it may be that many of these are actually the same pathway, modified by virus or host response (180). Newly discovered and better characterised endocytic mechanisms mean that studying virus entry has become more complex. Mechanisms of virus entry that were once thought understood have come under further scrutiny as more specific and sensitive methodologies are employed; paramyxoviruses such as RSV are one such family of viruses.

Paramyxovirus entry is conventionally thought to occur through virus-cell membrane fusion and is mediated by their attachment proteins and fusion protein F (183). The F protein undergoes conformational change upon attachment, which results in membrane fusion. The events that occur subsequent to receptor binding, that leads to the triggering of the F protein, remains largely unknown and appear to be diverse even amongst viruses of the same family. The paramyxovirus family contains many common human pathogenic viruses, including measles, mumps, the parainfluenza viruses, RSV, human metapneumovirus (HMPV), and the zoonotic henipaviruses, Hendra and Nipah and avian virus Newcastle disease. Evidence for an alternative mechanism of entry by some members of the paramyxovirus family has been postulated. Newcastle disease virus, although able to enter cells by direct fusion, has been shown, through chemical inhibition studies, to also use caveolae-dependant endocytosis (184). Similarly, Schowalter *et al* describe that HMPV entry may require endocytosis, evidenced by up to 90% reduction in infectivity following clathrin-mediated endocytosis inhibition (185, 186).

There is some evidence suggesting that endocytosis could at least be partially involved in RSV entry. Entry of RSV into host cells is specifically dependent on interactions between its surface glycoproteins G and F proteins, which bind to cellular glycosaminoglycans (187). A specific cellular receptor had yet to be described until 2011 when Hegele *et al* showed that RSV interacts with host-cell nucleolin via the viral fusion envelope glycoprotein and binds specifically to nucleolin at the apical cell surface.

Studies on RSV entry have mostly concluded that RSV, similarly to the other paramyxoviruses, fuses its membrane directly with the plasma membrane of target cells (8). Some more recent studies however contest this. Kolokoltsov *et al* inhibited RSV infection of HeLa cells using targeted siRNA knockdown of clathrin light chain, Eps15, and AP-2 surmising that RSV makes use of clathrin-mediated endocytosis (10). San-Juan-Vergara *et al* argue that in primary bronchial epithelial cells, RSV entry is a two-step process; RSV docks to cholesterol-rich plasma membrane domains facilitating hemifusion between the viral envelope and the plasma membrane followed by endocytosis (188). In 2013, Helenius *et al* investigated RSV entry into HeLa cells and A549 cells using multiple endocytosis assays, concluding that the mechanism of entry had all the hallmarks of macropinocytosis including blebbing of the plasma membrane, elevated fluid uptake, and internalisation of intact RSV particles into macropinosomes (11, 188).

Macropinocytosis is used by a number of viruses to gain host entry e.g. vaccinia virus and herpesvirus (174, 189). Virus particles are capable of triggering membrane *'ruffling'*. Vacuole formation occurs at the plasma membrane and viruses are internalised in macropinosomes. Penetration by the virus can then occur through the macropinosome membrane and virus enters the cytosol. Proving macropinocytosis as the mechanism of uptake is difficult. Visualization of virus particles at the site of membrane *'ruffles'* or within large irregular vesicles, were used to demonstrate a role for macropinocytosis in the entry of human immunodeficiency virus type 1 into macrophages (190).

It is not clear if viruses interact differently with immune and non-immune cells. It is likely that individual viruses use alternative mechanisms to enter different cell types. It may be that mechanisms used by virus to enter epithelial cells and replicate, conversely result in degradation in immune cells. For example, uptake of RSV and subsequent presentation of viral antigen to T lymphocytes by bovine DCs occurs via a caveolae-dependent endocytic mechanism. Caveolae, a type of plasma membrane lipid raft, are formed and maintained by the protein caveolin. In epithelial cells, caveolae

provide a safe route for virus to enter the cell, but in APCs, caveolae target the virus for degradation prior to processing and presentation of viral antigens (191). Endocytic entry into neutrophils by any virus has not been extensively investigated; some work has been done in macrophages (192). Macrophages express viral PRRs, the purpose of which is for recognition of viruses and triggering of an immune response. However, viruses have been known to engage these receptors to attach to and enter immune cells (193). Neutrophils express similar PRRs, which may be significant in RSV uptake.

In this chapter I use confocal microscopy to confirm true internalisation of RSV in neutrophils, rather than surface membrane attachment, and to gain insight into the mechanism of entry into the cell. Preliminary data presented at the end of **Chapter 3** showed that RSV could be identified using indirect immunocytochemistry. In this chapter further images are presented which better identify the exact location of the virus. I also undertook work to find out whether RSV can be localised inside endosomes, using dextran as a marker of pinocytosis.

4.2 Hypothesis

RSV is taken up by macropinocytosis into neutrophils.

4.3 Aims

The specific aims of this chapter are:

1. To identify the location of RSV in the neutrophil.
2. To determine the mechanism of uptake.

4.4 Specific methods

As in the previous chapter, neutrophils were incubated with RSV (MOI 0.1) in DMEM in the presence of 5% autologous serum and GM-CSF. After the incubation period cytospin slides were made of cells, which were then labelled and stained for imaging as detailed in **Section 2.15**. A full list of the antibodies used can be found in **Table 2-7**.

4.4.1 Z stack

Taking a series of z-stack images is a technique whereby multiple images are combined to give a resulting image with a greater depth of field. Successive single images were taken at different focal depths, by moving the objective lens, and these sets of images, known as z stacks, were reconstructed to create either a single 2D stack (the maximal pixel intensity was taken), or a 3D image using Imaris software. Orthogonal views have been used to display this data. In addition to a XY image, the XZ and YZ images for a certain spot are shown to demonstrate internalisation of the virus inside the neutrophil.

4.5 Results

4.5.1 Validation of RSV F monoclonal antibody by Western blot

To confirm that the monoclonal antibody that I planned to use in the immunocytochemistry experiments was specific for the RSV F protein in neutrophils, I used a Western blot technique. Neutrophils that had been incubated with RSV for 2 or 4 hours, and epithelial cells that had been infected with RSV for 24 hours, were probed with the anti-RSV F antibody (Abcam) using the method described in **Section 2.13**. The Western blot confirmed the specificity and sensitivity of the antibody **(Figure 4-1)**.

4.5.2 Optimisation of RSV antibody using epithelial cells as a positive control

To optimise the antibody for confocal microscopy, RSV infected epithelial cells (BEAS-2Bs) were used as a positive control. Confluent BEAS-2B cells were infected with RSV (MOI 1) for 24 hours before being spun onto a slide, fixed and labelled with RSV F antibody (1/100) for 1 hour. The secondary IgG Alexa fluor® 594 antibody was used and the nuclear stain DAPI. **Figure 4-2** shows RSV infection of the epithelial cells with positive staining in the nucleus and cytoplasm. The isotype control was negative.

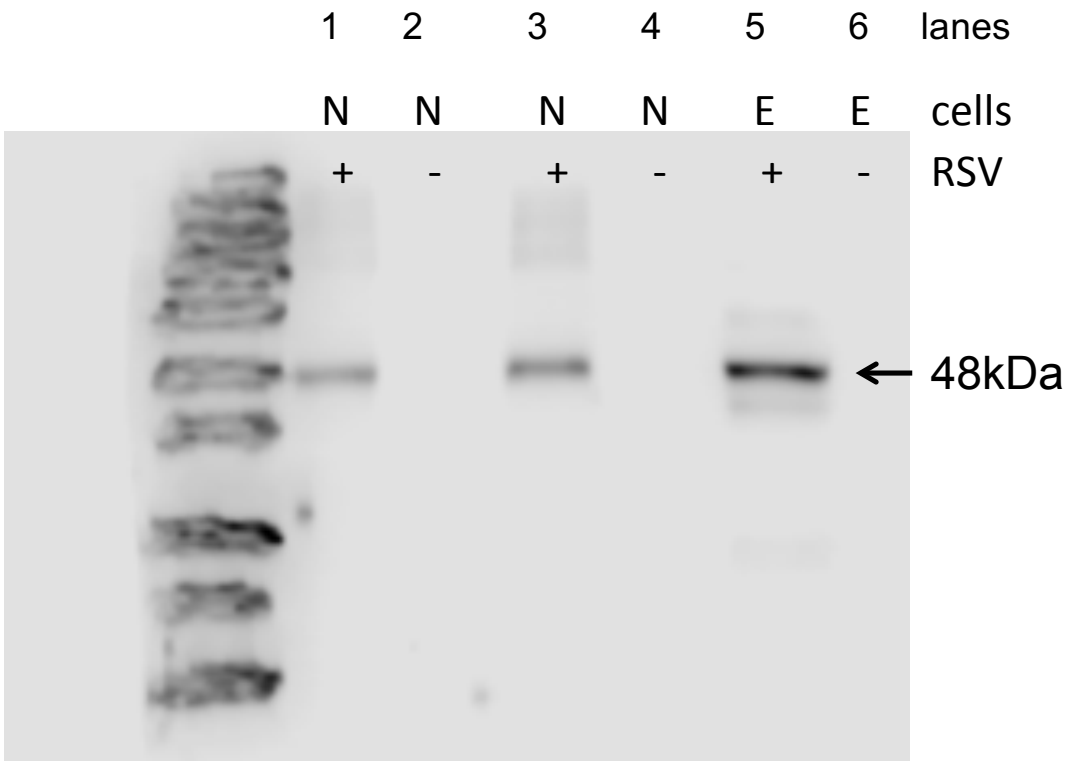

Figure 4-1 RSV F antibody validation by Western blot

Lanes 1-4 show the presence or absence of RSV F protein by Western blot analysis of neutrophil pellets (N). Lanes 5-6 show the presence or absence of RSV F protein from epithelial cell pellets (E). RSV F protein has a molecular weight of 48kDa, and the protein band seen was confirmed to be such using the ladder on the left side of the image. Neutrophils were incubated with RSV for 2 or 4 hours before being washed and pelleted. Epithelial cells were infected with RSV and cells harvested at 24 hours before being washed and pelleted. The RSV F monoclonal antibody is seen be sensitive and specific in epithelial cells and in neutrophils.

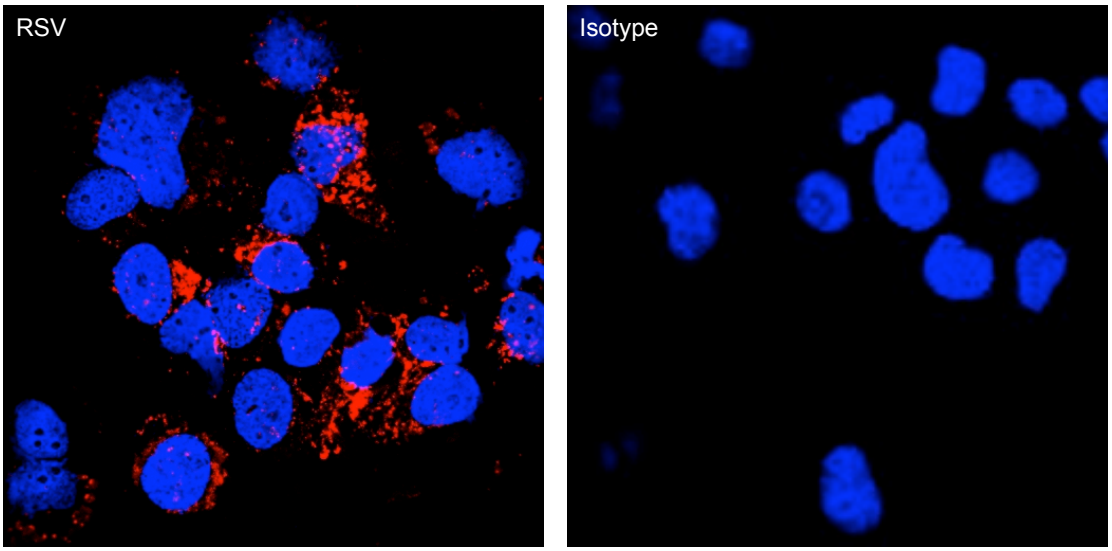

Figure 4-2 RSV antibody optimised to show BEAS2B RSV infection by confocal microscopy

Fluorescent confocal image of BEAS-2B cells visualised by their blue DAPI stained nucleus. RSV is visualised using RSV F antibody and IgG Alexa Fluor® 594 secondary and is illustrated in red. The isotype control, matched to primary antibody concentration, reveals no nonspecific binding.

4.5.3 RSV is internalised within the cytoplasm of the neutrophil

Neutrophils, incubated with RSV for 2 hours (**Chapter 2**), and then fixed on slides, were labelled using RSV F antibody and IgG Alexa Fluor® 594 antibody. The nuclei were stained using DAPI (1:10,000). Single images were taken as described in **Section 2.5.13**. These show RSV localised in the cytoplasm in discrete pockets **(Figure 4-3)**. Additional slides were labelled with the same primary antibody but with an IgG Alexa Fluor® 488 secondary. The cytoplasm was stained using Evans Blue, which emits at a similar wavelength to the previously used 594 secondary. Z-stacks were taken and are presented as orthogonal views. The z-stacks reveal that the RSV is indeed internalised within the cytoplasm as evidenced by the green speckles entirely surrounded by red stained cytoplasm **(Figure 4-4)**. Surface rendered 3D projections of the images were generated using Imaris (Bitplane). This surface can be given visualisation properties such as transparency. In this figure the solid rendered cytoplasm is made 70% transparent revealing the internalised RSV **(Figure 4-5)**. In the subsequent images, Imaris 'Spot object' was used to show localised RSV as small spheres. A representative neutrophil is shown in 3D with opaque surface render. When the cytoplasm is changed to 70% transparency, RSV can be seen, now represented by small green spheres **(Figure 4-6)**. In the next set of images a collection of neutrophils are shown, with z stacks processed to produce surface rendered 3D images which have then been, made partially transparent and then rotated 45^{o} to look through the neutrophils revealing the RSV inside **(Figure 4-7)**.

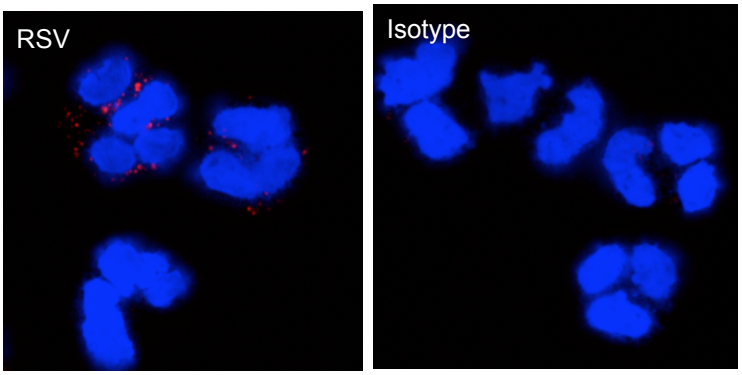

Figure 4-3 Neutrophils visualised by confocal microscopy showing positive staining for RSV F protein

Fluorescent confocal images of neutrophils, visualised with their nuclei stained with DAPI, in blue. RSV is visualised by positive staining for RSV F antibody and is shown in red.

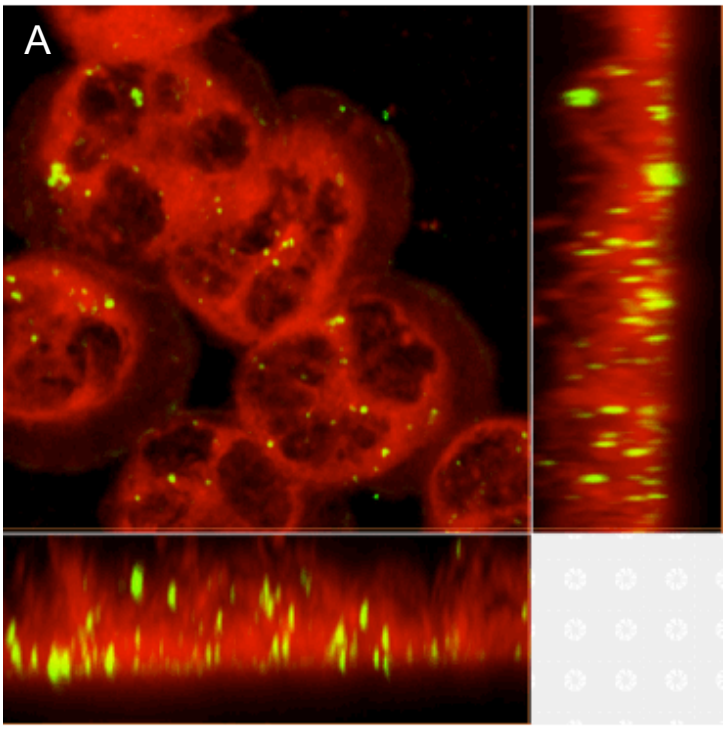

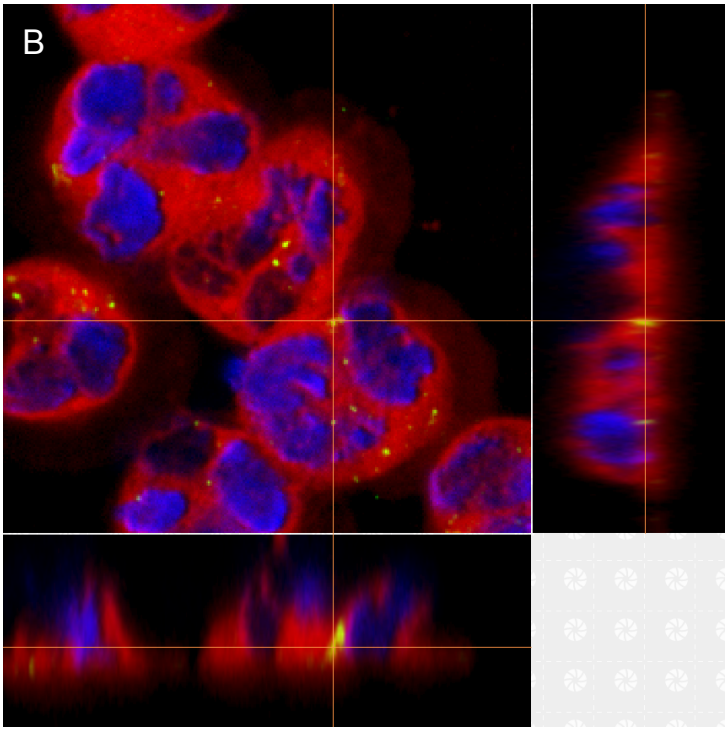

Figure 4-4 Orthogonal view showing RSV within the neutrophil cytoplasm

(A) Z stack orthogonal view of neutrophils, showing RSV (green) throughout the cytoplasm (red) (B) The same image is presented in the second panel but with the red pointer focused on an RSV antigen inside the cell, entirely surrounded by red in the ZX and YZ images. In this image the nucleus stain channel is shown (blue).

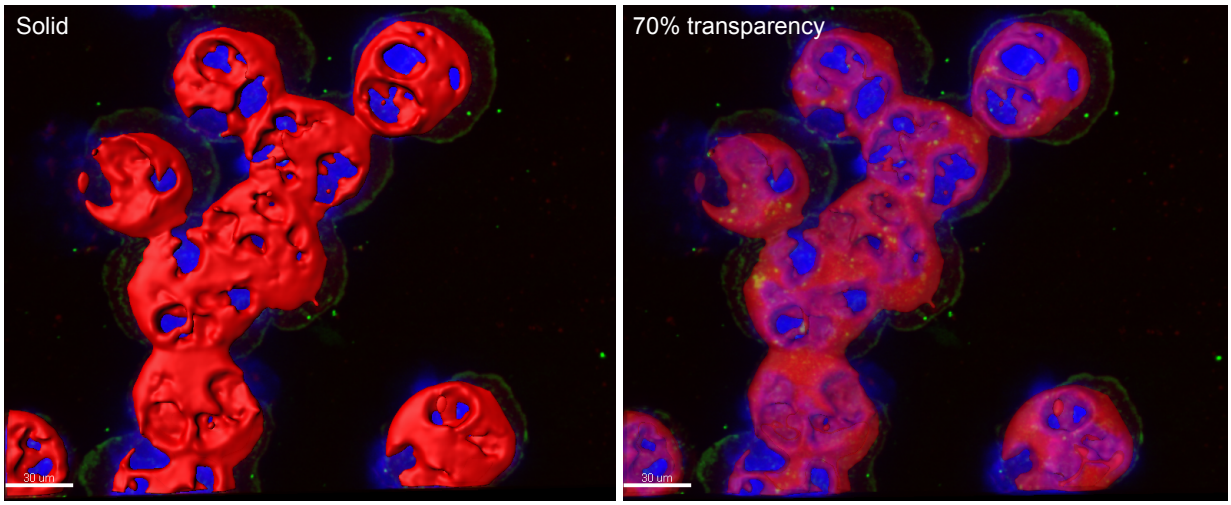

Figure 4-5 Surface-rendered neutrophil projection

Representative neutrophils are shown after image analysis reveals the surface rendered fluorescence from Evans Blue cytoplasmic stain (red). The 3D rendered z-stack confocal image of the cells is visible in the first image with solid cytoplasm. In the second image the cytoplasmic dependent fluorescence intensity is decreased, becoming 70% transparent, the internal RSV (green) is readily visible within the cytoplasm (red).

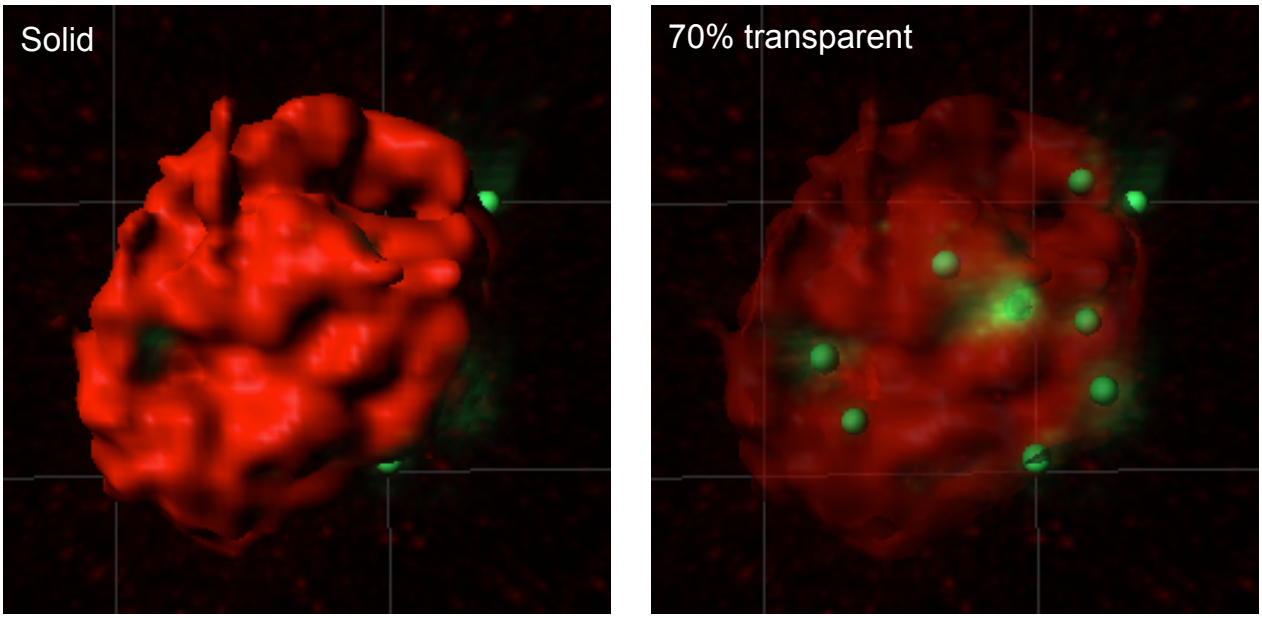

Figure 4-6 Surface rendered neutrophil

The opaque 3D neutrophil image reveals the surface rendered fluorescence of the Evans Blue stained cytoplasm (red). When the render is made 70% transparent, RSV (green) becomes readily visible inside the cytoplasm.

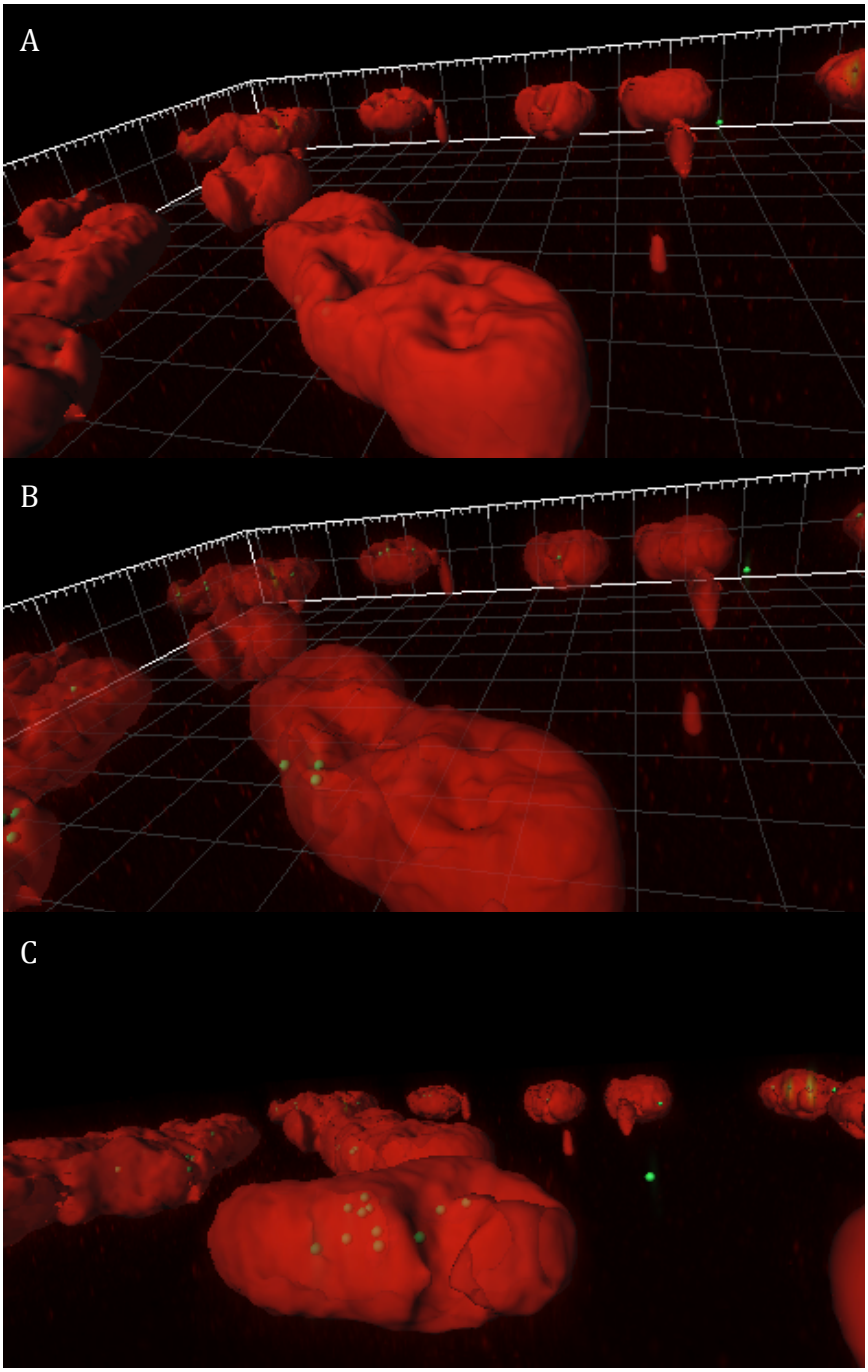

Figure 4-7 3D reconstruction of neutrophils and internalised RSV

The top panel (A) shows the 3D rendering of z-stacks taken through the neutrophils. The surface has been rendered and the Evans Blue stained cytoplasm (red) is opaque. In the middle panel (B) the surface render (cytoplasm) has been made 70% transparent, revealing internalised RSV (green) surrounded by cytoplasm. In the bottom panel (C), to better analyse the location of the RSV, the image has been rotated 45^{o} along its y-axis. This image clearly shows the spatial position of the RSV with respect to the cytoplasm.

4.5.4 Measurement of discrete RSV labelled areas within neutrophils

Using Fiji calibration and measurement tools, the size of discrete areas of RSV staining were measured (139) and were between 0.5 – 1.3μm **(Figure 4-8)**.

4.5.5 RSV is not co-localised with dextran in endosomes

To ascertain whether RSV was localised in endosomes, dextran was used as an endosomal marker. Tracing internalisation of extra-cellularly introduced fluorescent dextran is a standard technique for analysing fluid-phase endocytosis such as macropinocytosis (194-196). Neutrophils were incubated with RSV at the usual conditions but with or without the addition of a fluorescently labelled dextran. Dextran 10,000MW, alexa fluor® 594 labelled, anionic fixable (life technologies) was used at 25μg/ml. Preliminary experiments optimising this method appeared to show that the location of the dextran and RSV were mutually exclusive **(Figure 4-9)**. In view of this, multiple images were taken of neutrophils exposed to both dextran and RSV. FIJI colocalisation analysis was used to measure the degree of spatial overlap between the fluorescently labelled RSV and dextran. Manders coefficient, which expresses the fraction of colocalising objects in a dual colour image, with 1 being total colocalisation, was used (197). The mean Manders coefficient for dextran and RSV colocalisation was 0.03 (+/- 0.02), which indicates that they were not colocalised **(Figure 4-10)**.

4.5.6 RSV uptake is not prevented by inhibitors

Pharmacological inhibitors were tested to determine if they prevented uptake of RSV into the neutrophil. A selection of drugs with differing properties was used to narrow down the mechanism of uptake, specifically, amiloride (100μM), nystatin (50μM), monodansylcadaverine (MDC) (100μM) and cytochalasin D (10ug/ml) (all Sigma).

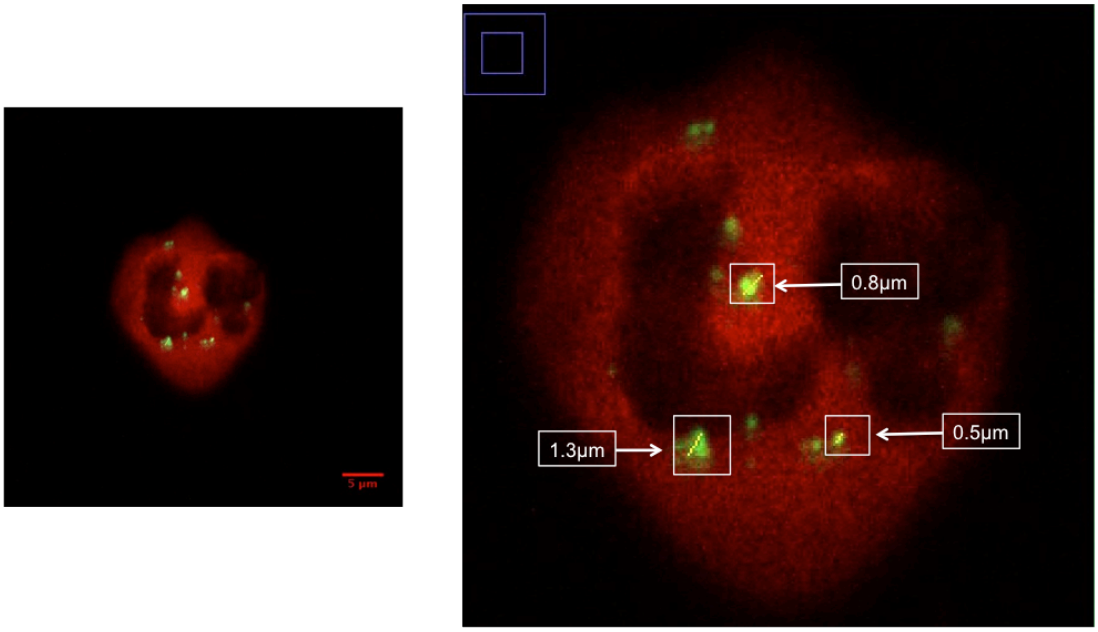

Figure 4-8 Measurement of internalised RSV

A representative neutrophil is shown with the cytoplasm stained with Evans Blue (red) and RSV labelled with IgG Alexa Fluor® 488 (green). In the 2nd image the image has been zoomed in and 3 RSV areas are shown with a ruler and associated measurement as recorded in FIJI.

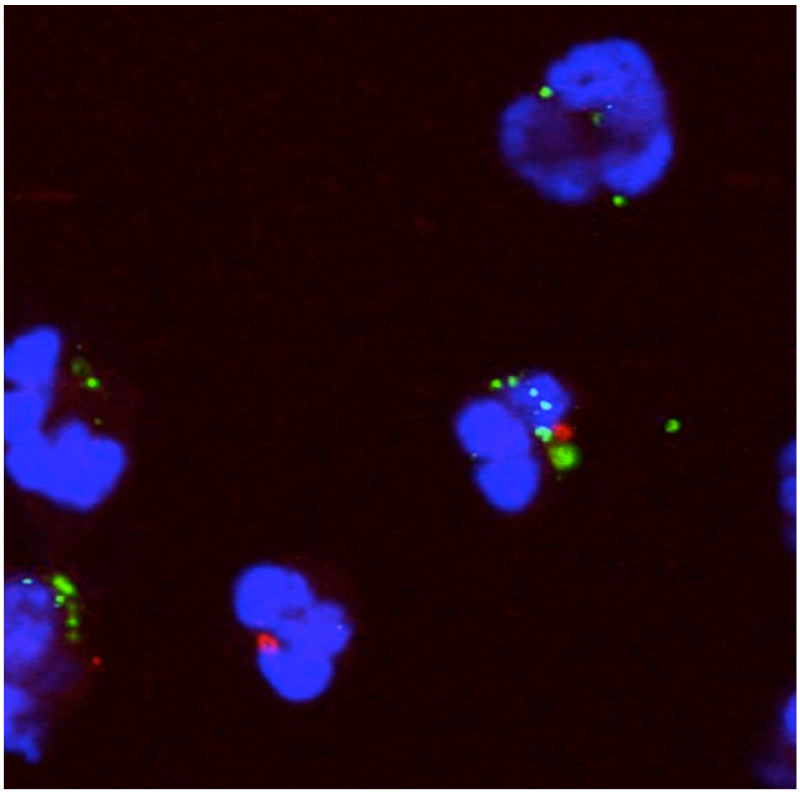

Figure 4-9 Dextran and RSV visualised by confocal in a neutrophil

Neutrophils were imaged following incubation with Alexa fluor 594® labelled dextran 10,000MW. Dextran (red) can be seen in association with the neutrophil and RSV can be seen (green), both inside the neutrophil in close proximity but not overlapping. x40 magnification.

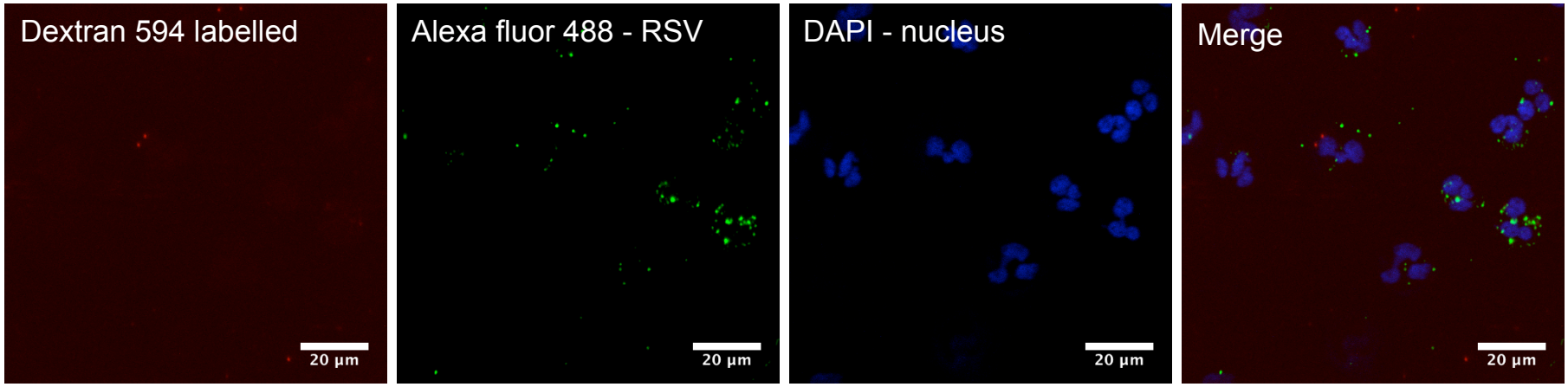

Figure 4-10 Dextran and RSV are not colocalised in neutrophils

Representative fluorescent image of neutrophils showing the 3 channels, dextran, RSV and nucleus and a composite image.

Amiloride inhibits macropinocytosis through the blockade of sodium-proton exchange (198). Nystatin inhibits caveolae-mediated endocytosis by distorting the structure and function of the cholesterol rich membrane domain (199). MDC is a specific blocker of clathrin-mediated endocytosis (200) (201). Cytochalasin D is an F-actin depolymerizing drug that inhibits phagosome formation. It is generally considered to be a global and non-selective uptake inhibitor (152). Neutrophils were confirmed to be viable in the presence of the stated concentration of the inhibitors by Annexin V/PI flow cytometry analysis. Images of neutrophils were identical, whether exposed to the inhibitors or not, indicating that none of the inhibitors prevented RSV uptake. **Figure 4-11** shows the absence of nystatin inhibition as a representative example of the results of all inhibitors.

4.6 Discussion

In **Chapter 3**, I established that RSV genomic material and protein could be measured within neutrophil preparations following a two-hour incubation period. That this association was enhanced by the addition of serum and that the amount of RSV reduced over time, led to the question addressed in this chapter as to the mechanism of uptake. Although evidence suggested that the RSV was located intracellularly, rather than being attached to the cell surface, and preliminary confocal images appeared to show virus within the cytoplasm, conclusive evidence was sought to prove internalisation of the virus.

The use of the z stack series and subsequent image analysis revealed that the RSV was internalised within the neutrophil. It was consistently found to be in the cytoplasm, and never in association with the nucleus. It was located at all depths of the cytoplasm and the size of the discrete pockets of RSV staining (0.5 - 1.3μm) indicated that it could be within endosomes. RSV virions are 0.15 - 0.3μm, suggesting that either single or multiple virions were being observed together.

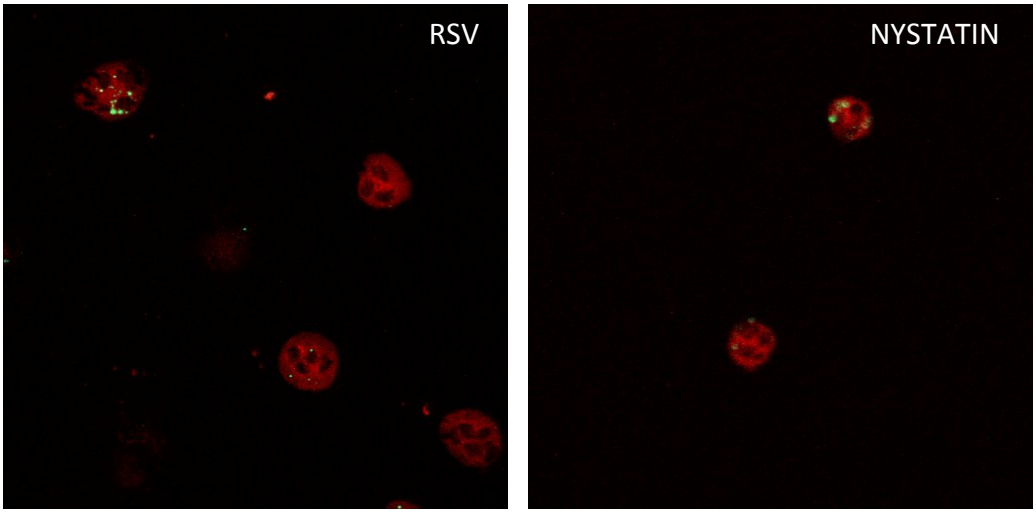

Figure 4-11 RSV visualised in neutrophils with and without inhibition

Representative confocal image of neutrophils incubated with RSV, in the presence or absence of the inhibitor nystatin. Neutrophil cytoplasm is seen in red (evans blue stain) and the RSV in green (IgG Alexa Fluor® 488).

Having established that the virus was intracellular, I investigated its mechanism of uptake. My hypothesis that uptake was via endocytosis was based on evidence from the literature, discussed in the introduction, indicating paramyxoviruses including RSV might use this mechanism to gain entry to host cells. The known endocytic pathways used by viruses to gain access into host cells is shown in **Figure 4-12**. This was supported by the appearance and size of the RSV 'pockets' within the cytoplasm. An externally introduced fluorescently labelled dextran to localise endosomes is a standard technique to visualise endocytosis (181, 202), as unless taken up by endocytosis, dextran is membrane impermeant. In addition, the use of florescence microscopy to investigate protein colocalisation is a widely used tool for assessing the extent of spatial coincidence between intracellular molecule (197, 203). Both of these techniques were exploited to investigate whether RSV could be localised within endosomes. The result was conclusive – RSV did not colocalise with dextran.

There are a number of possible explanations for this finding. Firstly, RSV passes through the endosomal pathway at a different rate to dextran and thus is not found in the same place at the same time. Secondly, the endosomal pathway classically described in macrophages differs in neutrophils, and that RSV and dextran are actually in different types of endosomes. Lastly, it is possible that RSV doesn't enter endosomes and the mechanism of uptake is not endocytosis. Each of these explanations will be dealt with in turn.

In neutrophils, the formation and maturation of endosomes differs from that of other phagocytic cells such as macrophages. Investigating the neutrophil endosomal pathway is difficult. Neutrophils are terminally differentiated and do not survive in long term culture, as such manipulating them, for example with genetic modification, in order to define pathways has not been possible. It is common therefore, for endocytic mechanisms characterised in macrophages to be extrapolated to neutrophils, despite their inherent differences (204).

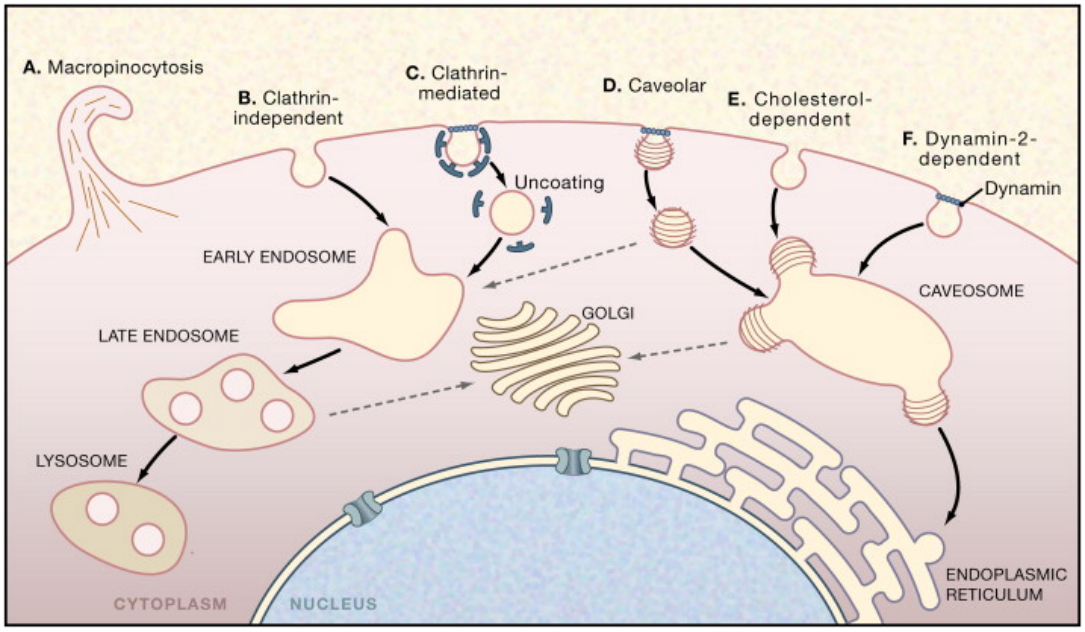

Figure 4-12 Endocytic pathways used by viruses

The six known pathways used by viruses to gain host cell entry are illustrated. Macropinocytosis (A) is involved in adenovirus entry and has been implicated in RSV uptake by Hep2 cells. Amiloride inhibits macropinocytosis. Clathrin-independent endocytosis (B) has been shown for entry of influenza virus. MDC is a specific blocker of this mechanism. Clathrin-mediated uptake (C) is the most commonly used pathway by virus. Caveolar pathway (D) is one of several cholesterol-dependant mechanisms and can be inhibited by nystatin. Cholesterol-dependant endocytosis (E), with no requirement for clathrin or caveolin, is used by polyomavirus. Dynamin 2-dependant pathway (F) is similar to D except it is dependant on dynamin 2. (Taken from Marsh & Helenius 2006 (180))

In macrophages, the process is well characterised and follows the traditional pathway of early and late endosomes (205). After internalisation, the contents of the endocytic vesicle are targeted to an early endosome. Those contents that are not recycled are then delivered to late endosomes where degradation may occur. Lastly the endocytic cargo is delivered to lysosomes for terminal degradation (206).

Neutrophils do not possess this classic endosomal pathway. Early and late endosomes are not found. Instead, neutrophils have a large number of pre-formed vesicles and granules that can fuse with the in-coming endosome. The timing of fusion of the different granule types has not been established. There are also very few studies which show how pathogens are handled within the endosomal pathway of the neutrophil (205). This deficit in available knowledge means that data derived from a method optimised to study macrophage endocytosis, may not mean the same for a neutrophil. For example, internalised particles in neutrophils might move through the cytoplasm in endosomes at different rates depending on their content. This would result in dextran and RSV being at different stages of endocytosis when visualised, unlike in macrophages where anything taken up by pinocytosis would pass through from early to late endosomes at a similar speed. Stopping the experiment at multiple time points to look at particle progression, and whether they ever colocalise would be a method to investigate this further.

Not enough is known about the endocytic mechanism of the neutrophil to know whether dextran and virus would end up in the same compartment together, even if they were both taken up by macropinocytosis. The neutrophil contains a variety of granules that fuse with incoming endosomes, delivering antimicrobial and cytotoxic substances to aid pathogen destruction (207). It may be that internalised virus is handled differently by the neutrophil to internalised dextran. Neutrophils also contain viral PRRs so could recognise virus as a threat and consequently handle it differently to inert dextran. However, the use of endocytosis by virus as a mechanism of entry into neutrophils suggests that it might confer some evolutionary advantage.

Endosomal conditions, such as low pH, can trigger un-coating of virus or enable release from the hostile endosome (208, 209). This could enable the virus to avoid degradation. If this were to be the case for RSV, then it might allow the virus to escape the endosome into the cytoplasm, hence the spatial separation from dextran, which might still be contained within the endosome.

Paramyxovirus entry to host cells is usually by means of plasma membrane fusion. However, some paramyxoviruses have also recently been shown to use endocytosis to gain entry into some cell types. The type of endocytosis used by a cell or pathogen seeking entry is determined by particle size, receptor availability, and cell tropism. I hypothesised that macropinocytosis would be the specific endocytic mechanism of uptake for RSV because this is the mechanism used by multiple other viruses including vaccinia, coxsackievirus, herpes simplex virus 1 and HIV (174, 210-212). Interestingly, HIV can also enter host cells by plasma membrane fusion, with its surface glycoproteins activated by binding to two surface receptors triggering conformational change, resulting in fusion of the virus envelope with the plasma membrane (213). Macropinosomes are irregular in size and shape, with a diameter of 0.5–10 μm, which would fit with the size and irregularity of the pockets seen in the neutrophil images. In addition, this mechanism has recently been demonstrated for RSV entry into HEP2 cells. That the virus does not appear to be within endosomes would suggest endocytosis, of any type, is not the mechanism involved in RSV uptake in neutrophils. Virus entry mechanisms into neutrophils have not been extensively investigated. It is evident however, that individual viruses can use different methods of entry depending on the host cell type. Although useful to gain knowledge about RSV entry into other cells, it does not necessarily extrapolate to the neutrophil.

As the colocalisation experiments were not able to provide an answer regarding the mechanism of uptake, I revisited the use of endocytosis inhibitors, using visualisation of internalised virus as the outcome measure. Quantifying virus uptake would have been ideal, to see if there was a measurable reduction in uptake with the use of inhibitors, as multiple

mechanisms of entry is a possibility. However, no method of quantification in previous optimisation experiments had proved reproducible. As none of the inhibitors appeared to prevent uptake, with the visual quantity of RSV identical with or without inhibitors, further quantification was not pursued.

Cytochalasin D has consistently failed to inhibit RSV uptake measured by PCR and now confocal microscopy. As discussed previously **(Chapter 3)**, the role of actin in macropinocytosis is accepted. However, whether the actin disruption effected by cytochalasin D disrupts macropinocytosis, inhibiting uptake, has been disputed. This is because the effect of cytochalasin D may vary depending on cell type (214). Keller *et al* also found that cytochalasin D could stimulate, rather than prevent, fluid pinocytosis and increase actin polymerization in neutrophils and that neutrophil pinosome formation differed depending on the stimulus. Thus cytochalasin D inhibited dextran uptake when used to inhibit phagocytosis of one strain of *S. Pyogenes* bacteria. However, pinocytic uptake occurred when it was similarly used to inhibit phagocytosis of a different strain (215). The authors concluded that the neutrophil actin filament network behaved differently dependant on different conditions. For these reasons I trialled a number of endocytosis inhibitors, all identified in a recent review of pharmacological inhibition of endocytosis (177). All these inhibitors had limitations and there is considerable overlap in their inhibitory effects on different endocytic processes. That they did not inhibit RSV uptake at all into neutrophils is likely because the mechanism of uptake was not endocytosis. However, it must also be considered that the inhibitors may not be, at the concentrations used, successful inhibitors in neutrophils. Testing them further using a variety of endocytic targets would be an appropriate next step to consider.

Given that all tested endocytosis inhibitors failed to stop uptake and that no evidence has been gained to show endosomal location of RSV, it would seem likely that viral endocytosis is not occurring and that direct plasma membrane fusion is the mechanism of entry. Additionally, it may be that RSV makes use of multiple internalisation pathways and therefore uptake might not be prevented by one inhibition method alone. It has been reported that

several tests and approaches are needed to define a macropinocytic pathway (174). As endocytosis involves multiple mechanisms that are not fully defined or understood, investigating this process in the neutrophil has proved problematic.

In this chapter, definitive evidence of RSV internalisation has been established, but not the mechanism of uptake. That there is far more to discover about both neutrophil endocytic pathways and methods of studying the neutrophil is evident. Several potential strategies to take this work further have been proposed. However, arguably more important than elucidating the precise mechanism of RSV entry into the neutrophil is the response of the cell to virus internalisation; this will be studied in the next chapters. Given the multitude of neutrophils within the RSV infected airway, this response may be critical to disease progression or recovery/resolution.

4.7 Summary

Data presented in this chapter reveal that RSV is internalised within the neutrophil cytoplasm but is not found within endosomes. The mechanism of uptake is unlikely to be macropinocytosis. That RSV enters at the plasma membrane by direct fusion has neither been ruled out nor confirmed but seems the probable mechanism of entry.

Chapter 5 Interaction of cord blood derived neutrophils with RSV

5.1 Introduction

Previous work in this thesis used adult neutrophils to study RSV-neutrophil interaction. However, bronchiolitis is a disease of infants and so I would have ideally liked to study infant neutrophils. This is not possible because of the ethics of taking a sufficient volume of blood, at least 10mls, from infants of the age affected by bronchiolitis, typically six weeks to six months. Many studies show that neutrophils from newborns differ from adult neutrophils in their response to pathogens. The literature is predominantly focused on bacterial and fungal microbes, presumably as these pathogens can cause severe disease in newborn infants (216-219). An alternative approach, used in this chapter, is to study cord blood neutrophils. This allows the study of neutrophil responses in a patient group approaching the age of the target demographic, and provides some evidence to validate my model based on adult neutrophils. The advantages are that cord blood is easily accessible, available in an adequate quantity compared to infant blood and can be acquired non-invasively through venepuncture of the placenta after delivery. I have repeated experiments on adult neutrophils presented in **Chapters 3** and **4**, to discover whether similar RSV uptake is seen by cord blood neutrophils.

In vitro studies on cord blood neutrophils may not accurately reflect the interaction of airway neutrophils in infants with RSV. The limitations of single cell *in vitro* cultures are covered in the discussion. For this reason I have extended the work further to investigate whether my results are simply an *in vitro* phenomenon or one that occurs *in vivo*. Thus, I have isolated neutrophils from BAL of RSV infected infants and used confocal imaging to visualise the RSV-neutrophil interaction.

5.2 Overall aim

To study the interaction between RSV and neutrophils from patient groups which reflect the demographic of those affected by RSV bronchiolitis, in order to validate the adult neutrophil model.

5.3 Specific aims

The specific aims of this chapter are:

3. To isolate highly purified neutrophils from cord blood of healthy term infants.
4. To establish the kinetics of RSV uptake in cord blood neutrophils and whether it is degraded similarly to that seen in adult neutrophils.
5. To visualise virus within the cord blood neutrophil by confocal microscopy.
6. To image *ex vivo* BAL neutrophils to establish whether the *in vitro* results are physiologically relevant.

5.4 Specific Methods

5.4.1 Cord blood collection

Liverpool Women's Hospital research midwives recruited mothers to the cord blood study (described in **Section 2.1.2**) at preoperative assessment clinic. Whole blood was collected from the placenta immediately after delivery. The cord was clamped and a needle inserted into one of the veins to withdraw blood. Blood was collected only when there were intact membranes, clear amniotic fluid, no signs of neonatal distress or infection during pregnancy and no concerns regarding baby's health, and if the gestational age was equal to or more than 37/40.

5.4.2 Cord blood neutrophil isolation

Cord blood neutrophils were isolated (outlined in **Section 2.2.1**) as for adult blood neutrophils. When using adult neutrophils, autologous serum was used. Due to the smaller volume of blood and hence serum from cord blood, AB serum (Sigma) has been used in its place for the experiments in this chapter.

5.4.3 BAL sample collection and processing

Infants were recruited to the mucin study (described in **Section 2.1.1**) by medical doctors on the respiratory team at Alder Hey Hospital. Members of the physiotherapy team collected non-bronchoscopic bronchoalveolar lavage (BAL) samples from children ventilated and muscle relaxed on PICU. European Respiratory Society (ERS) guidelines on collection of BAL in children were followed (220). A suction catheter was passed down the endo-tracheal tube until resistance was felt. 1ml/kg aliquot of 0.9% NaCl was instilled. BAL fluid was recovered with suction pressure and collected into a mucus trap.

5.4.4 BAL neutrophil isolation

All BAL samples were stored at 4^{o}C and used within an hour of collection. The total volume of sample obtained was first recorded. Each sample was pipetted vigorously and if the volume was less than 1 ml, the sample was diluted by a known amount using PBS. Samples were then centrifuged at 2000rpm for 10 minutes and the BAL supernatant was aliquoted into 1ml Eppendorf tubes, labelled with recruit number and stored at -80^{o}C. The cell pellet was resuspended in 1ml RoboSep™ buffer, and 25ul neutrophil enrichment cocktail added prior to 10 minutes incubation at room temperature. 50ul of RoboSep™ magnetic particles were added prior to another 10 minute incubation. The whole suspension was then made up to a total volume of 2.5ml by the addition of RoboSep™ buffer before being thoroughly mixed and placed into the EasySep™ magnet for 5 minutes. The desired fraction was poured off by inverting the magnet and tube into a new tube, which was then placed into the magnet for a further 5 minutes. This was repeated once, leaving the negatively selected enriched cells in the new tube ready for use.

5.5 Results

5.5.1 Maternal characteristics

In total 17 mothers consented to participate in the study, of which ten had cord blood collected. The reason for non-collection of other samples was

earlier delivery date than expected or complications subsequently making them ineligible. The mean maternal age was 32 years and all infants were between 38^{+2} and 39^{+2} weeks gestation. The mean infant weight was 3.48kg, (range 2.69 – 4.11kg). The mean volume of blood collected was 10mls (range 5mls – 16mls). A mean of 1.32 $x10^{6}$ neutrophils/ml of blood collected were isolated.

5.5.2 Cord blood neutrophils can be isolated to 98.7% purity as determined by CD66c positivity

To confirm that pure neutrophils could be isolated from cord blood in adequate volumes, purity was assessed using flow cytometry analysed CD66c positivity. Briefly, neutrophils were isolated using dextran sedimentation, percoll gradient and then highly purified using negative immunoselection. 98.7% of isolated cells were identified as neutrophils based on their expression of CD66c. Additionally, neutrophils were assessed by Romanowsky staining and were identified morphologically **(Figure 5-1).**

5.5.3 Cord blood neutrophil survival can be extended *in vitro* by GM-CSF

As for the adult neutrophils, to ensure that cord blood neutrophils remained viable throughout the course of the experiments, GM-CSF was used. Annexin V/PI analysis by flow cytometry of apoptosis and cell death was used to assess the percentage of viable neutrophils at time points up to 20 hours in the presence or absence of 5ng/ml human recombinant GM-CSF (Peprotech). Early apoptosis was identified by Annexin V positivity and cell death was identified by PI staining. In the absence of GM-CSF, mean (SEM) neutrophil survival was 97.20% (+/- 0.914), and 63.78% (+/- 7.717) at 4 and 20 hours respectively. There was a significant decrease in cell viability at 20 hours ($p=0.0033$) when compared to 4 hours. With the addition of GM-CSF cell viability increased to 97.33% (+/- 0.333), and 81.067% (+/- 6.583) at 4 and 20 hours. Cell viability was not significantly decreased at 20 hours in the presence of GM-CSF. 2-way ANOVA with Bonferroni's post hoc test incorporating correction for multiple testing was used **(Figure 5-2)**.

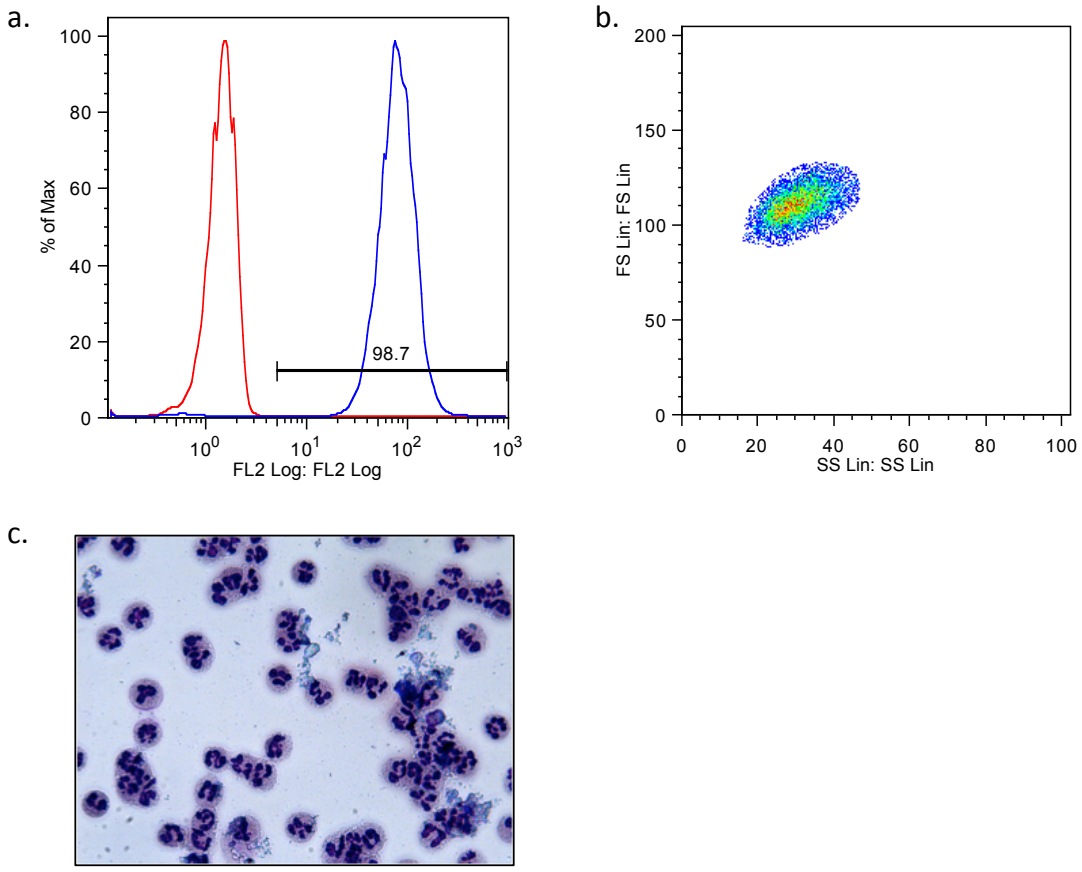

Figure 5-1 Cord blood neutrophil purity

a) Histogram showing percentage of cells that are CD66c positive measured by flow cytometry. Blue line = neutrophils labelled with a monoclonal antibody to CD66c conjugated to PE. Red line = matched isotype control. Following negative immunoselection where antibody complexes link to CD2, CD3, CD9, CD19, CD36, CD56 and glycophorin A and bind to magnetic particles leaving a pure preparation of neutrophils, 98.7% of neutrophils expressed CD66c. b) Flow cytometry scatter plot demonstrating the one cell population on the basis of forward and sidelight scatter properties. c) Neutrophils were spun onto a slide then stained using a Romanowsky staining protocol, before being imaged using a Leiss microscope. Cells were histologically identified as neutrophils by their multi-lobed nucleus and stain uptake pattern.

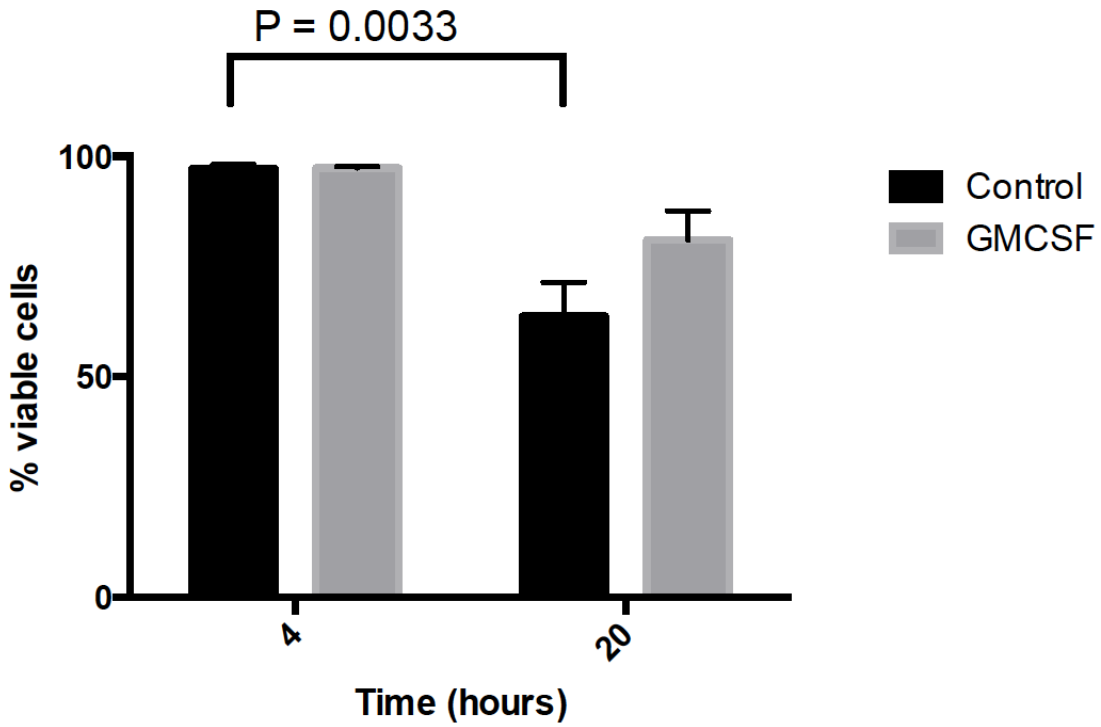

Figure 5-2 GM-CSF prevents significant neutrophil apoptosis

Grouped bar chart showing survival of GM-CSF treated and untreated cells at 4 and 20 hours. Control cells showed significant reduction in viability at 20 hours (p value = 0.0033). With GM-CSF treatment no significant neutrophil apoptosis was observed at 20 hours.

5.5.4 RSV uptake time course measured by western blot

RSV protein was measured from the neutrophils to ascertain whether RSV interacted with neutrophils, as seen with adult cells, and whether it was degraded over time. A Western blot was carried out on pellets harvested at 2, 4 and 20 hours from neutrophils incubated with RSV in DMEM, in the presence of GM-CSF and 5% AB serum. The polyclonal RSV antibody (1/100) was used with streptavidin secondary (1/1000). 4 bands were clearly seen and identified based on their predicted molecular weights as F, G, M and N. The density of the bands reduces at 20 hours **(**Figure 5-3**)** suggesting degradation of internalised RSV protein. The figure shown is representative of 3 identical, separate experiments, which revealed the same finding.

5.5.5 RSV is internalised within the cytoplasm of cord blood neutrophils

Neutrophils that had been in culture in the usual conditions with RSV preparation for 2 hours, in the presence of GM-CSF and 5% AB serum, were spun onto slides. Using the RSV monoclonal antibody to F protein (Abcam) used in the previous chapter, and an IgG Alexa Fluor® 488 secondary (Invitrogen), indirect immunocytochemistry was carried out, (as described in **Section 2.14)**. The cytoplasm was co-stained with Evans Blue. The image presented shows positive staining for RSV diffusely in the cytoplasmic area, with exclusion of the nucleus **(Figure 5-4)**. In addition to the single images, z-stacks were taken, (as described in **Section 4.4.1)**. These z-stacks are presented as orthogonal views and reveal that, identical to the adult neutrophil images, RSV is internalised throughout the cytoplasm, as indicated by the green speckles surrounded by red stained cytoplasm **(Figure 5-5)**.

5.5.6 RSV uptake not inhibited by phagocytosis inhibitor

Pharmacological inhibition of RSV uptake was tested using cytochalasin D (Sigma). Neutrophils were pre-incubated with cytochalasin D (10µg/ml) for 15 minutes prior to addition of RSV, and then cultured at the usual conditions

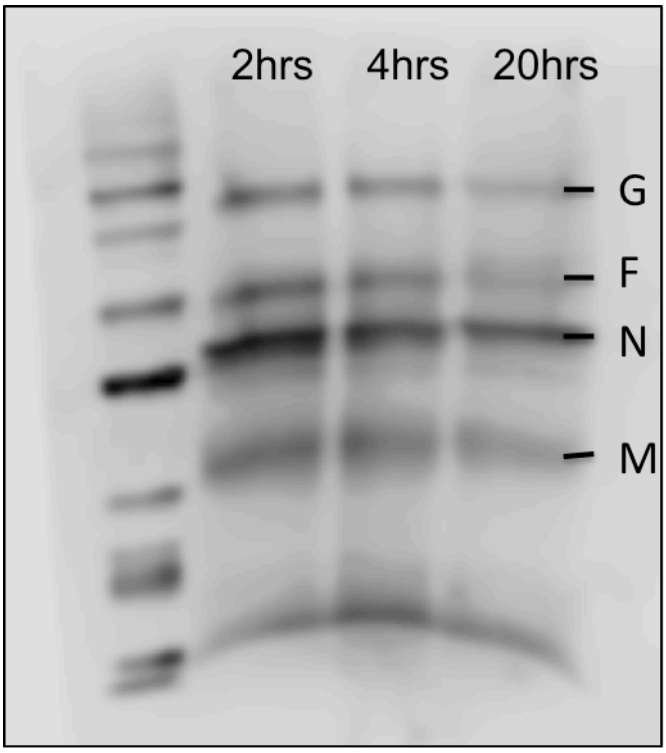

Figure 5-3 Western blot time course of RSV proteins from cord blood neutrophils

A Western blot was carried out on pellets harvested at 2, 4 and 20 hours from neutrophils incubated with RSV and 5% AB serum. The quantity of RSV, as shown by the density of the 4 RSV protein bands G, F, N and M, is reduced by 20 hours. The most distant band has not been identified and is of lower molecular mass than the full-length protein and may therefore represent fragments of proteolytic cleavage.

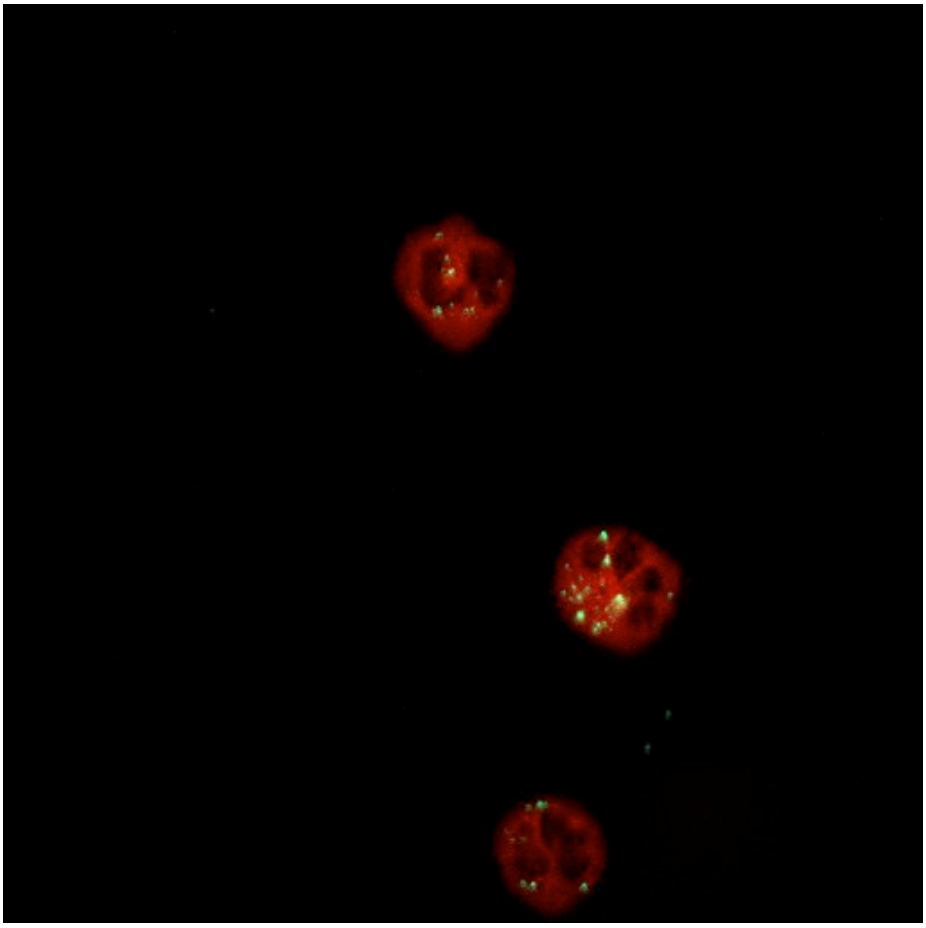

Figure 5-4 Cord blood neutrophils visualised by confocal microscopy showing RSV

Neutrophils that had been incubated for 2 hours with RSV were spun onto slides and fixed with methanol, following which they were stained for RSV (green) and co-stained with Evans Blue (red). Images were taken with a multiphoton Zeiss microscope.

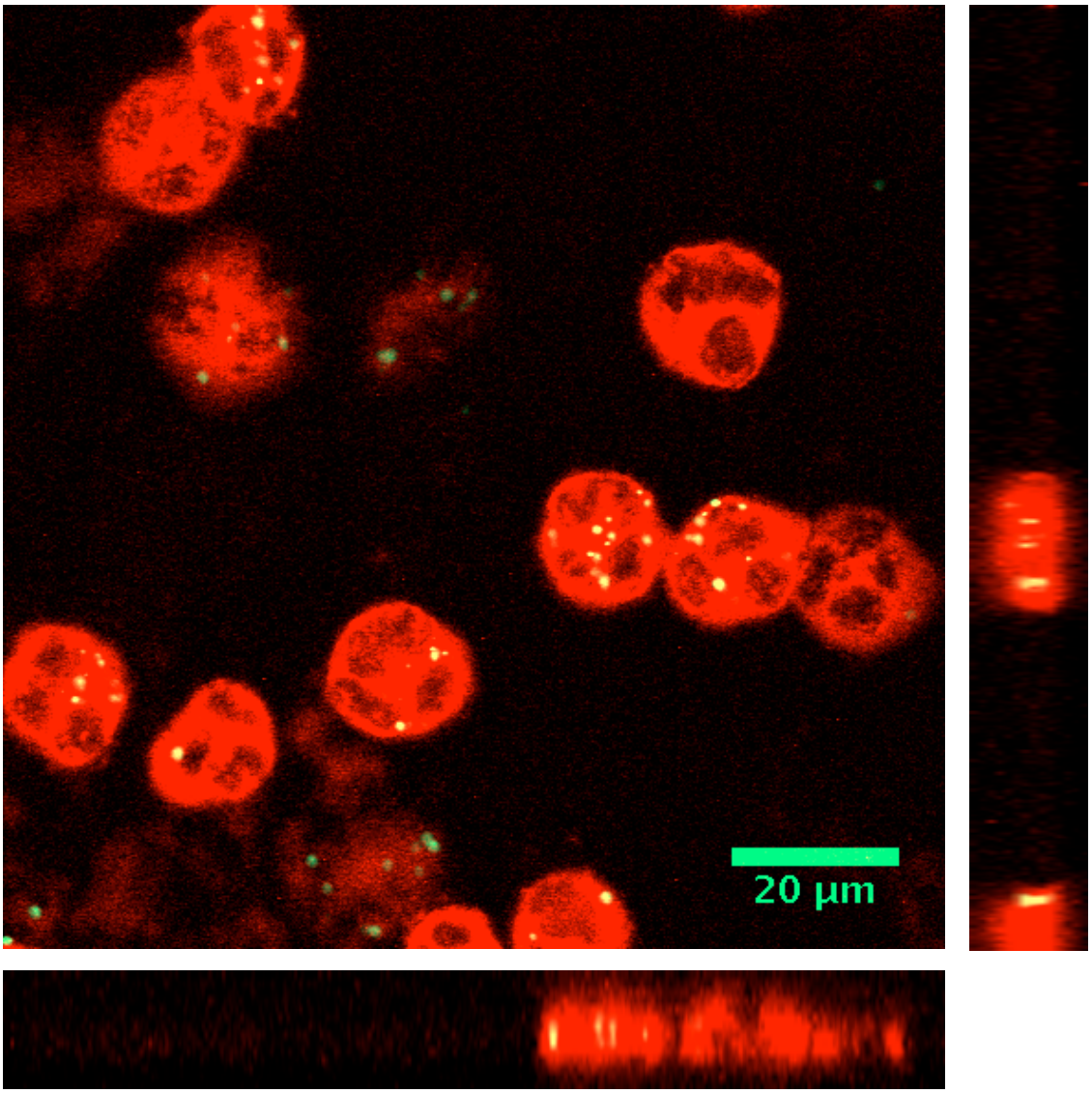

Figure 5-5 Orthogonal view showing RSV within the cord blood neutrophil cytoplasm

A z-stack orthogonal view of cord blood neutrophils showing RSV (green) throughout the cytoplasm (red).

for 2 hours prior to cytospin and immunocytochemistry analysis. Similarly to the adult neutrophils RSV uptake was not inhibited (figure not shown).

5.5.7 Bronchiolitis patients' characteristics

5 infants with RSV bronchiolitis were recruited and had a BAL sample collected for neutrophil isolation and cytospin. The characteristics of these patients are shown in **Table 5-1**. The mean GA at birth was 36 weeks (range 34 - 40 weeks). A mean of $9.7x10^5$ neutrophils/BAL sample collected were isolated.

GA at birth (weeks)	Corrected age at admission (weeks)	Time sample taken after intubation (hours)	Number of neutrophils isolated
40	3	18	2,300,000
34	15	24	400,000
35	27	23	150,000
37	3	24	1,500,000
35	1	7	500,000

Table 5-1 Table of RSV patient recruit characteristics

The gestational age (GA), corrected age on admission and the time the BAL was taken after intubation are shown for the 5 recruits. In addition, the number of neutrophils isolated from each BAL sample is shown.

5.5.8 RSV identified by confocal in *ex vivo* BAL neutrophils

Neutrophils were isolated from BAL (as described in **Section 5.4.2**). *Ex vivo* neutrophil cytospins were stained to identify RSV using the same method used for the *in vitro* neutrophils. Images were taken and are presented, firstly as single images revealing RSV positivity, and a negative isotype control **(Figure 5-6).** Secondly, a different recruit's BAL neutrophils are shown as an orthogonal image. In this image RSV can be seen throughout the cytoplasm, and in addition RSV can be seen attached to the neutrophil **(Figure 5-7)**.

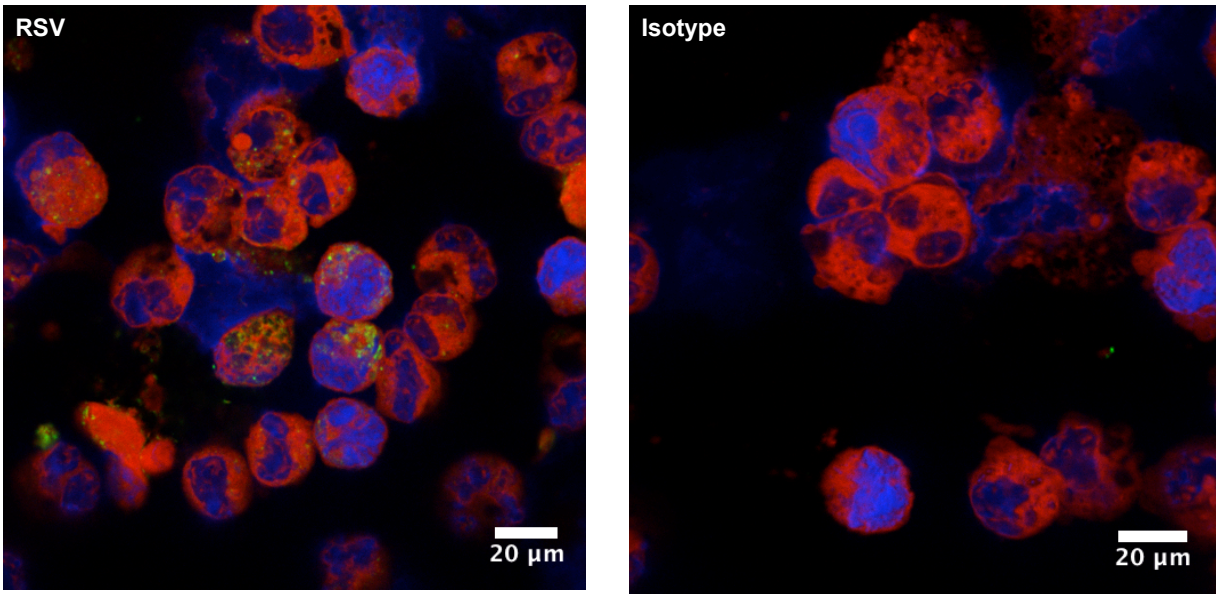

Figure 5-6 *Ex vivo* neutrophils showing RSV by immunocytochemistry

Neutrophils isolated from RSV infected infant's BAL fluid were fixed on slides and stained for RSV F protein, using an IgG Alexa Fluor® 488 secondary antibody. The cytoplasm is stained with Evans Blue (red), the RSV is seen in green and the nuclei are co-stained with DAPI (blue). The isotype (seen in the 2nd panel) was negative.

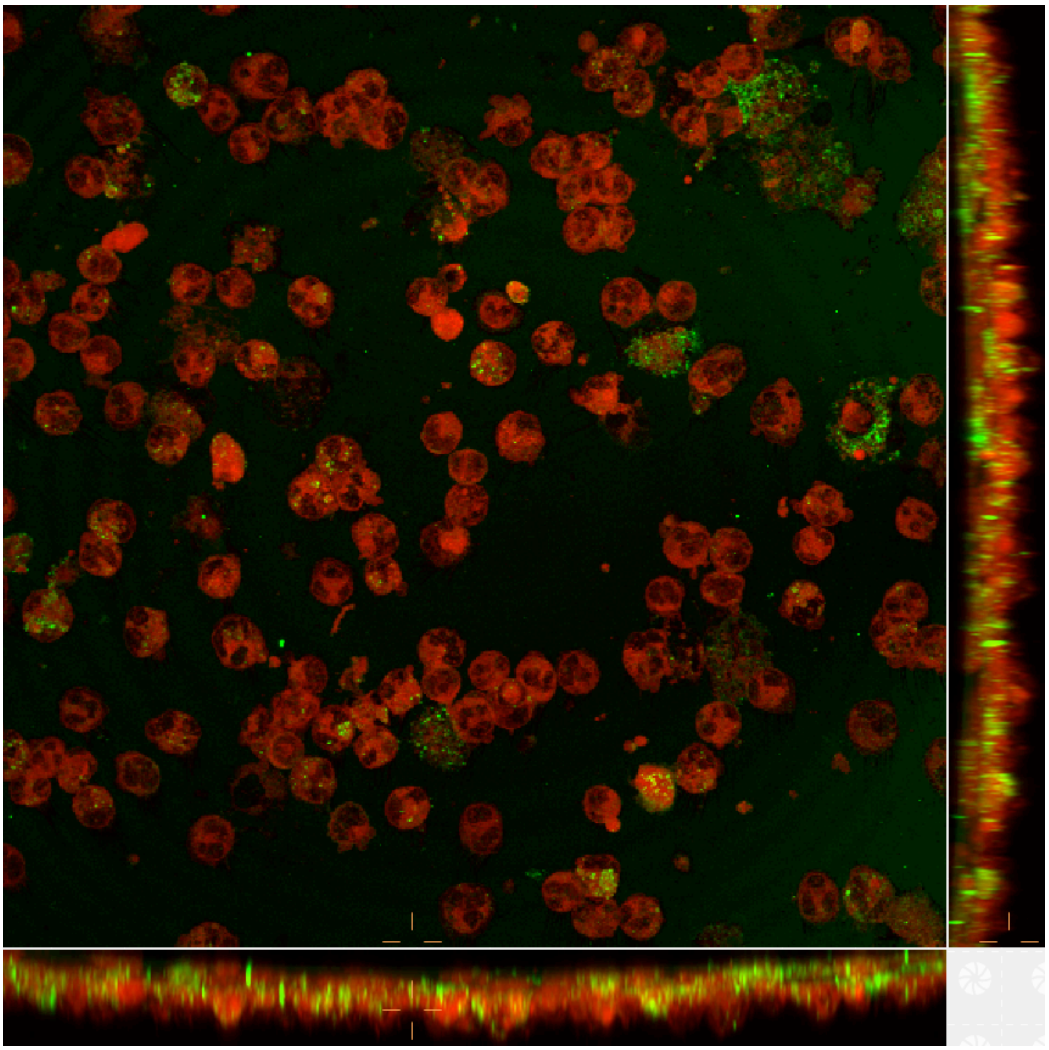

Figure 5-7 Orthogonal view of *ex vivo* neutrophils

Z-stack orthogonal views of ex vivo BAL neutrophils showing RSV (green) and cytoplasm, co-stained with Evans Blue (red). Neutrophils were isolated from RSV infected infant's BAL fluid and stained for RSV F protein, using an IgG Alexa Fluor® 488 secondary antibody.

5.6 Discussion

Data presented in this chapter show that cord blood neutrophils interact with RSV in a similar way to adult neutrophils. Thus, western blot revealed that RSV protein, seen at 2 and 4 hours, is reduced by 20 hours, suggesting that RSV is degraded once internalised. Confocal microscopy showed that the RSV is internalised within the cytoplasm in discrete pockets and that uptake is not prevented by cytochalasin D. That there appears to be no apparent difference between RSV and cord neutrophils, and RSV and adult neutrophils is perhaps unexpected, given the documented literature, discussed below, on cord blood impaired responses to pathogens.

Term newborns have blood neutrophil counts very similar to adults and older children (221), but some reports suggest they differ with respect to migration, phagocytosis, and oxidative burst. A recent study employed proteomic analysis to compare newborn cord blood neutrophils with peripheral adult neutrophils. This analysis indicated impaired function of newborn neutrophils, specifically relating to the proteasome, lysosome, phagosome and migration (222). In the literature the commonest observed functional difference is that of reduced chemotaxis, with newborn neutrophils migrating at about half the speed of adult neutrophils in *in vitro* studies (216, 223). Term newborns tend to establish normal chemotactic function by ten days to two weeks postnatal age (224, 225). Interpretations differ as to the phagocytic capacity of the newborn neutrophil with differences probably attributable to variation in experimental conditions, as some studies use cord blood neutrophils with serum from the newborn donor while some use adult serum. Specifically these differences in phagocytic ability appear to be dependant on adequate opsonisation. Thus phagocytosis of bacteria normalises in term infants' neutrophils when using infant blood and adult immunoglobulin and complement (216, 226). Respiratory burst activity of neutrophils harvested from cord blood of term infants does not differ significantly from adult neutrophils (227, 228). Intriguingly however, superoxide generation, the initial phase of respiratory burst, is increased in newborn neutrophils compared to those from adults (229).

It is a common approach to use cord blood as a source of immune cells when studying infant responses to a pathogen (230-232), although few studies have explored its suitability as a surrogate for infant blood. However, it would appear that cord blood neutrophils are markedly more immature than neutrophils from infants, even of a few weeks of age. One study showed that the impaired ability of the cord neutrophil to phagocytose was transient and that by day three, activity was similar to that seen in adult neutrophils (233). Similarly studies investigating neutrophil chemotaxis showed that adult-like chemotactic ability is achieved by two weeks of age (224, 225).

If cord blood neutrophil responses lack maturity when compared to those from a 2-week-old infant, why in this study do they appear to have responded similarly to adult neutrophils? It could be that the use of GM-CSF has activated and thus matured them. GM-CSF has been used as a pro-survival factor throughout this research. It is a haematopoietic growth factor that regulates proliferation and differentiation of precursor cells and has also been found to exert functional effects on neonatal and adult neutrophils (234, 235). The presence of GM-CSF can prolong neutrophil longevity *in vivo* and *in vitro* (236-239). Part of my justification for using GM-CSF was that it is produced by airway epithelial cells and is found in high concentrations in the airways of infants with severe RSV infection (240, 241). I found that GM-CSF prevented significant neutrophil apoptosis at 20 hours for the cord blood but not adult neutrophils. In **Chapter 2** GM-CSF exposed adult neutrophils showed improved survival compared to untreated neutrophils, but still significant apoptosis at 20 hours **(Figure 2.6)**. Most studies using GM-CSF have looked at its action on adult neutrophil function, but work carried out investigating the response of the neonatal neutrophil to GM-CSF revealed that it enhanced chemotaxis, and improved the respiratory oxidative burst to a greater degree than in adult neutrophils (242). That the cord blood neutrophil is more sensitive to the effects of GM-CSF may explain the similarity in response to the adult neutrophil.

A challenge of any *in vitro* study occurs when extrapolating back to the biology of the intact organism (243). Immunocytochemistry of the *ex vivo*

neutrophil has revealed RSV, internalised within the neutrophil and distributed throughout the cytoplasm, in a pattern corresponding to that seen in the *in vitro* experiments, which confirms the biological relevance of the work to this point. There are a number of limitations to the *in vitro* model that could result in the interaction observed not accurately reflecting human RSV infection and disease. Firstly, the interaction of just one immune cell with RSV is modelled. Neutrophils have been removed from their natural environment, eliminating interaction with other cell types, and simplifying the events that would occur in the airways of infants infected with RSV. Even though neutrophil influx occurs early in infection, epithelial cells and alveolar macrophages would also be present within the airway and would interact with the neutrophil. However, the main advantage of single cell type *in vitro* models is their ability to provide information on that cell's particular reaction to an infectious microbe. Secondly, it is not possible to know the correct ratio of virus to neutrophil and imitate that in a physiologically relevant space. Nonetheless, that the neutrophil does encounter RSV and that an interaction occurs has been confirmed in multiple patients' BAL samples. The magnitude of RSV seen in individual samples did vary, presumably reflecting the personal viral load of the different recruits. The *ex vivo* neutrophil results lend support to the RSV neutrophil interaction being a genuine disease phenomenon.

5.7 Summary

Data presented here shows that the cord blood neutrophil-RSV interaction is very similar to the adult blood neutrophil-RSV interaction. In addition, BAL from infants with bronchiolitis shows a similar distribution of RSV within the neutrophils, lending support for the use of the *in vitro* model to examine RSV-neutrophil interactions.

Chapter 6 Innate antiviral response to RSV

6.1 Introduction

RSV infection triggers a robust innate immune response characterised by high levels of airway cellularity. Neutrophils make up a large proportion of the cells, and throughout this study evidence of RSV entry into the neutrophil has been presented. This has been examined in an *in vitro* model system, showing that viral replication is not supported within the neutrophil, and in *ex vivo* neutrophils in which RSV was visualised. A 2015 review by Pickles and DeVincenzo highlights the lack of knowledge regarding the interaction of the neutrophil with RSV, in particular, how RSV affects neutrophil function and consequently impacts disease severity (244). This thesis attempts to fill that gap in understanding, but thus far, the response of the neutrophil to RSV has not been examined.

Neutrophils can express and produce a wide range of cytokines, either constitutively or upon activation, which influence antiviral defence. Activation of the neutrophil, can be effected through an array of receptors including colony stimulating, and cytokine receptors, G protein coupled-, Fcy- and complement receptors and many PRRs (105). The PRRs, RIG-I and MDA-5 are present in the neutrophil, enabling the cell to recognise intracellular viral components, as discussed in **Chapter 1**. Once stimulated, neutrophils can control cytokine production through regulation at the transcriptional level (102, 245). The RSV infected airway contains a melange of pro-inflammatory and anti-viral cytokines. The neutrophil's contribution to this environment is not known with any certainty but the expanding list of neutrophil derived cytokines means they probably contribute considerably, either directly or indirectly. Our group has previously shown large amounts of TNF-α in the RSV infected airway (246). Neutrophils produce low-levels of TNF-α (105, 247, 248), and through the expression of TRAIL, which is expressed on and secreted by neutrophils, are thought to play an active role in the early defence against viral infection. Neutrophil antiviral activities, specifically in a murine model of CMV infection were shown to act through the

TRAIL/TRAILR pathway (248). RSV specific studies in humans have shown increased levels of MIP-1 α (CCL3) and CXCL8, cytokines that neutrophils are known to produce (118). IL-9 was found in abundance in the BAL of term infants with RSV, immunostaining showed that neutrophils were the main source of this type 2 cytokine (249).

The neutrophil's contribution to immune modulation is far more than cytokine production alone. Since the 2000s, a number of high-throughput studies, using proteomic analysis, oligonucleotide array and microarray, have examined the scope of neutrophil gene expression during an inflammatory response (250-252). Microarray allows analysis of the regulation of gene expression at the transcriptional level for thousands of genes at one time. Microarrays have enhanced our knowledge of the number of transcripts involved in neutrophil biology and has revealed pathways not traditionally associated with the neutrophil such as cell to cell signalling, and regulation of T cell activation (253). *In vivo* work has then proceeded to confirm these functions. In influenza A, neutrophils have been shown to be capable of acting as APCs for CD8+T cells in the lungs, expressing MHCI, CD80 and CD86 (254).

Although transcriptional studies of neutrophils are becoming more commonplace, I have only been able to identify one study that has investigated the transcriptional response to a virus, specifically influenza H3N2 and none have specifically investigated the response to RSV (151). One study did undertake whole blood gene expression in infants with RSV. There were 2,317 differentially regulated transcripts in total. Two of the top ten overexpressed genes related to neutrophil function, and neutrophil related genes were significantly overexpressed in patients with RSV compared to other respiratory viral infections (255). That the neutrophil may contribute to the anti-viral response to RSV seems likely, and investigating their transcriptional profile by microarray, would appear to be a suitable method of elucidating this contribution.

6.2 Hypothesis

RSV uptake by neutrophils induces change in transcription in these cells, characterised by an antiviral response.

6.3 Aims

To answer the above hypothesis the work described in this chapter aimed to:

1. Utilise gene microarray technology to identify differentially expressed genes from RSV exposed neutrophils.

2. Use pathway analysis to determine the pattern of differentially expressed genes.

3. Validate the microarray analysis by measuring select, pertinent genes by RT qPCR.

6.4 Specific methods

6.4.1 Microarray

The aim of this experiment was to identify differentially expressed genes in RSV exposed and control human neutrophils. Blood was collected from 4 healthy adult volunteers (2 male, 2 female; mean (range) age 25 (20 – 33) years). Neutrophils were isolated and ultrapurified as described in **Section 2.2**. They were incubated at 37^{o}C/5% $C0_2$ for up to 20 hours, in DMEM containing 5% AB serum, either in the presence or absence of RSV (MOI 0.1). Samples were collected at 4 and 20 hours.

16 RNA samples were prepared from neutrophils using the method described in **Section 2.10.2**. However, an additional step of DNA digestion was incorporated into the protocol after RNA extraction, to remove contaminating DNA. RNase-Free DNase Set (Quiagen) was used. RNA solution was mixed with 10ul Buffer RDD and 2.5ul DNAse I stock solution, and made up to 100ul with RNase-free water. This was incubated for 10 minutes at room temperature, after which Quiagen RNA cleanup protocol was followed. The samples were assessed using Agilent 2100 Bioanalyser RNA 6000 Nano chips. 100ng of total RNA, dried by speed-vac, was used for one-colour target labelling and amplification using an Agilent Low-Input

Amplification Kit (LIQA) according to the manufacturer's instructions (sample IDs and information can be found in **Appendix 4**). 600ng of Cy3 labelled RNA was fragmented and loaded onto the arrays, which were then hybridised for 17 hours at 65°C and 10rpm in an Agilent hybridisation oven. Following this, the arrays were washed and scanned by the Agilent Scanner, using the G3_GX_1 colour protocol and 3uM resolution. The data were extracted with Agilent Feature Extraction software v11.01.1.1, using Design ID 039494 and Protocol GE1_1100_Jul11. Dr Lucille Rainbow (Centre for Genomic Research (CGR), University of Liverpool) carried out both the RNA sample quality assessment and the microarray.

6.4.2 qPCR validation of microarray findings

In order to validate the findings of the microarray analysis, qPCR was utilised. Analysis was carried out on the 4 original microarray RNA samples and in addition 2 further samples, which were produced using the same method, described in **Section 2.10.2**.

6.4.2.1 cDNA synthesis

RNA samples were converted to cDNA using Moloney Murine Leukaemia Virus reverse transcriptase (Bioline). RNA samples were incubated at 60°C for 5 minutes to denature RNA. RT mastermix, made up as shown in **Table 6-1**, was added immediately (20µl per 30µl RNA sample). Samples were incubated at 42°C for 1 hour, then at 80°C for 10 minutes to inactivate the RT enzyme. cDNA samples were diluted with 450µl sterile dH20 and stored at -20°C prior to use.

For 1 reaction	**30µl RNA sample (µl)**
Deoxynucleotide triphosphosphates dNTPs 40mM (Bioline)	1.5
Random Hexamer (AB)	1.0
UBioscript 5x RT Bufer (Bioline)	5.0
Bioscript RT Enzyme (Bioline)	0.5
Sterile distilled H20	12.0

Table 6-1 Reverse transcription mastermix used in cDNA synthesis Table stating the quantities of components used for the reverse transcription mastermix for cDNA synthesis.

6.4.2.2 Quantitative Polymerase Chain Reaction

For all reactions, 0.5µl gene expression assay (Taqman®) probe, 5.0µl Taqman® mastermix, 2.5µl sterile dH_20 and 2µl cDNA were used. Plates were sealed with adhesive film and run on Applied Biosystems 7500 fast Real-Time PCR System. Cycling conditions were: 2 minutes at 50°C, hold at 95° for 10 minutes, followed by 40-60 cycles of 95°C for 15 seconds and 60°C for 60 seconds.

6.4.3 Housekeeping gene selection

In **Chapter 3**, when qPCR was previously used, it was found that L32, the housekeeping gene utilised was not efficient in the neutrophil system. In order for relative quantification to take place, the efficiency of a probe must be 90 – 100%, which was not the case for L32. For this reason housekeeping gene selection was carried out using the GeNorm™ reference gene selection kit and software package (Primerdesign). This enabled the choice of a housekeeping gene combination, which had been shown to be stable within the human neutrophil cell type and across the different experimental conditions.

6 housekeeping genes were selected for testing, B2M, ACTB, GAPDH, YWHAZ, UBC and SDAH. 6 cDNA samples were probed for each of these genes in duplicate using a standard qPCR technique. The results were analysed in qbase^{PLUS} (Biogazelle). 2 parameters are used in this package in order to assess the suitability of the genes; the M value which measures the expression stability of each of the genes and the V value which determines the combination and number of housekeeping genes required for an experimental condition.

M value: This indicates the average expression stability value (M) of reference genes during a stepwise exclusion of the least stably expressed reference gene. Starting from the least stable gene on the left, the genes are ranked according to increasing expression stability, ending with the most stable gene on the right, which were B2M and GAPDH **(Figure 6-1)**.

V value: This determines the optimum number of reference genes required by showing the variation in average stability. The chart shows sequential addition of each reference gene starting with the two most stably expressed genes on the left with the inclusion of a 3rd, 4th… etc moving to the right. A proposed value of 0.15 is given, as guidance for the determination of optimal number of reference genes, which was 2 in this system **(Figure 6-2).**

From these results B2M and GAPDH were chosen as housekeeping genes and amplification curves were produced as described in **Section 2.14.1 (Table 6-2)**. All subsequent **ΔΔ**CT quantification analysis was carried out using the average of these two housekeeping genes.

Gene	R^2	Slope	Efficiency (%)	Threshold
GAPDH	0.97	-3.49	93	0.015
B2M	0.97	-3.50	93	0.15

Table 6-2 Standard curve characteristics of qRT-PCR experiments

Table showing the efficiency of the housekeeping genes B2M and GAPDH and the threshold used for each gene.

Gene	Assay ID	Supplier
GAPDH	Hs99999905_m1	Life technologies
B2M	Hs00984230_m1	Life technologies

Table 6-3 Pre-designed gene expression assays used for qPCR analysis

Table detailing the assay IDs and supplier for the housekeeping genes

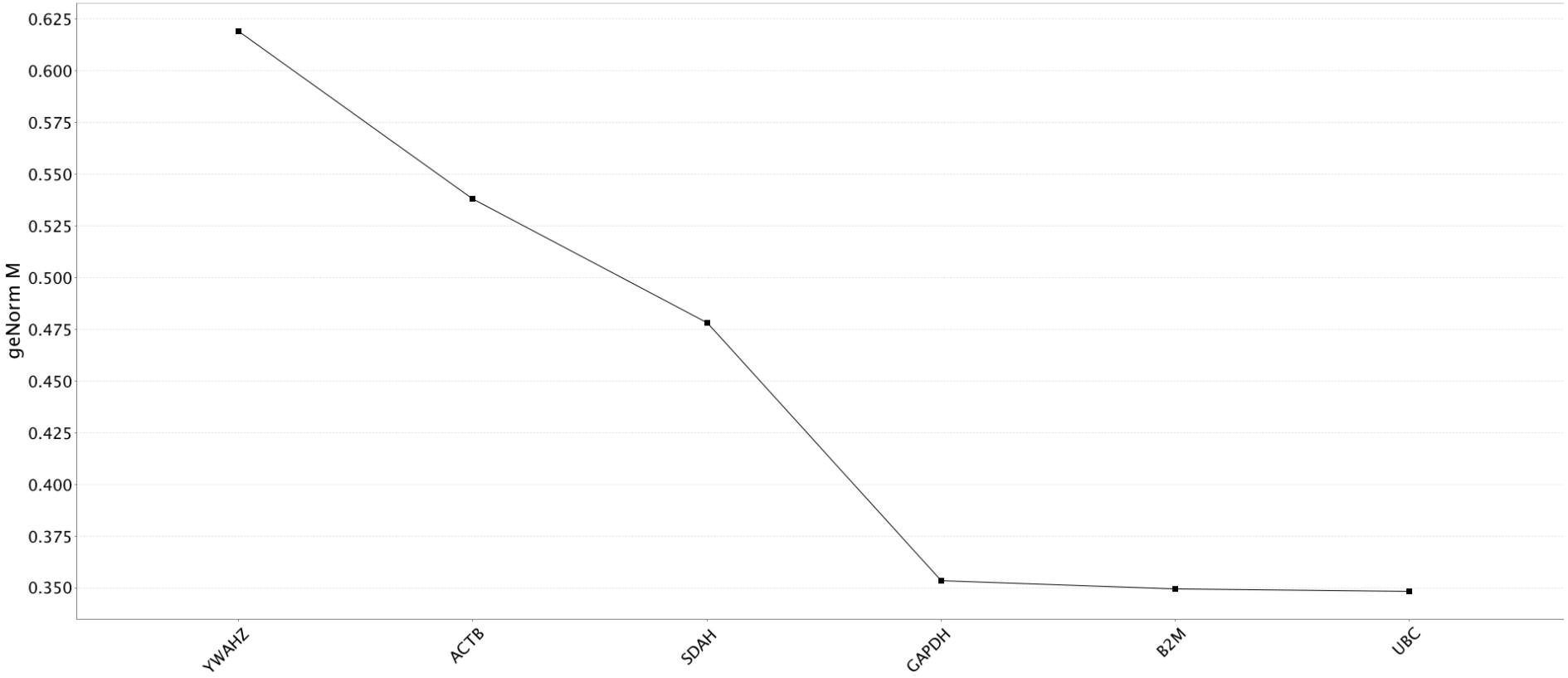

Figure 6-1 Average expression stability of reference targets

Line graph showing the geNorm M value (expression stability) for each of the 6 housekeeping genes tested. The genes start with the least stable gene at the left side of the x-axis and move towards the right side to the most stable gene.

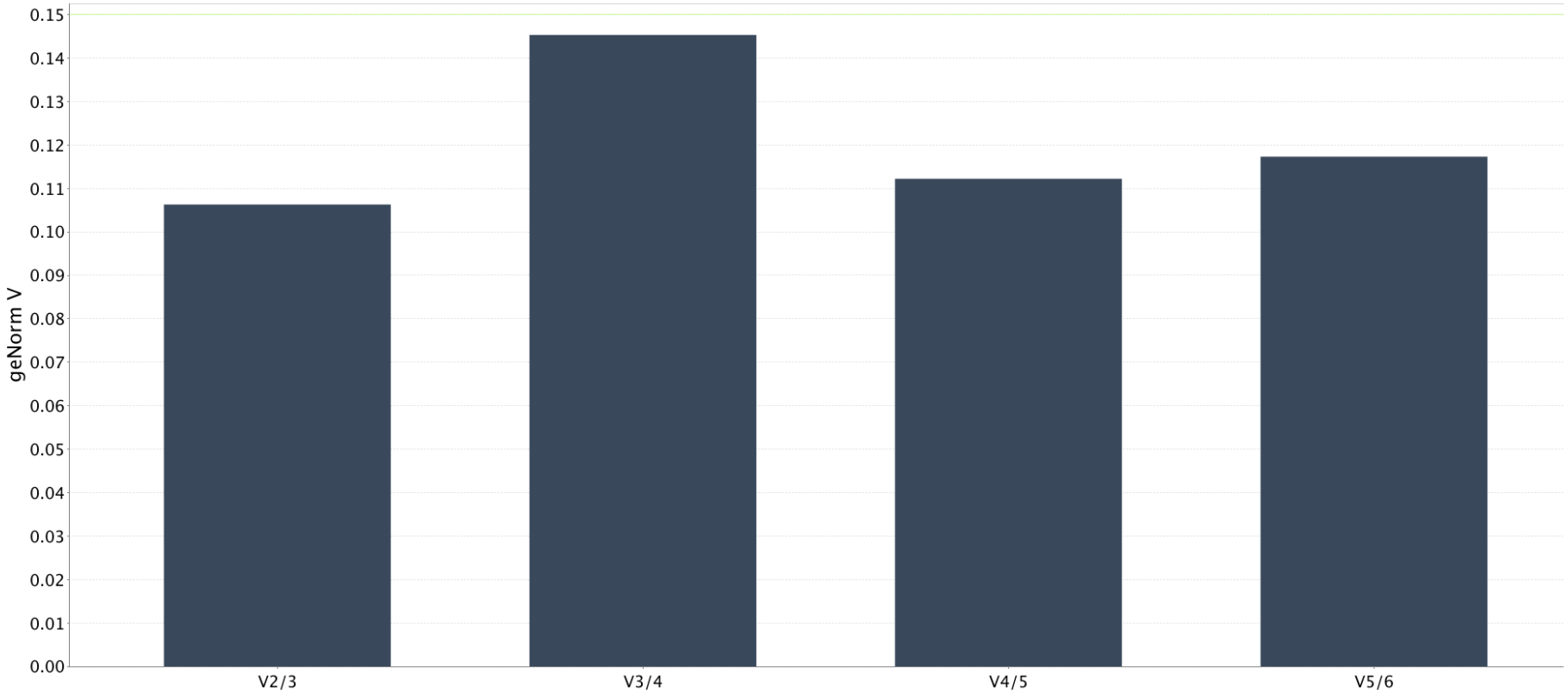

Figure 6-2 Determination of the optimal number of reference targets

Bar chart showing the V value as an additional gene is added sequentially. The optimal number of reference genes required for normalisation was determined by pairwise variation (geNorm V value of n/n+1). A value below 0.15 indicates consistent normalisation gene expression and indicates the minimum number (n) of genes required. In this experiment a combination of two reference genes was sufficient for normalisation since V2/3 was 0.105.

6.5 Results

6.5.1 RNA Pico chip traces

RNA samples were assessed to see whether they were of good enough quality to be analysed by microarray. 1µl of each RNA sample to be used for microarray was diluted to 5ng/µl and run on a Pico chip **(Figure 6-3)**. The RNA integrity number (RIN) (256), a mathematical interpretation of sample quality, was above 6.50 for all samples, indicating that although a small amount of RNA degradation was present the samples were of good enough quality to be used for microarray analysis **(Figure 6-4)**.

6.5.2 Data quality assessment

Once the data had been extracted, a general data quality assessment was performed by analysing the processed signal for each array feature. Firstly, normalisation was carried out. When running experiments that involve multiple high-density oligonucleotide arrays, it is important to remove sources of variation between the arrays that are not of biological origin. **Figure 6-5** shows the density distribution curve of the expression values before and after normalisation. This shows that the expression curves for different samples become almost identical after applying a quantile normalisation method to the expression data (257).

Variation assessment was carried out using Principal Component Analysis (PCA) (258). **Figure 6-6** is a PCA plot of the log expression of all the arrays. The plot reveals that samples from the two time points can be well discriminated based on the 2nd principal component. However, the RSV exposed (RSV) and control (CON) samples cannot be separated clearly. This suggests that there might not be a large percentage of genes that are differentially expressed.

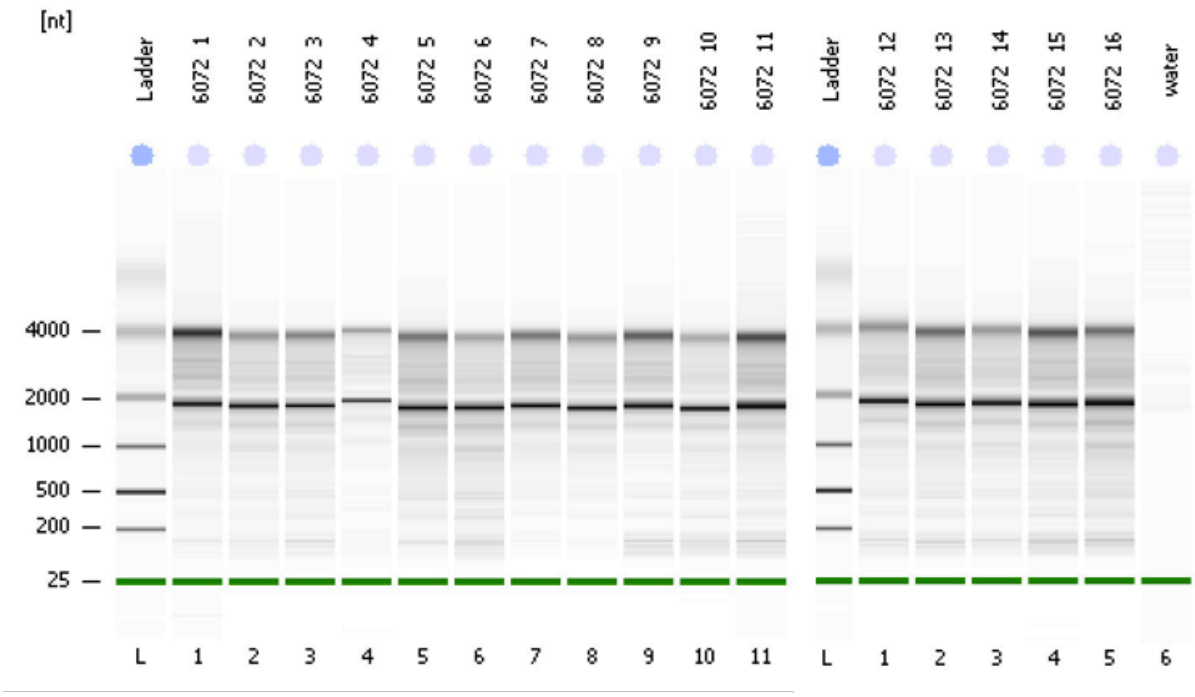

Figure 6-3 Electrophoresis run summary of total RNA on Pico chip

This is the image of a digital gel, produced on a bioanlayzer, for all 16 samples and a water control. The top band represents the 28S ribosomal band and the lower band the 18S

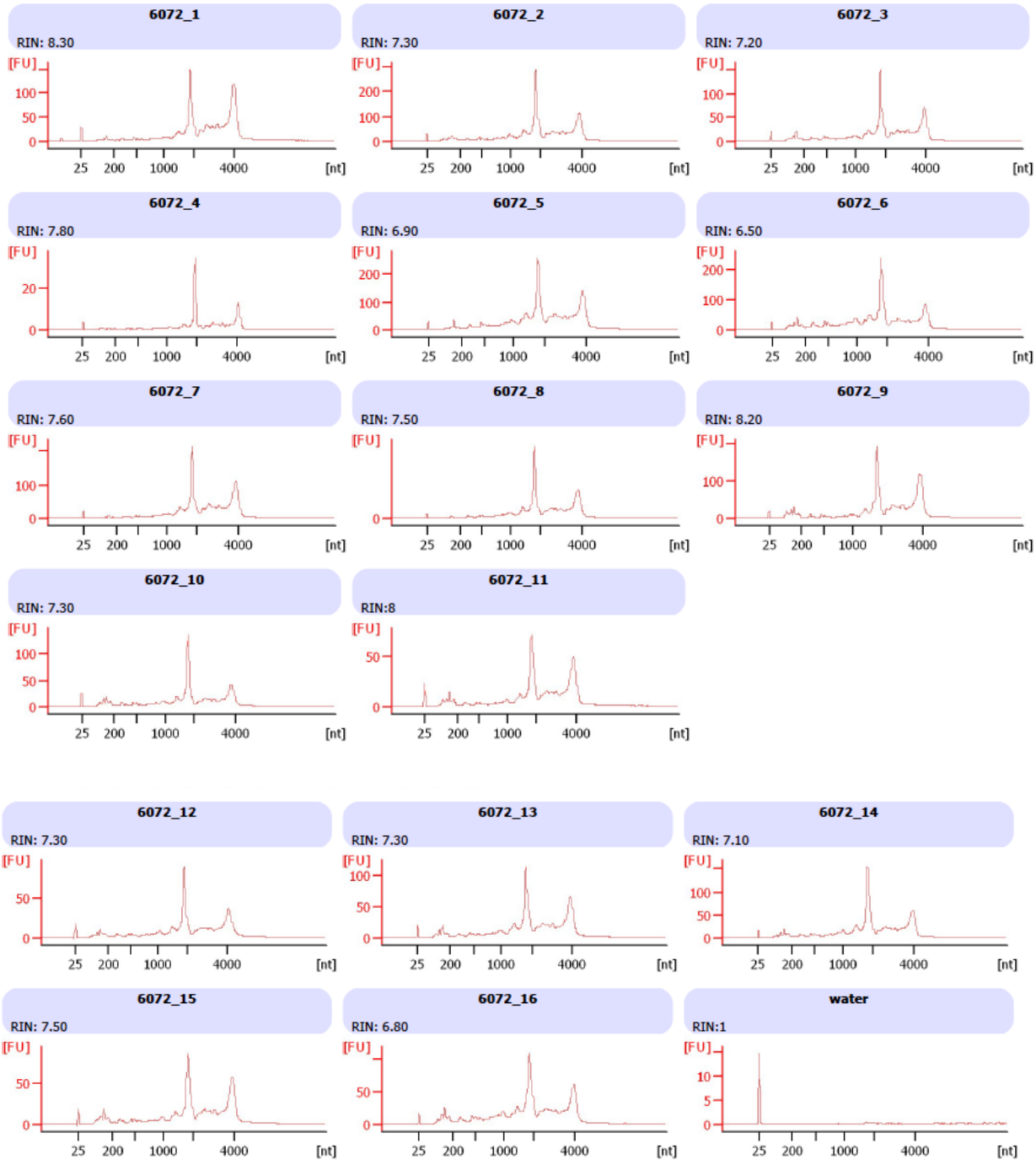

Figure 6-4 Electropherogram graphs and calculated RIN

The electropherograms show the analysis of each total RNA analysis. The first (left) peak is 18S ribosomal peak and the second (right) peak is 28S ribosomal peak. The sample integrity is determined mathematically, by the software, using the entire electrophoretic trace of the RNA sample. This includes the presence or absence of degradation products. The presence of a mildly wavy baseline indicates a small amount of RNA degradation. However, all RIN was > 6.50, which was adequate for continuing with the microarray analysis. These graphs show the same result as the electrophoresis blots just visualised in an alternate way to illustrate the 18S:28S ratio.

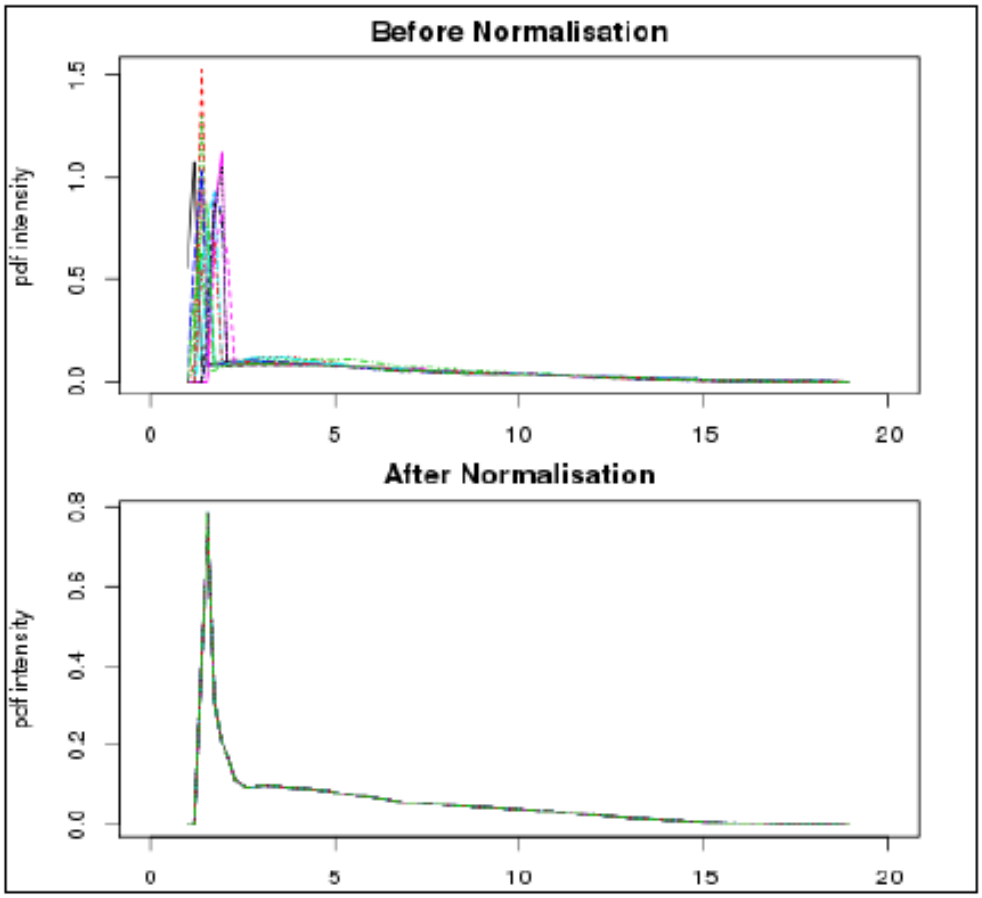

Figure 6-5 Distribution of log expression signal before and after normalisation

The upper panel presents the density distribution of the expression values. Different line style and colour combinations represent different samples. Expression distribution for different samples are very similar when expression level >5 (2.3 on the log2 scale). The lower panel shows that the expression density curves for different samples become almost identical after normalisation of the data.

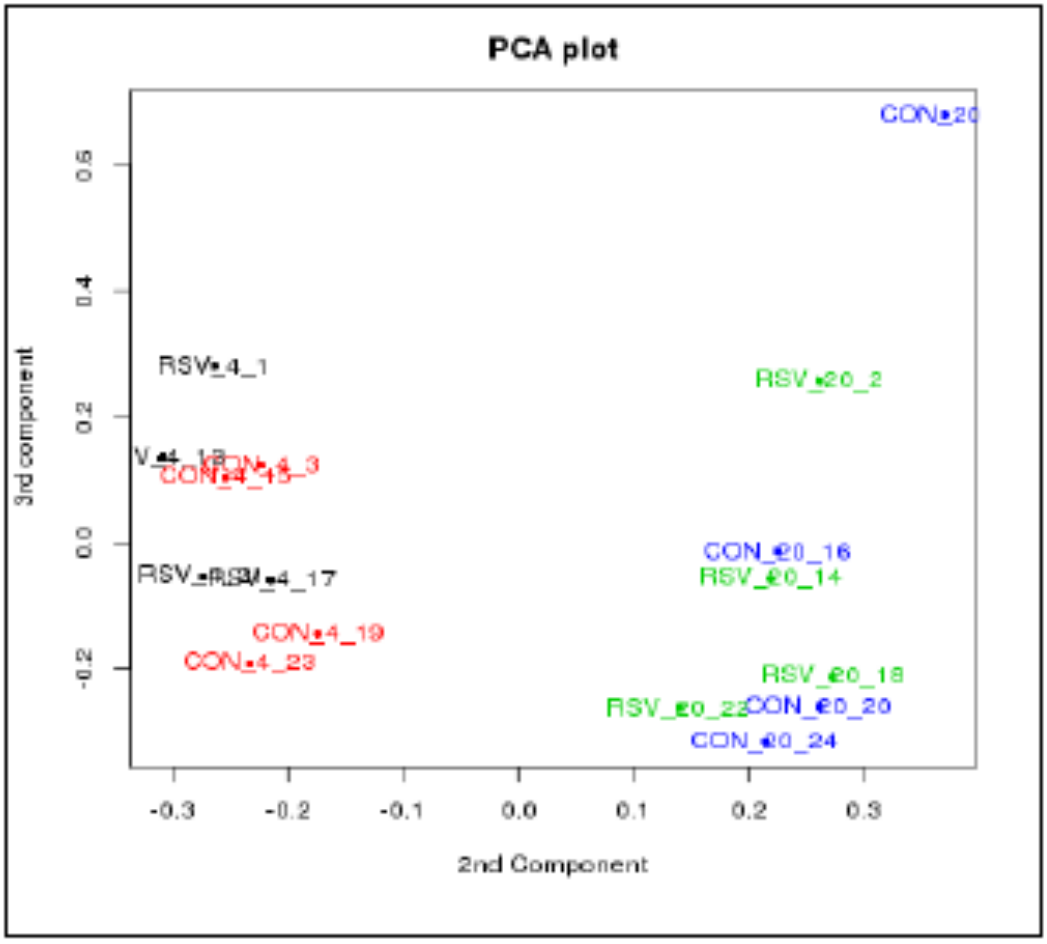

Figure 6-6 PCA plot of log2 gene expression for all samples

The plot reveals that the samples from two time points can be well discriminated based on the 2nd principal component. However the RSV and CON samples cannot be separated as clearly. This suggests that there may not be a large percentage of genes identified as differentially expressed.

6.5.3 Differential gene expression analysis

The differential expression analysis was performed in R using the package limma (259). The Agilent human genome v2 microarray used contained 62 976 reportable features, which belong to 50 739 unique probes. These probes are annotated to 36 344 uniquely named genes. The feature level expression data was de-replicated to probe and then gene level, in order to have only one value for each gene, despite multiple features/probes measuring for that particular gene. The mean expression of multi-features was taken as the de-replicated expression value for the gene. The $\log_2$ gene expression data was modelled using a linear model with 4 model parameters representing the expression for grouped samples. The model parameters were estimated using the maximum likelihood approach. This process generated $\log_2$ fold change (logFC) values for both RSV 4 hour/CON 4 hour and RSV 20 hour/CON 20 hour. These fold changes were tested using a t-test. P-values, associated with the logFC were adjusted for multiple testing using the False Discovery Rate (FDR) approach (260). Significant differential expression was defined as those with an FDR-adjusted P-value < 0.05. The results of this analysis are summarised in **Table 6-4**. Dr Yonxiang Fang (CGR, University of Liverpool) carried out data normalisation and differential gene expression analysis.

Regulation Direction	RSV 4/CON 4	RSV 20/CON 20
Probes		
Total Number	1197	217
Up	692	149
Down	505	68
Genes		
Total Number	911	180
Up	518	122
Down	393	58

Table 6-4 Number of differentially expressed probes and genes and regulation direction

Table detailing the number of differentially expressed probes and genes at each time point. The data is then divided to show the total number of probes and genes that have gone up and down at each time point.

6.5.4 Ingenuity Pathway Analysis

Data were analysed through the use of QIAGEN's Ingenuity® Pathway Analysis (IPA) (261). IPA initially maps the genes to an IPA Knowledge Base and produces an annotated data set. Of the 1091 genes that were differentially expressed over the two time points, 128 were unmapped. In total, there were 794 mapped genes at the early time point of 4 hours and 157 at the late time point of 20 hours (Full list of genes in **Appendix 5**). The q-value (FDR corrected p-value) was set at < 0.05, which incorporated all of the genes inputted, as this had previously been used in the analysis to identify differentially expressed genes. I used IPA to:

1. Determine over-represented signalling and metabolic canonical pathways.
2. Divide data into diseases and functions that are over-represented in the dataset.
3. Create molecular networks (algorithmically generated pathways).

6.5.5 IPA statistics

Fisher's exact test p-value is calculated to answer the null hypothesis: Is the proportion of genes mapping to a function or pathways in my samples similar to the proportion that map in the entire population? P values quoted in the results are p-values of Fisher's exact test. P value < 0.05 was taken as indicative of a statistically significant, non-random association.

6.5.6 Canonical pathways

IPA maps the differentially expressed genes against known canonical pathways, generated prior to data input based on known literature. Two measures of association are calculated, firstly a ratio of the number of genes from the list that map to the pathways, divided by the total number of genes that map to the same pathway, secondly, a p-value of the Fisher's exact test **(Table 6-5) (Table 6-6).**

Name	p-value	Ratio
Activation of IRF by cytosolic PRRs	5.19E-04	9/58 (0.155)
Death receptor signalling	1.15E-03	11/91 (0.121)
Retinoic acid mediated apoptosis signalling	1.83E-03	8/56 (0.143)
Salvage pathways of pyrimidine ribonucleotides	3.56E-03	10/90 (0.11)
p53 signalling	6.08E-03	10/97 (0.103)

Table 6-5 Top canonical pathways of early response

Table of the top 5 canonical pathways at the early time point of 4 hours with associated ratio and p-value.

Name	p-value	Ratio
Agranulocyte adhesion and diapedesis	3.92E-05	8/167 (0.048)
Granulocyte adhesion and diapedesis	1.89E-04	7/157 (0.045)
Pyrimidine deoxyribonucleotides de novo biosynthesis	4.38E-04	3/20 (0.15)
Salvage pathways of pyrimidine ribonucleotides	5.98E-04	5/90 (0.056)
Communication between innate & adaptive immune cells	1.94E-03	4/70 (0.057)

Table 6-6 Top canonical pathways of late response

Table of the top 5 canonical pathways at the late time point of 20 hours with the associated ratio and p-value.

6.5.7 Disease and function analysis

IPA divides the data into diseases and biological functions that are over represented in the data. IPA provides these categories based on high quality gene ontology information and manually curated IPA content. For each potential disease/function two statistical measurements are made. Firstly the overlap p-value, which assesses the significance of the overlap between dataset genes and known targets. Secondly, the activation z-score, which is used to infer the activation state of the regulators **(Table 6-7) (Table 6-8).**

6.5.8 Upstream regulator analysis

IPA identifies the upstream transcriptional regulators that could explain the observed gene expression in the dataset. This can help identify the biological activities occurring in the neutrophil. This analysis is achieved by using prior knowledge of expected effects between transcriptional regulators and their target genes. The analysis examines how many known targets of each

transcription regulator are present in the dataset and considers the direction of change to what might be expected from the literature. A prediction can thus be made with regards to the activation state of the regulator; activated or inhibited. For each potential regulator two statistical measurements are made. A p-value assesses the significance of the overlap between dataset genes and known targets and the activation z-score, which is used to infer the activation state of the process **(Table 6-9)**.

Categories	Diseases/Functions Annotation	p-Value	Predicted Activation State	Activation z-score	No. of Molecules	Molecules
Inflammatory Response	innate immune response	1.35E-07	Increased	2.538	25	APOBEC3A, APOBEC3F, APOBEC3G BST2, DDX58, FFAR2, FFAR3, IFIH1, IFIT2, IRF7, ISG15, MX1, OTULIN, PM PPARG, STAT1, TNFRSF10A, TRIM1 TRIM14, TRIM21, TRIM26, TRIM5, TRIM56, TRIM8, ZBP1
Antimicrobial Response, Inflammatory Response	antiviral response	1.22E-05	Increased	2.931	20	APOBEC3F, APOBEC3G, BST2, DDX58, DHX58, FOSL1, HYAL2, IFIH1 IFIT1, IFIT1B, IFIT2, IFIT3, IRF7, ISG2 MB21D1, MX1, PML, STAT1, TRIM5, USP21
Antimicrobial Response	inhibition of virus	2.10E-04	Increased	2.271	9	APOBEC3B, APOBEC3F, APOBEC3G BST2, GSK3B, IL27, MX1, SP100, TRIM5
Antimicrobial Response, Inflammatory Response	antimicrobial response	3.50E-04	Increased	2.931	24	APOBEC3F, APOBEC3G, BST2, DDX58, DHX58, FOSL1, HYAL2, IFIH1 IFIT1, IFIT1B, IFIT2, IFIT3, IRF7, ISG1 ISG20, MB21D1, MICA, MX1, PML, PPM1D, STAT1, TLR6, TRIM5, USP21
Cell Signalling	replication of viral replicon	1.34E-06	Decreased	-3.148	12	APOBEC3A, APOBEC3B, APOBEC3C APOBEC3F, APOBEC3G, BST2,

						DICER1, IFIT1, ISG15, ISG20, MX1, PARP10
Infectious Disease	replication of Herpesviridae	8.82E-06	Decreased	-2.556	12	CXCL10, DDX58, IFIH1, ISG20, PARP12, PML, SAMHD1, SP100, STAT1, TGFBR2, ZBP1, ZEB2
Cell Signalling	viral life cycle	9.26E-06	Decreased	-2.377	14	APOBEC3A, APOBEC3B, APOBEC3C APOBEC3F, APOBEC3G, BST2, DICER1, IFIT1, ISG15, ISG20, MX1, NUP62, PARP10, PSIP1
Infectious Disease	replication of virus	8.90E-05	Decreased	-3.326	49	AGO4, APOBEC3B, APOBEC3C, APOBEC3F, APOBEC3G, ATP6V1A, BST2, CCR1, CD58, CNOT7, CXCL10 DDX58, DICER1, FSCN1, GSK3B, HERC5, IFIH1, IFIT1, IL27, IRF2, IRF7 ISG15, ISG20, MID1IP1, MX1, NUP62, PARP12, PIKFYVE, PML, PRKAG2, PSIP1, RAB11FIP1, RACGAP1, RAF1, RHOH, SAMHD1, SGPL1, SP100, SPHK1, STAT1, TGFBR2, TNK2, TRADD, TRIM14, TRIM21, TRIM5, USP21, ZBP1, ZEB2

Table 6-7 Disease and function table of early response

Table showing the top and most relevant disease and functions the dataset has mapped to, including a p-value, z-score, predicted activation direction, the number of genes involved in any given function and the specific genes involved.

Categories	Disease/Functions Annotation	p-value	Predicted Activation State	Activation Z-score	No. of molecules	Molecules
Cellular Movement, Haematological System Development and Function, Immune Cell Trafficking	cell movement of myeloid cells	1.57E-06	Increased	2.386	18	CCL4, CD69, CXCL2, CXCR1, CXCF CYBB, EGLN1, HIF1A, IL1A, IL1RN, ITGAM, MADCAM1, PPBP, SEMA4A SERPINB1, TICAM1, TMSB10/TMSB4X, TXN
Cellular Movement, Immune Cell Trafficking	leukocyte migration	4.51E-06	Increased	2.491	23	CCL4, CD22, CD69, CD80, CXCL2, CXCR1, CXCR2, CYBB, EGLN1, GG HIF1A, IL1A, IL1RN, ITGAM, MADCAM1, PPBP, PRMT2, RARA, SEMA4A, SERPINB1, TICAM1, TMSB10/TMSB4X, TXN
Haematological System Development and Function, Tissue Morphology	quantity of leukocytes	5.34E-06	Increased	2.902	23	AFF1, CCL4, CD22, CD69, CD80, CISH, CXCL2, CXCR2, CYBB, HIF1A IL1A, IL1RN, ITGAM, KLF10, MPZL2 PIM1, PIM2, RARA, SERPINB1, SIGIRR, SIGLEC1, THRA, TICAM1
Cellular Movement, Haematological System Development and Function, Immune Cell Trafficking	cell movement of leukocytes	6.05E-06	Increased	2.213	21	CCL4, CD22, CD69, CD80, CXCL2, CXCR1, CXCR2, CYBB, EGLN1, HIF1A, IL1A, IL1RN, ITGAM, MADCAM1, PPBP, RARA, SEMA4A, SERPINB1, TICAM1, TMSB10/TMSB4X, TXN

Cell Death and Survival	cell viability	9.82E-06	Increased	2.106	28	AGRN, CAMK1G, CCL4, CD22, CD8 CISH, CXCL2, CYBB, DAB2, HIF1A, IGFBP7, IL1A, IL1RN, ITGAM, NME PIM1, PIM2, PPBP, PPFIA4, PPP1R12B, RARA, RRM1, SERPINE SHFM1, TICAM1, TNK2, TPK1, TXN
Cell Death and Survival	apoptosis of blood cells	2.46E-05	Decreased	-2.458	15	AGRN, CCL4, CD22, CD69, CD80, CXCL2, CYBB, HIF1A, IL1RN, ITGA PIM1, PIM2, RARA, THRA, TICAM1
Cell Death and Survival	apoptosis of hematopoietic cells	1.41E-03	Decreased	-2.621	7	AGRN, CCL4, HIF1A, PIM1, PIM2, RARA, THRA
Cellular Compromise	degeneration of cells	8.61E-03	Decreased	-2.236	8	AFF1, HIF1A, IL1RN, LRPAP1, MME SEMA4A, THRA, TXN

Table 6-8 Disease and function table of late response

Table showing the top and most relevant disease and functions the data has been mapped to, including a p-value, z-score, predicted activation direction, the number of genes involved in any given function and the specific genes involved.

Upstream regulator	Activation Z score	p-value	Predicted activation state
IFNA2	5.565	1.16E-16	activated
IFNL1	4.727	1.00E-15	activated
IRF7 (log ratio +2.556)	5.146	2.71E-15	activated
IRF3	4.277	6.15E-11	activated
TLR4	2.680	7.44E-10	activated
MAVS	3.536	1.83E-09	activated
DDX58 (log ratio +3.373)	2.651	4.08E-08	activated
STAT1 (log ratio +2.793)	3.697	5.89E-07	activated
MAPK1	-5.773	1.92E-13	inhibited
TRIM24	-4.122	3.45E-12	inhibited
IL1RN (log ratio +2.745)	-3.207	1.11E-04	inhibited

Table 6-9 Upstream regulators of early response

Table of selected upstream regulators, including an associated activation Z score, p-value and the predicted activation state at the 4-hour time point. Those upstream regulators that were found differentially expressed in the dataset have their log ratio included also.

6.5.9 Validation of microarray results by qPCR

12 RNA samples (6 control and 6 RSV exposed) for the 4 hour time point were analysed using qPCR. RNA was converted to cDNA and qPCR undertaken as described in **Section 6.1.4** to look for the expression of 7 differentially expressed genes purposively selected from the microarray data on the basis of their high expression value (2.5 - 7.9), and involvement at different steps of the pathways of relevance. These genes were DDX58, DHX58, IRF7, MX1, STAT1, and USP18, which were all up-regulated. One down regulated gene was chosen, DICER. The microarray results were confirmed with a statistically significant change in the expected direction for all genes **(Figure 6-7)**. A 12.87 fold increase was found for IRF7 following RSV exposure (p=0.026) A 41.08 fold increase was found for MX1 (p=0.0022). A 129.64 fold increase was found for USP18 (p=0.0022). A 9.15 fold increase was found for STAT1 (p=0.0022). A 21.55 fold increase was found for DDX58 (p=0.0022). A 90.42 fold increase was found for DHX58 (p=0.0095). Expression of DICER was significantly decreased in response to RSV (p=0.0022). Statistical analysis was performed using Mann Whitney U tests and confirmed on two statistical programmes (PRISM, StatsDirect).

6.5.10 RSV uptake with reduction over time confirmed

All of the 8 RSV exposed neutrophil cDNA samples were analysed to quantify the amount of RSV in each sample compared to the mean of the internal housekeeping genes B2M and GAPDH. RSV N gene was quantified at 4 hours and 20 hours and a statistically significant decrease at 20 hours was observed (p value = 0.0152) **(Figure 6-8)**. Mann Whitney U test was used.

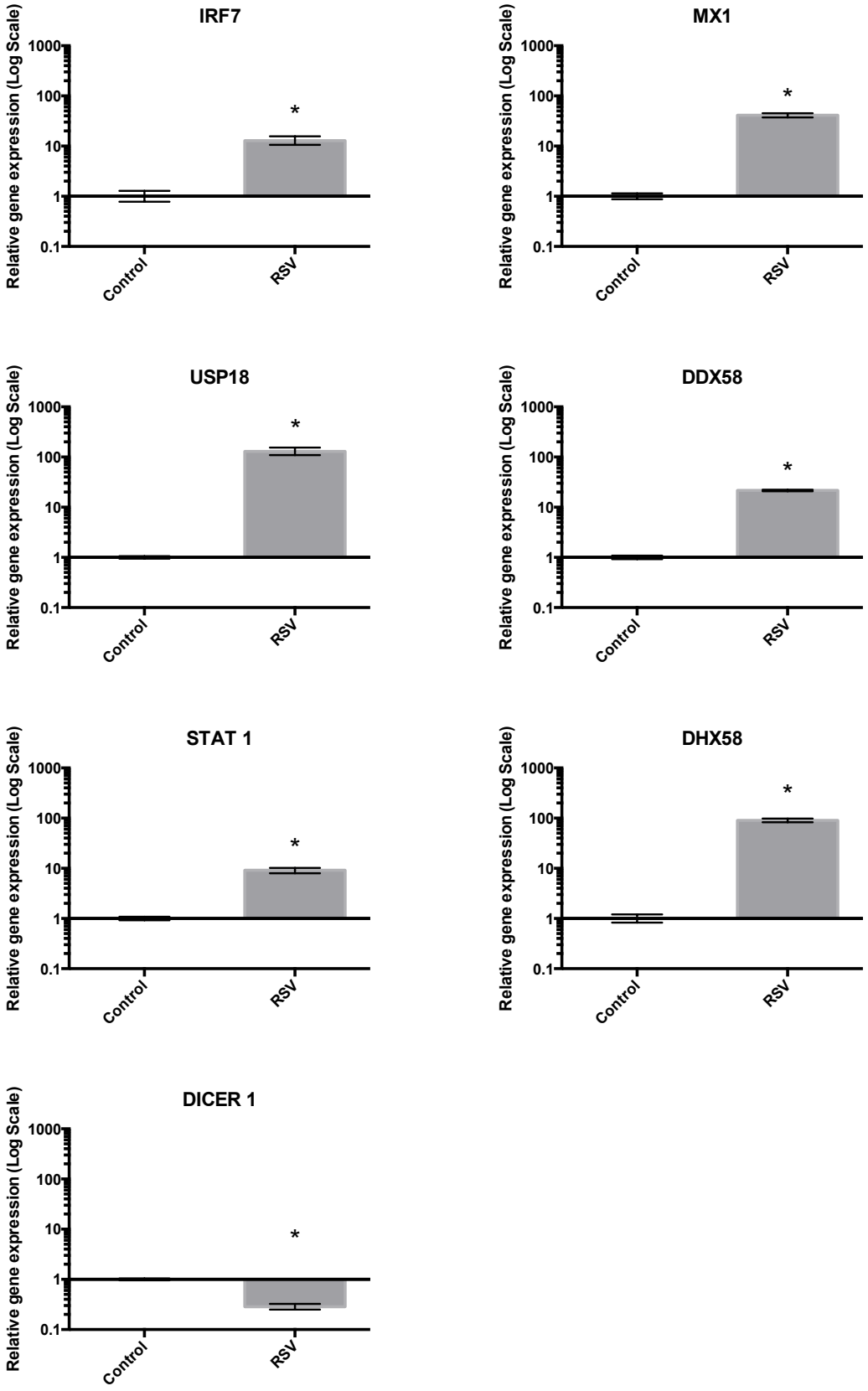

Figure 6-7 Target genes from microarray validated by qPCR

Expression of IRF7, MX1, USP18, DXD58, STAT1, DHX58 and DICER 1 were measured by qPCR. All were significantly upregulated in RSV exposed neutrophils compared to control except for DICER 1, which was significantly downregulated. IRF7 p value = 0.026, MX1, USP18, STAT1, DICER1, DDX58 p values = 0.0022 and DHX58 p value= 0.0095.

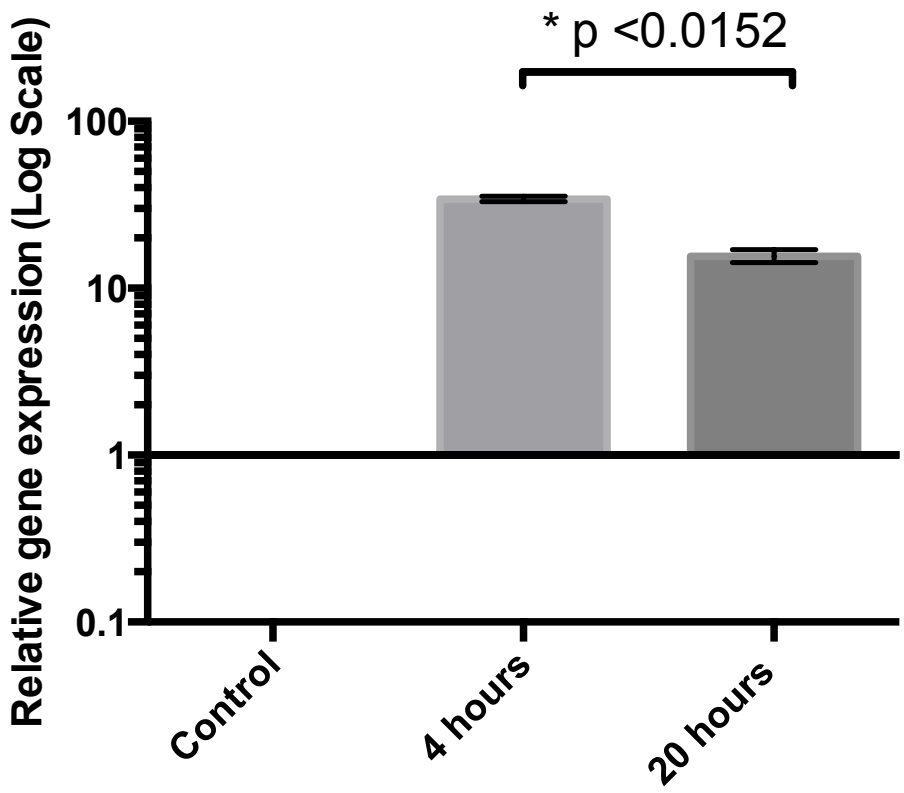

Figure 6-8 Relative RSV gene expression

RSV N gene expression was measured by qPCR at 4 and 20 hours, and is expressed relative to the internal housekeeping genes B2M and GAPDH on a log axis. RSV N gene was found in the neutrophil at both time points and there was a significant decrease in RSV N gene at 20 hours compared to 4 hours.

6.6 Discussion

There are two possible sources of experimental variation when analysing samples using microarray; the biological samples and the performance of the technology. By using the CGR facility and staff with their established and standardised laboratory protocols, the latter was minimised. The data quality assessment carried out, to ensure data suitability to address the hypothesis, included analysis of the expression density curves for all samples. The results implied that there was no flaw in the data with respect to cross-chip/cross-array normalisation.

The two data sets, from the early time point of 4 hours and the later time point of 20 hours, were markedly different, as shown by the principal component analysis **(Figure 6-6)**. Neutrophils are short-lived cells, and it is thus not that surprising that their transcriptional profiles would change over this relatively short period of time. Therefore, I will discuss the results of their RSV induced transcriptional changes in two separate sections and finish with a section relating to the persistent changes across both time points, of which there were 87 shared differentially expressed genes.

As described in **Chapter 3**, RSV does not replicate inside neutrophils. This was confirmed in this study and the reduction in RSV at 20 hours from 4 hours was found to be statistically significant. This significance, compared to the non-significant trend in **Chapter 3**, is likely due to a more robust RT-PCR method, using an optimised pair of housekeeping genes as the internal reference to RSV expression. The microarray data and subsequent PCR validation sheds light on the mechanisms at play in the neutrophil that allow inhibition of viral replication.

6.6.1 Early response

Ingenuity pathway analysis revealed activation of IFN regulatory factor (IRF) and IFN signalling pathways as the most significantly over-represented pathways at 4 hours. In addition, the majority of the disease/function groups identified were related to anti-viral function. The predicted upstream

regulators also reflect this antiviral response. To validate the microarray data, RT-PCR was performed for several of the IFN-related genes, including DDX58 (RIG-I), DHX58, IRF7, USP18, MX1, and STAT1. Correlating with the microarray data, there was upregulation of these genes at the early time point of 4 hours providing evidence for an early anti-viral response to RSV by the neutrophil. In the sections below, I will detail the known pathways and antiviral mechanisms using relevant literature relating to the anti-viral genes identified at work in the neutrophil.

6.6.2 Pattern recognition receptors

Interferon responses are essential for the immune response to virus and are triggered through the actions of cytoplasmic helicases RIG-I (DDX58) and MDA5 (IFIHI) (40, 262, 263). Intracellular viral products such as RNA initiate the signalling. Transcription of both these PRR genes was upregulated in my data set at 4 hours. Signalling through both RIG-I and MDA5 involves interaction with interferon promoter-stimulating factor 1 (IPS-1) adaptor protein, also known as MAVS (mitochondrial antiviral signalling protein). MAVS was identified as an activated upstream regulator. This interaction results in activation of two parallel signalling pathways leading to nuclear translocation of NF-κB and IFN regulatory factors (IRFs), and the consequent production of IFN and chemokines. The rapid production of IFN-α/β leads to the expression of hundreds of Interferon Stimulated Genes (ISGs), which have antiviral and immunomodulatory properties directed at limiting infection (264). RIG-I has specifically been shown to be triggered by RSV, playing a role in inhibiting viral replication and spread (45, 262, 265). MDA5 induction has more recently been found to be required to prevent early degradation of IRF3, a key transcriptional regulator of type I IFN responses (266). LGP2, encoded by DHX58 (DEXH (Asp-Glu-X-His) box polypeptide 58), or RIG-I like receptor, is a regulator of both RIG-I and MDA5 mediated signalling, which can bind both ssRNA and dsRNA.

TLR4 was also identified as a potential upstream regulator in this data set. A study, which examined the response of TLR4 deficient mice to RSV, found an impaired ability of the mice to respond to RSV with delayed viral

clearance. The authors suggested that the innate immune response to RSV may be mediated by signalling through TLR4 (267). More recently Blanco *et al* have shown the interaction is between RSV F protein and TLR4 co-receptor MD-2 (268). TLR4 activation leads to signal transduction and gene expression via the NF-κB pathway. The upregulation in the PRRs RIG-1 and MDA5, and the apparent involvement of the upstream regulators TLR4 and MAVS indicate that the neutrophil is recognising and responding to the presence of RSV. In addition a number of molecules involved in key antiviral pathway were also differentially expressed, such as LGP2 and IRF7. The two key pathways identified, interferon regulatory (IRF) pathway and the JAK-STAT pathway, are discussed and illustrated below.

6.6.3 The interferon regulatory factor pathway

Recognition of RSV by the PRRs RIG-1 and MDA5 activates the IRF pathway **(Figure 6-9).** In the early phase of infection signalling through these PRRs is by LGP2 and effected by MAVS. This results in upregulation of interferon stimulated genes (ISGs) and induction of cytokines, in particular interferons. Type I IFNs then upregulate IRF7 leading to further induction of IFNs through phosphorylation of STAT, enhancing the antiviral state of the cell.

IRFs are a family of transcription factors, which control type I IFN expression. Nine human IRFs have been identified. Of these, IRF1, 3 and 7 are the key regulators of the type I IFN response to viral infection (269, 270). IRF7 is usually expressed at low levels until viral contact, when it is induced, phosphorylated, undergoes dimerization and nuclear translocation. It was one of the key upstream regulators found within my microarray dataset. The IRF7 gene was also differentially transcribed, and this was confirmed by PCR. RSV induced IRF1 and -7 activation has been described in alveolar epithelial cells in a time dependant manner, with expression peaking at 6 hours post infection (271).

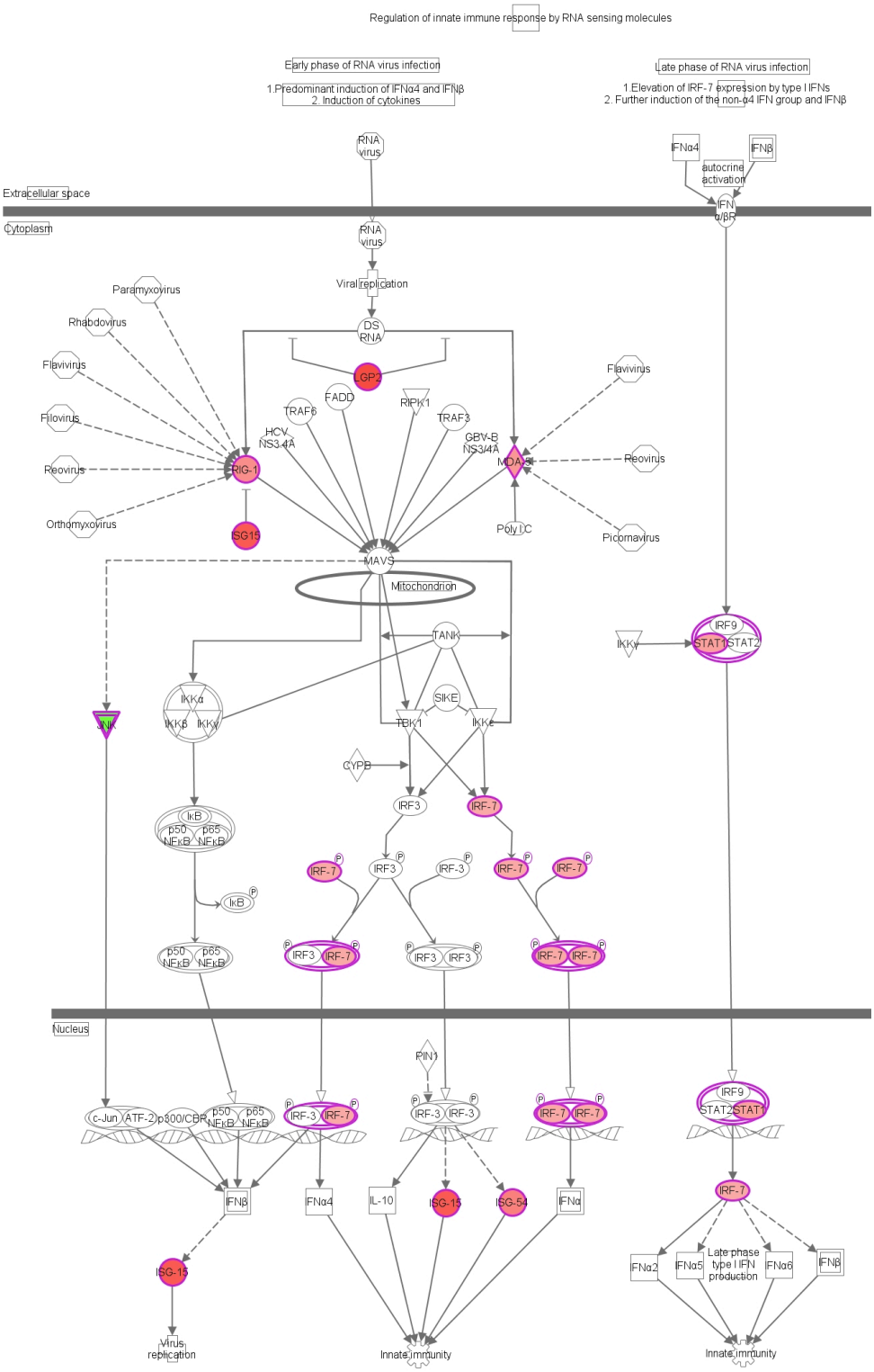

Figure 6-9 Regulation of the innate immune response by RNA sensing molecules

Two pathways are shown which are involved in the regulation of the innate immune response by RNA sensing molecules. Firstly, on the left, is the response to the early phase of infection. RIG-1 detects RSV; single stranded RNA virions and potentially any dsRNA made by attempts to replicate. MDA5, another PRR also detects virus. LGP2 regulates signalling of both these PRRs. Signalling by MDA5 and RIG-1 is effected through MAVS, identified as an activated upstream regulator, leading to upregulation of interferon stimulated genes (ISGs) and induction of cytokines including IFNs. The second pathway, on the right, is the response to the late phase of RNA virus. Upregulation of IRF7 is triggered by type I IFNs that then leads to further induction of IFNs through the phosphorylation of STAT. These pathways drive the cell into an antiviral state.

6.6.4 Jak-STAT Pathways

STAT 1 (Signal transducer and activator of transcription 1) is involved in mediating cellular responses to IFNs. Following type I IFN binding to cell surface receptors, signalling via protein kinases leads to activation of Jak kinases and phosphorylation of STAT1. This is illustrated in **Figure 6-10**. STAT1, which is shown transcriptionally upregulated by RSV, becomes phosphorylated and then associates with ISGF3G/IRF-9 to form ISGF3 transcription factor. This enters the nucleus where it acts as a transcription activator of IFN stimulated genes (ISGs), which drive the cell into an antiviral state. **Figure 6-10** shows the well-characterised downstream effect of this interferon-signalling pathway, i.e. the production of IFI35, IFIT1, MX1 and IFIT 3, all transcriptionally upregulated in my dataset.

6.6.5 IFN stimulated genes (ISGs)

Interferon-stimulated genes modulate biologic effects of IFNs. There are >300 ISGs which can be assigned to functional categories. The specific function of a large proportion of these is unclear, but some are known to play key roles in host defence (272). Below I outline some of the highly differentially transcribed ISGs within my dataset and highlight those that are particularly pertinent to RSV infection.

6.6.5.1 Ubiquitin Specific Peptidase 18

Ubiquitin Specific Peptidase 18 (USP18), also known as ISG43, was the highest upregulated mRNA at the early time point (FC 7.95). This protein cleaves ubiquitin from ubiquitinylated substrates, specifically ISG15 fusions. ISG15 is a ubiquitin-like protein that is conjugated to intracellular target proteins (ISGylation) upon activation by IFN. ISGylation may modulate the JAK-STAT pathway. The secreted form of ISG15 has a number of roles; it can induce natural killer cell proliferation, act as a chemotactic factor for neutrophils and as an IFN-γ-inducing cytokine. The ISG15/USP18 pathway has been found highly expressed in response to a number of viruses, including hepatitis C and vesicular stomatitis virus (273, 274).

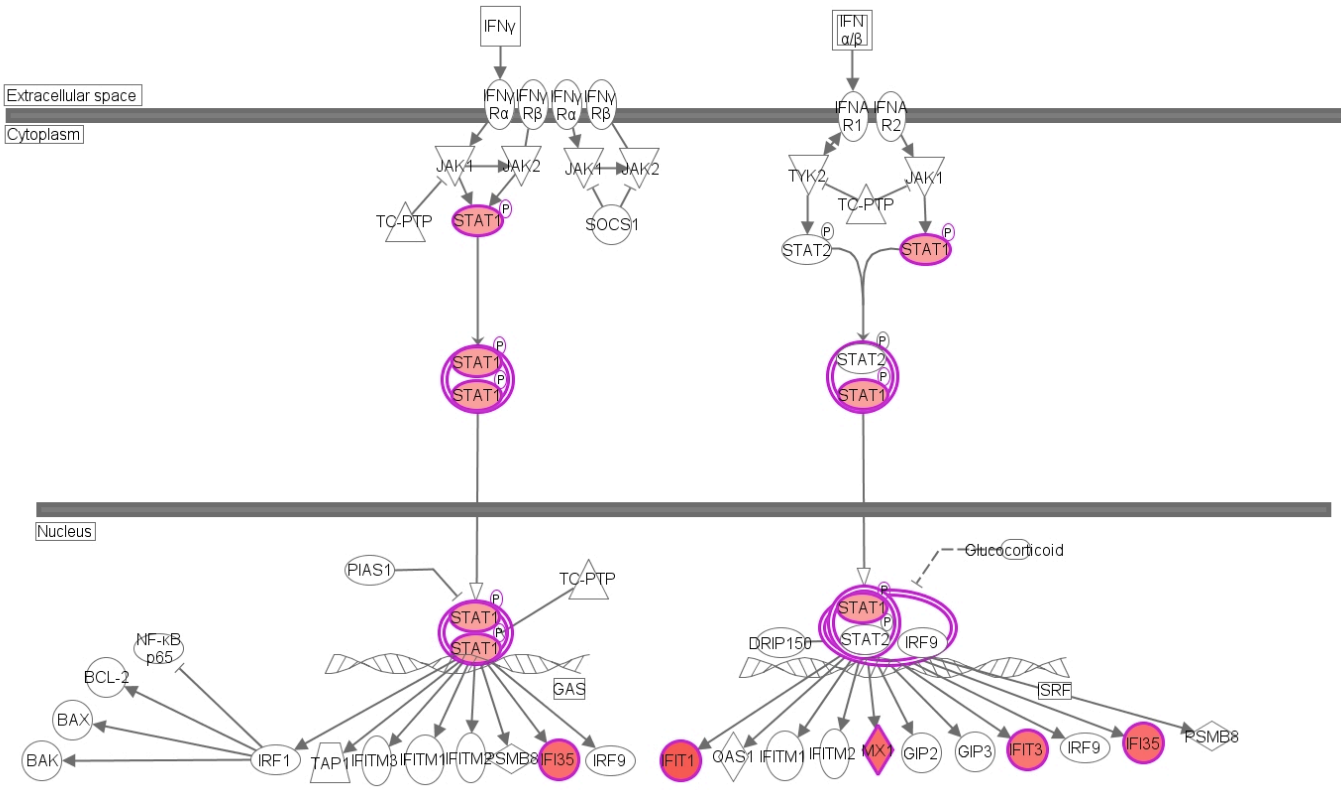

Figure 6-10 Interferon signalling pathway through Jak-STAT pathway

The cell response to IFN can be mediated through the Jak-Stat pathway. Activation of Jak kinases and phosphorylation of STAT1 allows association with IRF-9 to form ISGF3 transcription factor, which enters the nucleus and drives the cell into an antiviral state. Downstream IFI35, IFIT1, MX1 and IFIT 3 were all transcriptionally upregulated in the microarray data.

6.6.5.2 Myxovirus resistance 1

Myxovirus Resistance 1 (MX1) gene encodes a GTP-metabolising protein that participates in the cellular antiviral response. It is activated through the Jak-STAT pathway, induced by type I and II IFNs and antagonises the replication process of RNA (particularly negative stranded) and DNA viruses. It achieves this by binding and inactivating their ribonucleocapsid. MX genes were discovered around 50 years ago by Lindenmann *et al* (275). The protein encoded by MX1, called MXA, has a broad antiviral activity, which has been studied in the context of infection with a large number of different RNA viruses (276). In measles, a member of the paramyxoviridae family, MX1 has been shown to inhibit virus in a human mononuclear cell line (277). In contrast RSV infection of Vero cells was resistant to the antiviral effects of MxA (278). In a study using RSV infected cotton rats MX1 and 2 were highly expressed in the lungs early in infection and in a dose dependant fashion, which the authors concluded, was evidence of a robust type 1 IFN response (279).

6.6.5.3 Tetherin

Tetherin, encoded by the BST2 gene, is expressed as part of the IFN dependant antiviral response pathway and is a viral 'restriction' factor. This was significantly upregulated at the early time point. A mechanism whereby tetherin inhibits enveloped virus release by tethering the budding virus like particles has been proposed (280). Tetherin has been associated with all tested retroviruses, and some filoviruses. It has been recently reported that tetherin can act as a PRR inducing NF-kB dependant pro-inflammatory gene expression in virus infected cells (281).

6.6.5.4 Double stranded RNA-specific endoribonuclease

Double stranded RNA-specific endoribonuclease (DICER) gene encodes a protein that possesses an RNA helicase motif containing a DEXH box. This ISG was down-regulated by RSV exposure, a finding confirmed by PCR. It functions as a ribonuclease and plays a central role in short dsRNA-mediated post-transcriptional gene silencing. Gene silencing, mediated by RNA inference, controls the elimination of transcripts from mobile and

repetitive DNA elements of the genome, and the degradation of exogenous RNA of viral origin. Reduced DICER expression in the cord blood of infants subsequently admitted with severe RSV disease has recently been reported. The authors hypothesized that this reduction might have led to diminished anti-viral activity and impairment of innate cellular function (282). They did not measure the level of DICER in the patients at the time of illness. It is possible that those children who are already predisposed by low DICER levels and thus a reduced ability to interfere with viral replication are made more so by RSV mediated down regulation of DICER.

A number of groups of genes, whose antiviral functions have previously been recognised, were well represented in the data, including the APOBEC3, TRIM and IFIT families. The mechanism by which many of these genes inhibit viral replication is not fully known, but it is possible that they interfere with one or more of the following: viral entry, viral DNA synthesis, intracellular movement of viral nucleic acids and viral gene expression (283-285).

6.6.5.5 APOBEC3 enzymes

APOBEC3 (apolipoprotein B mRNA editing enzyme, catalytic polypeptide-like) is a superfamily of enzymes encoded by the APOBEC3 gene. They are capable of deaminating cytidines in single stranded DNA replication intermediates, leading to cytidine being changed to uridine and guanine to adenine, a phenomenon termed DNA editing. APOBEC3G is the most widely studied member of the family. In my dataset, APOBEC3 -A, -B, -C, -F and -G were upregulated, with APOBEC3-F and –G being the most highly expressed. RNA virus replication of measles, mumps and RSV, has been found to be sensitive to A3G (APOBEC3G) inhibition in *in vitro* study (284).

6.6.5.6 TRIM Proteins

A number of genes encoding proteins of the TRIM (tripartite motif-containing proteins) family were differentially expressed within my dataset. Thus TRIM 5, 14, 21, 26, 34 and 56 were up-regulated and TRIM 8 and 11, down-regulated. The TRIM family is a diverse family of RING finger domain-

containing protein that are classified into 11 subgroups. They are involved in the regulation of innate immune responses through modulation of PRR signalling pathways including TLRs and RIG-I. Many TRIM proteins are induced by type I IFN stimulation (286, 287). TRIM 21 has previously been shown to be induced by RNA viral infection, and is an essential modulator of IRF3 stability (288). TRIM proteins can exert antiviral activity through modulation of viral proteins as well as interacting with the innate immune signalling pathways (289). TRIM 56 was recently identified to associate with the N-terminal protease of bovine diarrhoea virus and inhibit its replication (285). TRIM 5, 11, 26 and 31 have been demonstrated to inhibit HIV entry. TRIM 11, which was down-regulated in the analysis, inhibits RIG-1 mediated IFN beta production by targeting the TBK1 complex (290).

6.6.5.7 IFIT protein encoding genes

IFIT (interferon-induced protein with tetratricopeptide repeats) protein encoding genes were over-represented at 4 hours, all by a >3 fold change, specifically –1, -1B, -2, -3, -5. Their transcription can be induced by viral infection. IFIT proteins show antiviral activity in two ways. They bind to both viral nucleic acids and to eIF3 (eukaryotic initiation factor 3) thereby inhibiting the translation process (283). IFIT1-5 genes were expressed in the whole blood analysis of infants with RSV (255).

6.6.6 Late response

The number of differentially expressed genes at the later time point was less than I expected. This may relate to variability in the quality of the data, with less genes reaching acceptable levels of significance, rather than less genes actually being differentially expressed. There are limitations to carrying out pathway analysis based on a small number of differentiated genes. A large number of pathways may be highlighted showing one or two differentially expressed genes rather than identification of a small number of significantly overrepresented pathways. In addition, the limitations of my model become apparent at this timepoint. Neutrophils present in the airways of an infant with RSV bronchiolitis for 20 hours would have been exposed to cytokines/chemokines and had direct contact to many other immune cells,

rather than just RSV, and their responses may change accordingly. In this *in vitro* system however, the top function networks relate to the movement and activation of lymphocytes and leukocytes. Genes for molecules that are chemoattractants such as CCL4, CYBB, EGLN1, HIF1A, IL1RN, TICAM, IL1A were all upregulated. Neutrophils, as they age and potentially become apoptotic, appear to be stimulating the influx of other immune cells to the site of inflammation. This would seem to include strong signals for further neutrophil migration. PPBP encodes a protein CXCL7, which is a potent chemoattractant and activator of neutrophils, and was the second highest upregulated molecule (LogFC 5.2). In contrast, there also appears to be an attempt at modulating/down-regulating neutrophil activation. Both CXCR1 and CXCR2, receptors for the neutrophil activating and migration factor CXCL8, are down-regulated at 20 hours. A picture of inflammatory balance is emerging at both time points, between inflammatory anti-viral processes and an attempt to keep the inflammation in check by the use of regulators. CISH (cytokine inducible SH2-containing protein) a cytokine signalling suppressor that works through a negative feedback system of the STAT pathway was upregulated at 20 hours. This was also found at 4 hours, although less pronounced, suggesting that this regulation of inflammation and anti-viral response is constant during neutrophil exposure to RSV.

Microarray data indicating an ability for neutrophils to interact with cells of the innate and adaptive immune systems occurred at both time points, so will be discussed in combination.

6.6.7 Immune crosstalk

Some evidence that the neutrophil is capable of modulating the function of other immune cells in response to RSV can be found in the microarray data. Further work would need to be done to confirm the interactions, but intriguing hypotheses can be built. The gene for IL-27, a novel IL-12 cytokine family member was upregulated. This is an immunoregulatory cytokine, which has been found in mice to have a dominant role in the suppression of immune hyperactivity, with IL-27 receptor deficient mice succumbing to $CD4^+$ T cell mediated inflammatory disease (291). IL-27 appears to have inhibitory

effects on Th1, Th2 and Th17 responses. Interestingly IL-27 has been shown to inhibit vaccine enhanced pulmonary disease following RSV infection (292). In addition, IL-27 receptor deficient mice experience severe RSV-induced disease, characterised by mucus secretion, enhanced expression of the Th17-related cytokine IL-17a and Th2-related cytokines IL-5 and IL-13, and inhibition of the Th1-associated cytokine IFNγ (293). Effective, efficient clearance of RSV from the airways relies on a balanced Th cell response, and IL-27 appears to play a regulatory role within this process (294). The neutrophil may contribute to airway levels of this cytokine.

A number of investigators have recently speculated that the neutrophil may play a role as antigen-presenting cells (APCs) particularly to T cells (295, 296). Antigen presentation involves the appearance of antigens, such as virus or bacteria, on major histocompatibility complex (MHC) molecules on the cell surface in order to be recognised by other immune cells. Intracellular antigens, such as internalised virus, can be presented on MHC class I or II molecules, in order that CD4+T cells recognise the antigen and kill the target cell. DCs, macrophages and B cells are the three main professional APCs. Only MHC II expressing APCs, such as DCs, are able to both present antigen to the T cell and to prime them.

Neutrophils have been found to have resting, cytoplasmic stores of molecules required for antigen presentation and T cell stimulation i.e. major histocompatibility complex class II (DR) antigen, CD80 and CD86 (297, 298). CD80, a protein that provides a co-stimulatory signal needed for T cell activation and survival, was upregulated at 20 hours in my dataset. This suggests a maturation process by the neutrophil, following RSV entry, similar to that seen by DCs. Support for this concept is the concurrent upregulation of CD11c (ITGAX). Recent reports have described the existence of neutrophil-dendritic cell hybrids during inflammation, characterised by co-expression of DC surface markers (including CD11c and CD80), and neutrophil markers (including Ly6G). It has been hypothesized that these may be important for bacterial clearance and antigen presentation (299, 300). The differential expression of these genes does not necessarily mean

that the respective proteins are expressed on the cell surface membrane but it does lend some weight to the concept that the neutrophils may act as APCs in RSV infection.

The microarray approach taken in this chapter begins to explore the antiviral response of the neutrophil to RSV, but is only able to provide data on transcriptional change. Genes can be regulated in a number of ways and mRNA upregulation might not necessarily equate with protein production as mRNA can be transcribed yet not translated. Advancing this work further would need to involve measurement of proteins translated from the differentially expressed mRNA, in order to give a more complete picture of the neutrophil antiviral response. A further limitation of this study is that the RSV lysate used is not pure. The RSV has been propagated, as described in **Section 2.4**, in Hep2 cells and this process is likely to have resulted in the RSV lysate containing other activators, which may also contribute to the differential expression measured. This limitation of the *in vitro* model and its implications is discussed in more detail in **Chapter 7**.

6.7 Summary

In this chapter, I have shown that the neutrophil is a transcriptionally active cell, which alters its gene expression profile in response to virus exposure. The microarray data reveals potential contributions by the neutrophil to both innate and adaptive arms of the host immunity.

Chapter 7 General discussion

RSV bronchiolitis is characterised by airway neutrophilia and inflammation (39, 55). Compared to other cells within the airway, the immune response of neutrophils to RSV has been somewhat neglected. This is in part due to the traditionally held view of the neutrophil as a short lived, phagocytic cell with limited capacity to interact with and affect the environment and cells around it. However, the neutrophil has an armoury of pro- and anti-inflammatory capabilities and is increasingly being recognised as a cell with immune-regulatory potential (102). In this thesis, the interaction and transcriptional response of the neutrophil to RSV has been examined in detail for the first time.

The overall aim of work described in this thesis was to investigate the nature of the interaction between neutrophils and RSV. The first specific aim was to establish an *in vitro* model of neutrophil-RSV interaction. In **Chapter 2** this model was established and optimised using ultra-purified adult neutrophils and laboratory propagated RSV. Previously, the majority of *in vitro* virus work, including RSV, has been carried out on immortalised cell lines such as A549 cells, which are not good physiological models of the human airway epithelium. The increasing use of primary epithelial cells better models clinical disease. However, the epithelium is not the only cell type encountered by the virus, and therefore immune cells, particularly the highly abundant phagocytic cells, should be considered. Neutrophils are difficult to work with, due to their short lifespan *in vitro*; they are not amenable to long term culture or storage and revival. This has resulted in the extrapolation of results from other similar, but not identical phagocytic cells, such as macrophages, the limitations of which were discussed in **Section 4.6**. In this thesis, the examination of human neutrophils, not an immortalised neutrophil-like cell line such as HL-60, or a ‘similar’ phagocytic cell, has been undertaken. In doing so the virus interaction is better modelled and results are more readily translated back to the disease and patient.

Any *in vitro* model is an imperfect representation of the *in vivo* situation. Acknowledgement of the model's limitations is important and where possible confirmation of the findings *in vivo* should be sought. The RSV preparation used throughout this study was produced by propagation in Hep2 cells. Although Hep2 cell debris was spun out of the RSV containing supernatant, Hep2 derived cytokines may have been present in the supernatant. The implication of this is that the neutrophil responses observed cannot be seen solely as a consequence of RSV, but of RSV plus epithelial cell line derived factors, which potentially include cytokines and chemokines. In this work I have not attempted to identify or quantify these proteins. Although Hep2 cells are a transformed epithelial cell line, originating from laryngeal carcinoma, their cytokine response to RSV infection is not dissimilar to that seen by primary epithelial cells. They have been shown to produce CCL2, CCL3, CCL5, IL-8, and IL-6 in response to RSV (301). The limitation of single cell models has been discussed in **Section 5.6** and it could be argued that exposing the neutrophils not only to RSV but also to epithelial cell derived cytokines represents an enhanced physiological model, more closely resembling the *in vivo* environment found in the airway of an infant with bronchiolitis.

In order to identify neutrophil transcriptional changes due to RSV alone, lengthy RSV purification techniques would be needed. I did trial a sucrose density gradient ultra-purification method for RSV isolation. However, ultracentrifugation in sucrose has previously been found to damage virus and result in low yields on culture (302, 303). I also found this to be the case with RSV. In addition, sucrose, which has high viscosity and hyper-osmotic properties, can be toxic to cells used with the RSV preparation, whether neutrophils or epithelial cells, affecting downstream work.

The second and third aims of the study were to determine whether RSV is taken up into the neutrophil and whether it productively replicates inside the neutrophil. The results presented in **Chapters 3 and 4** reveal that RSV becomes internalised inside the neutrophil. Although RSV was localised to endosomal-sized pockets, the mechanism of uptake was not been confirmed

to be any form of endocytosis. Rather, my supposition was that uptake was by fusion at the plasma membrane.

My data did not support the suggestion that neutrophils are a host for productive replication, nor that they were capable of transmitting RSV infection to epithelial cells. On the contrary, both RSV genomic material and protein measured from neutrophils exposed to virus decreased over time, suggesting virus degradation by the neutrophil. This novel discovery suggests a role for neutrophils in viral clearance. In RSV-infected mice depleted of neutrophils, a reduction in early viral load was observed but then a subsequent delay in viral clearance (304). This perhaps suggests that the neutrophils, through interaction with other cells, are indirectly concerned with viral clearance. The same study did show a reduction in lung DCs, and virus specific CD4 and CD8 cells in neutrophil depleted mice, suggesting that neutrophils are key to bringing about viral clearance in a timely fashion (304).

It is conceivable that virus could be spread by neutrophils, as they have the capacity to move around the lung, and to reverse migrate out of the lung. *In vitro* work on the interaction between CMV and neutrophils sets a precedent for this. A study by Saez-Lopez *et al* showed that neutrophils could transmit CMV to naïve fibroblasts after co-culture with virus suggesting a role for neutrophils in virus dissemination (235). The study by Halfhide *et al,* examining neutrophils from RSV infected infants, did show infant blood neutrophils to be positive for viral proteins and genes, in addition to the BAL neutrophils (129). If viable infective RSV was present within these neutrophil, dissemination out of the lung could be a possibility. However, neutrophils in my study were not shown to be capable of producing infective RSV progeny making this scenario unlikely. In addition, neither RSV viraemia nor satellite RSV infection outside the lung is a common occurrence in the immune-competent patient so the disease relevance of this finding is uncertain.

The findings in **Chapters 3 and 4** highlight the importance of using multiple techniques to dissect neutrophil and viral interaction. Microscopic or biochemical methods used alone to follow virus do not distinguish productive

and non-replicative virus. As discussed more fully in **Chapter 3**, a number of studies have claimed infection of immune cells, including neutrophils, without evidence of replication (142, 305). A combination of approaches is needed, which incorporates visual, biochemical and functional method. In so doing, my work has built up a picture of non-productive viral entry.

The fourth aim of this work was to compare neutrophil-RSV interaction in adult and infant neutrophils. In **Chapter 5**, cord blood neutrophils, modelling infant neutrophils, were shown to interact with RSV in the same way as adult neutrophils, confirming their applicability to neutrophils from young infants, the age group most at risk of severe RSV disease. The validity of my findings was confirmed through visualisation of RSV inside BAL neutrophils of infants with bronchiolitis. The similar distribution lent support to the RSV neutrophil interaction being a genuine disease phenomenon.

The fifth and final aim was to investigate the response of the neutrophil to RSV. The microarray data in **Chapter 6** revealed an RNA virus specific transcriptional response to RSV within the adult neutrophil. RSV replication and transcription involves the formation of RNA replication intermediates, which can then act as viral molecular patterns recognized by PRRs. These have been shown previously to modulate the activation state of a variety of cells, such as macrophages, dendritic cells, and natural killer cells. The same is likely to be true for the neutrophil. Previous studies have shown RNA receptors RIG-1, MDA5, and TLR8 mRNA and protein in neutrophils (115). My data revealed upregulation of both RIG-1 and MDA5 in response to RSV. Whether these PRRs are detecting whole virus or replication intermediates was not determined, but our previous finding of RSV mRNA transcripts in BAL neutrophils, raises the possibility of abortive transcription of RSV inside the neutrophil (129). Differentially expressed genes identified in these experiments need to be investigated in patient samples, something discussed in more detail below.

What impact, both good and bad, might the neutrophil be having, based on the findings of this *in vitro* work, on RSV disease? It is possible that the

regulation, activation state and/or number of neutrophils determine whether an immune response to RSV is 'appropriate' leading to viral clearance, activation of the adaptive response and resolution of the infection or 'overly robust' leading to lung inflammation and damage, and consequent severe disease. Neutrophils could undoubtedly result in immune mediated damage through the pro-inflammatory release of chemokines and granular enzymes (119, 126). In addition, pathological findings from RSV patients include signs of airway obstruction due to sloughing of epithelial cells, mucus secretion, and accumulated immune cells (39). Airway obstruction and oedema contribute to reduced lung function. Although in the minority compared to mononuclear cells, neutrophils contribute to the debris found in the airway lumen. (39) Microarray data in **Chapter 6** reveal the potential for the neutrophil to produce a number of chemoattractants in response to RSV, driving not only their own but also other immune cell's pulmonary recruitment. The RSV stimulated upregulation of ISGs has the potential to drive the neutrophil into an antiviral state, potentiating the pre-existing surrounding inflammatory environment resulting from infection, leading to further recruitment of immune cells, and pro-inflammatory chemokine production. However, the neutrophil also has a role to play in the resolution of the inflammation. The late response microarray data revealed downregulation of neutrophil activation receptors including CXCR1 and CXCR2. Neutrophils have previously been shown to have anti-inflammatory capabilities through their ability to block and scavenge chemokines such as CCL3 and CCL5, and produce anti-inflammatory cytokines such as IL-1RA and TGFβ1&2 (101, 102). The *in vitro* work in **Chapter 3** suggested that the neutrophil has a role in viral clearance. This combined with its ability to upregulate an antiviral response, provides strong evidence of a vital immune role against RSV infection. The balance between these different roles of the neutrophil may be important to RSV disease pathogenesis and hence severity. Neutrophils are required for an adequate immune response, but it may be that an excess of activated neutrophils results in unregulated, excessive inflammation.

Neutrophils are now considered to have a key role in the pathogenesis of inflammatory, infectious, autoimmune and neoplastic disease (102). Future work may involve translating recent insights in neutrophil biology into neutrophil-targeted therapies for treatment of inflammatory conditions. The challenge will be doing this without compromising immunity. One potential therapeutic area is that of apoptosis manipulation. Knowledge of the molecular mechanisms of apoptosis have allowed development of apoptosis modulators, which target different points of the pathway. For example, chemical mimetics of Smac have been developed which increase caspase activity and thus neutrophil apoptosis (306, 307). Inhibition of NF_kB can be achieved by a number of drugs and there is *in vivo* evidence of inflammation resolution enhancement in a rat model of pleurisy using one of these molecules, PGD_2 (308). As a number of apoptosis mechanisms are unique to the neutrophil, it is possible that pharmacological intervention could be used to target this cell to control inflammation (309). It does require however, a clearer understanding of the importance of airway neutrophilia on disease resolution. It could be that in certain situations increased neutrophil survival is the goal.

7.1 Future directions

There are a number of aspects of the study, which on reflection I may have done differently. In future work, it might be possible to use a novel method now available to overcome the impurity of the virus, in order to confirm the contribution RSV alone is making to the neutrophil response. This method involves the use of magnetic particles to capture and concentrate virus (a similar technique to that used for the neutrophil ultra-purification). The viral particles are captured by magnetic nanoparticles on the basis of electrostatic and hydrophobic interaction and a magnetic field concentrates the magnetic beads (Ozbiosciences) (310). The viral particles can then be suspended in a smaller volume to concentrate them. This technology might either allow the use of a purer preparation of RSV or potentially the use of the supernatant minus RSV so that a true control, identical except for the presence of RSV could be used.

It would have been useful to perform the microarray analysis earlier in the study, as data on new areas and pathways that I would have liked to investigate further was generated. There are a number of avenues for future work. Firstly, I need to confirm that the genes found differentially regulated in the microarray results translate to the protein level and produce the expected up- or down-expression of the individual proteins. This is best done using the RSV exposed *in vitro* neutrophils, as measuring target cytokines in BAL may confirm their presence but identifying the source as being the neutrophil would be less easy. BAL neutrophils could however be used to look for the transcriptional responses observed *in vitro*. Future work will need to consider the interaction between the neutrophil and the other important immune cells in RSV disease. The microarray data have revealed the potential for the RSV exposed neutrophil to prime and/or activate T cells. Mechanistic work, exposing T cells to RSV primed neutrophils, could confirm this and further our understanding of T cell responses in RSV disease.

A major limitation is that we can only study cells from the lower airways in BAL from severely infected patients. Ideally, we need to be able to compare the neutrophils across the spectrum of RSV disease to understand their impact on disease. It is possible that studying circulating neutrophils from patients could shed some light on the different functions of the neutrophils dependant on disease severity. Halfhide *et al* studied activation of matched BAL and blood neutrophil samples from infants intubated with RSV infection and showed that neutrophils become partially activated in the peripheral circulation (48). This might be ethically acceptable, as it would involve a minimum of 5mls of peripheral blood, and the advantage would be that it could be collected from any RSV infected patient regardless of severity. This may allow a better understanding of how the under- or over-activation of the neutrophil affects the severity of disease. The caveat being that the severity of disease could be the driving force to the neutrophil and not vice versa.

7.2 Final conclusions

Evidence presented in this thesis supports a novel role for neutrophils as innate cells at the frontline of antiviral immunity in RSV disease. For the first

time the degradation of internalised RSV has been shown in the neutrophil suggesting a role for this cell in viral clearance. In addition, a robust transcriptional response to RSV preparation has been revealed, specifically highlighting a number of interferon regulatory pathways. That severe RSV bronchiolitis is characterised by immunopathogenesis driven to a large degree by neutrophils is acknowledged in the literature. However, this thesis describes for the first time, the function of the neutrophil as a cell of importance in the immune response to RSV infection.

Appendix 1

Parent/Guardian Information Document

(For parents/guardians of children with bronchiolitis on the intensive care unit)

"The role of mucus in respiratory disease in childhood"

You are being invited to take part in a research study. Your child is on the paediatric intensive care unit at the moment and has a tube helping them to breath. We would like to collect some samples from your child's chest through the tube. Before you decide whether or not you wish to take part, it is important for you to understand why the research is being done and what it will involve. Please take time to read the following information carefully. Ask us if there is anything that is not clear or if you would like more information.

What is the study about?

Mucus plays a very important part in all respiratory diseases in childhood. It comes from cells lining the airways. If too much is produced these airways become blocked, making it difficult to breathe. This happens in illnesses such as bronchiolitis, asthma, cystic fibrosis and pneumonia. Studies in adults have shown that different amounts and types of mucus are produced in some chest diseases. What happens in children is not known, but we think that the mucus produced in a child's lung is very different from that in an adult lung.

By looking at the lung fluid in the airways and also the cells lining the airways, we want to discover how much and what types of mucus are produced in both health and disease. We also hope to find out what causes mucus production. We want to grow airway cells in the laboratory and stimulate them with different proteins, bacteria and viruses. Our long-term aim is to find ways of decreasing mucus production so that we can help children with respiratory disease.

Why has my child been chosen?

Your child has been chosen because they have bronchiolitis and are on the intensive care unit.

What will happen if I agree for my child to take part?

- As part of being on the intensive care unit, your child will need to have blood tests taken. When this is done some extra blood will be taken and stored.
- At the moment your child has a tube down helping them to breathe. As part of your child's routine care, fluid from this tube and your child's chest is regularly washed out and thrown away. We will take some of this fluid back to the laboratory and test it for different types of mucus. We will also use a very small brush to brush up some cells from the airways through the tube.
- Using these blood and airway samples, we will also test for genes which may be important in chest diseases. If we find any that are of interest, we will put these into a secure on-line database so that other investigators can study them as well. It will not be possible to identify your child from what is published.

Are there any disadvantages to my child taking part in this study?
If your child is sedated, then there will be no disadvantages from taking part in the study. If your child is not sedated, the brushing technique and the suction of fluid from your child's chest may cause them to cough immediately afterward.

Are there any benefits to my child taking part in this study?
No, there are none. While this study will not benefit your child directly, it may help us to understand more about childhood respiratory disease and help us to find treatments for other children in the future.

Will my child's GP be informed of their participation in this study?
Your child's GP will be informed unless you wish otherwise.

Does my child have to take part?

No. It is up to you to decide whether or not to take part. You are free to withdraw from the research at any time and without giving a reason. Your decisions about this will not affect the standard of care your child receives.

If you would like to take part, you will be given this information sheet to keep and be asked to sign a consent form.

Will the information on my child be kept confidential?
Yes, all personal information will be kept confidential and secure. Only people involved in the study will have access to the information. This study will be published in a medical journal but it won't be possible to identify individual children or parents from what is written. This study has been approved by the Liverpool Children's Research Ethics Committee, which includes lay members representing the local community.

What if you have any problems or would like further information about the study?
You can either contact:

Dr Paul McNamara,
Institute of Child Health,
Alder Hey Children's Hospital,
Eaton Rd,
Liverpool, L12 2AP
email: mcnamp@liv.ac.uk

The Patient Advisory Liaison Service (PALS)
Alder Hey Children's Hospital,
Eaton Rd,
Liverpool, L12 2AP
Tele: 0151 252 5161
Email: pals@alderhey.nhs.uk

Appendix 2

Alder Hey Children's Hospital, Eaton Road,
Liverpool L12 2AP
Telephone: 0151 228 4811

Centre Number:
Study Number:
Participant Identification Number for this study:

CONSENT FORM FOR RESEARCH
For parent/person with parental responsibility

Title of Project: The Role of mucus in respiratory disease in childhood

Name of Researcher: _____ Job title: _____

Please initial box

1. I confirm that I have read and understand the information sheet dated ..... (version .....) for the above study. I have had the opportunity to consider the information, ask questions and have had these answered satisfactorily. ☐

2. I understand that my child's participation is voluntary and that I am free to withdraw my child at any time, without giving any reason. If I do withdraw, his/her medical care and legal rights will not be affected in any way. ☐

3. I understand that relevant sections of any of my child's medical notes or data collected during the study may be looked at by responsible individuals. These individuals will be from regulatory authorities and/or the Alder Hey Children's Hospital NHS Foundation Trust. I give permission for these individuals to have access to my child's medical records and study data. ☐

4. I agree to the use of my childs blood, DNA, and respiratory samples in this research project, as described on the patient information sheet. I agree to anonymised data about my child such as age, gender and medical condition being held on a secure on-line database with limited access ☐

5. I agree for my child to take part in the above study. ☐

Name of patient _____

Name of Parent/Guardian	Date	Signature
Name of Person taking consent (if different from researcher)	Date	Signature
Researcher	Date	Signature

When completed: 1 for patient; 1 for researcher site file; 1 (original) to be kept in medical notes (Version 1.2 – 28 Oct 2013)

Appendix 3

Information sheet (Patient)

The immune response of the newborn to inflammation and infection

Name of Researchers:

Dr Paul McNamara

Dr Gemma Saint

Dr Brian Flanagan

Dr Mark Turner

You are being invited to take part in the above research project. Before you decide, it is important for you to understand why the research is being done and what it will involve. Please take time to read the following information carefully and discuss it with friends, or relatives. Ask us if there is anything you do not understand or if you would like more information. Take time to decide whether or not you wish to take part. Thank you for reading this.

What is the purpose of the study?

The purpose of the study is to look at the immune system of newborn babies. We have found that babies who get a severe infection when they are a few months old fight infections differently from adults. We now want to do some laboratory tests on blood cells from newborn babies in order to see whether the differences are present when babies are born.

Why have I been chosen?

You have been chosen because you are about to deliver a newborn who we believe is healthy and has not been exposed to infections in the womb.

Do I have to take part?

Entering the trial is completely voluntary. If you do decide to take part you will be given this information sheet to keep and be asked to sign a consent form. If you decide to take part you are still free to withdraw without giving a reason. This will not affect the standard of care you receive.

What will happen to me if I take part?

If you decide to take part in this study, we will ask you to sign a consent form. Taking part in this study will mean that we will take about 10 -30 mls of blood from the umbilical cord after the baby is born and the cord has been cut. The placenta and umbilical cord, once cut and removed from the baby in the first few minutes after birth, is normally disposed of in a respectful manner. However it still contains some of your baby's blood and this can be used to study the immune system of the newborn.

What are the possible benefits of taking part?

There will be no direct benefits to you from taking part in this study. However, the information we get from this study may be of benefit to other babies in the future. It will help us to determine how newborn babies fight infections and this may lead to the development of new treatments. We will not be able to predict if your baby is more, or less, likely to get an infection than other babies.

What if something goes wrong?

It is very unlikely that you or your baby will be harmed by this study. The blood samples are collected only after the baby is born and from the large umbilical vein of the cord after it is no longer attached to the baby. This study does not involve blood tests for you or your baby. If you are harmed by taking part in this research project, there are no special compensation arrangements. If you are harmed due to someone's negligence, then you may have grounds for a legal action but you may have to pay for it. Regardless of this, if you wish to complain about any aspect of the way you have been approached or treated during the course of this study, the normal National Health Service complaints mechanisms are available to you.

Will my taking part in this study be kept confidential?

All information collected about you or your baby during the course of the research will be kept strictly confidential. Any information about you or your baby, which leaves the hospital, will have all personal details removed so that you cannot be recognised from it. Your medical notes as well as the baby's medical notes may be looked at to obtain information relevant to this study but this will only involve the checking that you and the baby do not have any illnesses and the baby's sex and gestational age.

What will happen to the results of the research study?

The results will be published in scientific journals and presented at conferences to further our understanding of the immune response to infection.

Who is organising the research?

The research is being organised by the University Of Liverpool.

Who has reviewed the study?

The Liverpool Research Ethics Committee.

How can I know the results of this study?

If you wish to obtain a summary of the investigation that is easy to read once data collection and analysis are complete please contact the research team.

Contact for Further Information

Dr Mark Turner

Liverpool Women's NHS Foundation Trust

Crown Street

Liverpool L8 7SS

Tel: 0151 708 9988

Thank you for reading this.

Liverpool Women's NHS
NHS Foundation Trust

Royal Liverpool Children's NHS
NHS Trust

CONSENT FORM

The immune response of the newborn to inflammation and infection

Name of Researchers:

Dr Paul McNamara	Dr Mark Turner
Dr Brian Flanagan	Dr Gemma Saint

Please initial box

1. I confirm that I have read and understand the information sheet for the above study. ☐

2. I understand that my participation is voluntary and that I am free to withdraw at any time without my medical care or legal rights being affected. ☐

3. I understand that sections of any of my medical notes may be looked at by responsible individuals from Liverpool Women's NHS Foundation Trust, or from regulatory authorities where it is relevant to my taking part in research. I give permission for these individuals to have access to my records and my baby records. ☐

4. I agree to take part in the above study. ☐

_____	_____	_____
Name of Patient	Date	Signature
_____	_____	_____
Researcher	Date	Signature
_____	_____	_____
Name of Person taking consent (If different from researcher)	Date	Signature

If you wish to obtain a summary of the investigation that is easy to read once data collection and analysis are complete please contact the research team.

1 copy for patient, 1 copy for research, 1 copy to be kept with hospital notes

Appendix 4

Tube ID	Sample name	Description	Concentration (ng/ul)	Sample volume (ul)	260/280	260/230	amount for 100ng input	volume of H_2O to 11.4 ul for SV	
6072_1	1	RSV 1 4hrs	11.59	30	1.97	0.46	8.63	2.77	
6072_2	2	RSV 1 20hrs	12.25	30	1.83	0.8	8.16	3.24	
6072_3	3	Con 1 4hrs	8.77	30	1.63	0.1	11.40	0.00	
6072_4	4	Con 1 20hrs	14.25	30	1.93	0.08	7.02	4.38	
6072_5	13	RSV 4 4hrs	35.99	30	2.01	0.87	2.78	8.62	
6072_6	14	RSV 4 20hrs	9.89	30	1.78	1.38	10.11	1.29	
6072_7	15	Con 4 4hrs	51.08	30	2.16	0.14	1.96	9.44	
6072_8	16	Con 4 20hrs	52.77	30	2.14	2.49	1.90	9.50	
6072_9	17	RSV 5 4hrs	30.41	30	1.97	0.35	3.29	8.11	
6072_10	18	RSV 5 20hrs	33.42	30	2.07	1.04	2.99	8.41	
6072_11	19	Con 5 4hrs	38.05	30	2.08	0.97	2.63	8.77	
6072_12	20	Con 5 20hrs	28.22	30	2.01	0.83	3.54	7.86	
6072_13	21	RSV 6 4hrs	60.91	30	2.06	1.49	1.64	9.76	
6072_14	22	RSV 6 20hrs	53.01	30	2.07	1.8	1.89	9.51	
6072_15	23	Con 6 4hrs	47.04	30	2.13	1.7	2.13	9.27	
6072_16	24	Con 6 20hrs	62.87	30	2.01	0.48	1.59	9.81	

RNA sample information

Sample IDs, description, concentration, volume, and nanodrop measurements are shown. The volume used for labelling in order to use 100ng of RNA is shown, as is the volume of water needed to equalise the volumes across all the samples.

Appendix 5

Gene	Description	Location	Action
39142	N(alpha)-acetyltransferase 60, NatF catalytic subunit	Cytoplasm	enzyme
ABTB1	ankyrin repeat and BTB (POZ) domain containing 1	Cytoplasm	translation regulator
ACN9	ACN9 homolog (S. cerevisiae)	Cytoplasm	other
ACOT9	acyl-CoA thioesterase 9	Cytoplasm	enzyme
ACSS2	acyl-CoA synthetase short-chain family member 2	Cytoplasm	enzyme
ACTL10	actin-like 10	Extracellular Space	other
ACTN3	actinin, alpha 3	Plasma Membrane	other
ADCK3	aarF domain containing kinase 3	Cytoplasm	kinase
ADCY7	adenylate cyclase 7	Plasma Membrane	enzyme
ADNP	activity-dependent neuroprotector homeobox	Nucleus	transcription regulator
ADPGK	ADP-dependent glucokinase	Other	kinase
ADPRHL2	ADP-ribosylhydrolase like 2	Cytoplasm	enzyme
ADRBK1	adrenergic, beta, receptor kinase 1	Cytoplasm	kinase
ADRBK2	adrenergic, beta, receptor kinase 2	Cytoplasm	kinase
AEN	apoptosis enhancing nuclease	Nucleus	enzyme
AFF1	AF4/FMR2 family, member 1	Nucleus	transcription regulator
AGO4	argonaute RISC catalytic component 4	Cytoplasm	translation regulator
AGRN	agrin	Plasma Membrane	other
AK091028	GMDS antisense RNA 1 (head to head)	Other	other
AKAP10	A kinase (PRKA) anchor protein 10	Cytoplasm	other
AKIRIN1	akirin 1	Cytoplasm	enzyme
ALKBH7	alkB, alkylation repair homolog 7 (E. coli)	Cytoplasm	other
AMPD2	adenosine monophosphate deaminase 2	Cytoplasm	enzyme
ANKFY1	ankyrin repeat and FYVE domain containing 1	Cytoplasm	transcription regulator
ANKMY1	ankyrin repeat and MYND domain containing 1	Other	other
ANKRD34B	ankyrin repeat domain 34B	Nucleus	transcription regulator
ANXA2R	annexin A2 receptor	Plasma Membrane	other
ANXA9	annexin A9	Plasma Membrane	transmembrane receptor
AP1S3	adaptor-related protein complex 1, sigma 3 subunit	Cytoplasm	transporter

AP4B1	adaptor-related protein complex 4, beta 1 subunit	Cytoplasm	transporter
APAF1	apoptotic peptidase activating factor 1	Cytoplasm	other
APOBEC3A	apolipoprotein B mRNA editing enzyme, catalytic polypeptide-like 3A	Cytoplasm	enzyme
APOBEC3B	apolipoprotein B mRNA editing enzyme, catalytic polypeptide-like 3B	Cytoplasm	enzyme
APOBEC3C	apolipoprotein B mRNA editing enzyme, catalytic polypeptide-like 3C	Other	enzyme
APOBEC3F	apolipoprotein B mRNA editing enzyme, catalytic polypeptide-like 3F	Cytoplasm	enzyme
APOBEC3G	apolipoprotein B mRNA editing enzyme, catalytic polypeptide-like 3G	Nucleus	enzyme
APTR	Alu-mediated CDKN1A/p21 transcriptional regulator (non-protein coding)	Other	other
ARID4B	AT rich interactive domain 4B (RBP1-like)	Nucleus	other
ARL8B	ADP-ribosylation factor-like 8B	Plasma Membrane	enzyme
ARSB	arylsulfatase B	Cytoplasm	enzyme
ASNSD1	asparagine synthetase domain containing 1	Other	enzyme
ATF7IP	activating transcription factor 7 interacting protein	Nucleus	transcription regulator
ATG2B	autophagy related 2B	Other	other
ATP1B1	ATPase, Na+/K+ transporting, beta 1 polypeptide	Plasma Membrane	transporter
ATP6V1A	ATPase, H+ transporting, lysosomal 70kDa, V1 subunit A	Plasma Membrane	transporter
ATP6V1E2	ATPase, H+ transporting, lysosomal 31kDa, V1 subunit E2	Cytoplasm	transporter
ATP6V1F	ATPase, H+ transporting, lysosomal 14kDa, V1 subunit F	Cytoplasm	enzyme
ATXN2	ataxin 2	Nucleus	other
ATXN7L1	ataxin 7-like 1	Other	other
AZI2	5-azacytidine induced 2	Cytoplasm	other
B3GALNT1	beta-1,3-N-acetylgalactosaminyltransferase 1 (globoside blood group)	Cytoplasm	enzyme
B4GALT3	UDP-Gal:betaGlcNAc beta 1,4- galactosyltransferase, polypeptide 3	Cytoplasm	enzyme
BAALC	brain and acute leukemia, cytoplasmic	Cytoplasm	other
BAG1	BCL2-associated athanogene	Cytoplasm	other
BARD1	BRCA1 associated RING domain 1	Nucleus	transcription regulator
BATF2	basic leucine zipper transcription factor, ATF-like 2	Other	other
BC013229	UDP-GlcNAc:betaGal beta-1,3-N-	Cytoplasm	enzyme

	acetylglucosaminyltransferase 5		
BHLHE40	basic helix-loop-helix family, member e40	Nucleus	transcription regulator
BICD2	bicaudal D homolog 2 (Drosophila)	Cytoplasm	other
BLZF1	basic leucine zipper nuclear factor 1	Cytoplasm	transcription regulator
BMI1	BMI1 proto-oncogene, polycomb ring finger	Nucleus	transcription regulator
BNIPL	BCL2/adenovirus E1B 19kD interacting protein like	Cytoplasm	other
BOD1L1	biorientation of chromosomes in cell division 1-like 1	Nucleus	other
BRCA2	breast cancer 2, early onset	Nucleus	transcription regulator
BREA2	breast cancer estrogen-induced apoptosis 2	Other	other
BRF2	BRF2, RNA polymerase III transcription initiation factor 50 kDa subunit	Nucleus	transcription regulator
BRICD5	BRICHOS domain containing 5	Other	enzyme
BST2	bone marrow stromal cell antigen 2	Plasma Membrane	other
BTG1	B-cell translocation gene 1, anti-proliferative	Nucleus	transcription regulator
C10orf105	chromosome 10 open reading frame 105	Other	other
C10orf120	chromosome 10 open reading frame 120	Other	other
C10orf131	chromosome 10 open reading frame 131	Other	other
C11orf68	chromosome 11 open reading frame 68	Other	other
C12orf75	chromosome 12 open reading frame 75	Other	other
C15orf48	chromosome 15 open reading frame 48	Nucleus	other
C17orf62	chromosome 17 open reading frame 62	Other	other
C17orf67	chromosome 17 open reading frame 67	Other	other
C17orf75	chromosome 17 open reading frame 75	Extracellular Space	other
C17orf96	chromosome 17 open reading frame 96	Other	other
C19orf12	chromosome 19 open reading frame 12	Other	other
C19orf33	chromosome 19 open reading frame 33	Nucleus	other
C19orf66	chromosome 19 open reading frame 66	Other	other
C1GALT1	core 1 synthase, glycoprotein-N-acetylgalactosamine 3-beta-galactosyltransferase 1	Plasma Membrane	enzyme
C1GALT1C1	C1GALT1-specific chaperone 1	Cytoplasm	enzyme
C21orf91	chromosome 21 open reading frame 91	Other	other
C2orf44	chromosome 2 open reading frame 44	Other	other
C2orf80	chromosome 2 open reading frame 80	Other	other
C3orf18	chromosome 3 open reading frame 18	Other	other
C4orf45	chromosome 4 open reading frame 45	Other	other

C5orf24	chromosome 5 open reading frame 24	Other	other
C5orf30	chromosome 5 open reading frame 30	Cytoplasm	other
C5orf56	chromosome 5 open reading frame 56	Other	other
C5orf58	chromosome 5 open reading frame 58	Other	other
C6orf1	chromosome 6 open reading frame 1	Other	other
C7orf60	chromosome 7 open reading frame 60	Other	other
C8orf88	chromosome 8 open reading frame 88	Other	other
C9orf139	chromosome 9 open reading frame 139	Other	other
C9orf24	chromosome 9 open reading frame 24	Cytoplasm	other
CAB39L	calcium binding protein 39-like	Cytoplasm	kinase
CACNA1A	calcium channel, voltage-dependent, P/Q type, alpha 1A subunit	Plasma Membrane	ion channel
CACUL1	CDK2-associated, cullin domain 1	Other	other
CAMK1G	calcium/calmodulin-dependent protein kinase IG	Cytoplasm	kinase
CAMK2G	calcium/calmodulin-dependent protein kinase II gamma	Cytoplasm	kinase
CARHSP1	calcium regulated heat stable protein 1, 24kDa	Cytoplasm	other
CARKD	carbohydrate kinase domain containing	Cytoplasm	enzyme
CASP9	caspase 9, apoptosis-related cysteine peptidase	Cytoplasm	peptidase
CBWD5	COBW domain containing 5	Other	other
CBX7	chromobox homolog 7	Nucleus	other
CBX8	chromobox homolog 8	Nucleus	other
CC2D1B	coiled-coil and C2 domain containing 1B	Nucleus	other
CCDC112	coiled-coil domain containing 112	Extracellular Space	other
CCDC167	coiled-coil domain containing 167	Other	other
CCDC170	coiled-coil domain containing 170	Extracellular Space	other
CCDC28A	coiled-coil domain containing 28A	Other	other
CCDC85B	coiled-coil domain containing 85B	Cytoplasm	other
CCL4	chemokine (C-C motif) ligand 4	Extracellular Space	cytokine
CCL4L2	chemokine (C-C motif) ligand 4-like 1	Plasma Membrane	other
CCND2	cyclin D2	Nucleus	other
CCR1	chemokine (C-C motif) receptor 1	Plasma Membrane	G-protein coupled receptor
CCT6B	chaperonin containing TCP1, subunit 6B (zeta 2)	Cytoplasm	transporter
CD164	CD164 molecule, sialomucin	Plasma Membrane	other
CD22	CD22 molecule	Plasma	transmembrane

		Membrane	receptor
CD274	CD274 molecule	Plasma Membrane	enzyme
CD58	CD58 molecule	Plasma Membrane	transmembrane receptor
CD68	CD68 molecule	Plasma Membrane	other
CD69	CD69 molecule	Plasma Membrane	transmembrane receptor
CD80	CD80 molecule	Plasma Membrane	transmembrane receptor
CDC123	cell division cycle 123	Cytoplasm	other
CDC14C	cell division cycle 14C	Nucleus	other
CDC40	cell division cycle 40	Nucleus	other
CDC42SE2	CDC42 small effector 2	Plasma Membrane	other
CDC73	cell division cycle 73	Nucleus	other
CDK19	cyclin-dependent kinase 19	Nucleus	kinase
CDK5R1	cyclin-dependent kinase 5, regulatory subunit 1 (p35)	Nucleus	kinase
CDK7	cyclin-dependent kinase 7	Nucleus	kinase
CEBPA	CCAAT/enhancer binding protein (C/EBP), alpha	Nucleus	transcription regulator
CEBPD	CCAAT/enhancer binding protein (C/EBP), delta	Nucleus	transcription regulator
CENPF	centromere protein F, 350/400kDa	Nucleus	other
CEP44	centrosomal protein 44kDa	Cytoplasm	other
CEP85L	centrosomal protein 85kDa-like	Cytoplasm	other
CEP97	centrosomal protein 97kDa	Cytoplasm	other
CERS4	ceramide synthase 4	Cytoplasm	transcription regulator
CHMP5	charged multivesicular body protein 5	Cytoplasm	other
CHRM4	cholinergic receptor, muscarinic 4	Plasma Membrane	G-protein coupled receptor
CHRNB1	cholinergic receptor, nicotinic, beta 1 (muscle)	Plasma Membrane	transmembrane receptor
CIDEC	cell death-inducing DFFA-like effector c	Cytoplasm	other
CIDECP	cell death-inducing DFFA-like effector c pseudogene	Other	other
CISH	cytokine inducible SH2-containing protein	Cytoplasm	other
CLCF1	cardiotrophin-like cytokine factor 1	Extracellular Space	cytokine
CLEC4A	C-type lectin domain family 4, member A	Plasma	transmembrane

		Membrane	receptor
CLINT1	clathrin interactor 1	Cytoplasm	other
CLPX	caseinolytic mitochondrial matrix peptidase chaperone subunit	Cytoplasm	enzyme
CLU	clusterin	Cytoplasm	other
CMAHP	cytidine monophospho-N-acetylneuraminic acid hydroxylase, pseudogene	Cytoplasm	other
CMTM1	CKLF-like MARVEL transmembrane domain containing 1	Other	other
CMTR1	cap methyltransferase 1	Nucleus	enzyme
CNEP1R1	CTD nuclear envelope phosphatase 1 regulatory subunit 1	Other	other
CNOT2	CCR4-NOT transcription complex, subunit 2	Nucleus	transcription regulator
CNOT7	CCR4-NOT transcription complex, subunit 7	Nucleus	transcription regulator
CNP	2',3'-cyclic nucleotide 3' phosphodiesterase	Cytoplasm	enzyme
CNPY3	canopy FGF signaling regulator 3	Cytoplasm	other
CNTF	ciliary neurotrophic factor	Extracellular Space	cytokine
COL12A1	collagen, type XII, alpha 1	Extracellular Space	other
CORO1A	coronin, actin binding protein, 1A	Cytoplasm	other
CPS1	carbamoyl-phosphate synthase 1, mitochondrial	Cytoplasm	enzyme
CT83	cancer/testis antigen 83	Nucleus	other
CTAGE1	cutaneous T-cell lymphoma-associated antigen 1	Other	other
CTC-338M12.4	uncharacterized LOC101928649	Other	other
CTSLP8	cathepsin L pseudogene 8	Other	other
CUEDC1	CUE domain containing 1	Other	other
CXCL10	chemokine (C-X-C motif) ligand 10	Extracellular Space	cytokine
CXCL2	chemokine (C-X-C motif) ligand 2	Extracellular Space	cytokine
CXCL6	chemokine (C-X-C motif) ligand 6	Extracellular Space	cytokine
CXCR1	chemokine (C-X-C motif) receptor 1	Plasma Membrane	G-protein coupled receptor
CXCR2	chemokine (C-X-C motif) receptor 2	Plasma Membrane	G-protein coupled receptor
CXorf21	chromosome X open reading frame 21	Other	enzyme
CXorf38	chromosome X open reading frame 38	Other	other

CYBB	cytochrome b-245, beta polypeptide	Cytoplasm	enzyme
CYR61	cysteine-rich, angiogenic inducer, 61	Extracellular Space	other
CYTH3	cytohesin 3	Cytoplasm	other
DAB2	Dab, mitogen-responsive phosphoprotein, homolog 2 (Drosophila)	Plasma Membrane	other
DAGLB	diacylglycerol lipase, beta	Plasma Membrane	enzyme
DAPL1	death associated protein-like 1	Other	other
DAPP1	dual adaptor of phosphotyrosine and 3-phosphoinositides	Cytoplasm	other
DBF4B	DBF4 zinc finger B	Nucleus	other
DBP	D site of albumin promoter (albumin D-box) binding protein	Nucleus	transcription regulator
DCAF4L1	DDB1 and CUL4 associated factor 4-like 1	Other	other
DCAF4L2	DDB1 and CUL4 associated factor 4-like 2	Other	other
DCLRE1C	DNA cross-link repair 1C	Nucleus	enzyme
DCP2	decapping mRNA 2	Nucleus	enzyme
DCTN6	dynactin 6	Cytoplasm	enzyme
DCUN1D3	DCN1, defective in cullin neddylation 1, domain containing 3	Cytoplasm	other
DDX28	DEAD (Asp-Glu-Ala-Asp) box polypeptide 28	Nucleus	enzyme
DDX58	DEAD (Asp-Glu-Ala-Asp) box polypeptide 58	Cytoplasm	enzyme
DDX60L	DEAD (Asp-Glu-Ala-Asp) box polypeptide 60-like	Other	other
DESI2	desumoylating isopeptidase 2	Cytoplasm	other
DHTKD1	dehydrogenase E1 and transketolase domain containing 1	Cytoplasm	enzyme
DHX58	DEXH (Asp-Glu-X-His) box polypeptide 58	Cytoplasm	enzyme
DICER1	dicer 1, ribonuclease type III	Cytoplasm	enzyme
DICER1-AS1	DICER1 antisense RNA 1	Other	other
DIP2B	DIP2 disco-interacting protein 2 homolog B (Drosophila)	Cytoplasm	other
DKC1	dyskeratosis congenita 1, dyskerin	Nucleus	enzyme
DNAJC13	DnaJ (Hsp40) homolog, subfamily C, member 13	Cytoplasm	other
DOCK11	dedicator of cytokinesis 11	Cytoplasm	other
DPF2	D4, zinc and double PHD fingers family 2	Nucleus	other
DRAP1	DR1-associated protein 1 (negative cofactor 2 alpha)	Nucleus	transcription regulator
DSTYK	dual serine/threonine and tyrosine protein kinase	Cytoplasm	kinase
DUS2	dihydrouridine synthase 2	Cytoplasm	other
DUSP11	dual specificity phosphatase 11 (RNA/RNP complex 1-interacting)	Nucleus	phosphatase

DUSP5	dual specificity phosphatase 5	Nucleus	phosphatase
DYNLT1	dynein, light chain, Tctex-type 1	Cytoplasm	other
EDEM1	ER degradation enhancer, mannosidase alpha-like 1	Cytoplasm	enzyme
EDN1	endothelin 1	Extracellular Space	cytokine
EFNA1	ephrin-A1	Plasma Membrane	other
EFNA4	ephrin-A4	Plasma Membrane	kinase
EGLN1	egl-9 family hypoxia-inducible factor 1	Cytoplasm	enzyme
EIF4A1	eukaryotic translation initiation factor 4A1	Cytoplasm	translation regulator
EIF4E	eukaryotic translation initiation factor 4E	Cytoplasm	translation regulator
ELMSAN1	ELM2 and Myb/SANT-like domain containing 1	Nucleus	other
EML4	echinoderm microtubule associated protein like 4	Cytoplasm	other
EMP1	epithelial membrane protein 1	Plasma Membrane	other
ENST00000287667	NODAL modulator 1	Plasma Membrane	other
ENST00000316517	olfactory receptor, family 56, subfamily B, member 3 pseudogene	Other	other
ENST00000390300	immunoglobulin lambda variable 5-37	Other	other
ENST00000390465	T cell receptor alpha variable 38-2/delta variable 8	Other	other
ENST00000391437	uncharacterized protein DKFZp667F0711	Other	other
ENST00000525262	unc-93 homolog B6 (C. elegans)	Other	other
ENST00000582047	keratin 17 pseudogene 1	Other	other
EPB41	erythrocyte membrane protein band 4.1	Plasma Membrane	other
EPHB6	EPH receptor B6	Plasma Membrane	kinase
EPS15L1	epidermal growth factor receptor pathway substrate 15-like 1	Plasma Membrane	other
ERP27	endoplasmic reticulum protein 27	Other	other
ERP29	endoplasmic reticulum protein 29	Cytoplasm	transporter
EVI5	ecotropic viral integration site 5	Cytoplasm	other
EXOC3L1	exocyst complex component 3-like 1	Cytoplasm	other
EXTL3	exostosin-like glycosyltransferase 3	Cytoplasm	enzyme
EYA3	EYA transcriptional coactivator and phosphatase 3	Nucleus	phosphatase
F8A1	coagulation factor VIII-associated 1	Nucleus	other
F8A2	coagulation factor VIII-associated 1	Nucleus	other
FAM101B	family with sequence similarity 101, member B	Other	other

FAM106CP	family with sequence similarity 106, member C, pseudogene	Other	other
FAM117A	family with sequence similarity 117, member A	Other	transporter
FAM122C	family with sequence similarity 122C	Other	other
FAM174A	family with sequence similarity 174, member A	Extracellular Space	other
FAM184B	family with sequence similarity 184, member B	Other	other
FAM212B	family with sequence similarity 212, member B	Other	other
FAM214A	family with sequence similarity 214, member A	Other	other
FAM217B	family with sequence similarity 217, member B	Other	other
FAM222A	family with sequence similarity 222, member A	Other	other
FAM27E2	family with sequence similarity 27, member E2	Other	other
FAM27E3	family with sequence similarity 27, member E3	Other	other
FAM46A	family with sequence similarity 46, member A	Other	other
FAM53B	family with sequence similarity 53, member B	Other	other
FAM63A	family with sequence similarity 63, member A	Cytoplasm	other
FAM72A	family with sequence similarity 72, member A	Cytoplasm	other
FAM72D	family with sequence similarity 72, member D	Nucleus	other
FAM83H-AS1	FAM83H antisense RNA 1 (head to head)	Other	other
FANCA	Fanconi anemia, complementation group A	Nucleus	other
FAR1	fatty acyl CoA reductase 1	Cytoplasm	enzyme
FBRS	fibrosin	Extracellular Space	cytokine
FBXL20	F-box and leucine-rich repeat protein 20	Cytoplasm	other
FBXO6	F-box protein 6	Cytoplasm	enzyme
FBXW4	F-box and WD repeat domain containing 4	Other	other
FCHO1	FCH domain only 1	Plasma Membrane	other
FDFT1	farnesyl-diphosphate farnesyltransferase 1	Cytoplasm	enzyme
FFAR2	free fatty acid receptor 2	Plasma Membrane	G-protein coupled receptor
FFAR3	free fatty acid receptor 3	Plasma Membrane	G-protein coupled receptor
FHL2	four and a half LIM domains 2	Nucleus	transcription regulator
FIBP	fibroblast growth factor (acidic) intracellular binding protein	Nucleus	other
FKBP15	FK506 binding protein 15, 133kDa	Plasma Membrane	enzyme
FLJ32255	uncharacterized LOC643977	Other	other

FLJ40194	uncharacterized FLJ40194	Other	other
FLJ42393	uncharacterized LOC401105	Other	other
FLOT1	flotillin 1	Plasma Membrane	other
FMR1	fragile X mental retardation 1	Nucleus	other
FNTB	farnesyltransferase, CAAX box, beta	Cytoplasm	enzyme
FOSL1	FOS-like antigen 1	Nucleus	transcription regulator
FOXO3	forkhead box O3	Nucleus	transcription regulator
FOXO4	forkhead box O4	Nucleus	transcription regulator
FSCN1	fascin actin-bundling protein 1	Cytoplasm	other
FUT11	fucosyltransferase 11 (alpha (1,3) fucosyltransferase)	Cytoplasm	enzyme
FUT7	fucosyltransferase 7 (alpha (1,3) fucosyltransferase)	Cytoplasm	enzyme
FYCO1	FYVE and coiled-coil domain containing 1	Cytoplasm	other
GAB3	GRB2-associated binding protein 3	Other	other
GALK1	galactokinase 1	Cytoplasm	kinase
GCC1	GRIP and coiled-coil domain containing 1	Cytoplasm	other
GDE1	glycerophosphodiester phosphodiesterase 1	Plasma Membrane	enzyme
GDPD3	glycerophosphodiester phosphodiesterase domain containing 3	Cytoplasm	enzyme
GGT5	gamma-glutamyltransferase 5	Plasma Membrane	enzyme
GIT2	G protein-coupled receptor kinase interacting ArfGAP 2	Nucleus	other
GLRX2	glutaredoxin 2	Cytoplasm	enzyme
GLUL	glutamate-ammonia ligase	Cytoplasm	enzyme
GMNN	geminin, DNA replication inhibitor	Nucleus	transcription regulator
GNG11	guanine nucleotide binding protein (G protein), gamma 11	Plasma Membrane	enzyme
GNG12	guanine nucleotide binding protein (G protein), gamma 12	Plasma Membrane	enzyme
GNPAT	glyceronephosphate O-acyltransferase	Cytoplasm	enzyme
GNPDA1	glucosamine-6-phosphate deaminase 1	Cytoplasm	enzyme
GPR27	G protein-coupled receptor 27	Plasma Membrane	G-protein coupled receptor
GPX3	glutathione peroxidase 3 (plasma)	Extracellular Space	enzyme
GRINA	glutamate receptor, ionotropic, N-methyl D-aspartate-	Other	ion channel

	associated protein 1 (glutamate binding)		
GRM1	glutamate receptor, metabotropic 1	Plasma Membrane	G-protein coupled receptor
GSDMD	gasdermin D	Extracellular Space	other
GSK3B	glycogen synthase kinase 3 beta	Nucleus	kinase
GSTO1	glutathione S-transferase omega 1	Cytoplasm	enzyme
GTF2B	general transcription factor IIB	Nucleus	transcription regulator
GTPBP2	GTP binding protein 2	Extracellular Space	enzyme
H19	H19, imprinted maternally expressed transcript (non-protein coding)	Cytoplasm	other
H2AFX	H2A histone family, member X	Nucleus	transcription regulator
HAS1	hyaluronan synthase 1	Plasma Membrane	enzyme
HAVCR1	hepatitis A virus cellular receptor 1	Plasma Membrane	other
HAX1	HCLS1 associated protein X-1	Cytoplasm	other
HBEGF	heparin-binding EGF-like growth factor	Extracellular Space	growth factor
HEATR5B	HEAT repeat containing 5B	Cytoplasm	other
HELZ2	helicase with zinc finger 2, transcriptional coactivator	Nucleus	transcription regulator
HERC5	HECT and RLD domain containing E3 ubiquitin protein ligase 5	Cytoplasm	enzyme
HERPUD1	homocysteine-inducible, endoplasmic reticulum stress-inducible, ubiquitin-like domain member 1	Cytoplasm	other
HES4	hes family bHLH transcription factor 4	Other	other
HEXIM1	hexamethylene bis-acetamide inducible 1	Nucleus	transcription regulator
HIF1A	hypoxia inducible factor 1, alpha subunit (basic helix-loop-helix transcription factor)	Nucleus	transcription regulator
HK1	hexokinase 1	Cytoplasm	kinase
HMG20A	high mobility group 20A	Nucleus	transcription regulator
HMGA1	high mobility group AT-hook 1	Nucleus	transcription regulator
HMHA1	histocompatibility (minor) HA-1	Cytoplasm	transporter
HNRNPLL	heterogeneous nuclear ribonucleoprotein L-like	Other	other

HRH4	histamine receptor H4	Plasma Membrane	G-protein coupled receptor
HS6ST1	heparan sulfate 6-O-sulfotransferase 1	Plasma Membrane	enzyme
HSPBAP1	HSPB (heat shock 27kDa) associated protein 1	Other	other
HVCN1	hydrogen voltage-gated channel 1	Plasma Membrane	ion channel
HYAL2	hyaluronoglucosaminidase 2	Cytoplasm	enzyme
ID	Description	Location	Family
ID2	inhibitor of DNA binding 2, dominant negative helix-loop-helix protein	Nucleus	transcription regulator
IER5	immediate early response 5	Other	other
IFI35	interferon-induced protein 35	Nucleus	other
IFIH1	interferon induced with helicase C domain 1	Nucleus	enzyme
IFIT1	interferon-induced protein with tetratricopeptide repeats 1	Cytoplasm	other
IFIT1B	interferon-induced protein with tetratricopeptide repeats 1B	Cytoplasm	other
IFIT2	interferon-induced protein with tetratricopeptide repeats 2	Cytoplasm	other
IFIT3	interferon-induced protein with tetratricopeptide repeats 3	Cytoplasm	other
IFIT5	interferon-induced protein with tetratricopeptide repeats 5	Plasma Membrane	other
IGFBP7	insulin-like growth factor binding protein 7	Extracellular Space	transporter
IKBIP	IKBKB interacting protein	Cytoplasm	other
IL1A	interleukin 1, alpha	Extracellular Space	cytokine
IL1RN	interleukin 1 receptor antagonist	Extracellular Space	cytokine
IL27	interleukin 27	Extracellular Space	cytokine
IMPA2	inositol(myo)-1(or 4)-monophosphatase 2	Cytoplasm	phosphatase
INTS6	integrator complex subunit 6	Nucleus	enzyme
IQCK	IQ motif containing K	Other	other
IRF2	interferon regulatory factor 2	Nucleus	transcription regulator
IRF2BPL	interferon regulatory factor 2 binding protein-like	Nucleus	other
IRF7	interferon regulatory factor 7	Nucleus	transcription regulator

ISG15	ISG15 ubiquitin-like modifier	Extracellular Space	other
ISG20	interferon stimulated exonuclease gene 20kDa	Nucleus	enzyme
ITGAM	integrin, alpha M (complement component 3 receptor 3 subunit)	Plasma Membrane	transmembrane receptor
ITGAX	integrin, alpha X (complement component 3 receptor 4 subunit)	Plasma Membrane	transmembrane receptor
ITPR1	inositol 1,4,5-trisphosphate receptor, type 1	Cytoplasm	ion channel
ITPRIPL2	inositol 1,4,5-trisphosphate receptor interacting protein-like 2	Other	other
JADE1	jade family PHD finger 1	Nucleus	other
JDP2	Jun dimerization protein 2	Nucleus	transcription regulator
KAT5	K(lysine) acetyltransferase 5	Nucleus	transcription regulator
KIAA0226	KIAA0226	Cytoplasm	other
KIAA0226L	KIAA0226-like	Other	other
KIAA0232	KIAA0232	Extracellular Space	other
KIAA0368	KIAA0368	Cytoplasm	other
KIAA1033	KIAA1033	Cytoplasm	other
KIAA1257	KIAA1257	Other	other
KIAA1467	KIAA1467	Other	other
KIF28P	kinesin family member 28, pseudogene	Cytoplasm	other
KIF3B	kinesin family member 3B	Cytoplasm	transporter
KLF10	Kruppel-like factor 10	Nucleus	transcription regulator
KLF3	Kruppel-like factor 3 (basic)	Nucleus	transcription regulator
KLHDC7B	kelch domain containing 7B	Other	other
KLHL28	kelch-like family member 28	Other	other
KLHL6	kelch-like family member 6	Other	other
KLHL8	kelch-like family member 8	Nucleus	other
KNSTRN	kinetochore-localized astrin/SPAG5 binding protein	Cytoplasm	other
KPTN	kaptin (actin binding protein)	Other	other
KRT14	keratin 14	Cytoplasm	other
KRT16P2	keratin 16 pseudogene 2	Other	other
KRT17	keratin 17	Cytoplasm	other
KRT33A	keratin 33A	Extracellular Space	other
KRTAP5-10	keratin associated protein 5-10	Other	other
LACTB	lactamase, beta	Cytoplasm	other

LAMP3	lysosomal-associated membrane protein 3	Plasma Membrane	other
LASP1	LIM and SH3 protein 1	Cytoplasm	transporter
LCE6A	late cornified envelope 6A	Other	other
LCMT1	leucine carboxyl methyltransferase 1	Cytoplasm	enzyme
LDHB	lactate dehydrogenase B	Cytoplasm	enzyme
LEP	leptin	Extracellular Space	growth factor
LETM2	leucine zipper-EF-hand containing transmembrane protein 2	Other	other
LGALS8	lectin, galactoside-binding, soluble, 8	Extracellular Space	other
LINC00173	long intergenic non-protein coding RNA 173	Other	other
LINC00211	long intergenic non-protein coding RNA 211	Other	other
LINC00310	long intergenic non-protein coding RNA 310	Other	other
LINC00334	long intergenic non-protein coding RNA 334	Other	other
LINC00461	long intergenic non-protein coding RNA 461	Other	other
LINC00487	long intergenic non-protein coding RNA 487	Other	other
LINC00877	long intergenic non-protein coding RNA 877	Other	other
LINC00930	long intergenic non-protein coding RNA 930	Other	other
LINC00957	long intergenic non-protein coding RNA 957	Other	other
LINC01262	long intergenic non-protein coding RNA 1262	Other	other
LMO2	LIM domain only 2 (rhombotin-like 1)	Nucleus	other
LNPEP	leucyl/cystinyl aminopeptidase	Cytoplasm	peptidase
LOC100129550	uncharacterized LOC100129550	Other	other
LOC100130539	uncharacterized LOC100130539	Other	other
LOC100294362	uncharacterized LOC100294362	Other	other
LOC100506023	uncharacterized LOC100506023	Other	other
LOC100506036	uncharacterized LOC100506036	Other	other
LOC100506801	uncharacterized LOC100506801	Other	other
LOC100507131	uncharacterized LOC100507131	Other	other
LOC100507501	uncharacterized LOC100507501	Other	other
LOC101926887	uncharacterized LOC101926887	Other	other
LOC101927027	uncharacterized LOC101927027	Other	other
LOC101927207	uncharacterized LOC101927207	Other	other
LOC101927522	uncharacterized LOC101927522	Other	other
LOC101927759	uncharacterized LOC101927759	Other	other
LOC101928092	uncharacterized LOC101928092	Other	other
LOC101928173	uncharacterized LOC101928173	Other	other
LOC101929128	uncharacterized LOC101929128	Other	other
LOC101930017	transcription initiation factor TFIID subunit 4-like	Other	other
LOC101930333	uncharacterized LOC101930333	Other	other

LOC101930532	uncharacterized LOC101930532	Other	other
LOC102723759	uncharacterized LOC102723759	Other	other
LOC153684	uncharacterized LOC153684	Other	other
LOC200830	uncharacterized LOC200830	Other	other
LOC283177	uncharacterized LOC283177	Other	other
LOC389765	kinesin family member 27 pseudogene	Other	other
LOC648987	uncharacterized LOC648987	Other	other
LOC728554	THO complex 3 pseudogene	Other	other
LPAR6	lysophosphatidic acid receptor 6	Plasma Membrane	G-protein coupled receptor
LRG1	leucine-rich alpha-2-glycoprotein 1	Extracellular Space	other
LRMP	lymphoid-restricted membrane protein	Cytoplasm	other
LRPAP1	low density lipoprotein receptor-related protein associated protein 1	Plasma Membrane	transmembrane receptor
LRRC25	leucine rich repeat containing 25	Other	other
LRRC37A2	leucine rich repeat containing 37, member A3	Other	other
LRRC37A3	leucine rich repeat containing 37, member A3	Other	other
LRRC4	leucine rich repeat containing 4	Plasma Membrane	other
LSM2	LSM2 homolog, U6 small nuclear RNA associated (S. cerevisiae)	Nucleus	other
LY6K	lymphocyte antigen 6 complex, locus K	Nucleus	other
LYRM1	LYR motif containing 1	Cytoplasm	other
LYSMD1	LysM, putative peptidoglycan-binding, domain containing 1	Other	other
LYSMD2	LysM, putative peptidoglycan-binding, domain containing 2	Other	other
MAD2L1BP	MAD2L1 binding protein	Nucleus	other
MADCAM1	mucosal vascular addressin cell adhesion molecule 1	Plasma Membrane	other
MAL2	mal, T-cell differentiation protein 2 (gene/pseudogene)	Plasma Membrane	transporter
MANSC1	MANSC domain containing 1	Other	other
MAP2K4	mitogen-activated protein kinase kinase 4	Cytoplasm	kinase
MAP3K14	mitogen-activated protein kinase kinase kinase 14	Cytoplasm	kinase
MAP3K3	mitogen-activated protein kinase kinase kinase 3	Cytoplasm	kinase
MAPRE2	microtubule-associated protein, RP/EB family, member 2	Cytoplasm	other
MASTL	microtubule associated serine/threonine kinase-like	Cytoplasm	kinase
MB21D1	Mab-21 domain containing 1	Cytoplasm	other

MBD4	methyl-CpG binding domain protein 4	Nucleus	enzyme
MCMBP	minichromosome maintenance complex binding protein	Nucleus	other
MCU	mitochondrial calcium uniporter	Cytoplasm	ion channel
MDK	midkine (neurite growth-promoting factor 2)	Extracellular Space	growth factor
MED21	mediator complex subunit 21	Nucleus	transcription regulator
MED28	mediator complex subunit 28	Nucleus	other
MED30	mediator complex subunit 30	Nucleus	transcription regulator
MEF2D	myocyte enhancer factor 2D	Nucleus	transcription regulator
MEGF9	multiple EGF-like-domains 9	Other	other
MEMO1	mediator of cell motility 1	Cytoplasm	other
MET	MET proto-oncogene, receptor tyrosine kinase	Plasma Membrane	kinase
METTL17	methyltransferase like 17	Nucleus	other
MFAP1	microfibrillar-associated protein 1	Extracellular Space	other
MFSD2A	major facilitator superfamily domain containing 2A	Plasma Membrane	transporter
MGRN1	mahogunin ring finger 1, E3 ubiquitin protein ligase	Cytoplasm	enzyme
MIA3	melanoma inhibitory activity family, member 3	Cytoplasm	other
MICA	MHC class I polypeptide-related sequence A	Plasma Membrane	other
MID1IP1	MID1 interacting protein 1	Cytoplasm	other
MIS18BP1	MIS18 binding protein 1	Nucleus	other
MKL1	megakaryoblastic leukemia (translocation) 1	Nucleus	transcription regulator
MKNK2	MAP kinase interacting serine/threonine kinase 2	Cytoplasm	kinase
MME	membrane metallo-endopeptidase	Plasma Membrane	peptidase
MOB3A	MOB kinase activator 3A	Other	other
MOB3C	MOB kinase activator 3C	Other	other
MPDU1	mannose-P-dolichol utilization defect 1	Cytoplasm	other
MPZL2	myelin protein zero-like 2	Plasma Membrane	other
MRFAP1L1	Morf4 family associated protein 1-like 1	Other	other
MRPL16	mitochondrial ribosomal protein L16	Cytoplasm	other
MRPL17	mitochondrial ribosomal protein L17	Cytoplasm	other
MRPL24	mitochondrial ribosomal protein L24	Cytoplasm	other

MRPS6	mitochondrial ribosomal protein S6	Cytoplasm	other
MRVI1-AS1	MRVI1 antisense RNA 1	Other	other
MSL1	male-specific lethal 1 homolog (Drosophila)	Nucleus	other
MSL2	male-specific lethal 2 homolog (Drosophila)	Nucleus	other
MT1A	metallothionein 1A	Cytoplasm	other
MT1B	metallothionein 1B	Cytoplasm	other
MT1E	metallothionein 1E	Other	other
MT1HL1	metallothionein 1H-like 1	Other	other
MT1L	metallothionein 1L (gene/pseudogene)	Cytoplasm	other
MT1M	metallothionein 1M	Other	other
MT1X	metallothionein 1X	Other	other
MT2A	metallothionein 2A	Cytoplasm	other
MTL5	metallothionein-like 5, testis-specific (tesmin)	Cytoplasm	other
MTMR6	myotubularin related protein 6	Cytoplasm	phosphatase
MX1	MX dynamin-like GTPase 1	Cytoplasm	enzyme
MXI1	MAX interactor 1, dimerization protein	Nucleus	transcription regulator
MYL12A	myosin, light chain 12A, regulatory, non-sarcomeric	Cytoplasm	other
N4BP2	NEDD4 binding protein 2	Cytoplasm	kinase
NAA50	N(alpha)-acetyltransferase 50, NatE catalytic subunit	Cytoplasm	enzyme
NACC2	NACC family member 2, BEN and BTB (POZ) domain containing	Nucleus	transcription regulator
NAGK	N-acetylglucosamine kinase	Cytoplasm	kinase
NAPA	N-ethylmaleimide-sensitive factor attachment protein, alpha	Cytoplasm	transporter
NCAPD2	non-SMC condensin I complex, subunit D2	Nucleus	other
NCK1	NCK adaptor protein 1	Cytoplasm	kinase
NCOA4	nuclear receptor coactivator 4	Nucleus	transcription regulator
NDE1	nudE neurodevelopment protein 1	Nucleus	other
NDEL1	nudE neurodevelopment protein 1-like 1	Nucleus	other
NEURL3	neuralized E3 ubiquitin protein ligase 3	Other	other
NFASC	neurofascin	Plasma Membrane	other
NFATC3	nuclear factor of activated T-cells, cytoplasmic, calcineurin-dependent 3	Nucleus	transcription regulator
NFX1	nuclear transcription factor, X-box binding 1	Nucleus	transcription regulator
NGFRAP1	nerve growth factor receptor (TNFRSF16) associated protein 1	Cytoplasm	other
NKIRAS2	NFKB inhibitor interacting Ras-like 2	Cytoplasm	enzyme
NKRF	NFKB repressing factor	Nucleus	transcription

			regulator
NME1	NME/NM23 nucleoside diphosphate kinase 1	Cytoplasm	kinase
NME2	NME/NM23 nucleoside diphosphate kinase 2	Nucleus	kinase
NNMT	nicotinamide N-methyltransferase	Cytoplasm	enzyme
NOMO1	NODAL modulator 1	Plasma Membrane	other
NPAP1	nuclear pore associated protein 1	Cytoplasm	other
NPRL2	nitrogen permease regulator-like 2 (S. cerevisiae)	Cytoplasm	kinase
NPVF	neuropeptide VF precursor	Extracellular Space	other
NR2F6	nuclear receptor subfamily 2, group F, member 6	Nucleus	ligand-dependent nuclear receptor
NRBF2	nuclear receptor binding factor 2	Nucleus	transcription regulator
NRDE2	NRDE-2, necessary for RNA interference, domain containing	Other	other
NRIP3	nuclear receptor interacting protein 3	Other	other
NRM	nurim (nuclear envelope membrane protein)	Nucleus	other
NSUN6	NOP2/Sun domain family, member 6	Other	enzyme
NT5C2	5'-nucleotidase, cytosolic II	Cytoplasm	phosphatase
NT5C3A	5'-nucleotidase, cytosolic IIIA	Cytoplasm	phosphatase
NTNG2	netrin G2	Plasma Membrane	other
NUB1	negative regulator of ubiquitin-like proteins 1	Nucleus	other
NUDT4	nudix (nucleoside diphosphate linked moiety X)-type motif 4	Cytoplasm	phosphatase
NUMB	numb homolog (Drosophila)	Plasma Membrane	other
NUP62	nucleoporin 62kDa	Nucleus	transporter
NUPR1	nuclear protein, transcriptional regulator, 1	Nucleus	transcription regulator
NXT1	nuclear transport factor 2-like export factor 1	Nucleus	transporter
OAZ2	ornithine decarboxylase antizyme 2	Cytoplasm	other
OLIG2	oligodendrocyte lineage transcription factor 2	Nucleus	transcription regulator
OR51A4	olfactory receptor, family 51, subfamily A, member 4	Plasma Membrane	other
OR51G2	olfactory receptor, family 51, subfamily G, member 2	Plasma Membrane	G-protein coupled receptor

ORAI1	ORAI calcium release-activated calcium modulator 1	Plasma Membrane	ion channel
OTULIN	OTU deubiquitinase with linear linkage specificity	Cytoplasm	peptidase
OXR1	oxidation resistance 1	Cytoplasm	other
P2RY12	purinergic receptor P2Y, G-protein coupled, 12	Plasma Membrane	G-protein coupled receptor
P4HA1	prolyl 4-hydroxylase, alpha polypeptide I	Cytoplasm	enzyme
PAICS	phosphoribosylaminoimidazole carboxylase, phosphoribosylaminoimidazole succinocarboxamide synthetase	Cytoplasm	enzyme
PAIP1	poly(A) binding protein interacting protein 1	Cytoplasm	translation regulator
PAPD5	PAP associated domain containing 5	Nucleus	enzyme
PAPD7	PAP associated domain containing 7	Nucleus	enzyme
PARP10	poly (ADP-ribose) polymerase family, member 10	Cytoplasm	enzyme
PARP12	poly (ADP-ribose) polymerase family, member 12	Nucleus	other
PARP4	poly (ADP-ribose) polymerase family, member 4	Cytoplasm	enzyme
PARP9	poly (ADP-ribose) polymerase family, member 9	Nucleus	enzyme
PATL1	protein associated with topoisomerase II homolog 1 (yeast)	Cytoplasm	translation regulator
PCED1B	PC-esterase domain containing 1B	Other	other
PCM1	pericentriolar material 1	Cytoplasm	other
PCP2	Purkinje cell protein 2	Cytoplasm	other
PDGFRL	platelet-derived growth factor receptor-like	Plasma Membrane	kinase
PDK1	pyruvate dehydrogenase kinase, isozyme 1	Cytoplasm	kinase
PDSS1	prenyl (decaprenyl) diphosphate synthase, subunit 1	Cytoplasm	enzyme
PDZD8	PDZ domain containing 8	Extracellular Space	other
PEF1	penta-EF-hand domain containing 1	Cytoplasm	other
PELI2	pellino E3 ubiquitin protein ligase family member 2	Cytoplasm	other
PER1	period circadian clock 1	Nucleus	other
PF4V1	platelet factor 4 variant 1	Extracellular Space	cytokine
PGBD2	piggyBac transposable element derived 2	Other	other
PHACTR2	phosphatase and actin regulator 2	Other	other
PHF11	PHD finger protein 11	Other	other
PHF20	PHD finger protein 20	Nucleus	other
PHOSPHO1	phosphatase, orphan 1	Extracellular Space	enzyme
PI4K2A	phosphatidylinositol 4-kinase type 2 alpha	Cytoplasm	kinase

PI4K2B	phosphatidylinositol 4-kinase type 2 beta	Cytoplasm	kinase
PIGY	phosphatidylinositol glycan anchor biosynthesis, class Y	Plasma Membrane	other
PIKFYVE	phosphoinositide kinase, FYVE finger containing	Cytoplasm	kinase
PIM1	Pim-1 proto-oncogene, serine/threonine kinase	Cytoplasm	kinase
PIM2	Pim-2 proto-oncogene, serine/threonine kinase	Other	kinase
PLA2G16	phospholipase A2, group XVI	Nucleus	enzyme
PLEKHA4	pleckstrin homology domain containing, family A (phosphoinositide binding specific) member 4	Cytoplasm	other
PLEKHB2	pleckstrin homology domain containing, family B (evectins) member 2	Other	other
PLEKHM3	pleckstrin homology domain containing, family M, member 3	Other	other
PLK2	polo-like kinase 2	Nucleus	kinase
PLSCR2	phospholipid scramblase 2	Other	other
PML	promyelocytic leukemia	Nucleus	transcription regulator
PNMA5	paraneoplastic Ma antigen family member 5	Other	other
PNMA6A	paraneoplastic Ma antigen family member 6A	Cytoplasm	other
PNPT1	polyribonucleotide nucleotidyltransferase 1	Cytoplasm	enzyme
POC5	POC5 centriolar protein	Cytoplasm	other
POLB	polymerase (DNA directed), beta	Nucleus	enzyme
POM121	POM121 transmembrane nucleoporin	Nucleus	other
POMZP3	POM121 and ZP3 fusion	Nucleus	other
POPDC2	popeye domain containing 2	Other	other
PPA1	pyrophosphatase (inorganic) 1	Cytoplasm	enzyme
PPAPDC1B	phosphatidic acid phosphatase type 2 domain containing 1B	Other	phosphatase
PPARD	peroxisome proliferator-activated receptor delta	Nucleus	ligand-dependent nuclear receptor
PPARG	peroxisome proliferator-activated receptor gamma	Nucleus	ligand-dependent nuclear receptor
PPBP	pro-platelet basic protein (chemokine (C-X-C motif) ligand 7)	Extracellular Space	cytokine
PPFIA4	protein tyrosine phosphatase, receptor type, f polypeptide (PTPRF), interacting protein (liprin), alpha 4	Plasma Membrane	phosphatase
PPIL1	peptidylprolyl isomerase (cyclophilin)-like 1	Plasma	enzyme

		Membrane	
PPM1D	protein phosphatase, Mg2+/Mn2+ dependent, 1D	Cytoplasm	phosphatase
PPM1K	protein phosphatase, Mg2+/Mn2+ dependent, 1K	Cytoplasm	phosphatase
PPP1R12A	protein phosphatase 1, regulatory subunit 12A	Cytoplasm	phosphatase
PPP1R12B	protein phosphatase 1, regulatory subunit 12B	Other	phosphatase
PRDX4	peroxiredoxin 4	Cytoplasm	enzyme
PRKAG2	protein kinase, AMP-activated, gamma 2 non-catalytic subunit	Cytoplasm	kinase
PRKD2	protein kinase D2	Cytoplasm	kinase
PRMT2	protein arginine methyltransferase 2	Nucleus	enzyme
PRORY	proline rich, Y-linked	Other	other
PRPF38B	pre-mRNA processing factor 38B	Other	other
PRPS2	phosphoribosyl pyrophosphate synthetase 2	Cytoplasm	kinase
PRR12	proline rich 12	Extracellular Space	other
PRSS16	protease, serine, 16 (thymus)	Extracellular Space	peptidase
PRUNE	prune exopolyphosphatase	Nucleus	enzyme
PSIP1	PC4 and SFRS1 interacting protein 1	Nucleus	other
PSMA4	proteasome (prosome, macropain) subunit, alpha type, 4	Cytoplasm	peptidase
PSMB6	proteasome (prosome, macropain) subunit, beta type, 6	Other	peptidase
PWWP2A	PWWP domain containing 2A	Other	other
PYGO2	pygopus family PHD finger 2	Nucleus	other
RAB11FIP1	RAB11 family interacting protein 1 (class I)	Cytoplasm	other
RAB13	RAB13, member RAS oncogene family	Plasma Membrane	enzyme
RAB20	RAB20, member RAS oncogene family	Cytoplasm	enzyme
RAB2A	RAB2A, member RAS oncogene family	Cytoplasm	enzyme
RAB36	RAB36, member RAS oncogene family	Cytoplasm	enzyme
RAB37	RAB37, member RAS oncogene family	Cytoplasm	enzyme
RAB8A	RAB8A, member RAS oncogene family	Plasma Membrane	enzyme
RACGAP1	Rac GTPase activating protein 1	Cytoplasm	transporter
RAF1	Raf-1 proto-oncogene, serine/threonine kinase	Cytoplasm	kinase
RAPGEF6	Rap guanine nucleotide exchange factor (GEF) 6	Plasma Membrane	other
RARA	retinoic acid receptor, alpha	Nucleus	ligand-dependent nuclear receptor

RASGRP3	RAS guanyl releasing protein 3 (calcium and DAG-regulated)	Cytoplasm	other
RASSF1	Ras association (RalGDS/AF-6) domain family member 1	Nucleus	other
RBBP6	retinoblastoma binding protein 6	Nucleus	enzyme
RBCK1	RanBP-type and C3HC4-type zinc finger containing 1	Cytoplasm	transcription regulator
RBM11	RNA binding motif protein 11	Nucleus	other
RBM14	RNA binding motif protein 14	Nucleus	transcription regulator
RBM20	RNA binding motif protein 20	Nucleus	other
RBM47	RNA binding motif protein 47	Other	other
RBM4B	RNA binding motif protein 4B	Nucleus	other
RCBTB2	regulator of chromosome condensation (RCC1) and BTB (POZ) domain containing protein 2	Cytoplasm	other
RCN1	reticulocalbin 1, EF-hand calcium binding domain	Cytoplasm	other
RCOR1	REST corepressor 1	Nucleus	transcription regulator
RDH16	retinol dehydrogenase 16 (all-trans)	Cytoplasm	enzyme
RELL1	RELT-like 1	Other	other
REXO1L2P	REX1, RNA exonuclease 1 homolog (S. cerevisiae)-like 2 (pseudogene)	Other	other
RFC1	replication factor C (activator 1) 1, 145kDa	Nucleus	transcription regulator
RFWD2	ring finger and WD repeat domain 2, E3 ubiquitin protein ligase	Cytoplasm	enzyme
RGS14	regulator of G-protein signaling 14	Cytoplasm	other
RGS18	regulator of G-protein signaling 18	Cytoplasm	other
RGS2	regulator of G-protein signaling 2	Nucleus	other
RHBDD2	rhomboid domain containing 2	Plasma Membrane	other
RHBDF2	rhomboid 5 homolog 2 (Drosophila)	Cytoplasm	other
RHOH	ras homolog family member H	Plasma Membrane	enzyme
RHOT1	ras homolog family member T1	Cytoplasm	enzyme
RIF1	replication timing regulatory factor 1	Nucleus	other
RILP	Rab interacting lysosomal protein	Cytoplasm	other
RIN2	Ras and Rab interactor 2	Cytoplasm	other
RLF	rearranged L-myc fusion	Nucleus	transcription regulator
RMI1	RecQ mediated genome instability 1	Nucleus	other
RNF139	ring finger protein 139	Cytoplasm	enzyme

RNF213	ring finger protein 213	Cytoplasm	enzyme
RNF44	ring finger protein 44	Other	other
RPN1	ribophorin I	Cytoplasm	enzyme
RPRD2	regulation of nuclear pre-mRNA domain containing 2	Other	other
RPS27L	ribosomal protein S27-like	Cytoplasm	translation regulator
RPS6KA1	ribosomal protein S6 kinase, 90kDa, polypeptide 1	Cytoplasm	kinase
RPS6KB2	ribosomal protein S6 kinase, 70kDa, polypeptide 2	Cytoplasm	kinase
RRM1	ribonucleotide reductase M1	Nucleus	enzyme
RRM2B	ribonucleotide reductase M2 B (TP53 inducible)	Nucleus	enzyme
RTF1	Rtf1, Paf1/RNA polymerase II complex component, homolog (S. cerevisiae)	Nucleus	other
SAMD8	sterile alpha motif domain containing 8	Cytoplasm	other
SAMD9	sterile alpha motif domain containing 9	Cytoplasm	other
SAMD9L	sterile alpha motif domain containing 9-like	Extracellular Space	other
SAMHD1	SAM domain and HD domain 1	Nucleus	enzyme
SAP25	Sin3A-associated protein, 25kDa	Other	other
SAP30	Sin3A-associated protein, 30kDa	Nucleus	transcription regulator
SCAMP1-AS1	SCAMP1 antisense RNA 1	Other	other
SCARB2	scavenger receptor class B, member 2	Plasma Membrane	other
SCARF1	scavenger receptor class F, member 1	Plasma Membrane	transmembrane receptor
SCHIP1	schwannomin interacting protein 1	Cytoplasm	other
SCRG1	stimulator of chondrogenesis 1	Extracellular Space	other
SCRN3	secernin 3	Other	other
SEC11A	SEC11 homolog A (S. cerevisiae)	Cytoplasm	peptidase
SEC16A	SEC16 homolog A (S. cerevisiae)	Cytoplasm	phosphatase
SEMA4A	sema domain, immunoglobulin domain (Ig), transmembrane domain (TM) and short cytoplasmic domain, (semaphorin) 4A	Plasma Membrane	other
SEMA6B	sema domain, transmembrane domain (TM), and cytoplasmic domain, (semaphorin) 6B	Plasma Membrane	other
SERPINB1	serpin peptidase inhibitor, clade B (ovalbumin), member 1	Cytoplasm	other
SERPINB5	serpin peptidase inhibitor, clade B (ovalbumin), member 5	Extracellular Space	other
SESN3	sestrin 3	Extracellular Space	other

SETD2	SET domain containing 2	Cytoplasm	enzyme
SETDB2	SET domain, bifurcated 2	Nucleus	enzyme
SGPL1	sphingosine-1-phosphate lyase 1	Cytoplasm	enzyme
SGSH	N-sulfoglucosamine sulfohydrolase	Cytoplasm	enzyme
SH2D3A	SH2 domain containing 3A	Cytoplasm	other
SH2D3C	SH2 domain containing 3C	Cytoplasm	other
SHFM1	split hand/foot malformation (ectrodactyly) type 1	Nucleus	peptidase
SIGIRR	single immunoglobulin and toll-interleukin 1 receptor (TIR) domain	Plasma Membrane	transmembrane receptor
SIGLEC1	sialic acid binding Ig-like lectin 1, sialoadhesin	Plasma Membrane	other
SIGLEC14	sialic acid binding Ig-like lectin 14	Plasma Membrane	other
SIK1	salt-inducible kinase 1	Nucleus	kinase
SLC15A2	solute carrier family 15 (oligopeptide transporter), member 2	Plasma Membrane	transporter
SLC19A1	solute carrier family 19 (folate transporter), member 1	Plasma Membrane	transporter
SLC19A2	solute carrier family 19 (thiamine transporter), member 2	Plasma Membrane	transporter
SLC22A5	solute carrier family 22 (organic cation/carnitine transporter), member 5	Plasma Membrane	transporter
SLC25A3	solute carrier family 25 (mitochondrial carrier; phosphate carrier), member 3	Cytoplasm	transporter
SLC25A45	solute carrier family 25, member 45	Cytoplasm	transporter
SLC27A3	solute carrier family 27 (fatty acid transporter), member 3	Cytoplasm	transporter
SLC38A2	solute carrier family 38, member 2	Plasma Membrane	transporter
SLC40A1	solute carrier family 40 (iron-regulated transporter), member 1	Plasma Membrane	transporter
SLC51A	solute carrier family 51, alpha subunit	Plasma Membrane	transporter
SLC5A3	solute carrier family 5 (sodium/myo-inositol cotransporter), member 3	Plasma Membrane	transporter
SLC7A5	solute carrier family 7 (amino acid transporter light chain, L system), member 5	Plasma Membrane	transporter
SLFN13	schlafen family member 13	Nucleus	enzyme
SLX4	SLX4 structure-specific endonuclease subunit	Nucleus	other
SMIM3	small integral membrane protein 3	Other	ion channel
SMIM9	small integral membrane protein 9	Other	other
SNAR-A3	small ILF3/NF90-associated RNA A3	Other	other

SNAR-B2	small ILF3/NF90-associated RNA B2	Other	other
SNAR-D	small ILF3/NF90-associated RNA D	Other	other
SNAR-F	small ILF3/NF90-associated RNA F	Other	other
SNAR-G2	small ILF3/NF90-associated RNA G2	Other	other
SNAR-H	small ILF3/NF90-associated RNA H	Other	other
SNHG7	small nucleolar RNA host gene 7 (non-protein coding)	Other	other
SNORD35B	small nucleolar RNA, C/D box 35B	Other	other
SNRK	SNF related kinase	Cytoplasm	kinase
SNRPD2	small nuclear ribonucleoprotein D2 polypeptide 16.5kDa	Nucleus	other
SNX1	sorting nexin 1	Cytoplasm	transporter
SOCS2-AS1	SOCS2 antisense RNA 1	Other	other
SOCS5	suppressor of cytokine signaling 5	Extracellular Space	cytokine
SORL1	sortilin-related receptor, L(DLR class) A repeats containing	Cytoplasm	transporter
SP100	SP100 nuclear antigen	Nucleus	transcription regulator
SP140L	SP140 nuclear body protein-like	Other	other
SPAG4	sperm associated antigen 4	Cytoplasm	other
SPECC1L	sperm antigen with calponin homology and coiled-coil domains 1-like	Extracellular Space	other
SPHK1	sphingosine kinase 1	Cytoplasm	kinase
SPHKAP	SPHK1 interactor, AKAP domain containing	Cytoplasm	other
SPINK6	serine peptidase inhibitor, Kazal type 6	Extracellular Space	other
SPINT2	serine peptidase inhibitor, Kunitz type, 2	Extracellular Space	other
SPOPL	speckle-type POZ protein-like	Other	other
SPTA1	spectrin, alpha, erythrocytic 1	Cytoplasm	other
SQRDL	sulfide quinone reductase-like (yeast)	Cytoplasm	enzyme
SRGAP2B	SLIT-ROBO Rho GTPase activating protein 2B	Other	other
SRGAP2C	SLIT-ROBO Rho GTPase activating protein 2C	Other	other
SSB	Sjogren syndrome antigen B (autoantigen La)	Nucleus	enzyme
ST3GAL4	ST3 beta-galactoside alpha-2,3-sialyltransferase 4	Cytoplasm	enzyme
ST3GAL4-AS1	ST3GAL4 antisense RNA 1 (head to head)	Other	other
STAT1	signal transducer and activator of transcription 1, 91kDa	Nucleus	transcription regulator
STIM1	stromal interaction molecule 1	Plasma Membrane	ion channel
STK38L	serine/threonine kinase 38 like	Cytoplasm	kinase
STOML1	stomatin (EPB72)-like 1	Other	other

STRAP	serine/threonine kinase receptor associated protein	Plasma Membrane	other
STX17	syntaxin 17	Plasma Membrane	transporter
STXBP3	syntaxin binding protein 3	Plasma Membrane	transporter
SURF6	surfeit 6	Nucleus	other
TACC1	transforming, acidic coiled-coil containing protein 1	Nucleus	other
TAPT1	transmembrane anterior posterior transformation 1	Plasma Membrane	G-protein coupled receptor
TBC1D10C	TBC1 domain family, member 10C	Nucleus	other
TCF20	transcription factor 20 (AR1)	Nucleus	transcription regulator
TCP11L2	t-complex 11, testis-specific-like 2	Other	other
TDRD6	tudor domain containing 6	Cytoplasm	other
TDRD7	tudor domain containing 7	Cytoplasm	other
TECPR2	tectonin beta-propeller repeat containing 2	Other	other
TET3	tet methylcytosine dioxygenase 3	Nucleus	other
TEX2	testis expressed 2	Other	other
TFAP2E	transcription factor AP-2 epsilon (activating enhancer binding protein 2 epsilon)	Other	other
TFEC	transcription factor EC	Nucleus	transcription regulator
TGFBR2	transforming growth factor, beta receptor II (70/80kDa)	Plasma Membrane	kinase
TGM2	transglutaminase 2	Cytoplasm	enzyme
THBD	thrombomodulin	Plasma Membrane	transmembrane receptor
THRA	thyroid hormone receptor, alpha	Nucleus	ligand-dependent nuclear receptor
TICAM1	toll-like receptor adaptor molecule 1	Nucleus	other
TINF2	TERF1 (TRF1)-interacting nuclear factor 2	Nucleus	other
TKT	transketolase	Cytoplasm	enzyme
TLDC2	TBC/LysM-associated domain containing 2	Other	other
TLR6	toll-like receptor 6	Plasma Membrane	transmembrane receptor
TM2D2	TM2 domain containing 2	Extracellular Space	other
TM4SF1	transmembrane 4 L six family member 1	Plasma	other

		Membrane	
TMEM123	transmembrane protein 123	Plasma Membrane	other
TMEM126B	transmembrane protein 126B	Other	other
TMEM140	transmembrane protein 140	Other	other
TMEM255A	transmembrane protein 255A	Extracellular Space	other
TMEM30B	transmembrane protein 30B	Other	other
TMEM62	transmembrane protein 62	Other	enzyme
TMEM81	transmembrane protein 81	Other	other
TMLHE-AS1	TMLHE antisense RNA 1	Other	other
TMOD2	tropomodulin 2 (neuronal)	Cytoplasm	other
TMSB10	thymosin beta 10	Cytoplasm	other
TMX4	thioredoxin-related transmembrane protein 4	Cytoplasm	enzyme
TNFRSF10A	tumor necrosis factor receptor superfamily, member 10a	Plasma Membrane	transmembrane receptor
TNFRSF10B	tumor necrosis factor receptor superfamily, member 10b	Plasma Membrane	transmembrane receptor
TNK2	tyrosine kinase, non-receptor, 2	Cytoplasm	kinase
TNK2-AS1	TNK2 antisense RNA 1	Other	other
TOM1L2	target of myb1-like 2 (chicken)	Cytoplasm	transporter
TOPBP1	topoisomerase (DNA) II binding protein 1	Nucleus	other
TOR1A	torsin family 1, member A (torsin A)	Cytoplasm	enzyme
TOR1AIP1	torsin A interacting protein 1	Nucleus	other
TOR1B	torsin family 1, member B (torsin B)	Cytoplasm	enzyme
TOX2	TOX high mobility group box family member 2	Nucleus	transcription regulator
TP53INP1	tumor protein p53 inducible nuclear protein 1	Nucleus	other
TPD52L1	tumor protein D52-like 1	Cytoplasm	other
TPI1P2	triosephosphate isomerase 1 pseudogene 2	Other	other
TPK1	thiamin pyrophosphokinase 1	Cytoplasm	kinase
TPM2	tropomyosin 2 (beta)	Other	other
TPT1-AS1	TPT1 antisense RNA 1	Other	other
TRADD	TNFRSF1A-associated via death domain	Cytoplasm	other
TRAFD1	TRAF-type zinc finger domain containing 1	Other	other
TRIM11	tripartite motif containing 11	Cytoplasm	enzyme
TRIM14	tripartite motif containing 14	Cytoplasm	other
TRIM21	tripartite motif containing 21	Nucleus	enzyme
TRIM26	tripartite motif containing 26	Cytoplasm	other
TRIM34	tripartite motif containing 34	Cytoplasm	other
TRIM5	tripartite motif containing 5	Cytoplasm	enzyme
TRIM56	tripartite motif containing 56	Cytoplasm	enzyme

TRIM8	tripartite motif containing 8	Nucleus	other
TRIOBP	TRIO and F-actin binding protein	Nucleus	other
TSC22D3	TSC22 domain family, member 3	Nucleus	transcription regulator
TTC21A	tetratricopeptide repeat domain 21A	Extracellular Space	other
TTC26	tetratricopeptide repeat domain 26	Extracellular Space	other
TTC38	tetratricopeptide repeat domain 38	Cytoplasm	other
TUSC2	tumor suppressor candidate 2	Nucleus	other
TXN	thioredoxin	Cytoplasm	enzyme
UBE2W	ubiquitin-conjugating enzyme E2W (putative)	Nucleus	enzyme
UBFD1	ubiquitin family domain containing 1	Other	other
UBR2	ubiquitin protein ligase E3 component n-recognin 2	Nucleus	enzyme
UBXN7	UBX domain protein 7	Nucleus	other
UCK2	uridine-cytidine kinase 2	Cytoplasm	kinase
UNC93B1	unc-93 homolog B1 (C. elegans)	Cytoplasm	other
UPP1	uridine phosphorylase 1	Cytoplasm	enzyme
UQCRC1	ubiquinol-cytochrome c reductase core protein I	Cytoplasm	enzyme
USP18	ubiquitin specific peptidase 18	Cytoplasm	peptidase
USP21	ubiquitin specific peptidase 21	Cytoplasm	peptidase
USP25	ubiquitin specific peptidase 25	Other	peptidase
USP3	ubiquitin specific peptidase 3	Cytoplasm	peptidase
USP41	ubiquitin specific peptidase 41	Other	other
USP49	ubiquitin specific peptidase 49	Other	peptidase
USPL1	ubiquitin specific peptidase like 1	Extracellular Space	other
UTP14C	UTP14, U3 small nucleolar ribonucleoprotein, homolog C (yeast)	Nucleus	other
VAT1	vesicle amine transport 1	Plasma Membrane	transporter
VNN3	vanin 3	Extracellular Space	enzyme
VPS26B	vacuolar protein sorting 26 homolog B (S. pombe)	Cytoplasm	transporter
WAC	WW domain containing adaptor with coiled-coil	Nucleus	other
WDR93	WD repeat domain 93	Other	other
WIPI2	WD repeat domain, phosphoinositide interacting 2	Cytoplasm	other
WRAP73	WD repeat containing, antisense to TP73	Nucleus	other
XPO7	exportin 7	Nucleus	transporter
YAP1	Yes-associated protein 1	Nucleus	transcription regulator
YME1L1	YME1-like 1 ATPase	Cytoplasm	peptidase

YPEL2	yippee-like 2 (Drosophila)	Nucleus	other
YPEL3	yippee-like 3 (Drosophila)	Other	other
ZBP1	Z-DNA binding protein 1	Cytoplasm	other
ZBTB18	zinc finger and BTB domain containing 18	Nucleus	transcription regulator
ZBTB33	zinc finger and BTB domain containing 33	Nucleus	other
ZBTB34	zinc finger and BTB domain containing 34	Nucleus	other
ZBTB43	zinc finger and BTB domain containing 43	Nucleus	other
ZBTB47	zinc finger and BTB domain containing 47	Other	other
ZCCHC2	zinc finger, CCHC domain containing 2	Cytoplasm	other
ZDHHC18	zinc finger, DHHC-type containing 18	Cytoplasm	enzyme
ZEB2	zinc finger E-box binding homeobox 2	Nucleus	transcription regulator
ZER1	zyg-11 related, cell cycle regulator	Other	enzyme
ZFP91	ZFP91 zinc finger protein	Nucleus	transcription regulator
ZFYVE26	zinc finger, FYVE domain containing 26	Cytoplasm	other
ZMYND10	zinc finger, MYND-type containing 10	Cytoplasm	other
ZMYND8	zinc finger, MYND-type containing 8	Nucleus	transcription regulator
ZNF106	zinc finger protein 106	Cytoplasm	other
ZNF18	zinc finger protein 18	Nucleus	transcription regulator
ZNF182	zinc finger protein 182	Nucleus	other
ZNF398	zinc finger protein 398	Nucleus	transcription regulator
ZNF552	zinc finger protein 552	Other	other
ZNF586	zinc finger protein 586	Other	other
ZNF614	zinc finger protein 614	Other	other
ZNF667	zinc finger protein 667	Nucleus	other
ZNF672	zinc finger protein 672	Other	other
ZNF684	zinc finger protein 684	Nucleus	other
ZNF775	zinc finger protein 775	Other	other
ZNF784	zinc finger protein 784	Other	other
ZNF814	zinc finger protein 814	Other	other
ZNFX1	zinc finger, NFX1-type containing 1	Nucleus	transcription regulator
ZYG11B	zyg-11 family member B, cell cycle regulator	Other	other

References

1. Hospital Episode Statistics 2012/13. accessed 15th January 2015]. Available from: http://www.hscic.gov.uk.

2. Blount RE, Jr., Morris JA, Savage RE. Recovery of cytopathogenic agent from chimpanzees with coryza. Proc Soc Exp Biol Med. 1956;92(3):544-9.

3. Chanock R, Finberg L. Recovery from infants with respiratory illness of a virus related to chimpanzee coryza agent (CCA). II. Epidemiologic aspects of infection in infants and young children. American journal of hygiene. 1957;66(3):291-300.

4. Carter SD, Dent KC, Atkins E, Foster TL, Verow M, Gorny P, et al. Direct visualization of the small hydrophobic protein of human respiratory syncytial virus reveals the structural basis for membrane permeability. FEBS letters. 2010;584(13):2786-90.

5. Spann KM, Tran KC, Collins PL. Effects of nonstructural proteins NS1 and NS2 of human respiratory syncytial virus on interferon regulatory factor 3, NF-kappaB, and proinflammatory cytokines. Journal of virology. 2005;79(9):5353-62.

6. Bitko V, Shulyayeva O, Mazumder B, Musiyenko A, Ramaswamy M, Look DC, et al. Nonstructural proteins of respiratory syncytial virus suppress premature apoptosis by an NF-kappaB-dependent, interferon-independent mechanism and facilitate virus growth. Journal of virology. 2007;81(4):1786-95.

7. Kahn JS, Schnell MJ, Buonocore L, Rose JK. Recombinant vesicular stomatitis virus expressing respiratory syncytial virus (RSV) glycoproteins: RSV fusion protein can mediate infection and cell fusion. Virology. 1999;254(1):81-91.

8. Srinivasakumar N, Ogra PL, Flanagan TD. Characteristics of fusion of respiratory syncytial virus with HEp-2 cells as measured by R18 fluorescence dequenching assay. Journal of virology. 1991;65(8):4063-9.

9. Collins PL, Fearns R, Graham BS. Respiratory syncytial virus: virology, reverse genetics, and pathogenesis of disease. Current topics in microbiology and immunology. 2013;372:3-38.

10. Kolokoltsov AA, Deniger D, Fleming EH, Roberts NJ, Jr., Karpilow JM, Davey RA. Small interfering RNA profiling reveals key role of clathrin-mediated endocytosis and early endosome formation for infection by respiratory syncytial virus. J Virol. 2007;81(14):7786-800.

11. Krzyzaniak MA, Zumstein MT, Gerez JA, Picotti P, Helenius A. Host cell entry of respiratory syncytial virus involves macropinocytosis followed by proteolytic activation of the F protein. PLoS Pathog. 2013;9(4):e1003309.

12. Bermingham A, Collins PL. The M2-2 protein of human respiratory syncytial virus is a regulatory factor involved in the balance between RNA replication and transcription. Proceedings of the National Academy of Sciences of the United States of America. 1999;96(20):11259-64.

13. Graham BS, Anderson LJ. Challenges and opportunities for respiratory syncytial virus vaccines. Curr Top Microbiol Immunol. 2013;372:391-404.

14. Glezen WP, Taber LH, Frank AL, Kasel JA. Risk of primary infection and reinfection with respiratory syncytial virus. Am J Dis Child. 1986;140(6):543-6.

15. Oymar K, Skjerven HO, Mikalsen IB. Acute bronchiolitis in infants, a review. Scandinavian journal of trauma, resuscitation and emergency medicine. 2014;22:23.

16. Zorc JJ, Hall CB. Bronchiolitis: recent evidence on diagnosis and management. Pediatrics. 2010;125(2):342-9.

17. Hall CB, Weinberg GA, Iwane MK, Blumkin AK, Edwards KM, Staat MA, et al. The burden of respiratory syncytial virus infection in young children. The New England journal of medicine. 2009;360(6):588-98.

18. Everard M L. Respiratory syncytial virus bronchiolitis and pneumonia. In: Taussig L. LL, editor. Paediatric Respiratory Medicine. St Louis: Mosby; 2009. p. 491-500.

19. MacDonald NE, Hall CB, Suffin SC, Alexson C, Harris PJ, Manning JA. Respiratory syncytial viral infection in infants with congenital heart disease. The New England journal of medicine. 1982;307(7):397-400.

20. Hall CB, Powell KR, MacDonald NE, Gala CL, Menegus ME, Suffin SC, et al. Respiratory syncytial viral infection in children with compromised immune function. The New England journal of medicine. 1986;315(2):77-81.

21. Boyce TG, Mellen BG, Mitchel EF, Jr., Wright PF, Griffin MR. Rates of hospitalization for respiratory syncytial virus infection among children in medicaid. The Journal of pediatrics. 2000;137(6):865-70.

22. Welliver RC. Review of epidemiology and clinical risk factors for severe respiratory syncytial virus (RSV) infection. The Journal of pediatrics. 2003;143(5 Suppl):S112-7.

23. Nair H, Nokes DJ, Gessner BD, Dherani M, Madhi SA, Singleton RJ, et al. Global burden of acute lower respiratory infections due to respiratory syncytial virus in young children: a systematic review and meta-analysis. Lancet. 2010;375(9725):1545-55.

24. World Health Organisation 'Immunization, Vaccines and Biologicals' 2014. Available from: http://www.who.int/immunization/research/meetings_workshops/pdvac/en/.

25. Kapikian AZ, Bell JA, Mastrota FM, Johnson KM, Huebner RJ, Chanock RM. An outbreak of febrile illness and pneumonia associated with respiratory syncytial virus infection. Am J Hyg. 1961;74:234-48.

26. Henderson FW, Collier AM, Clyde WA, Jr., Denny FW. Respiratory-syncytial-virus infections, reinfections and immunity. A prospective, longitudinal study in young children. The New England journal of medicine. 1979;300(10):530-4.

27. Hall CB. Respiratory syncytial virus. Feigin R, Cherry J, editors. Philadelphia: WB Saunders; 1998.

28. Heikkinen T, Thint M, Chonmaitree T. Prevalence of various respiratory viruses in the middle ear during acute otitis media. The New England journal of medicine. 1999;340(4):260-4.

29. Hall CB, McCarthy CA. Respiratory Syncytial Virus. 5th ed. Mandell GL, Bennett JE, editors. Philadelphia: Churchill Livingstone Inc; 2000. 1782-801 p.

30. Stein RT, Sherrill D, Morgan WJ, Holberg CJ, Halonen M, Taussig LM, et al. Respiratory syncytial virus in early life and risk of wheeze and allergy by age 13 years. Lancet. 1999;354(9178):541-5.

31. Simoes EA, Groothuis JR, Carbonell-Estrany X, Rieger CH, Mitchell I, Fredrick LM, et al. Palivizumab prophylaxis, respiratory syncytial virus, and subsequent recurrent wheezing. The Journal of pediatrics. 2007;151(1):34-42, e1.

32. Diagnosis and management of bronchiolitis. Pediatrics. 2006;118(4):1774-93.

33. Simões EA, DeVincenzo JP, Boeckh M, Bont L, Crowe JE, Griffiths P, et al. Challenges and opportunities in developing respiratory syncytial virus therapeutics. J Infect Dis. 2015;211 Suppl 1:S1-S20.

34. DeVincenzo JP, Whitley RJ, Mackman RL, Scaglioni-Weinlich C, Harrison L, Farrell E, et al. Oral GS-5806 activity in a respiratory syncytial virus challenge study. N Engl J Med. 2014;371(8):711-22.

35. Johnson S, Oliver C, Prince GA, Hemming VG, Pfarr DS, Wang SC, et al. Development of a humanized monoclonal antibody (MEDI-493) with potent in vitro and in vivo activity against respiratory syncytial virus. The Journal of infectious diseases. 1997;176(5):1215-24.

36. Harkensee C, Brodlie M, Embleton ND, McKean M. Passive immunisation of preterm infants with palivizumab against RSV infection. The Journal of infection. 2006;52(1):2-8.

37. Feltes TF, Cabalka AK, Meissner HC, Piazza FM, Carlin DA, Top FH, Jr., et al. Palivizumab prophylaxis reduces hospitalization due to respiratory

syncytial virus in young children with hemodynamically significant congenital heart disease. The Journal of pediatrics. 2003;143(4):532-40.

38. Public Health England Respiratory syncytial virus: the green book, chapter 27a March 2013 [25th February 2015]. Available from: http://www.gov.uk/government/publications/respiratory-syncytial-virus-the-green-book-chapter-27a.

39. Johnson JE, Gonzales RA, Olson SJ, Wright PF, Graham BS. The histopathology of fatal untreated human respiratory syncytial virus infection. Mod Pathol. 2007;20(1):108-19.

40. Sen GC, Sarkar SN. Hitching RIG to action. Nat Immunol. 2005;6(11):1074-6.

41. Schroder M, Bowie AG. TLR3 in antiviral immunity: key player or bystander? Trends in immunology. 2005;26(9):462-8.

42. Garcia-Sastre A, Biron CA. Type 1 interferons and the virus-host relationship: a lesson in detente. Science. 2006;312(5775):879-82.

43. Doyle S, Vaidya S, O'Connell R, Dadgostar H, Dempsey P, Wu T, et al. IRF3 mediates a TLR3/TLR4-specific antiviral gene program. Immunity. 2002;17(3):251-63.

44. Rudd BD, Burstein E, Duckett CS, Li X, Lukacs NW. Differential role for TLR3 in respiratory syncytial virus-induced chemokine expression. Journal of virology. 2005;79(6):3350-7.

45. Liu P, Jamaluddin M, Li K, Garofalo RP, Casola A, Brasier AR. Retinoic acid-inducible gene I mediates early antiviral response and Toll-like receptor 3 expression in respiratory syncytial virus-infected airway epithelial cells. Journal of virology. 2007;81(3):1401-11.

46. Murawski MR, Bowen GN, Cerny AM, Anderson LJ, Haynes LM, Tripp RA, et al. Respiratory syncytial virus activates innate immunity through Toll-like receptor 2. Journal of virology. 2009;83(3):1492-500.

47. Monick MM, Yarovinsky TO, Powers LS, Butler NS, Carter AB, Gudmundsson G, et al. Respiratory syncytial virus up-regulates TLR4 and sensitizes airway epithelial cells to endotoxin. The Journal of biological chemistry. 2003;278(52):53035-44.

48. Halfhide CP, Brearey SP, Flanagan BF, Hunt JA, Howarth D, Cummerson J, et al. Neutrophil TLR4 expression is reduced in the airways of infants with severe bronchiolitis. Thorax. 2009;64(9):798-805.

49. McNamara PS, Flanagan BF, Hart CA, Smyth RL. Production of chemokines in the lungs of infants with severe respiratory syncytial virus bronchiolitis. The Journal of infectious diseases. 2005;191(8):1225-32.

50. Kumagai Y, Takeuchi O, Kato H, Kumar H, Matsui K, Morii E, et al. Alveolar macrophages are the primary interferon-alpha producer in pulmonary infection with RNA viruses. Immunity. 2007;27(2):240-52.

51. Kimpen JL. Respiratory syncytial virus and asthma. The role of monocytes. American journal of respiratory and critical care medicine. 2001;163(3 Pt 2):S7-9.

52. Domurat F, Roberts NJ, Walsh EE, Dagan R. Respiratory syncytial virus infection of human mononuclear leukocytes in vitro and in vivo. J Infect Dis. 1985;152(5):895-902.

53. Wang SZ, Forsyth KD. The interaction of neutrophils with respiratory epithelial cells in viral infection. Respirology. 2000;5(1):1-10.

54. Bueno SM, Gonzalez PA, Riedel CA, Carreno LJ, Vasquez AE, Kalergis AM. Local cytokine response upon respiratory syncytial virus infection. Immunology letters. 2011;136(2):122-9.

55. Everard ML, Swarbrick A, Wrightham M, McIntyre J, Dunkley C, James PD, et al. Analysis of cells obtained by bronchial lavage of infants with respiratory syncytial virus infection. Archives of disease in childhood. 1994;71(5):428-32.

56. Hussell T, Openshaw PJ. Intracellular IFN-gamma expression in natural killer cells precedes lung CD8+ T cell recruitment during respiratory syncytial virus infection. The Journal of general virology. 1998;79 (Pt 11):2593-601.

57. Wang H, Peters N, Schwarze J. Plasmacytoid dendritic cells limit viral replication, pulmonary inflammation, and airway hyperresponsiveness in respiratory syncytial virus infection. J Immunol. 2006;177(9):6263-70.

58. Boogaard I, van Oosten M, van Rijt LS, Muskens F, Kimman TG, Lambrecht BN, et al. Respiratory syncytial virus differentially activates murine myeloid and plasmacytoid dendritic cells. Immunology. 2007;122(1):65-72.

59. Groothuis JR. The role of RSV neutralizing antibodies in the treatment and prevention of respiratory syncytial virus infection in high-risk children. Antiviral research. 1994;23(1):1-10.

60. Siber GR, Leombruno D, Leszczynski J, McIver J, Bodkin D, Gonin R, et al. Comparison of antibody concentrations and protective activity of respiratory syncytial virus immune globulin and conventional immune globulin. J Infect Dis. 1994;169(6):1368-73.

61. Falsey AR, Singh HK, Walsh EE. Serum antibody decay in adults following natural respiratory syncytial virus infection. J Med Virol. 2006;78(11):1493-7.

62. Glezen WP, Paredes A, Allison JE, Taber LH, Frank AL. Risk of respiratory syncytial virus infection for infants from low-income families in relationship to age, sex, ethnic group, and maternal antibody level. J Pediatr. 1981;98(5):708-15.

63. Groothuis JR, Simoes EA. Immunoprophylaxis and immunotherapy: role in the prevention and treatment of repiratory syncytial virus. International journal of antimicrobial agents. 1993;2(2):97-103.

64. Mejias A, Ramilo O. Review of palivizumab in the prophylaxis of respiratory syncytial virus (RSV) in high-risk infants. Biologics : targets & therapy. 2008;2(3):433-9.

65. Graham BS, Bunton LA, Wright PF, Karzon DT. Role of T lymphocyte subsets in the pathogenesis of primary infection and rechallenge with respiratory syncytial virus in mice. J Clin Invest. 1991;88(3):1026-33.

66. Cannon MJ, Openshaw PJ, Askonas BA. Cytotoxic T cells clear virus but augment lung pathology in mice infected with respiratory syncytial virus. J Exp Med. 1988;168(3):1163-8.

67. McNamara PS, Smyth RL. The pathogenesis of respiratory syncytial virus disease in childhood. British medical bulletin. 2002;61:13-28.

68. Collins PL, Graham BS. Viral and host factors in human respiratory syncytial virus pathogenesis. Journal of virology. 2008;82(5):2040-55.

69. Griffin MR, Walker FJ, Iwane MK, Weinberg GA, Staat MA, Erdman DD. Epidemiology of respiratory infections in young children: insights from the new vaccine surveillance network. The Pediatric infectious disease journal. 2004;23(11 Suppl):S188-92.

70. Miller EK, Lu X, Erdman DD, Poehling KA, Zhu Y, Griffin MR, et al. Rhinovirus-associated hospitalizations in young children. The Journal of infectious diseases. 2007;195(6):773-81.

71. Hall CB, Long CE, Schnabel KC. Respiratory syncytial virus infections in previously healthy working adults. Clinical infectious diseases : an official publication of the Infectious Diseases Society of America. 2001;33(6):792-6.

72. Lo MS, Brazas RM, Holtzman MJ. Respiratory syncytial virus nonstructural proteins NS1 and NS2 mediate inhibition of Stat2 expression and alpha/beta interferon responsiveness. Journal of virology. 2005;79(14):9315-9.

73. Melero JA, Garcia-Barreno B, Martinez I, Pringle CR, Cane PA. Antigenic structure, evolution and immunobiology of human respiratory syncytial virus attachment (G) protein. The Journal of general virology. 1997;78 (Pt 10):2411-8.

74. Tripp RA, Moore D, Anderson LJ. TH(1)- and TH(2)-TYPE cytokine expression by activated t lymphocytes from the lung and spleen during the

inflammatory response to respiratory syncytial virus. Cytokine. 2000;12(6):801-7.

75. Arnold R, Konig B, Werchau H, Konig W. Respiratory syncytial virus deficient in soluble G protein induced an increased proinflammatory response in human lung epithelial cells. Virology. 2004;330(2):384-97.

76. Perkins SM, Webb DL, Torrance SA, El Saleeby C, Harrison LM, Aitken JA, et al. Comparison of a real-time reverse transcriptase PCR assay and a culture technique for quantitative assessment of viral load in children naturally infected with respiratory syncytial virus. J Clin Microbiol. 2005;43(5):2356-62.

77. DeVincenzo JP, El Saleeby CM, Bush AJ. Respiratory syncytial virus load predicts disease severity in previously healthy infants. J Infect Dis. 2005;191(11):1861-8.

78. Buckingham SC, Bush AJ, Devincenzo JP. Nasal quantity of respiratory syncytical virus correlates with disease severity in hospitalized infants. Pediatr Infect Dis J. 2000;19(2):113-7.

79. DeVincenzo JP, Wilkinson T, Vaishnaw A, Cehelsky J, Meyers R, Nochur S, et al. Viral load drives disease in humans experimentally infected with respiratory syncytial virus. Am J Respir Crit Care Med. 2010;182(10):1305-14.

80. Welliver TP, Garofalo RP, Hosakote Y, Hintz KH, Avendano L, Sanchez K, et al. Severe human lower respiratory tract illness caused by respiratory syncytial virus and influenza virus is characterized by the absence of pulmonary cytotoxic lymphocyte responses. J Infect Dis. 2007;195(8):1126-36.

81. Lukens MV, van de Pol AC, Coenjaerts FE, Jansen NJ, Kamp VM, Kimpen JL, et al. A systemic neutrophil response precedes robust CD8(+) T-cell activation during natural respiratory syncytial virus infection in infants. Journal of virology. 2010;84(5):2374-83.

82. El Saleeby CM, Somes GW, DeVincenzo JP, Gaur AH. Risk factors for severe respiratory syncytial virus disease in children with cancer: the importance of lymphopenia and young age. Pediatrics. 2008;121(2):235-43.

83. Murphy BR, Olmsted RA, Collins PL, Chanock RM, Prince GA. Passive transfer of respiratory syncytial virus (RSV) antiserum suppresses the immune response to the RSV fusion (F) and large (G) glycoproteins expressed by recombinant vaccinia viruses. J Virol. 1988;62(10):3907-10.

84. Melendi GA, Hoffman SJ, Karron RA, Irusta PM, Laham FR, Humbles A, et al. C5 modulates airway hyperreactivity and pulmonary eosinophilia during enhanced respiratory syncytial virus disease by decreasing C3a receptor expression. J Virol. 2007;81(2):991-9.

85. Kim HW, Leikin SL, Arrobio J, Brandt CD, Chanock RM, Parrott RH. Cell-mediated immunity to respiratory syncytial virus induced by inactivated vaccine or by infection. Pediatr Res. 1976;10(1):75-8.

86. McNamara PS, Ritson P, Selby A, Hart CA, Smyth RL. Bronchoalveolar lavage cellularity in infants with severe respiratory syncytial virus bronchiolitis. Archives of disease in childhood. 2003;88(10):922-6.

87. Sung RY, Hui SH, Wong CK, Lam CW, Yin J. A comparison of cytokine responses in respiratory syncytial virus and influenza A infections in infants. European journal of pediatrics. 2001;160(2):117-22.

88. Jones W. The blood corpuscle considered in its different phases of development in the animal series. Philos Trans R Soc London. 1846;1(63).

89. Erhlich PaLE. Die Anaemie. Wein. 1898;8(49).

90. Waller A. Microscopic observations on the perforation of the capillaries by the corpuscles of blood and on the origin of mucus and pus globules. London Edinburgh Philos Mag J Sci. 1846;29:271.

91. Metchnikoff E, editor. Immunity in Infective Diseases. London: Cambridge University Press; 1905.

92. Wintrobe MM, editor. Clinical Hematology. Philadelphia: Lea & Febiger; 1967.

93. Scmid-Schonbein G. W SYY, Chen, S. Morphometry of human leukocytes. Blood. 1980;56:866.

94. Lekstrom-Himes JA, Gallin JI. Immunodeficiency diseases caused by defects in phagocytes. The New England journal of medicine. 2000;343(23):1703-14.

95. Kolaczkowska E, Kubes P. Neutrophil recruitment and function in health and inflammation. Nat Rev Immunol. 2013;13(3):159-75.

96. Ley K, Laudanna C, Cybulsky MI, Nourshargh S. Getting to the site of inflammation: the leukocyte adhesion cascade updated. Nat Rev Immunol. 2007;7(9):678-89.

97. Brinkmann V, Reichard U, Goosmann C, Fauler B, Uhlemann Y, Weiss DS, et al. Neutrophil extracellular traps kill bacteria. Science. 2004;303(5663):1532-5.

98. Okrent DG, Lichtenstein AK, Ganz T. Direct cytotoxicity of polymorphonuclear leukocyte granule proteins to human lung-derived cells and endothelial cells. Am Rev Respir Dis. 1990;141(1):179-85.

99. Segel GB, Halterman MW, Lichtman MA. The paradox of the neutrophil's role in tissue injury. J Leukoc Biol. 2011;89(3):359-72.

100. Leitch AE, Duffin R, Haslett C, Rossi AG. Relevance of granulocyte apoptosis to resolution of inflammation at the respiratory mucosa. Mucosal Immunol. 2008;1(5):350-63.

101. Ariel A, Fredman G, Sun YP, Kantarci A, Van Dyke TE, Luster AD, et al. Apoptotic neutrophils and T cells sequester chemokines during immune response resolution through modulation of CCR5 expression. Nature immunology. 2006;7(11):1209-16.

102. Mantovani A, Cassatella MA, Costantini C, Jaillon S. Neutrophils in the activation and regulation of innate and adaptive immunity. Nat Rev Immunol. 2011;11(8):519-31.

103. Serhan CN, Chiang N, Van Dyke TE. Resolving inflammation: dual anti-inflammatory and pro-resolution lipid mediators. Nature reviews Immunology. 2008;8(5):349-61.

104. Hayashi F, Means TK, Luster AD. Toll-like receptors stimulate human neutrophil function. Blood. 2003;102(7):2660-9.

105. Tecchio C, Micheletti A, Cassatella MA. Neutrophil-derived cytokines: facts beyond expression. Frontiers in immunology. 2014;5:508.

106. Scapini P, Lapinet-Vera JA, Gasperini S, Calzetti F, Bazzoni F, Cassatella MA. The neutrophil as a cellular source of chemokines. Immunological reviews. 2000;177:195-203.

107. van Gisbergen KP, Ludwig IS, Geijtenbeek TB, van Kooyk Y. Interactions of DC-SIGN with Mac-1 and CEACAM1 regulate contact between dendritic cells and neutrophils. FEBS letters. 2005;579(27):6159-68.

108. Scapini P, Nardelli B, Nadali G, Calzetti F, Pizzolo G, Montecucco C, et al. G-CSF-stimulated neutrophils are a prominent source of functional BLyS. The Journal of experimental medicine. 2003;197(3):297-302. Epub 2003/02/05.

109. Costantini C, Cassatella MA. The defensive alliance between neutrophils and NK cells as a novel arm of innate immunity. Journal of leukocyte biology. 2011;89(2):221-33.

110. Douglas RG, Jr., Alford RH, Cate TR, Couch RB. The leukocyte response during viral respiratory illness in man. Annals of internal medicine. 1966;64(3):521-30.

111. Stevens DA, Ferrington RA, Jordan GW, Merigan TC. Cellular events in zoster vesicles: relation to clinical course and immune parameters. The Journal of infectious diseases. 1975;131(5):509-15.

112. Van Strijp JA, Van Kessel KP, van der Tol ME, Verhoef J. Complement-mediated phagocytosis of herpes simplex virus by granulocytes. Binding or ingestion. The Journal of clinical investigation. 1989;84(1):107-12.

113. Tamassia N, Cassatella MA. Cytoplasmic receptors recognizing nucleic acids and mediating immune functions in neutrophils. Current opinion in pharmacology. 2013;13(4):547-54.

114. Tamassia N, Le Moigne V, Rossato M, Donini M, McCartney S, Calzetti F, et al. Activation of an immunoregulatory and antiviral gene expression program in poly(I:C)-transfected human neutrophils. J Immunol. 2008;181(9):6563-73.

115. Berger M, Hsieh CY, Bakele M, Marcos V, Rieber N, Kormann M, et al. Neutrophils express distinct RNA receptors in a non-canonical way. The Journal of biological chemistry. 2012;287(23):19409-17.

116. Becker S, Koren HS, Henke DC. Interleukin-8 expression in normal nasal epithelium and its modulation by infection with respiratory syncytial virus and cytokines tumor necrosis factor, interleukin-1, and interleukin-6. American journal of respiratory cell and molecular biology. 1993;8(1):20-7.

117. Patel JA, Jiang Z, Nakajima N, Kunimoto M. Autocrine regulation of interleukin-8 by interleukin-1alpha in respiratory syncytial virus-infected pulmonary epithelial cells in vitro. Immunology. 1998;95(4):501-6.

118. Harrison AM, Bonville CA, Rosenberg HF, Domachowske JB. Respiratory syncytical virus-induced chemokine expression in the lower airways: eosinophil recruitment and degranulation. American journal of respiratory and critical care medicine. 1999;159(6):1918-24.

119. Abu-Harb M, Bell F, Finn A, Rao WH, Nixon L, Shale D, et al. IL-8 and neutrophil elastase levels in the respiratory tract of infants with RSV bronchiolitis. The European respiratory journal. 1999;14(1):139-43.

120. Gern JE, Martin MS, Anklam KA, Shen K, Roberg KA, Carlson-Dakes KT, et al. Relationships among specific viral pathogens, virus-induced interleukin-8, and respiratory symptoms in infancy. Pediatric allergy and immunology : official publication of the European Society of Pediatric Allergy and Immunology. 2002;13(6):386-93.

121. Gill MA, Palucka AK, Barton T, Ghaffar F, Jafri H, Banchereau J, et al. Mobilization of plasmacytoid and myeloid dendritic cells to mucosal sites in children with respiratory syncytial virus and other viral respiratory infections. The Journal of infectious diseases. 2005;191(7):1105-15.

122. Fiedler MA, Wernke-Dollries K, Stark JM. Respiratory syncytial virus increases IL-8 gene expression and protein release in A549 cells. The American journal of physiology. 1995;269(6 Pt 1):L865-72.

123. Smyth RL, Mobbs KJ, O'Hea U, Ashby D, Hart CA. Respiratory syncytial virus bronchiolitis: disease severity, interleukin-8, and virus genotype. Pediatric pulmonology. 2002;33(5):339-46.

124. Stark JM, Godding V, Sedgwick JB, Busse WW. Respiratory syncytial virus infection enhances neutrophil and eosinophil adhesion to cultured

respiratory epithelial cells. Roles of CD18 and intercellular adhesion molecule-1. J Immunol. 1996;156(12):4774-82.

125. Wang SZ, Xu H, Wraith A, Bowden JJ, Alpers JH, Forsyth KD. Neutrophils induce damage to respiratory epithelial cells infected with respiratory syncytial virus. The European respiratory journal. 1998;12(3):612-8.

126. Gern JE, Busse WW. Relationship of viral infections to wheezing illnesses and asthma. Nat Rev Immunol. 2002;2(2):132-8.

127. Kaul TN, Faden H, Baker R, Ogra PL. Virus-induced complement activation and neutrophil-mediated cytotoxicity against respiratory syncytial virus (RSV). Clinical and experimental immunology. 1984;56(3):501-8.

128. Stokes K, Moore M. Examining the Role of Neutrophils in Respiratory Syncytial Virus (RSV) Infection. The Journal of Immunology. 2012;188:168.26.

129. Halfhide CP, Flanagan BF, Brearey SP, Hunt JA, Fonceca AM, McNamara PS, et al. Respiratory syncytial virus binds and undergoes transcription in neutrophils from the blood and airways of infants with severe bronchiolitis. J Infect Dis. 2011;204(3):451-8.

130. Prince LR, Graham KJ, Connolly J, Anwar S, Ridley R, Sabroe I, et al. Staphylococcus aureus induces eosinophil cell death mediated by alpha-hemolysin. PloS one. 2012;7(2):e31506.

131. Sabroe I, Prince LR, Dower SK, Walmsley SR, Chilvers ER, Whyte MK. What can we learn from highly purified neutrophils? Biochemical Society transactions. 2004;32(Pt3):468-9.

132. Simons ER. Measurement of phagocytosis and of the phagosomal environment in polymorphonuclear phagocytes by flow cytometry. Current protocols in cytometry / editorial board, J Paul Robinson, managing editor [et al]. 2010;Chapter 9:Unit9 31.

133. Orlando C, Pinzani P, Pazzagli M. Developments in quantitative PCR. Clinical chemistry and laboratory medicine : CCLM / FESCC. 1998;36(5):255-69.

134. Livak KJ, Schmittgen TD. Analysis of relative gene expression data using real-time quantitative PCR and the 2(-Delta Delta C(T)) Method. Methods. 2001;25(4):402-8.

135. Pfaffl MW. A new mathematical model for relative quantification in real-time RT-PCR. Nucleic acids research. 2001;29(9):e45.

136. Whelan JA, Russell NB, Whelan MA. A method for the absolute quantification of cDNA using real-time PCR. Journal of immunological methods. 2003;278(1-2):261-9.

137. Larionov A, Krause A, Miller W. A standard curve based method for relative real time PCR data processing. BMC bioinformatics. 2005;6:62.

138. Dewhurst-Maridor G, Simonet V, Bornand JE, Nicod LP, Pache JC. Development of a quantitative TaqMan RT-PCR for respiratory syncytial virus. Journal of virological methods. 2004;120(1):41-9.

139. Schindelin J, Arganda-Carreras I, Frise E, Kaynig V, Longair M, Pietzsch T, et al. Fiji: an open-source platform for biological-image analysis. Nat Methods. 2012;9(7):676-82.

140. Bai F, Kong KF, Dai J, Qian F, Zhang L, Brown CR, et al. A paradoxical role for neutrophils in the pathogenesis of West Nile virus. The Journal of infectious diseases. 2010;202(12):1804-12.

141. Gu J, Xie Z, Gao Z, Liu J, Korteweg C, Ye J, et al. H5N1 infection of the respiratory tract and beyond: a molecular pathology study. Lancet. 2007;370(9593):1137-45.

142. Zhao Y, Lu M, Lau LT, Lu J, Gao Z, Liu J, et al. Neutrophils may be a vehicle for viral replication and dissemination in human H5N1 avian influenza. Clin Infect Dis. 2008;47(12):1575-8.

143. Larochelle B, Flamand L, Gourde P, Beauchamp D, Gosselin J. Epstein-Barr virus infects and induces apoptosis in human neutrophils. Blood. 1998;92(1):291-9.

144. von Laer D, Serr A, Meyer-Konig U, Kirste G, Hufert FT, Haller O. Human cytomegalovirus immediate early and late transcripts are expressed in all major leukocyte populations in vivo. The Journal of infectious diseases. 1995;172(2):365-70.

145. Velzing J, Rothbarth PH, Kroes AC, Quint WG. Detection of cytomegalovirus mRNA and DNA encoding the immediate early gene in peripheral blood leukocytes from immunocompromised patients. Journal of medical virology. 1994;42(2):164-9.

146. Grefte A, Harmsen MC, van der Giessen M, Knollema S, van Son WJ, The TH. Presence of human cytomegalovirus (HCMV) immediate early mRNA but not ppUL83 (lower matrix protein pp65) mRNA in polymorphonuclear and mononuclear leukocytes during active HCMV infection. The Journal of general virology. 1994;75 (Pt 8):1989-98.

147. Gerna G, Percivalle E, Baldanti F, Sozzani S, Lanzarini P, Genini E, et al. Human cytomegalovirus replicates abortively in polymorphonuclear leukocytes after transfer from infected endothelial cells via transient microfusion events. Journal of virology. 2000;74(12):5629-38.

148. Hashimoto Y, Moki T, Takizawa T, Shiratsuchi A, Nakanishi Y. Evidence for phagocytosis of influenza virus-infected, apoptotic cells by neutrophils and macrophages in mice. J Immunol. 2007;178(4):2448-57.

149. Manicassamy B, Manicassamy S, Belicha-Villanueva A, Pisanelli G, Pulendran B, Garcia-Sastre A. Analysis of in vivo dynamics of influenza virus infection in mice using a GFP reporter virus. Proceedings of the National Academy of Sciences of the United States of America. 2010;107(25):11531-6.

150. Cassidy LF, Lyles DS, Abramson JS. Synthesis of viral proteins in polymorphonuclear leukocytes infected with influenza A virus. Journal of clinical microbiology. 1988;26(7):1267-70.

151. Ivan FX, Tan KS, Phoon MC, Engelward BP, Welsch RE, Rajapakse JC, et al. Neutrophils infected with highly virulent influenza H3N2 virus exhibit augmented early cell death and rapid induction of type I interferon signaling pathways. Genomics. 2013;101(2):101-12.

152. Peterson JR, Mitchison TJ. Small molecules, big impact: a history of chemical inhibitors and the cytoskeleton. Chem Biol. 2002;9(12):1275-85.

153. Fonceca AM, Flanagan BF, Trinick R, Smyth RL, McNamara PS. Primary airway epithelial cultures from children are highly permissive to respiratory syncytial virus infection. Thorax. 2012;67(1):42-8.

154. Bannister R, Rodrigues D, Murray EJ, Laxton C, Westby M, Bright H. Use of a highly sensitive strand-specific quantitative PCR to identify abortive replication in the mouse model of respiratory syncytial virus disease. Virology journal. 2010;7:250.

155. Boukhvalova MS, Prince GA, Blanco JC. Respiratory syncytial virus infects and abortively replicates in the lungs in spite of preexisting immunity. Journal of virology. 2007;81(17):9443-50.

156. Zhang L, Peeples ME, Boucher RC, Collins PL, Pickles RJ. Respiratory syncytial virus infection of human airway epithelial cells is polarized, specific to ciliated cells, and without obvious cytopathology. Journal of virology. 2002;76(11):5654-66.

157. Neilson KA, Yunis EJ. Demonstration of respiratory syncytial virus in an autopsy series. Pediatric pathology / affiliated with the International Paediatric Pathology Association. 1990;10(4):491-502.

158. Le Nouën C, Munir S, Losq S, Winter CC, McCarty T, Stephany DA, et al. Infection and maturation of monocyte-derived human dendritic cells by human respiratory syncytial virus, human metapneumovirus, and human parainfluenza virus type 3. Virology. 2009;385(1):169-82.

159. Arnold R, Konig B, Galatti H, Werchau H, Konig W. Cytokine (IL-8, IL-6, TNF-alpha) and soluble TNF receptor-I release from human peripheral blood mononuclear cells after respiratory syncytial virus infection. Immunology. 1995;85(3):364-72.

160. Franke-Ullmann G, Pfortner C, Walter P, Steinmuller C, Lohmann-Matthes ML, Kobzik L, et al. Alteration of pulmonary macrophage function by respiratory syncytial virus infection in vitro. J Immunol. 1995;154(1):268-80.

161. Babior BM. NADPH oxidase. Current opinion in immunology. 2004;16(1):42-7.

162. Dahlgren C, Karlsson A. Respiratory burst in human neutrophils. Journal of immunological methods. 1999;232(1-2):3-14.

163. Klebanoff SJ. Myeloperoxidase: friend and foe. Journal of leukocyte biology. 2005;77(5):598-625.

164. Faurschou M, Borregaard N. Neutrophil granules and secretory vesicles in inflammation. Microbes and infection / Institut Pasteur. 2003;5(14):1317-27.

165. Roitt I, Brostoff J, Male D. Immunology. 6th ed: Mosby; 2001.

166. Niedergang F, Chavrier P. Signaling and membrane dynamics during phagocytosis: many roads lead to the phagos(R)ome. Current opinion in cell biology. 2004;16(4):422-8.

167. Kaksonen M, Toret CP, Drubin DG. Harnessing actin dynamics for clathrin-mediated endocytosis. Nature reviews Molecular cell biology. 2006;7(6):404-14.

168. Mercer J, Helenius A. Gulping rather than sipping: macropinocytosis as a way of virus entry. Curr Opin Microbiol. 2012;15(4):490-9.

169. Botelho RJ, Tapper H, Furuya W, Mojdami D, Grinstein S. Fc gamma R-mediated phagocytosis stimulates localized pinocytosis in human neutrophils. J Immunol. 2002;169(8):4423-9.

170. Kliks SC, Nisalak A, Brandt WE, Wahl L, Burke DS. Antibody-dependent enhancement of dengue virus growth in human monocytes as a risk factor for dengue hemorrhagic fever. The American journal of tropical medicine and hygiene. 1989;40(4):444-51.

171. Takada A, Feldmann H, Ksiazek TG, Kawaoka Y. Antibody-dependent enhancement of Ebola virus infection. Journal of virology. 2003;77(13):7539-44.

172. Willey S, Aasa-Chapman MM, O'Farrell S, Pellegrino P, Williams I, Weiss RA, et al. Extensive complement-dependent enhancement of HIV-1 by autologous non-neutralising antibodies at early stages of infection. Retrovirology. 2011;8:16.

173. Petros RA, DeSimone JM. Strategies in the design of nanoparticles for therapeutic applications. Nat Rev Drug Discov. 2010;9(8):615-27.

174. Mercer J, Helenius A. Virus entry by macropinocytosis. Nat Cell Biol. 2009;11(5):510-20.

175. Takada A, Kawaoka Y. Antibody-dependent enhancement of viral infection: molecular mechanisms and in vivo implications. Reviews in medical virology. 2003;13(6):387-98.

176. Gimenez HB, Chisholm S, Dornan J, Cash P. Neutralizing and enhancing activities of human respiratory syncytial virus-specific antibodies. Clinical and diagnostic laboratory immunology. 1996;3(3):280-6.

177. Ivanov AI. Pharmacological inhibition of endocytic pathways: is it specific enough to be useful? Methods Mol Biol. 2008;440:15-33.

178. Sastre P, Oomens AG, Wertz GW. The stability of human respiratory syncytial virus is enhanced by incorporation of the baculovirus GP64 protein. Vaccine. 2007;25(27):5025-33.

179. JORDAN WS. Growth characteristics of respiratory syncytial virus. J Immunol. 1962;88:581-90.

180. Marsh M, Helenius A. Virus entry: open sesame. Cell. 2006;124(4):729-40.

181. Doherty GJ, McMahon HT. Mechanisms of endocytosis. Annu Rev Biochem. 2009;78:857-902.

182. Sieczkarski SB, Whittaker GR. Dissecting virus entry via endocytosis. J Gen Virol. 2002;83(Pt 7):1535-45.

183. Lamb RA, Kolakofksy D. Paramyxoviridae: the viruses and their replication. 3rd ed. Fields BN, Knipe DM, Howley PM, Chanock RM, Melnick JL, Monath TP, et al., editors. Philadephia: Lippincott-Raven; 1996.

184. Cantín C, Holguera J, Ferreira L, Villar E, Muñoz-Barroso I. Newcastle disease virus may enter cells by caveolae-mediated endocytosis. J Gen Virol. 2007;88(Pt 2):559-69.

185. Smith EC, Popa A, Chang A, Masante C, Dutch RE. Viral entry mechanisms: the increasing diversity of paramyxovirus entry. FEBS J. 2009;276(24):7217-27.

186. Schowalter RM, Chang A, Robach JG, Buchholz UJ, Dutch RE. Low-pH triggering of human metapneumovirus fusion: essential residues and importance in entry. J Virol. 2009;83(3):1511-22.

187. Hallak LK, Collins PL, Knudson W, Peeples ME. Iduronic acid-containing glycosaminoglycans on target cells are required for efficient respiratory syncytial virus infection. Virology. 2000;271(2):264-75.

188. San-Juan-Vergara H, Sampayo-Escobar V, Reyes N, Cha B, Pacheco-Lugo L, Wong T, et al. Cholesterol-rich microdomains as docking

platforms for respiratory syncytial virus in normal human bronchial epithelial cells. J Virol. 2012;86(3):1832-43.

189. Raghu H, Sharma-Walia N, Veettil MV, Sadagopan S, Chandran B. Kaposi's sarcoma-associated herpesvirus utilizes an actin polymerization-dependent macropinocytic pathway to enter human dermal microvascular endothelial and human umbilical vein endothelial cells. J Virol. 2009;83(10):4895-911.

190. Maréchal V, Prevost MC, Petit C, Perret E, Heard JM, Schwartz O. Human immunodeficiency virus type 1 entry into macrophages mediated by macropinocytosis. J Virol. 2001;75(22):11166-77.

191. Harris J, Werling D. Binding and entry of respiratory syncytial virus into host cells and initiation of the innate immune response. Cell Microbiol. 2003;5(10):671-80.

192. Mercer J, Greber UF. Virus interactions with endocytic pathways in macrophages and dendritic cells. Trends Microbiol. 2013;21(8):380-8.

193. Lozach PY, Kühbacher A, Meier R, Mancini R, Bitto D, Bouloy M, et al. DC-SIGN as a receptor for phleboviruses. Cell Host Microbe. 2011;10(1):75-88.

194. Plank C, Oberhauser B, Mechtler K, Koch C, Wagner E. The influence of endosome-disruptive peptides on gene transfer using synthetic virus-like gene transfer systems. J Biol Chem. 1994;269(17):12918-24.

195. Lencer WI, Weyer P, Verkman AS, Ausiello DA, Brown D. FITC-dextran as a probe for endosome function and localization in kidney. Am J Physiol. 1990;258(2 Pt 1):C309-17.

196. Falcone S, Cocucci E, Podini P, Kirchhausen T, Clementi E, Meldolesi J. Macropinocytosis: regulated coordination of endocytic and exocytic membrane traffic events. J Cell Sci. 2006;119(Pt 22):4758-69.

197. Manders EMM, Verbeek FJ, Aten JA. Measurement of co-localization of objects in dual-colour confocal images. Journal of Microscopy. 1993;169:375-82.

198. West MA, Bretscher MS, Watts C. Distinct endocytotic pathways in epidermal growth factor-stimulated human carcinoma A431 cells. J Cell Biol. 1989;109(6 Pt 1):2731-9.

199. Ros-Baro A, Lopez-Iglesias C, Peiro S, Bellido D, Palacin M, Zorzano A, et al. Lipid rafts are required for GLUT4 internalization in adipose cells. Proc Natl Acad Sci U S A. 2001;98(21):12050-5.

200. Davies PJ, Davies DR, Levitzki A, Maxfield FR, Milhaud P, Willingham MC, et al. Transglutaminase is essential in receptor-mediated endocytosis of alpha 2-macroglobulin and polypeptide hormones. Nature. 1980;283(5743):162-7.

201. Bradley JR, Johnson DR, Pober JS. Four different classes of inhibitors of receptor-mediated endocytosis decrease tumor necrosis factor-induced gene expression in human endothelial cells. J Immunol. 1993;150(12):5544-55.

202. Dunn KW, Kamocka MM, McDonald JH. A practical guide to evaluating colocalization in biological microscopy. Am J Physiol Cell Physiol. 2011;300(4):C723-42.

203. Bolte S, Cordelières FP. A guided tour into subcellular colocalization analysis in light microscopy. J Microsc. 2006;224(Pt 3):213-32.

204. Lee WL, Harrison RE, Grinstein S. Phagocytosis by neutrophils. Microbes Infect. 2003;5(14):1299-306.

205. Nordenfelt P, Tapper H. Phagosome dynamics during phagocytosis by neutrophils. J Leukoc Biol. 2011;90(2):271-84.

206. Mukherjee S, Ghosh RN, Maxfield FR. Endocytosis. Physiol Rev. 1997;77(3):759-803.

207. Underhill DM, Goodridge HS. Information processing during phagocytosis. Nat Rev Immunol. 2012;12(7):492-502.

208. Suomalainen M, Greber UF. Uncoating of non-enveloped viruses. Curr Opin Virol. 2013;3(1):27-33.

209. Barlan AU, Danthi P, Wiethoff CM. Lysosomal localization and mechanism of membrane penetration influence nonenveloped virus activation of the NLRP3 inflammasome. Virology. 2011;412(2):306-14.

210. Mercer J, Helenius A. Vaccinia virus uses macropinocytosis and apoptotic mimicry to enter host cells. Science. 2008;320(5875):531-5.

211. Coyne CB, Shen L, Turner JR, Bergelson JM. Coxsackievirus entry across epithelial tight junctions requires occludin and the small GTPases Rab34 and Rab5. Cell Host Microbe. 2007;2(3):181-92.

212. Garner JA. Herpes simplex virion entry into and intracellular transport within mammalian cells. Adv Drug Deliv Rev. 2003;55(11):1497-513.

213. Berger EA, Murphy PM, Farber JM. Chemokine receptors as HIV-1 coreceptors: roles in viral entry, tropism, and disease. Annu Rev Immunol. 1999;17:657-700.

214. Keller H, Niggli V. Effects of cytochalasin D on shape and fluid pinocytosis in human neutrophils as related to cytoskeletal changes (actin, alpha-actinin and microtubules). Eur J Cell Biol. 1995;66(2):157-64.

215. Bauer S, Tapper H. Membrane retrieval in neutrophils during phagocytosis: inhibition by M protein-expressing S. pyogenes bacteria. J Leukoc Biol. 2004;76(6):1142-50.

216. Carr R. Neutrophil production and function in newborn infants. British journal of haematology. 2000;110(1):18-28.

217. Falconer AE, Carr R, Edwards SW. Impaired neutrophil phagocytosis in preterm neonates: lack of correlation with expression of immunoglobulin or complement receptors. Biol Neonate. 1995;68(4):264-9.

218. Sadeghi K, Berger A, Langgartner M, Prusa AR, Hayde M, Herkner K, et al. Immaturity of infection control in preterm and term newborns is associated with impaired toll-like receptor signaling. J Infect Dis. 2007;195(2):296-302.

219. Melvan JN, Bagby GJ, Welsh DA, Nelson S, Zhang P. Neonatal sepsis and neutrophil insufficiencies. Int Rev Immunol. 2010;29(3):315-48.

220. de Blic J, Midulla F, Barbato A, Clement A, Dab I, Eber E, et al. Bronchoalveolar lavage in children. ERS Task Force on bronchoalveolar lavage in children. European Respiratory Society. The European respiratory journal. 2000;15(1):217-31.

221. Manroe BL, Weinberg AG, Rosenfeld CR, Browne R. The neonatal blood count in health and disease. I. Reference values for neutrophilic cells. The Journal of pediatrics. 1979;95(1):89-98.

222. Zhu J, Zhang H, Guo T, Li W, Li H, Zhu Y, et al. Quantitative proteomics reveals differential biological processes in healthy neonatal cord neutrophils and adult neutrophils. Proteomics. 2014;14(13-14):1688-97.

223. Krause PJ, Herson VC, Boutin-Lebowitz J, Eisenfeld L, Block C, LoBello T, et al. Polymorphonuclear leukocyte adherence and chemotaxis in stressed and healthy neonates. Pediatric research. 1986;20(4):296-300.

224. Eisenfeld L, Krause PJ, Herson V, Savidakis J, Bannon P, Maderazo E, et al. Longitudinal study of neutrophil adherence and motility. The Journal of pediatrics. 1990;117(6):926-9.

225. Sacchi F, Rondini G, Mingrat G, Stronati M, Gancia GP, Marseglia GL, et al. Different maturation of neutrophil chemotaxis in term and preterm newborn infants. The Journal of pediatrics. 1982;101(2):273-4.

226. Dossett JH, Williams RC, Jr., Quie PG. Studies on interaction of bacteria, serum factors and polymorphonuclear leukocytes in mothers and newborns. Pediatrics. 1969;44(1):49-57.

227. Kallman J, Schollin J, Schalen C, Erlandsson A, Kihlstrom E. Impaired phagocytosis and opsonisation towards group B streptococci in preterm neonates. Archives of disease in childhood Fetal and neonatal edition. 1998;78(1):F46-50.

228. Bektas S, Goetze B, Speer CP. Decreased adherence, chemotaxis and phagocytic activities of neutrophils from preterm neonates. Acta paediatrica Scandinavica. 1990;79(11):1031-8.

229. Ambruso DR, Stork LC, Gibson BE, Thurman GW. Increased activity of the respiratory burst in cord blood neutrophils: kinetics of the NADPH oxidase enzyme system in subcellular fractions. Pediatric research. 1987;21(2):205-10.

230. Currie AJ, Curtis S, Strunk T, Riley K, Liyanage K, Prescott S, et al. Preterm infants have deficient monocyte and lymphocyte cytokine responses to group B streptococcus. Infection and immunity. 2011;79(4):1588-96.

231. Destin KG, Linden JR, Laforce-Nesbitt SS, Bliss JM. Oxidative burst and phagocytosis of neonatal neutrophils confronting Candida albicans and Candida parapsilosis. Early human development. 2009;85(8):531-5.

232. Reddy RK, Xia Y, Hanikyrova M, Ross GD. A mixed population of immature and mature leucocytes in umbilical cord blood results in a reduced expression and function of CR3 (CD11b/CD18). Clinical and experimental immunology. 1998;114(3):462-7.

233. Filias A, Theodorou GL, Mouzopoulou S, Varvarigou AA, Mantagos S, Karakantza M. Phagocytic ability of neutrophils and monocytes in neonates. BMC pediatrics. 2011;11:29.

234. Frenck RW, Buescher ES, Vadhan-Raj S. The effects of recombinant human granulocyte-macrophage colony stimulating factor on in vitro cord blood granulocyte function. Pediatr Res. 1989;26(1):43-8.

235. Saez-Lopez C, Ngambe-Tourere E, Rosenzwajg M, Petit JC, Nicolas JC, Gozlan J. Immediate-early antigen expression and modulation of apoptosis after in vitro infection of polymorphonuclear leukocytes by human cytomegalovirus. Microbes Infect. 2005;7(9-10):1139-49.

236. Hannah S, Mecklenburgh K, Rahman I, Bellingan GJ, Greening A, Haslett C, et al. Hypoxia prolongs neutrophil survival in vitro. FEBS letters. 1995;372(2-3):233-7.

237. Colotta F, Re F, Polentarutti N, Sozzani S, Mantovani A. Modulation of granulocyte survival and programmed cell death by cytokines and bacterial products. Blood. 1992;80(8):2012-20.

238. Brach MA, deVos S, Gruss HJ, Herrmann F. Prolongation of survival of human polymorphonuclear neutrophils by granulocyte-macrophage colony-stimulating factor is caused by inhibition of programmed cell death. Blood. 1992;80(11):2920-4.

239. Lee A, Whyte MK, Haslett C. Inhibition of apoptosis and prolongation of neutrophil functional longevity by inflammatory mediators. Journal of leukocyte biology. 1993;54(4):283-8.

240. Noah TL, Becker S. Respiratory syncytial virus-induced cytokine production by a human bronchial epithelial cell line. The American journal of physiology. 1993;265(5 Pt 1):L472-8.

241. Jones A, Qui JM, Bataki E, Elphick H, Ritson S, Evans GS, et al. Neutrophil survival is prolonged in the airways of healthy infants and infants with RSV bronchiolitis. The European respiratory journal. 2002;20(3):651-7.

242. Wolach B, Gavrieli R, Pomeranz A. Effect of granulocyte and granulocyte macrophage colony stimulating factors (G-CSF and GM-CSF) on neonatal neutrophil functions. Pediatric research. 2000;48(3):369-73.

243. Duell BL, Cripps AW, Schembri MA, Ulett GC. Epithelial cell coculture models for studying infectious diseases: benefits and limitations. J Biomed Biotechnol. 2011;2011:852419.

244. Pickles RJ, DeVincenzo JP. Respiratory syncytial virus (RSV) and its propensity for causing bronchiolitis. The Journal of pathology. 2015;235(2):266-76.

245. Cassatella MA. Neutrophil-derived proteins: selling cytokines by the pound. Advances in immunology. 1999;73:369-509.

246. McNamara PS, Flanagan BF, Selby AM, Hart CA, Smyth RL. Pro- and anti-inflammatory responses in respiratory syncytial virus bronchiolitis. The European respiratory journal. 2004;23(1):106-12.

247. Bazzoni F, Cassatella MA, Laudanna C, Rossi F. Phagocytosis of opsonized yeast induces tumor necrosis factor-alpha mRNA accumulation and protein release by human polymorphonuclear leukocytes. Journal of leukocyte biology. 1991;50(3):223-8.

248. Stacey MA, Marsden M, Pham NT, Clare S, Dolton G, Stack G, et al. Neutrophils recruited by IL-22 in peripheral tissues function as TRAIL-dependent antiviral effectors against MCMV. Cell host & microbe. 2014;15(4):471-83.

249. McNamara PS, Flanagan BF, Baldwin LM, Newland P, Hart CA, Smyth RL. Interleukin 9 production in the lungs of infants with severe respiratory syncytial virus bronchiolitis. Lancet. 2004;363(9414):1031-7.

250. Zhang X, Kluger Y, Nakayama Y, Poddar R, Whitney C, DeTora A, et al. Gene expression in mature neutrophils: early responses to inflammatory stimuli. Journal of leukocyte biology. 2004;75(2):358-72.

251. Fessler MB, Malcolm KC, Duncan MW, Worthen GS. A genomic and proteomic analysis of activation of the human neutrophil by lipopolysaccharide and its mediation by p38 mitogen-activated protein kinase. J Biol Chem. 2002;277(35):31291-302.

252. Kobayashi SD, Voyich JM, Somerville GA, Braughton KR, Malech HL, Musser JM, et al. An apoptosis-differentiation program in human polymorphonuclear leukocytes facilitates resolution of inflammation. J Leukoc Biol. 2003;73(2):315-22.

253. Lakschevitz FS, Visser MB, Sun C, Glogauer M. Neutrophil transcriptional profile changes during transit from bone marrow to sites of inflammation. Cellular & molecular immunology. 2015;12(1):53-65.

254. Hufford MM, Richardson G, Zhou H, Manicassamy B, Garcia-Sastre A, Enelow RI, et al. Influenza-infected neutrophils within the infected lungs act as antigen presenting cells for anti-viral CD8(+) T cells. PloS one. 2012;7(10):e46581.

255. Mejias A, Dimo B, Suarez NM, Garcia C, Suarez-Arrabal MC, Jartti T, et al. Whole blood gene expression profiles to assess pathogenesis and disease severity in infants with respiratory syncytial virus infection. PLoS medicine. 2013;10(11):e1001549.

256. Schroeder A, Mueller O, Stocker S, Salowsky R, Leiber M, Gassmann M, et al. The RIN: an RNA integrity number for assigning integrity values to RNA measurements. BMC molecular biology. 2006;7:3.

257. Bolstad BM, Irizarry RA, Astrand M, Speed TP. A comparison of normalization methods for high density oligonucleotide array data based on variance and bias. Bioinformatics. 2003;19(2):185-93.

258. H Abdi LW. Principal component analysis. Computational Statistics. 2: Wiley Interdisciplinary Reviews; 2010. p. 433-59.

259. G.K S. Limma: linear models for microarrat data In: R Gentleman VC, S Dudoit, R Irizarry, W Huber, editor. Bioinformatics and Computational Biology Solutions using R and Bioconductor New York: Springer; 2005. p. 397-420.

260. Benjamini Y, Hochberg Y. Controlling the false discovery rate: a practical and powerful approach to multiple testing. Journal of the Royal Statistical Society. 1995;Series B57:289-300.

261. QIAGEN's Ingenuity® Pathway Analysis (IPA®, QIAGEN Redwood City, http://www.qiagen.com/ingenuity.

262. Loo YM, Fornek J, Crochet N, Bajwa G, Perwitasari O, Martinez-Sobrido L, et al. Distinct RIG-I and MDA5 signaling by RNA viruses in innate immunity. Journal of virology. 2008;82(1):335-45.

263. Kawai T, Akira S. Innate immune recognition of viral infection. Nat Immunol. 2006;7(2):131-7.

264. Takaoka A, Yanai H. Interferon signalling network in innate defence. Cellular microbiology. 2006;8(6):907-22.

265. Yoboua F, Martel A, Duval A, Mukawera E, Grandvaux N. Respiratory syncytial virus-mediated NF-kappa B p65 phosphorylation at serine 536 is dependent on RIG-I, TRAF6, and IKK beta. Journal of virology. 2010;84(14):7267-77.

266. Grandvaux N, Guan X, Yoboua F, Zucchini N, Fink K, Doyon P, et al. Sustained activation of interferon regulatory factor 3 during infection by paramyxoviruses requires MDA5. Journal of innate immunity. 2014;6(5):650-62.

267. Kurt-Jones EA, Popova L, Kwinn L, Haynes LM, Jones LP, Tripp RA, et al. Pattern recognition receptors TLR4 and CD14 mediate response to respiratory syncytial virus. Nature immunology. 2000;1(5):398-401.

268. Rallabhandi P, Phillips RL, Boukhvalova MS, Pletneva LM, Shirey KA, Gioannini TL, et al. Respiratory syncytial virus fusion protein-induced toll-like receptor 4 (TLR4) signaling is inhibited by the TLR4 antagonists Rhodobacter sphaeroides lipopolysaccharide and eritoran (E5564) and requires direct interaction with MD-2. MBio. 2012;3(4).

269. Marie I, Durbin JE, Levy DE. Differential viral induction of distinct interferon-alpha genes by positive feedback through interferon regulatory factor-7. The EMBO journal. 1998;17(22):6660-9.

270. Matsuyama T, Kimura T, Kitagawa M, Pfeffer K, Kawakami T, Watanabe N, et al. Targeted disruption of IRF-1 or IRF-2 results in abnormal type I IFN gene induction and aberrant lymphocyte development. Cell. 1993;75(1):83-97.

271. Liu T, Castro S, Brasier AR, Jamaluddin M, Garofalo RP, Casola A. Reactive oxygen species mediate virus-induced STAT activation: role of tyrosine phosphatases. The Journal of biological chemistry. 2004;279(4):2461-9.

272. de Veer MJ, Holko M, Frevel M, Walker E, Der S, Paranjape JM, et al. Functional classification of interferon-stimulated genes identified using microarrays. Journal of leukocyte biology. 2001;69(6):912-20.

273. Chen L, Li S, McGilvray I. The ISG15/USP18 ubiquitin-like pathway (ISGylation system) in hepatitis C virus infection and resistance to interferon therapy. Int J Biochem Cell Biol. 2011;43(10):1427-31.

274. Ritchie KJ, Hahn CS, Kim KI, Yan M, Rosario D, Li L, et al. Role of ISG15 protease UBP43 (USP18) in innate immunity to viral infection. Nat Med. 2004;10(12):1374-8.

275. Lindenmann J, Lane CA, Hobson D. The Resistance of A2g Mice to Myxoviruses. J Immunol. 1963;90:942-51.

276. Verhelst J, Hulpiau P, Saelens X. Mx proteins: antiviral gatekeepers that restrain the uninvited. Microbiol Mol Biol Rev. 2013;77(4):551-66.

277. Schnorr JJ, Schneider-Schaulies S, Simon-Jodicke A, Pavlovic J, Horisberger MA, ter Meulen V. MxA-dependent inhibition of measles virus glycoprotein synthesis in a stably transfected human monocytic cell line. Journal of virology. 1993;67(8):4760-8.

278. Atreya PL, Kulkarni S. Respiratory syncytial virus strain A2 is resistant to the antiviral effects of type I interferons and human MxA. Virology. 1999;261(2):227-41.

279. Pletneva LM, Haller O, Porter DD, Prince GA, Blanco JC. Induction of type I interferons and interferon-inducible Mx genes during respiratory syncytial virus infection and reinfection in cotton rats. The Journal of general virology. 2008;89(Pt 1):261-70.

280. Jouvenet N, Neil SJ, Zhadina M, Zang T, Kratovac Z, Lee Y, et al. Broad-spectrum inhibition of retroviral and filoviral particle release by tetherin. Journal of virology. 2009;83(4):1837-44.

281. Sauter D. Counteraction of the multifunctional restriction factor tetherin. Frontiers in microbiology. 2014;5:163.

282. Inchley CS, Sonerud T, Fjaerli HO, Nakstad B. Reduced Dicer expression in the cord blood of infants admitted with severe respiratory syncytial virus disease. BMC infectious diseases. 2011;11:59.

283. Fensterl V, Sen GC. The ISG56/IFIT1 gene family. Journal of interferon & cytokine research : the official journal of the International Society for Interferon and Cytokine Research. 2011;31(1):71-8.

284. Fehrholz M, Kendl S, Prifert C, Weissbrich B, Lemon K, Rennick L, et al. The innate antiviral factor APOBEC3G targets replication of measles, mumps and respiratory syncytial viruses. J Gen Virol. 2012;93(Pt 3):565-76.

285. Wang J, Liu B, Wang N, Lee YM, Liu C, Li K. TRIM56 is a virus- and interferon-inducible E3 ubiquitin ligase that restricts pestivirus infection. Journal of virology. 2011;85(8):3733-45.

286. Rajsbaum R, Stoye JP, O'Garra A. Type I interferon-dependent and -independent expression of tripartite motif proteins in immune cells. European journal of immunology. 2008;38(3):619-30.

287. Carthagena L, Bergamaschi A, Luna JM, David A, Uchil PD, Margottin-Goguet F, et al. Human TRIM gene expression in response to interferons. PloS one. 2009;4(3):e4894.

288. Yang K, Shi HX, Liu XY, Shan YF, Wei B, Chen S, et al. TRIM21 is essential to sustain IFN regulatory factor 3 activation during antiviral response. J Immunol. 2009;182(6):3782-92.

289. Kawai T, Akira S. Regulation of innate immune signalling pathways by the tripartite motif (TRIM) family proteins. EMBO molecular medicine. 2011;3(9):513-27.

290. Lee Y, Song B, Park C, Kwon KS. TRIM11 negatively regulates IFNbeta production and antiviral activity by targeting TBK1. PloS one. 2013;8(5):e63255.

291. Villarino A, Hibbert L, Lieberman L, Wilson E, Mak T, Yoshida H, et al. The IL-27R (WSX-1) is required to suppress T cell hyperactivity during infection. Immunity. 2003;19(5):645-55.

292. Zeng R, Zhang H, Hai Y, Cui Y, Wei L, Li N, et al. Interleukin-27 inhibits vaccine-enhanced pulmonary disease following respiratory syncytial virus infection by regulating cellular memory responses. Journal of virology. 2012;86(8):4505-17.

293. de Almeida Nagata DE, Demoor T, Ptaschinski C, Ting HA, Jang S, Reed M, et al. IL-27R-mediated regulation of IL-17 controls the development of respiratory syncytial virus-associated pathogenesis. The American journal of pathology. 2014;184(6):1807-18.

294. Openshaw PJ, Chiu C. Protective and dysregulated T cell immunity in RSV infection. Curr Opin Virol. 2013;3(4):468-74.

295. Abi Abdallah DS, Egan CE, Butcher BA, Denkers EY. Mouse neutrophils are professional antigen-presenting cells programmed to instruct Th1 and Th17 T-cell differentiation. Int Immunol. 2011;23(5):317-26.

296. Ostanin DV, Kurmaeva E, Furr K, Bao R, Hoffman J, Berney S, et al. Acquisition of antigen-presenting functions by neutrophils isolated from mice with chronic colitis. J Immunol. 2012;188(3):1491-502.

297. Sandilands GP, Hauffe B, Loudon E, Marsh AG, Gondowidjojo A, Campbell C, et al. Detection of cytoplasmic CD antigens within normal human peripheral blood leucocytes. Immunology. 2003;108(3):329-37.

298. Sandilands GP, Ahmed Z, Perry N, Davison M, Lupton A, Young B. Cross-linking of neutrophil CD11b results in rapid cell surface expression of molecules required for antigen presentation and T-cell activation. Immunology. 2005;114(3):354-68.

299. Geng S, Matsushima H, Okamoto T, Yao Y, Lu R, Page K, et al. Emergence, origin, and function of neutrophil-dendritic cell hybrids in experimentally induced inflammatory lesions in mice. Blood. 2013;121(10):1690-700.

300. Matsushima H, Geng S, Lu R, Okamoto T, Yao Y, Mayuzumi N, et al. Neutrophil differentiation into a unique hybrid population exhibiting dual phenotype and functionality of neutrophils and dendritic cells. Blood. 2013;121(10):1677-89.

301. Martínez I, Lombardía L, Herranz C, García-Barreno B, Domínguez O, Melero JA. Cultures of HEp-2 cells persistently infected by human respiratory syncytial virus differ in chemokine expression and resistance to apoptosis as compared to lytic infections of the same cell type. Virology. 2009;388(1):31-41.

302. Trépanier P, Payment P, Trudel M. Concentration of human respiratory syncytial virus using ammonium sulfate, polyethylene glycol or hollow fiber ultrafiltration. J Virol Methods. 1981;3(4):201-11.

303. Mbiguino A, Menezes J. Purification of human respiratory syncytial virus: superiority of sucrose gradient over percoll, renografin, and metrizamide gradients. J Virol Methods. 1991;31(2-3):161-70.

304. Kolli D, Yueqing Z, Palkowetz K, Garofalo R, Casola A. Critical role of neutrophils in respiratory syncytial virus induced disease pathogenesis (INC8P.440). The Journal of Immunology. 2014;192 (1 supplement)(187.13).

305. Gu J, Xie Z, Gao Z, Liu J, Korteweg C, Ye J, et al. H5N1 infection of the respiratory tract and beyond: a molecular pathology study. Lancet. 2007;370(9593):1137-45.

306. Altznauer F, Conus S, Cavalli A, Folkers G, Simon HU. Calpain-1 regulates Bax and subsequent Smac-dependent caspase-3 activation in neutrophil apoptosis. J Biol Chem. 2004;279(7):5947-57.

307. Jost PJ, Grabow S, Gray D, McKenzie MD, Nachbur U, Huang DC, et al. XIAP discriminates between type I and type II FAS-induced apoptosis. Nature. 2009;460(7258):1035-9.

308. Lawrence T, Willoughby DA, Gilroy DW. Anti-inflammatory lipid mediators and insights into the resolution of inflammation. Nat Rev Immunol. 2002;2(10):787-95.

309. Geering B, Simon HU. Peculiarities of cell death mechanisms in neutrophils. Cell Death Differ. 2011;18(9):1457-69.

310. Vasudevan KK, Song K, Alford LM, Sale WS, Dymek EE, Smith EF, et al. FAP206 is a microtubule-docking adapter for ciliary radial spoke 2 and dynein c. Mol Biol Cell. 2015;26(4):696-710.